arXiv:1409.7055v2 [math.PR] 29 Feb 2016

Liouville quantum gravity as a mating of trees

Bertrand Duplantier, Jason Miller and Scott Sheffield

Abstract

There is a simple way to "glue together" a coupled pair of continuum random trees (CRTs) to produce a topological sphere. The sphere comes equipped with a measure and a space-filling curve (which describes the "interface" between the trees). We present an explicit and canonical way to embed the sphere in $\mathbf{C} \cup \{\infty\}$. In this embedding, the measure is Liouville quantum gravity (LQG) with parameter $\gamma \in (0,2)$, and the curve is space-filling $\mathrm{SLE}_{\kappa'}$ with $\kappa' = 16/\gamma^2$.

Achieving this requires us to develop an extensive suite of tools for working with LQG surfaces. We explain how to conformally weld so-called "quantum wedges" to obtain new quantum wedges of different weights. We construct finite-volume quantum disks and spheres of various types, and give a Poissonian description of the set of quantum disks cut off by a boundary-intersecting $\mathrm{SLE}_\kappa(\rho)$ process with $\kappa \in (0,4)$. We also establish a *Lévy tree* description of the set of quantum disks to the left (or right) of an $\mathrm{SLE}_{\kappa'}$ with $\kappa' \in (4,8)$. We show that given two such trees, sampled independently, there is a.s. a canonical way to "zip them together" and recover the $\mathrm{SLE}_{\kappa'}$.

The law of the CRT pair we study was shown in an earlier paper to be the scaling limit of the discrete tree/dual-tree pair associated to an FK-decorated random planar map (RPM). Together, these results imply that FK-decorated RPM scales to CLE-decorated LQG in a certain "tree structure" topology.

Contents

1 Introduction **4**
- 1.1 Constructing a topological sphere from a pair of trees 7
- 1.2 Liouville quantum gravity as a scaling limit 13
- 1.3 Gluing trees of disks 17
- 1.4 Quantum wedges, cones, disks, and spheres 18
- 1.5 Conformal structure and removability 27
- 1.6 Welding and cutting quantum wedges and cones 29
- 1.7 Matings of trees and trees of loops 35
- 1.8 Outline 52

2 Additional context **52**
- 2.1 Conformal mating in complex dynamics 52
- 2.2 Bottlenecks, baby universes and Liouville duality 54
- 2.3 Scaling exponents and KPZ 56

3 Preliminaries **57**
- 3.1 Reversing processes using local time 57
- 3.2 Bessel processes 60
- 3.3 $\mathrm{SLE}_\kappa(\rho)$ processes 63
- 3.4 Forward/reverse symmetries for $\mathrm{SLE}_\kappa(\rho)$ processes 68

4 Quantum surfaces **73**
- 4.1 Gaussian free fields 73
- 4.2 Thick quantum wedges 77
- 4.3 Quantum cones 82
- 4.4 Encoding surfaces using Bessel processes 84

5 Quantum disks and spheres as limits **90**
- 5.1 Unit area quantum disk 90
- 5.2 Unit boundary length quantum disk 100
- 5.3 Unit area quantum sphere 101

6 SLE/GFF couplings **103**
- 6.1 Reverse coupling 103
- 6.2 Forward coupling 107
- 6.3 Law of an $\mathrm{SLE}_\kappa(\rho)$ excursion 110

7 Structure theorems and quantum natural time **115**
- 7.1 Boundary-intersecting $\mathrm{SLE}_\kappa(\rho)$ processes 115
- 7.2 Radial and whole-plane $\mathrm{SLE}_\kappa(\rho)$ processes 125
- 7.3 $\mathrm{SLE}_{\kappa'}$ processes with $\kappa' \in (4, 8)$ 126
- 7.4 Zipping according to quantum natural time 134

8 Welding quantum wedges **141**
8.1 Welding a thick wedge and a weight 2 wedge . . . 142
8.2 Zipping up a thick wedge . . . 146
8.3 Welding more general wedges: proof of Theorem 1.9 . . . 148
8.4 Zipping up a thin wedge . . . 154
8.5 Gluing infinitesimally thin wedges: the Poissonian formulation . . . 155

9 Space-filling SLE and Brownian motion **157**

10 Trees determine embedding **162**
10.1 Theorem statement and proof using three lemmas . . . 162
10.2 Proof of variance bound . . . 168
10.3 Proof of basic distortion lemma . . . 170
10.4 Proof of KPZ lemma on diameter fourth powers . . . 171
10.5 Discrete models and topology strengthening . . . 181

11 KPZ interpretation **183**
11.1 General principles . . . 184
11.2 Non-intersecting paths and cut point dimension . . . 187
11.3 $\mathrm{SLE}_{\kappa'}$ double point dimension . . . 192
11.4 Boundary intersection dimension for $\mathrm{SLE}_\kappa(\rho)$ . . . 194
11.5 Intersection dimension of GFF flow lines . . . 195

12 Weldings of forested wedges and duality **196**
12.1 Brownian motion and SLE . . . 196
12.2 Surfaces with bottlenecks and atomic measures . . . 203

13 Open Questions **205**

References **206**

Acknowledgments. We have benefited from discussions with many individuals, including (and not limited to) Nathanael Berestycki, Dmitry Chelkak, Nicolas Curien, Hugo Duminil-Copin, Grégory Miermont, Richard Kenyon, Greg Lawler, Jean-François Le Gall, Asaf Nachmias, Rémi Rhodes, Steffen Rohde, Oded Schramm, Stanislav Smirnov, Xin Sun, Vincent Vargas, Sam Watson, Wendelin Werner, and Hao Wu. We also thank Ewain Gwynne for helpful comments on an earlier version of this article and Ken Stephenson for helping us use his circle packing software.

1 Introduction

This paper studies connections between the Schramm-Loewner evolution (SLE) [Sch00] and the "random surfaces" associated with Liouville quantum gravity (LQG). We derive an extensive collection of results about weldings and decompositions of surfaces of various types (spheres, disks, wedges, chains of disks, trees of disks, etc.) along with fundamental structural results about LQG. These results comprise a sort of "calculus of random surfaces" that combines the conformal welding theory of [She10] with the imaginary geometry theory of [MS12a, MS12b, MS12c, MS13a].

However, we begin with a construction that can be described without any *a priori* reference to SLE or LQG. Section 1.1 explains how to "mate" a pair of continuum random trees (CRTs) to produce what we will call a *peanosphere*. A peanosphere is a topological sphere endowed with a measure and a space-filling path in a certain random way. We then pose the question of how to put an explicit conformal structure on the peanosphere — i.e., how to explicitly embed the peanosphere in the complex plane $\mathbf{C} \cup \{\infty\}$. This paper shows that an instance of the peanosphere can a.s. be canonically embedded in the plane in a particular way, and that the embedded peanosphere has the law of an LQG quantum surface parameterized by $\mathbf{C} \cup \{\infty\}$ and decorated by a space-filling form of SLE. We will ultimately introduce a correlation parameter to the peanosphere construction that corresponds to the parameters $\gamma \in (0, 2)$, $\kappa = \gamma^2 \in (0, 4)$, and $\kappa' = 16/\kappa \in (4, \infty)$ that appear in the LQG and SLE constructions. Once the parameter is fixed, our result produces a one-to-one correspondence between instances of the peanosphere and instances of SLE-decorated LQG (defined for almost all instances).

One reason that this result is intriguing is that it allows one to convert many questions about SLE and LQG into questions about the peanosphere that can be asked without reference to conformal structure. In principle, this could allow future researchers to derive properties of SLE, LQG, and related structures in papers that never mention either Loewner evolution or the Gaussian free field. For example, the major open problem of endowing LQG with a metric space structure for general γ (see the discussion in [MS13b]) might turn out to be more easily addressed from the peanosphere perspective than from the conventional LQG perspective.

Another such open problem (which we state but will not solve here) is the following. Consider the graph whose vertices are the components of the complement of a chordal (non-space-filling) $\mathrm{SLE}_{\kappa'}$ trace with $\kappa' \in (4, 8)$, where two such components are adjacent if their boundaries intersect; is this graph a.s. connected? We will explain in Section 1.7 how topological properties of $\mathrm{SLE}_{\kappa'}$ (along with some geometric properties like quantum path length) are directly encoded by the CRTs used to construct the peanosphere, or by certain stable Lévy processes derived from these CRTs. This encoding reduces problems like the one just stated to questions about stable Lévy processes that can be asked without reference to SLE.

We also stress that, as explained in [She09], there is a simple procedure for constructing a conformal loop ensemble (CLE) from space-filling $\mathrm{SLE}_{\kappa'}$ when $\kappa' \in (4, 8)$, and that the procedure itself is topological, making no use of conformal structure. Hence the peanosphere encodes the CLE loops in a straightforward way, and many properties of CLE (e.g., quantum dimensions of different types of special points, quantum lengths of loops and areas of enclosed regions, properties of the graph whose vertices are loops with two loops adjacent when they intersect, etc.) could also be addressed directly from the peanosphere construction.

Another reason for interest in the peanosphere is discussed in Section 1.2, which explains at a high level how, in light of related recent work, our result completes a solution to one form of the problem of showing that CLE-decorated LQG is a scaling limit of random cluster-decorated planar maps. Essentially, the work in [She11] shows that certain trees associated to the latter scale to the pair of CRTs that this paper associates to the former, a fact that can be interpreted as scaling limit convergence within a topology native to the peanosphere.[1]

Update: As mentioned above this paper suggests that one natural way to study discrete statistical physics models on a planar maps (which we will discuss in Section 1.2) is try to identify a natural pair of trees induced by those models, and then use a combinatorial understanding of the trees to prove a relationship to SLE/LQG. Since this paper was posted to the arXiv, this approach has been

[1] Our scaling limit theorem does not by itself resolve the scaling limit conjectures of [DS11a, She10] (which require convergence in a topology that encodes conformal structure), because it does not address how the discrete models are embedded in the plane. There are a number of natural ways to embed the discrete models "conformally" in the plane; Figures 1.4 and 1.5 illustrate one way to do this using circle packings. Another approach is to view the faces of the planar map as regular unit-side-length polygons, stitched together along their boundaries to form a "quilt," and then to conformally map the quilt onto the plane. Proving that the curves in these embeddings are close to SLE curves appears to require a deeper understanding of the embeddings themselves, including the establishment of some technical lemmas that seem out of reach at the moment. However, Nicolas Curien, and Stanislav Smirnov and Roman Boikii, have announced some progress in this direction in private communication. Section 10.5 has some discussion about how one might try to "strengthen the topology" of the convergence theorem in this paper to establish the conjectures of [DS11a, She10] in a different way.

successfully applied by a number of authors to several well known combinatorial objects that had not previously been studied in the conformal probability context, including bipolar orientations and Schnyder woods as well as certain generalizations of the FK cluster model; see [KMSW15, GKMW16] (combined with [GHMS15]) and work in progress by Li and Sun, along with additional work in progress by Bernardi, Li and Sun. The new results allow us to add these models to the pantheon of canonical SLE/LQG-related models, which already includes loop-erased random walk, percolation, the Ising model, the uniform spanning tree, and the Gaussian free field. In particular, these are the first elements of the pantheon corresponding to $\kappa < 2$ and $\kappa' > 8$. We expect that these ideas will in time lead to additional bridges between combinatorics and conformal probability — in part because the "peanosphere convergence" results for random planar maps (as discussed in Section 1.2) are often more accessible than the analogous results for deterministic lattices, and can be established without a precise understanding of the discrete conformal structure.

A third reason for interest in these results is that they turn out to have consequences for the quantum zipper, as described in [She10], for $\mathrm{SLE}_{\kappa'}$ with $\kappa' \in (4, 8)$. We do not prove that $\mathrm{SLE}_{\kappa'}$ is removable (an issue raised as an open question in [She10]), but we obtain another way of showing that when $\kappa' \in (4, 8)$ the embedding of an $\mathrm{SLE}_{\kappa'}$ in the plane is a.s. determined by the two "quantum disk trees" it cuts out, one on its left and one on its right, which resolves other open problems from [She10, Section 6, Question 8]. This implies that the "welding" or "conformal mating" of the pair of trees is uniquely determined by the trees themselves. (See Figure 1.6.)

A fourth reason is that we intend to heavily use the matings mentioned just above, along with several other results from this paper, in forthcoming work about the quantum Loewner evolution (QLE), as introduced in [MS13b], and its relationship to the Brownian map. Both QLE and several approximations to QLE have analogs that can be constructed directly on the peanosphere itself. It will also turn out that the time-reversals of some of the QLE processes described in [MS13b] (the ones constructed using $\mathrm{SLE}_{\kappa'}$ for $\kappa' \in (4, 8)$) can be reformulated as ways to construct spheres by gluing trees of disks (more precisely, so-called *Lévy trees* of disks, of the sort described in Figure 1.6 and 1.7) to themselves. The Brownian map itself will also be obtained as a sort of "reshuffling" of the entire SLE_6 exploration tree associated to the peanosphere.

A fifth and more speculative reason to study the peanosphere is that developing objects like SLE, CLE and LQG in a framework that does not explicitly reference conformal structure may help us figure out how to construct interesting analogs of these objects in higher dimensions, where the tools of planar conformal geometry (such as the Riemann mapping theorem) no longer apply.

The remainder of this section is structured as follows. In Section 1.1, we describe how it is possible to construct a topological sphere by gluing a pair of trees to each

other. Section 1.2 explains how this article fits into a larger program to relate the scaling limits of random planar maps to LQG. Section 1.3 describes a variant of the construction of Section 1.1 to the setting of gluing trees of disks. In Section 1.4, we give an overview of the different types of quantum surfaces which will arise in this article. Section 1.6 gives our main results about welding quantum cones and wedges. Section 1.7 then describes our main results regarding different types of matings. Finally, Section 1.8 contains an outline of the remainder of the article.

1.1 Constructing a topological sphere from a pair of trees

Let us begin with something we can do easily. We will construct a topological sphere as a quotient of a pair of continuum random trees. This sphere will turn out to be naturally endowed with a measure and a space-filling curve that represents (intuitively) the interface between the two identified trees.

Let X_t and Y_t be independent Brownian excursions, both indexed by $t \in [0, T]$. Thus $X_0 = X_T = 0$ and $X_t > 0$ for $t \in (0, T)$ (and similarly for Y_t). Once X_t and Y_t are chosen, choose C large enough so that the graphs of X_t and $C - Y_t$ do not intersect. (The precise value of C does not matter.) Let $R = [0, T] \times [0, C]$, viewed as a Euclidean metric space.

Let $\cong$ denote the smallest equivalence relation on R that makes two points equivalent if they lie on the same vertical line segment with endpoints on the graphs of X_t and $C - Y_t$, or they lie on the same horizontal line segment that never goes above the graph of X_t (or never goes below the graph of $C - Y_t$). Maximal segments of this type are shown in Figure 1.1.

Observe that the vertical line segment corresponding to time $t \in [0, T]$ shares its lower (resp. upper) endpoint with a horizontal line segment if and only if $X_s > X_t$ (resp. $Y_s > Y_t$) for all s in a neighborhood of the form $(t, t + \epsilon)$ or $(t - \epsilon, t)$ for $\epsilon > 0$. It is easy to see that (aside from the $t = 0$ and $t = T$ segments) there almost surely exists no vertical line segment that shares both an upper and a lower endpoint with a horizontal line segment. [2] It is also easy to see that each of X_t and Y_t a.s. has at most countably many local minima, and that almost surely the values obtained by X_t or Y_t at these minima are distinct. It follows that a.s. each of the maximal horizontal segments of Figure 1.1 intersects the graph of X_t or $C - Y_t$ in two or three places (the two endpoints plus at most one additional point).

Thus the equivalence classes a.s. all have one of the following types:

[2] It can be shown the set of record minima of a one dimensional Brownian motion agrees in law with the zero set of a one dimensional Brownian motion; the fact that no such minima occur simultaneously is related to the fact that planar Brownian motion a.s. does not hit any specific point. More general statements, related to so-called "cone times," appear in [Eva85] and will be discussed in Section 9.

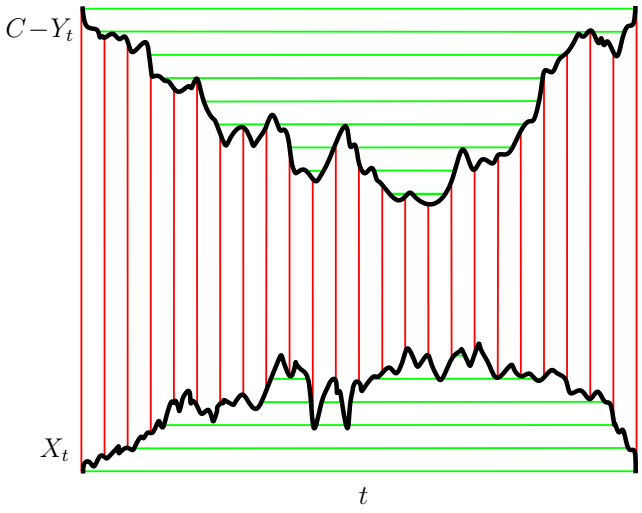

Figure 1.1: Points on the same vertical (or horizontal) line segment are equivalent.

Type 0: The outer boundary rectangle ∂R.

Type 1: A single vertical segment that does not share an endpoint with a horizontal segment.

Type 2: A single maximal horizontal segment beneath the graph of X_t or above the graph of $C - Y_t$, together with the two vertical segments with which it has an endpoint in common.

Type 3: A single maximal horizontal segment beneath the graph of X_t or above the graph of $C - Y_t$, together with the two vertical segments with which it has an endpoint in common, and one additional vertical segment with an endpoint in the interior of the horizontal segment.

Proposition 1.1. *The relation $\cong$ is a.s.* topologically closed. *That is, if $x_j \to x$, and $y_j \to y$, and $x_j \cong y_j$ for all j, then $x \cong y$.*

Proof. By passing to a subsequence, one may assume that the type of the equivalence class of $x_j \cong y_j$ is the same for all j. The equivalence class can be described by a finite collection of numbers (the endpoint coordinates for the line segments), and compactness implies that we can find a subsequence along which this collection of coordinates converges to a limit. We then observe that these limiting numbers describe an equivalence class (or a subset of an equivalence class) comprised of zero or one horizontal lines that lie either below the graph of X_t or above the graph of $C - Y_t$, and one or more incident vertical lines that lie between these graphs. Since x and y necessarily belong to this limiting equivalence class, we have $x \cong y$. □

Let $\widetilde{R}$ be the topological quotient $R/\cong$. Then we have the following:

Proposition 1.2. *The space $\widetilde{R}$ is a.s. topologically equivalent to the sphere $\mathbf{S}^2$. The map ϕ that sends t to the equivalence class containing (t, X_t) and $(t, C - Y_t)$ is a continuous surjective map from $[0, T]$ to $\widetilde{R}$.*

Proof. Let R' be obtained from R by identifying the outer boundary of R with a single point. Then R' is topologically a sphere, and $\cong$ induces a topologically closed relation on R'. The fact that $\widetilde{R}$ is topologically a sphere is immediate from the properties observed above and Proposition 1.3, stated just below. The continuity of ϕ is immediate from the fact that the quotient map from R to $\widetilde{R}$ is continuous. □

The following was established by R.L. Moore in 1925 [Moo25] (the formulation below is lifted from [Mil04]):

Proposition 1.3. *Let $\cong$ be any topologically closed equivalence relationship on the sphere $\mathbf{S}^2$. Assume that each equivalence class is connected, but is not the entire sphere. Then the quotient space $\mathbf{S}^2/\cong$ is itself homeomorphic to $\mathbf{S}^2$ if and only if no equivalence class separates the sphere into two or more connected components.*

If R_1 is the set of points in R on or under the graph of X, then $\widetilde{R}_1 = R_1/\cong$ is a random metric space called a *continuum random tree*, constructed and studied by Aldous in the early 1990's [Ald91a, Ald91b, Ald93]. Similarly, if R_2 is the set of points on or above the graph of $C - Y$, then $\widetilde{R}_2/\cong$ is another continuum random tree. Thus, $\widetilde{R}$ can be understood as a topological quotient of this pair of metric trees. We can define a measure ν on $\widetilde{R}$ by letting $\nu(A)$ be the Lebesgue measure of $\phi^{-1}(A)$. Observe that for Lebesgue almost all times t, the value $\phi^{-1}\big(\phi(t)\big)$ consists of the single point t. Thus ν is supported on points that are hit by the space-filling path exactly once. The set of double points (i.e., points in $\widetilde{R}$ hit twice by the path) a.s. has ν measure zero but is uncountable. The set of triple points (i.e. points in $\widetilde{R}$ hit three times by the path) a.s. has ν measure zero and is countable.

We next claim that given $\widetilde{R}$, ν, and ϕ (with the latter given only modulo monotone reparameterization), it is a.s. possible to reconstruct X_t and Y_t. We will not need this fact, but we nonetheless sketch the proof here. Observe first that we recover the parameterization of ϕ by requiring $\nu(\phi([0, t])) = t$. Second, given any t_0, the union of equivalence classes in R corresponding to $\phi([0, t_0])$ is given by the union of $[0, t_0] \times [0, C]$ and

1. all horizontal line segments with exactly one endpoint in $[0, t_0] \times [0, C]$.
2. all vertical segments that share an endpoint with one of these horizontal segments.

One may check that the complement of this set is connected and open, which implies that $\widetilde{R} \setminus \phi([0,t_0])$ is connected and open, hence homeomorphic to a disk. Moreover, the boundary of $\phi([0,t_0])$ consists of two arcs, separated from each other by $\phi(0)$ and $\phi(t_0)$, each corresponding to a branch of one of the two trees; the lengths of these arcs, which are given by X_t and Y_t, can then be determined as the $(1/2)$-Minkowski measure of the set of times $t > t_0$ at which these arcs are visited; this is related to the well known fact that the set of record times of a Brownian motion (i.e., the times at which a new positive value is reached for the first time) agrees in law with the set of zero times of a Brownian motion, and both of these sets have a natural *local time* structure (much more about Brownian motion local times can be found in the reference text [RY99]; see also [IM74, Section 2.2, 5) and 6)]).

Now observe the following:

Proposition 1.4. *The measure ν described above is a.s. non-atomic (i.e., assigns zero mass to each individual element of the sphere) and assigns positive measure to each non-empty open set of the sphere.*

Proof. If $x \in \widetilde{R}$ then $\phi^{-1}(x)$ consists of one, two or three points in $[0,T]$, hence has Lebesgue measure zero. If A is a non-empty open subset of $\widetilde{R}$, then since ϕ is continuous, we have that $\phi^{-1}(A)$ is a non-empty open subset of $[0,T]$, so the Lebesgue measure of $\phi^{-1}(A)$ is non-zero. □

A non-atomic measure on $\mathbf{S}^2$ that assigns positive mass to each open set is sometimes called a *good measure*. By the so-called von Neumann-Oxtoby-Ulam theorem, derived in 1941 [OU41] (and an extension in [Fat80], see also [MP83]), any topological sphere endowed with a good measure is isomorphic to any other topological sphere endowed with a good measure.

Proposition 1.5. *Suppose that μ and ν are two good measures on $\mathbf{S}^2$, both with total mass T. Then there exists a homeomorphism of $\mathbf{S}^2$ w.r.t. which the pullback of μ is ν.*

Let $\mathcal{G}_T$ denote the canonical (up to measure-preserving homeomorphism) good-measure endowed topological sphere. Proposition 1.5 implies that $\widetilde{R}$ is (as a good-measure endowed sphere) equivalent to $\mathcal{G}_T$. What makes $\widetilde{R}$ more interesting is that it comes with additional structure: namely, the space-filling path ϕ, which we call an *exploration structure* on $\mathcal{G}_T$. The pair $(\mathcal{G}_T, \phi)$ is what we call a *peanosphere*[3].

[3]This term emerged during a private discussion with Richard Kenyon, who also proposed that the term *peanofold* be used for variants of the peanosphere that are homeomorphic to the disk, or to higher genus surfaces. The term peanofold could also apply to analogous constructions in dimensions higher than two. It is an open question whether the construction presented in this

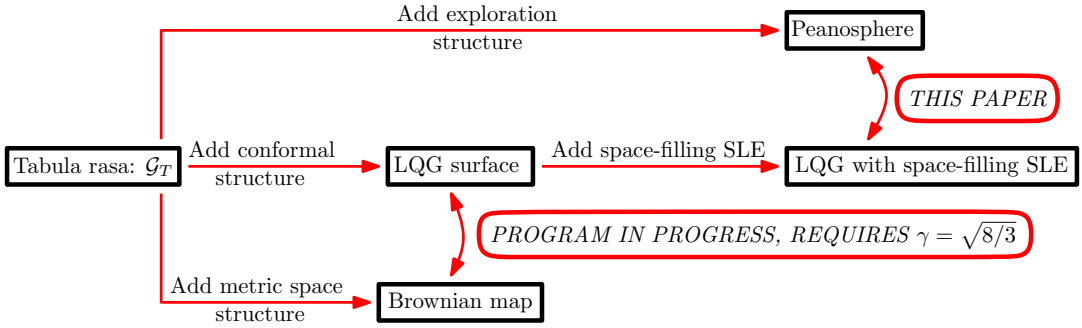

Figure 1.2: The two boxes on the right contain more information than the two in the middle column. As explained in Section 1.2, the objects on the right should be scaling limits of discrete models *decorated* by random statistical physics structure (such as an Ising spin or percolation cluster or spanning tree configuration) on top of the random planar map. The two objects in the center column (LQG surface and Brownian map) do not encode this extra decoration. The program to connect LQG surfaces (with $\gamma^2 = 8/3$) to the Brownian map has been partially begun and explained in [MS13b], has been advanced in [MS15c, MS15a, MS15b] and will be completed in [MS16a, MS16b].

Now let us make a couple of points about the role of the peanosphere in this paper. First, because it turns out to be simpler, we will work initially with a straightforward "infinite volume" variant of the peanosphere discussed above in which X_t and Y_t are Brownian motions indexed by all of $\mathbf{R}$.[4]

Second, throughout the remainder of this paper, we will actually work on a more general case in which (X_t, Y_t) is an affine transformation of a standard two dimensional Brownian motion such that

1. $X_t + Y_t$ is a standard Brownian motion,
2. $X_t - Y_t$ is an independent *constant multiple* of a standard Brownian motion.

section can be generalized to produce a three dimensional manifold as a topological quotient of three trees. Moore's theorem does not apply as generally as one might expect in higher dimensions (see [HR12] for a recent survey of what is and is not known to be true), and of course the Riemann mapping theorem fails in higher dimensions. However, the von Neumann-Oxtoby-Ulam theorem remains valid for compact manifolds in any dimension [Fat80].

[4]In this case, X_t and Y_t describe infinite-diameter CRTs, and the quotient is taken the same way as before. To clarify the construction, we note that we can draw it inside a finite rectangle as before if we rescale both time and space; if ϕ is a monotone continuous map from $\mathbf{R}$ onto $(0, 1)$, we can replace X_t and Y_t with $\widetilde{X}_t = \phi(X_{\phi^{-1}(t)})$ and $\widetilde{Y}_t = \widetilde{X}_t = \phi(X_{\phi^{-1}(t)})$, and then use $\widetilde{X}_t$ and $\widetilde{Y}_t$ in the construction described by Figure 1.1 to generate $\widetilde{R}$. The outer boundary of R again forms a single equivalence class, which corresponds to a "point at ∞" in the sense that every neighborhood of that point has infinite measure. It is straightforward to extend Proposition 1.2 to this setting.

The constant in question encodes how *correlated* the Brownian processes X_t and Y_t are with one another.[5] We remark that, as one may observe from Figure 1.1, replacing X_t and Y_t with aX_t and bY_t, where a and b are positive constants, does not actually affect the construction. Thus, if one assumes that (X_t, Y_t) is an affine transformation of a standard two dimensional Brownian motion, the correlation constant is the only parameter that is really relevant. Theorem 1.13 gives a relationship between this constant and the parameter $\kappa' = 16/\gamma^2$, a relationship proved to hold at least in the range $\kappa' \in (4, 8]$.

Using this generality, Figure 1.2 gives a sense of what will be accomplished in this paper, and how the corresponding peanospheres fit into the context of other objects the reader may have studied.[6] As suggested in Figure 1.2, we will show in this paper that an exploration structure on $\mathcal{G}_T$ actually determines a conformal structure on $\mathcal{G}_T$ in a natural way. Another way to say this is that we give a canonical way of defining a Brownian diffusion on the peanosphere. For us, "endowing $\widetilde{R}$ with a conformal structure" will mean explicitly embedding $\widetilde{R}$ in the complex sphere $\mathbf{C} \cup \{\infty\}$ and describing the corresponding measure and space-filling path on $\mathbf{C}$. The measure turns out to be Liouville quantum gravity with parameter $\gamma \in (0, 2)$ and the space-filling path is a form of the Schramm-Loewner evolution (SLE) with parameter $16/\gamma^2$. The parameter γ depends on the level of correlation between X_t and Y_t, and is $\sqrt{2}$ in the case of independent CRTs discussed above.

[5]The curious reader may try to repeat our proof of Proposition 1.2 in the setting where X_t and Y_t are correlated in this way. The key step is to show that, regardless of correlation constant, there is always a.s. some upper bound on the number of vertical line segments that can belong to a single $\cong$ equivalence class. Each of the countable set of equivalence classes that include local minima of X_t or Y_t involves exactly three vertical lines a.s., and other equivalence classes are alternating chains of vertical and horizontal line segments. One can use a "cone time" analysis following [Eva85] to derive an a.s. upper bound on the lengths of these chains. We will not give details of this argument here. Instead we note that this more general version of Proposition 1.2 will also follow as a consequence of our explicit embedding construction.

[6]We have *not* endowed a peanosphere with a non-trivial metric space structure, because we have not ruled out the possibility that the metric space quotient of $R/\cong$ is trivial (so that all points are distance zero from each other). Indeed, we believe that the metric space quotient actually *is* trivial but will not prove this here. The Brownian map is actually constructed in much the same way we constructed $\widetilde{R}$ above, except that while X_t is still taken to be a Brownian excursion, Y_t is defined using a Brownian motion indexed by the CRT that X_t describes. This guarantees that for every equivalence class containing a horizontal line segment below X_t, the points at the upper endpoints of the vertical lines in the equivalence class (points on the graph of $C - Y_t$) have the same y coordinates. In this case, one can start with the metric on the upper tree, take its quotient with respect to the induced equivalence on that tree, and note that the branches in the upper tree continue to be geodesics in the new quotient space (because the added equivalences introduce no shortcuts). Thus the quotient metric is a non-trivial metric on the corresponding topological quotient; this metric generates the spherical topology [LG07] and the two trees obtained correspond to the geodesic tree of the metric (rooted at a distinguished point in the sphere) and its planar dual.

Finally, let us stress that we will actually derive the upward direction of the double arrow in Figure 1.2 before the downward direction. That is, we proceed by studying SLE/LQG until we are able to show that an SLE/LQG pair encodes a pair of trees, each of which comes with a natural metric structure; then checking that the joint law of the pair of trees is the same as the law of the pair of CRTs discussed above; and only then showing *a posteriori* that the pair of CRTs almost surely determines the SLE/LQG structure in this construction.

1.2 Liouville quantum gravity as a scaling limit

In this section, we say more about how the result we began to describe in Section 1.1 fits into the context of Liouville quantum gravity, conformal loop ensembles, and random planar maps. As illustrated in Figure 1.3, this paper can be understood, in some sense, as a culmination of a multi-paper project aimed at establishing a connection between

1. random planar maps "decorated" by FK distinguished edge subsets (and the loops forming cluster/dual-cluster interfaces), and
2. Liouville quantum gravity (LQG) random surfaces "decorated" by independently sampled conformal loop ensembles (CLE).

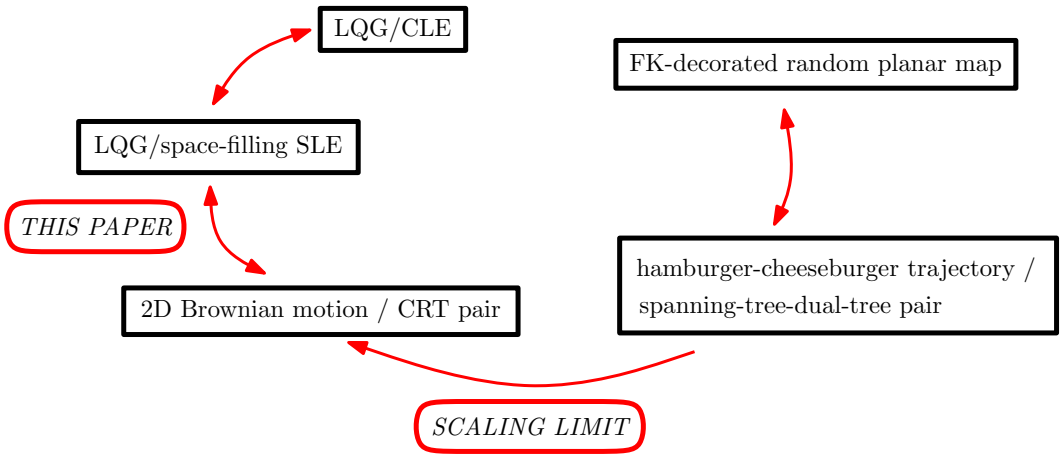

Figure 1.3: This paper focuses on the double arrow indicated above. The LQG/space-filling SLE box represents a space-filling $\mathrm{SLE}_{\kappa'}$ drawn on top of a γ-Liouville quantum gravity surface, where $\gamma \in (0,2)$, $\kappa' = 16/\kappa$, and $\kappa = \gamma^2$. The 2D Brownian motion/CRT pair box represents the coupled pair of CRTs described in Section 1.1.

This paper will focus narrowly on the double arrow of Figure 1.3 as the figure label indicates, and as was discussed in Section 1.1. We will not discuss the other arrows in Figure 1.3 outside of a few high level contextual remarks and references, which form the remainder of Section 1.2. The reader who prefers to focus on what is accomplished in this paper may skip these remarks and proceed directly to Section 1.3.

1. The double arrow on the right in Figure 1.3 is explained in detail in [She11]. In that paper, one considers a rooted planar map M with n edges, together with a distinguished subset E of those edges associated to the self-dual FK random cluster model with parameter q. The interfaces between clusters and dual clusters are understood as loops. Given an (M, E) pair, there is a canonical space-filling path that "explores" the loops, and also represents the interface between a special spanning tree T_1 and a special dual spanning tree T_2. The structure of these trees (and the way that they are "glued" together) is encoded by a walk in $\mathbf{Z}^2$, which is related in [She11] to a two-product LIFO (last in first out) inventory management ("hamburger-cheeseburger") model. The trees T_1 and T_2 arising in a computer simulation of this construction (together with the "space-filling loop" in between them) appear in Figures 1.4 and 1.5. These figures also illustrate a method of embedding the planar maps in the disk "conformally" using circle packing computed with [Ste10].

2. The "scaling limit" arrow in Figure 1.3 is also explained in [She11], where it is shown that the above mentioned walk in $\mathbf{Z}^2$ scales to a two-dimensional Brownian motion, with a diffusion rate depending on q.

3. The upper left double arrow in Figure 1.3 is explained in more detail in [She09] and [MS13a]. These works show that there is a space-filling variant of SLE_κ that "explores" the entire CLE_κ loop ensemble, and which may be understood as a continuum analog of the loop exploration path discussed in [She11]. In this context, the analog of the pair (T_1, T_2) discussed above is a pair $(\mathcal{T}_1, \mathcal{T}_2)$ of space-filling trees, which can be interpreted as flow-line and dual-flow-line trees within an "imaginary geometry" based on a Gaussian free field.

More references to the physics literature and discussion of the overall project are also found in [She11, She09, MS13a]. As discussed in [She11], the combination of the results summarized in Figure 1.3 implies that certain structures encoded by the discrete models, namely the trees (T_1, T_2), have scaling limits that agree in law with the analogous structures encoded by CLE-decorated LQG. Another way to state this fact is to say that CLE-decorated LQG is the scaling limit of FK-weighted random planar maps in a topology where two loop-decorated metric surfaces are considered

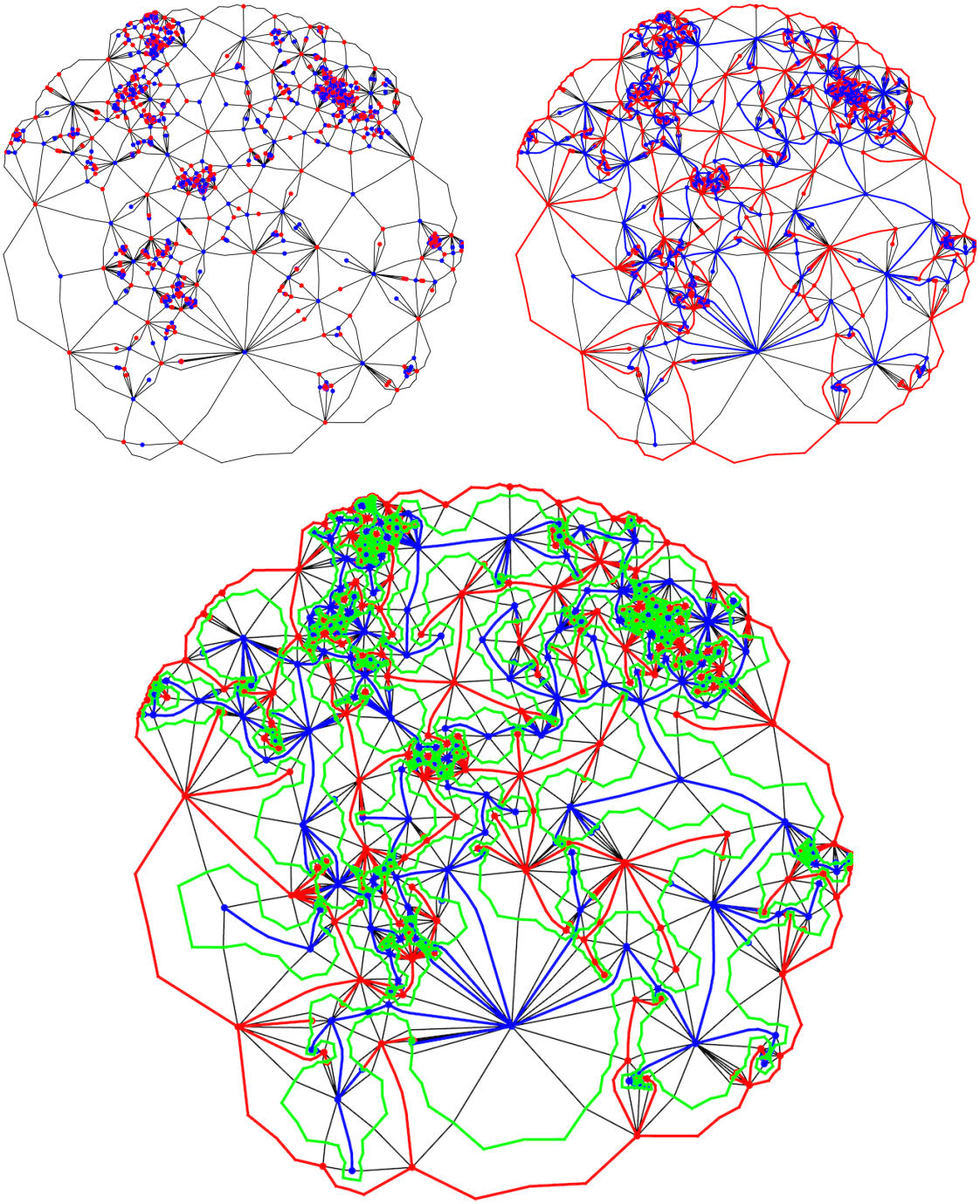

Figure 1.4: **Upper left:** random planar map sampled using the bijection from [She11] with $p = 0$ and embedded into $\mathbf{C}$ using [Ste10]. **Upper right:** same map with distinguished tree/dual tree pair. **Bottom:** map with path which snakes between the trees and visits all of the edges.

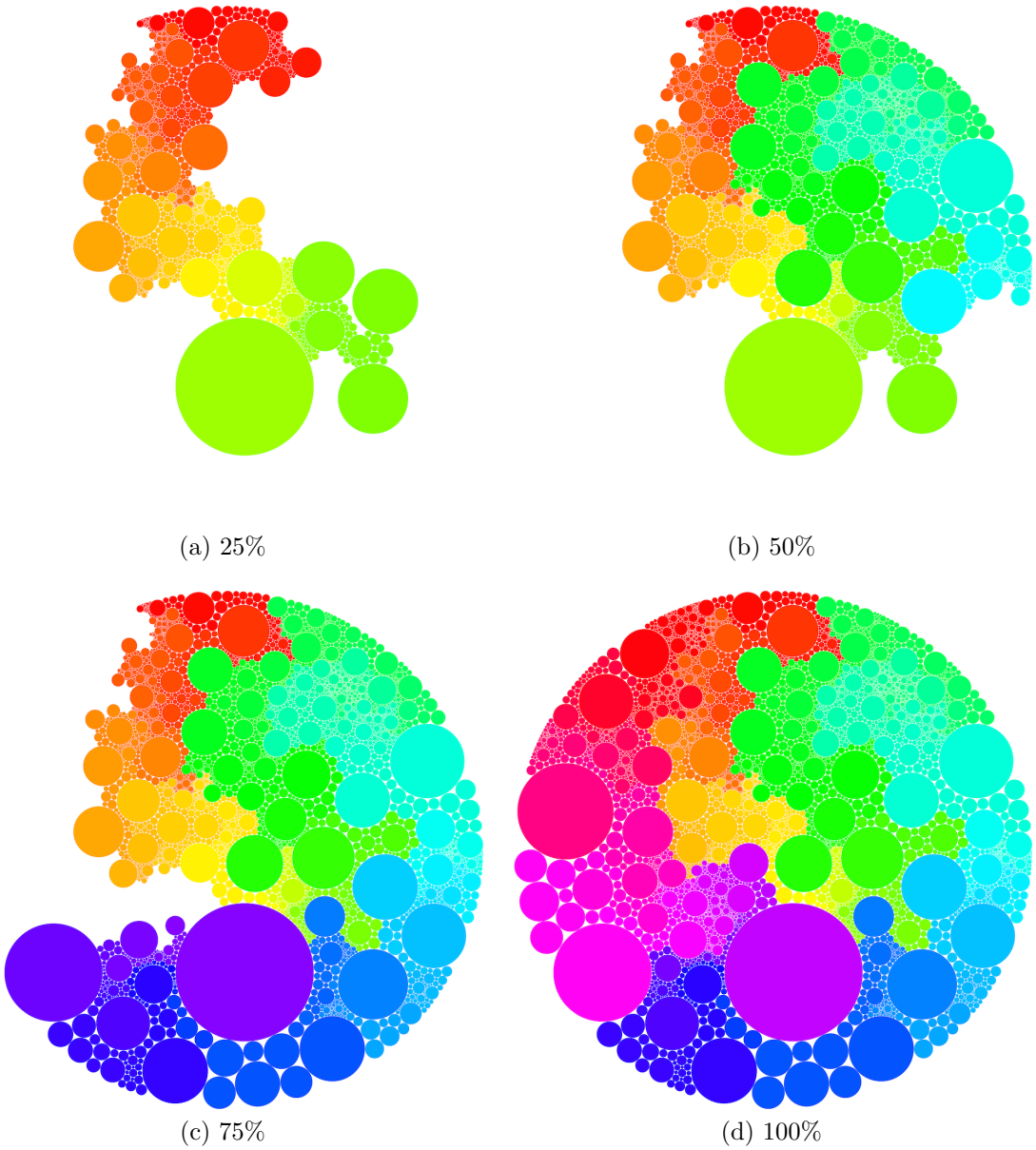

(a) 25%

(b) 50%

(c) 75%

(d) 100%

Figure 1.5: Shown is the circle packing associated with the map from Figure 1.4. The circles are colored according to the order in which they are visited by the space-filling path. The different panels show the circles visited by the path up to the first time that they cover 25%, 50%, 75%, and 100% of the total area.

close when their associated tree/dual-tree pairs are close as measure-endowed metric

spaces.[7]

1.3 Gluing trees of disks

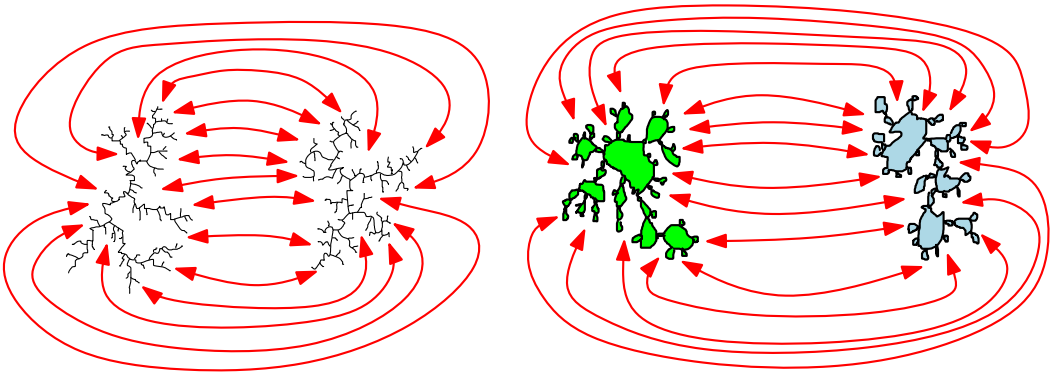

Figure 1.6: **Left:** If the two trees represented by the upper and lower graphs in Figure 1.1 are somehow embedded in the plane in a way that preserves the cyclic order around the tree (let us not worry about precisely how) then the vertical lines of Figure 1.1 correspond to the red lines shown, identifying points along one tree with points along the other. **Right:** Similar, but the trees are replaced with "trees of quantum disks", each somehow embedded in the plane (again, let us not worry about how). Both left and right identification procedures produce a topological sphere, which we embed canonically in $\mathbf{C} \cup \{\infty\}$. In both cases the cyclical ordering on the set of red lines describes a loop on the embedded sphere. In the left scenario, this loop is a space-filling form of $\mathrm{SLE}_{\kappa'}$, with $\kappa' > 4$. In the right scenario, it is a non-space-filling $\mathrm{SLE}_{\kappa'}$ with $\kappa' \in (4, 8)$.

Although we do not give any details in this subsection, we mention that we will also present another variant of the construction from Section 1.1 in which the CRTs represented by Figure 1.1 are replaced by "trees of quantum disks" that correspond to the so-called dual LQG surfaces and that can be obtained through a construction that assigns an independent disk to each jump of a stable Lévy excursion. The rough idea is illustrated in Figure 1.6 and Figure 1.7. (If we cut out the grey filled regions from one the trees in Figure 1.7, we obtain a tree of loops; this tree of loops was

[7]Readers familiar with SLE scaling limit results will recall that every statement of the form "these measures on discretized random paths converge to this measure on continuum random paths" is made w.r.t. to some topology on the set of measures. A standard approach is to begin with a topology on the set of paths themselves, and then consider the corresponding weak topology on the corresponding space of Borel measures. The choice of topology determines what properties of the paths we keep track of: whether the paths are treated as unparameterized paths, or natural-time-parameterized paths, or sets, or Loewner driving functions, etc.

also analyzed in the context of scaling limits of random planar maps in [CK13].) In some ways, this construction may seem more intuitive than the one from Section 1.1, since it produces a sphere as a quotient of objects that have non-empty interior to begin with. However, we will actually derive this construction as a consequence of the one described in Section 1.1, with $\kappa' \in (4, 8)$ taken to be the same value in the two pictures, as we explain in more detail in Section 1.7.

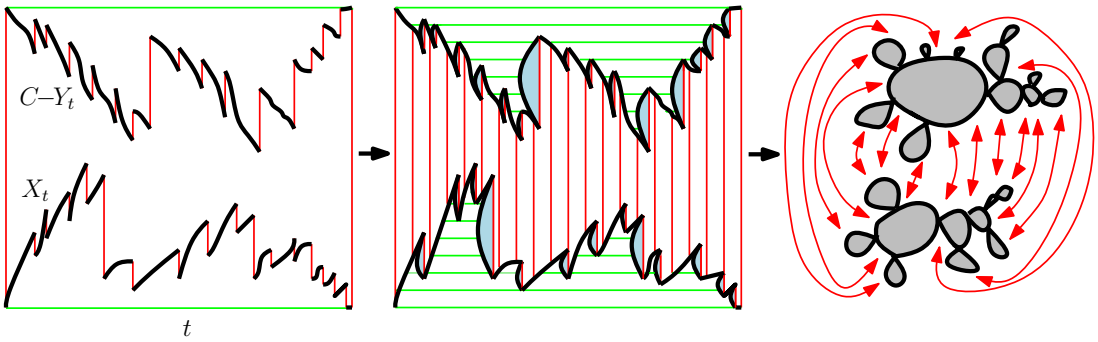

Figure 1.7: **Left:** X_t and Y_t are i.i.d. Lévy excursions, each with only negative jumps. Graphs of X_t and $C - Y_t$ are sketched; red segments indicate jumps. **Middle:** Add a black curve to the left of each jump, connecting its two endpoints; the precise form of the curve does not matter (as we care only about topology for now) but we insist that it intersect each horizontal line at most once and stay below the graph of X_t (or above the graph of $C - Y_t$) except at its endpoints. We also draw the vertical segments that connect one graph to another, as in Figure 1.1, declaring two points equivalent if they lie on the same such segment (or on the same jump segment). Shaded regions (one for each jump) are topological disks. **Right:** By collapsing green segments and red jump segments, one obtains two trees of disks with outer boundaries identified, as on the right side of Figure 1.6.

1.4 Quantum wedges, cones, disks, and spheres

A **quantum surface**, as in [DS11a, She10], is formally represented by a pair (D, h) where D is planar domain and h is an instance of (some form of) the Gaussian free field (GFF) on D. Intuitively, the quantum surface is the manifold conformally parameterized by D, with a metric tensor given by $e^{\gamma h(z)}$ times the Euclidean one, where $\gamma \in [0, 2)$ is a fixed constant. Since h is a distribution and not a function, this notion requires interpretation.

We can use a regularization procedure to define an area measure on D:

$$\mu = \mu_h := \lim_{\varepsilon \to 0} \varepsilon^{\gamma^2/2} e^{\gamma h_\varepsilon(z)} dz, \tag{1.1}$$

where dz is Lebesgue measure on D, $h_\varepsilon(z)$ is the mean value of h on the circle $\partial B(z,\epsilon)$ and the limit represents weak convergence in the space of measures on D. (The limit exists almost surely, at least if ε is restricted to powers of two [DS11a].) We interpret μ_h as the area measure of a random surface conformally parameterized by D. When $x \in \partial D$, we let $h_\varepsilon(x)$ be the mean value of h on $D \cap \partial B(x,\epsilon)$. Similarly, on a linear segment of ∂D, where h has free boundary conditions, we may define a boundary length measure by

$$\nu = \nu_h := \lim_{\varepsilon \to 0} \varepsilon^{\gamma^2/4} e^{\gamma h_\varepsilon(x)/2} dx, \tag{1.2}$$

where dx is Lebesgue measure on ∂D [DS11a].

One can parameterize the same quantum surface with a different domain $\widetilde{D}$, and our regularization procedure implies a simple rule for changing coordinates. Suppose that ψ is a conformal map from a domain $\widetilde{D}$ to D and write $\widetilde{h}$ for the distribution on $\widetilde{D}$ given by $h \circ \psi + Q \log |\psi'|$ where

$$Q := \frac{2}{\gamma} + \frac{\gamma}{2},$$

as in Figure 1.8. Then μ_h is almost surely the image under ψ of the measure $\mu_{\widetilde{h}}$. That is, $\mu_{\widetilde{h}}(A) = \mu_h(\psi(A))$ for $A \subseteq \widetilde{D}$. Similarly, ν_h is almost surely the image under ψ of the measure $\nu_{\widetilde{h}}$ in the case that ν_h and $\nu_{\widetilde{h}}$ are both defined and ψ extends to be a homeomorphism on the closure of the domain. In fact, [DS11a] formally defines a **quantum surface** to be an equivalence class of pairs (D,h) under the equivalence transformations (see Figure 1.8)

$$(D,h) \to \psi^{-1}(D,h) := (\psi^{-1}(D), h \circ \psi + Q \log |\psi'|) = (\widetilde{D}, \widetilde{h}), \tag{1.3}$$

noting that both area and boundary length are well-defined for such surfaces. The invariance of ν_h under (1.3) actually yields a definition of the quantum boundary length measure ν_h when the boundary of D is not piecewise linear—i.e., in this case, one simply maps to the upper half plane (or any other domain with a piecewise linear boundary) and computes the length there.

One can also define a **quantum surface with k marked points** to be an equivalence class of elements of the form $(D,h,x_1,x_2,\ldots,x_k)$, with each $x_i \in \overline{D}$, under maps of the form (1.3), where (1.3) is understood to map the $x_i \in \overline{D}$ to $\psi^{-1}(x_i)$.

We emphasize that the definition of equivalence for quantum surfaces does not require that D be simply connected or even connected.

Before we state our main results, we will first need to introduce certain types of random infinite LQG surfaces called *quantum wedges* and *quantum cones*, as defined in [She10]. Much of the paper will be concerned with studying the properties of

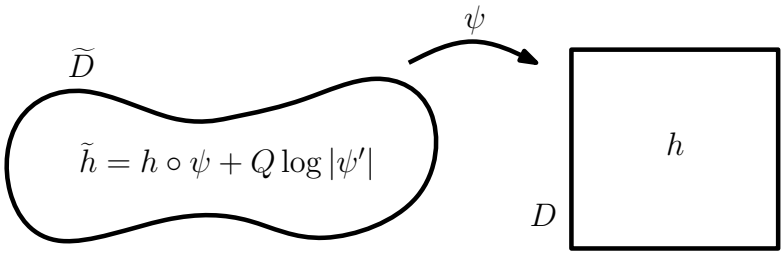

Figure 1.8: A quantum surface coordinate change.

these objects. The statement illustrated in Figure 1.3 will ultimately emerge as a consequence of this analysis. These objects are informally introduced in the present section; careful definitions are given in Section 4.

A quantum wedge is a kind of quantum surface, with two marked points, which we define below and discuss in more detail in Section 4. The two marked points divide the boundary of the quantum wedge into an infinite-length left boundary and an infinite-length right boundary, each isometric to $[0, \infty)$. It was shown in [She10] that if one glues (according to boundary length) the right boundary of one particular type of quantum wedge to the left boundary of a quantum wedge with the same law — and then conformally maps the combined surface to the complex upper half plane $\mathbf{H}$, then the image of the interface becomes an SLE curve. We generalize these results to different types of quantum wedges and to sequences of more than two independent quantum wedges. The interfaces one obtains from such weldings turn out to be closely related to the rays in the so-called "imaginary geometry" associated to a GFF [She10, MS12a, MS12b, MS12c, MS13a].

Before we define quantum wedges, let us give a closely related construction. We present below a list of three equivalent ways to parameterize a quantum surface (D, h) in which the h is only defined modulo a global additive constant (so that the surface is only defined modulo constant rescaling). We refer to the quantum surface described in the list below (defined modulo an additive constant for h) as an **unscaled quantum wedge**.

1. Let D be the infinite wedge $\mathbf{W}_\theta = \{z \in \mathbf{C} : \arg(z) \in [0, \theta]\}$ for some $\theta > 0$. Then take h to be an instance of the free boundary GFF on $\mathbf{W}_\theta$.

2. Parameterize instead by the upper half plane $\mathbf{H}$. If we conformally map $\mathbf{H}$ to $\mathbf{W}_\theta$ via the map $\psi_\theta(\widetilde{z}) = \widetilde{z}^{\theta/\pi}$, then the coordinate change rule (1.3) for quantum surfaces implies that we can represent this as $\widetilde{D} = \mathbf{H}$ and let $\widetilde{h}$ be an instance of the free boundary GFF on $\mathbf{H}$ *plus* the deterministic function $Q \log |\psi'_\theta|$, which up to additive constant is $Q \log |\widetilde{z}^{\theta/\pi - 1}| = Q(\frac{\theta}{\pi} - 1) \log |\widetilde{z}| = -\alpha \log |\widetilde{z}|$ for $\alpha := Q(1 - \theta/\pi)$.

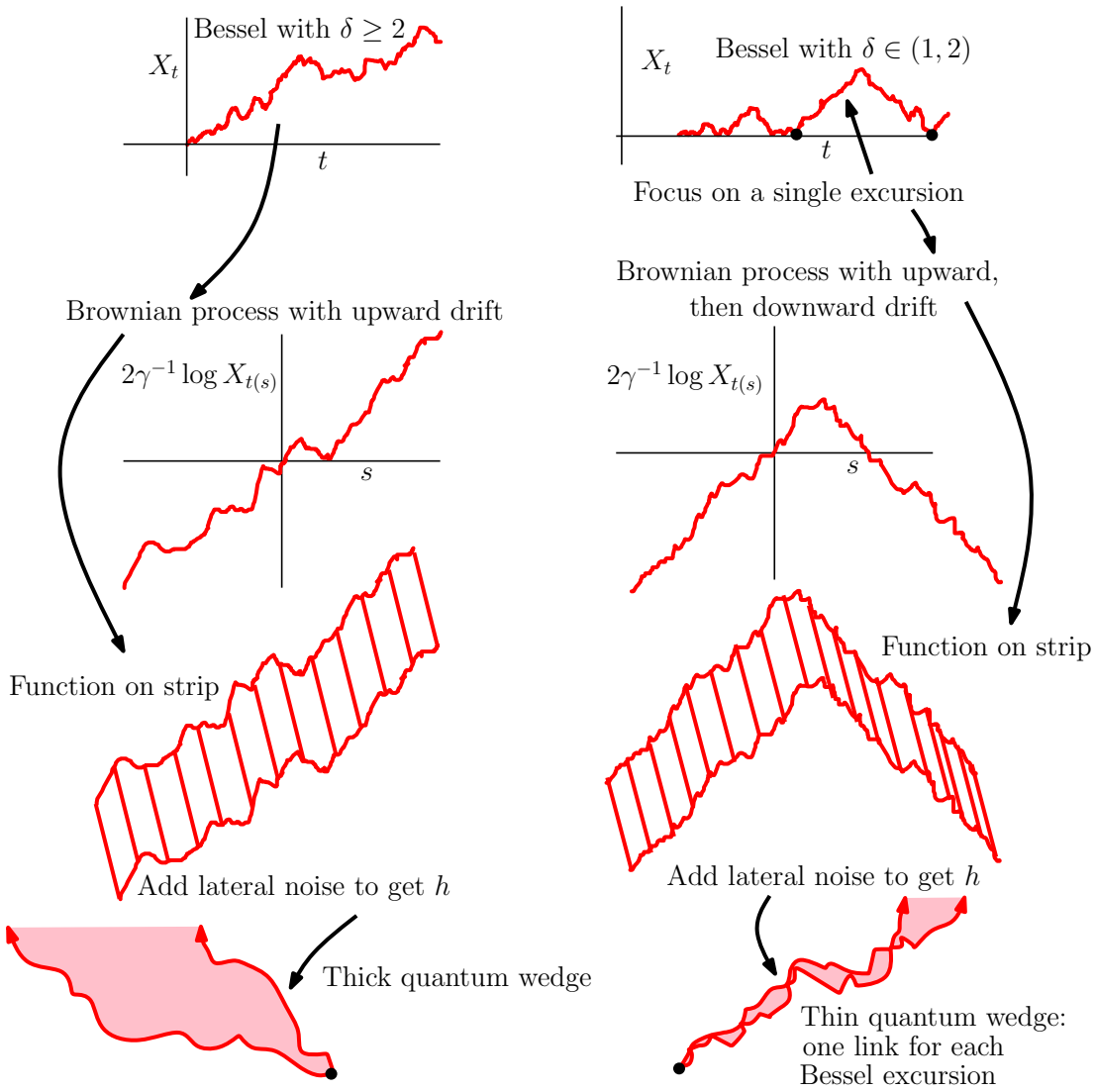

Figure 1.9: If X_t is a Bessel process with $\delta \geq 2$, then $2\gamma^{-1} \log X_t$ can be reparameterized to have quadratic variation $2du$ so that it evolves as $B_{2u} + au$ where B is a standard Brownian motion and a is a constant. The reparameterized graph is determined up to horizontal translation. When $\delta \in (1,2)$, the restriction of $2\gamma^{-1} \log X_t$ to a single Bessel excursion can be similarly reparameterized to obtain a Brownian process with a single maximum and a positive/negative drift on the left/right of that maximum (conditioned not to exceed the maximum); we obtain a map from the infinite strip $\mathcal{S} = \mathbf{R} \times [0, \pi]$ to $\mathbf{R}$ by applying this function to the first coordinate. After adding "lateral noise" obtained by $(\cdot,\cdot)_\nabla$-orthogonally projecting the free boundary GFF on $\mathcal{S}$ onto the subspace of functions with mean zero on all vertical segments, one obtains a field h. If $\delta \geq 2$ then $(\mathcal{S}, h)$ is a **thick quantum wedge**. If $\delta \in (1,2)$, one generates a quantum disk this way for each Bessel excursion, and the resulting chain is a **thin quantum wedge**.

3. Parameterize instead by the infinite strip $\mathcal{S} = \mathbf{R} \times [0, \pi]$. This can be mapped to $\mathbf{W}_\theta$ via the map $\phi_\theta(\widetilde{z}) = e^{(\theta/\pi)\widetilde{z}}$, and then the coordinate change rule (1.3) for quantum surfaces implies that we can represent the quantum surface by $\mathcal{S}$ using an instance of the free boundary GFF on $\mathcal{S}$ plus the deterministic function $Q \log |\phi'_\theta| = Q(\theta/\pi)\mathrm{Re}\,\widetilde{z} = (Q - \alpha)\mathrm{Re}\,\widetilde{z}$ (modulo additive constant).

The strip approach is convenient because it turns out that an instance of the free boundary GFF on $\mathcal{S}$ can be represented as $B_{2\mathrm{Re}\,z}$ (where B is standard Brownian motion defined up to additive constant — this function is constant on vertical line segments of the strip) plus a "lateral noise" given by the $(\cdot, \cdot)_\nabla$-orthogonal projection of the free boundary GFF on $\mathcal{S}$ onto the subspace of functions on $\mathcal{S}$ that have mean zero on each vertical segment (see Section 4.1.6). One obtains an unscaled quantum wedge by replacing B_{2t} with $B_{2t} + at$ where $a = Q - \alpha \geq 0$ (again defined modulo additive constant). We remark that the parameter space $\mathbf{W}_\theta$ is actually less convenient to work with than either the strip of the half plane, and it will not be used outside of this subsection. (Moreover, in the future, the parameter θ will be used for another purpose: namely, to describe an angle from the theory of imaginary geometry.)

A quantum wedge is the same as an unscaled quantum wedge except that B_t is replaced by a closely related process whose graph is defined modulo horizontal translation, instead of modulo vertical translation. One simple way to describe this process is to say that it is the log of a Bessel process (started at 0, with dimension $\delta = 2 + \frac{2}{\gamma}a$, with $\delta \geq 2$) parameterized to have quadratic variation $2du$ (see Figure 1.9). This process is essentially a Brownian motion with drift (as explained in Proposition 3.4) but the choice of how to translate the graph horizontally is somewhat arbitrary (and was chosen in Figure 1.9 to make the process reach 0 for the first time at time 0). In fact, if we use this approach, we can also consider Bessel processes of dimension $\delta \in (1, 2)$, and define a quantum surface for each component of the Bessel process, as illustrated in Figure 1.9.

The quantum surfaces obtained for $\delta \geq 2$, or equivalently, $\alpha \leq Q$, are called **thick quantum wedges**. A thick quantum wedge is a random quantum surface with two marked points (0 and ∞) whose law is invariant under constant rescalings. Each quantum wedge—when parameterized by $\mathcal{S}$ as discussed above—has an infinite amount of quantum mass, almost surely, but only a finite amount corresponding to any particular bounded subset of $\mathcal{S}$. (In particular, the law of a quantum wedge is not symmetric under reversing the two marked points, since every neighborhood of its second point has infinite mass, and this is not true of the first point.) A **thin quantum wedge**, obtained for $\delta \in (1, 2)$, or equivalently, $\alpha \in (Q, Q + \frac{\gamma}{2})$, is an infinite Poissonian "chain" (concatenation) of finite volume quantum surfaces, each with two marked boundary points; there is one quantum surface for each excursion of a Bessel process from 0, as Figure 1.9 illustrates. The thick-quantum wedge

condition $\alpha \leq Q$ corresponds in Liouville quantum theory to the so-called *Seiberg bound* [Sei90].[8]

	α	W	θ	δ	a	Δ
α	—	$\frac{\gamma}{2} + Q - \frac{1}{\gamma} W$	$\frac{\gamma}{2} + Q - \chi \frac{\theta}{\pi}$	$Q + \frac{\gamma}{2}(2 - \delta)$	$Q - a$	$\gamma(1 - \Delta)$
W	$\gamma(\frac{\gamma}{2} + Q - \alpha)$	—	$\chi\gamma \frac{\theta}{\pi}$	$\frac{\gamma^2}{2}(\delta - 1)$	$\gamma a + \frac{\gamma^2}{2}$	$2 + \gamma^2 \Delta$
θ	$\frac{\pi}{\chi}(\frac{\gamma}{2} + Q - \alpha)$	$\frac{\pi}{\chi\gamma} W$	—	$\frac{\pi\gamma}{2\chi}(\delta - 1)$	$\frac{\pi}{\chi}(a + \frac{\gamma}{2})$	$\frac{\pi}{\chi}(\frac{2}{\gamma} + \gamma\Delta)$
δ	$2 + \frac{2}{\gamma}(Q - \alpha)$	$1 + \frac{2}{\gamma^2} W$	$1 + \chi \frac{2}{\gamma} \frac{\theta}{\pi}$	—	$2 + \frac{2}{\gamma} a$	$2(\Delta + \frac{1}{\gamma} Q)$
a	$Q - \alpha$	$\frac{1}{\gamma} W - \frac{\gamma}{2}$	$\chi \frac{\theta}{\pi} - \frac{\gamma}{2}$	$\frac{\gamma}{2}(\delta - 2)$	—	$\chi + \gamma\Delta$
Δ	$1 - \frac{\alpha}{\gamma}$	$\frac{1}{\gamma^2}(W - 2)$	$\frac{\chi}{\gamma} \frac{\theta}{\pi} - \frac{2}{\gamma^2}$	$\frac{1}{2}\delta - \frac{1}{\gamma} Q$	$\frac{1}{\gamma}(a - \chi)$	—

Table 1.1: We can parameterize the space of **quantum wedges** using a number of different variables that are affine transformations of each other once γ is fixed. Shown are six such possibilities which are important for this article: multiple (α) of $-\log|\cdot|$ used when parameterizing by $\mathbf{H}$, weight (W), angle gap in imaginary geometry (θ), dimension of Bessel process (δ), drift for the corresponding Brownian motion (a) when parameterizing by the strip $\mathcal{S} = \mathbf{R} \times [0, \pi]$, and boundary quantum exponent at a quantum typical point in a fractal conditioned to intersect $\partial\mathbf{H}$ (Δ). (**Important:** The θ here is *not the same* as the one used to define $\mathbf{W}_\theta$ above.) Each element of the table gives the variable corresponding to the row as a function of the variable which corresponds to the column. Here, $Q = 2/\gamma + \gamma/2$ and $\chi = 2/\gamma - \gamma/2$ is a constant from imaginary geometry [MS12a, MS12b, MS12c, MS13a]. Recall that Theorem 1.9 gives the additivity of weights under the welding operation; by combining this with the table above, we can see how the other ways of parameterizing a wedge transform under the welding operation. In particular, the only other parameterization given above which is additive is θ.

We will assign a "weight" parameter to each quantum wedge and show that these weights are additive under gluing operations. In particular, a wedge of weight W can be produced by welding together n independent wedges of weight W/n. Taking the $n \to \infty$ limit, we will obtain a way to construct a wedge by gluing together countably many quantum surfaces that can in some sense be interpreted as wedges of weight zero. Explicitly, the **weight** of an α-quantum wedge is the number defined from α as follows:

$$W := \gamma\left(\gamma + \frac{2}{\gamma} - \alpha\right) = \gamma\left(\frac{\gamma}{2} + Q - \alpha\right). \tag{1.4}$$

[8] For an introduction, see, e.g., [GM93, DFGZJ95, Nak04]. The thin wedges correspond to values of α above this bound; however, as we shall see shortly, each of the concatenated finite volume quantum surfaces which form the thin wedge locally looks like an $\widetilde{\alpha}$-wedge with the reflected value $\widetilde{\alpha} = 2Q - \alpha$ near each of its endpoints, i.e., a thick wedge with $\widetilde{\alpha} \in (\frac{2}{\gamma}, Q)$.

	α	W	θ	δ	a	Δ
α	—	$Q - \frac{1}{2\gamma} W$	$Q - \chi \frac{\theta}{2\pi}$	$Q - \frac{\gamma}{4}(\delta - 2)$	$Q - a$	$\gamma(1 - \Delta)$
W	$2\gamma(Q - \alpha)$	—	$\gamma\chi \frac{\theta}{\pi}$	$\frac{\gamma^2}{2}(\delta - 2)$	$2a\gamma$	$\gamma^2(2\Delta - 1) + 4$
θ	$\frac{2\pi}{\chi}(Q - \alpha)$	$\frac{\pi}{\gamma\chi} W$	—	$\gamma \frac{\pi}{2\chi}(\delta - 2)$	$\frac{2\pi}{\chi} a$	$2\pi(1 + \frac{\gamma}{\chi}\Delta)$
δ	$2 + \frac{4}{\gamma}(Q - \alpha)$	$2 + \frac{2}{\gamma^2} W$	$2 + \chi \frac{2}{\gamma} \frac{\theta}{\pi}$	—	$2 + \frac{4}{\gamma} a$	$4\Delta + \frac{8}{\gamma^2}$
a	$Q - \alpha$	$\frac{1}{2\gamma} W$	$\chi \frac{\theta}{2\pi}$	$\frac{\gamma}{4}(\delta - 2)$	—	$\chi + \gamma\Delta$
Δ	$1 - \frac{\alpha}{\gamma}$	$\frac{1}{2} + \frac{1}{2\gamma^2}(W - 4)$	$\frac{\chi}{\gamma}(\frac{\theta}{2\pi} - 1)$	$\frac{1}{4}\delta - \frac{2}{\gamma^2}$	$\frac{1}{\gamma}(a - \chi)$	—

Table 1.2: As in the case of quantum wedges (Table 1.1), we can parameterize the space of **quantum cones** using a number of different variables. Shown are six such possibilities which are important for this article: multiple of $-\log|\cdot|$ (α) when parameterizing by $\mathbf{C}$, weight (W), "space of angles" in imaginary geometry (θ), dimension of Bessel process (δ), and drift for the corresponding Brownian motion (a) when parameterizing by the cylinder $\mathcal{Q} = \mathbf{R} \times [0, 2\pi]$ (with $\mathbf{R} \times \{0\}$ and $\mathbf{R} \times \{2\pi\}$ identified), and quantum exponent at a quantum typical point in a fractal in $\mathbf{H}$ (Δ). Each element of the table gives the variable corresponding to the row as a function of the variable which corresponds to the column. Here, $Q = 2/\gamma + \gamma/2$ and $\chi = 2/\gamma - \gamma/2$ is a constant from imaginary geometry [MS12a, MS12b, MS12c, MS13a].

We will usually describe an α-quantum wedge in terms of either α or its weight W depending on the context. Table 1.1 summarizes the relationships between several ways of parameterizing the space of wedges (all equivalent up to affine transformation, once γ is fixed). Two of these will be introduced at later points in this paper. We have already introduced α, W, δ, and a. The value Δ is a "quantum scaling exponent." It turns out that at a point conditioned to intersect a random fractal of quantum scaling exponent Δ (boundary or interior) in the KPZ framework, the surface typically has a logarithmic singularity or magnitude $\alpha = \gamma - \gamma\Delta$, see [DS11a, Equation (63)] and Section 2.3. The value θ is an imaginary geometry angle, see Proposition 8.14.

Taking $\alpha \leq Q$ corresponds to taking $W \geq \frac{\gamma^2}{2}$, which thus corresponds to a thick wedge. If we extend the formula relating W to α beyond this range, we find that taking $\alpha \in (Q, Q + \frac{\gamma}{2})$ formally corresponds to taking $W \in (0, \frac{\gamma^2}{2})$, which thus corresponds to a thin wedge.

For the reader who has read [She10], we briefly mention a few of the special wedge types discussed there:

1. Wedge obtained by zooming in at a boundary-measure-typical point: $\alpha = \gamma$, $W = 2$.
2. Wedge obtained by zooming in near the origin of a capacity invariant SLE_κ quantum zipper: $\alpha = -2/\gamma$, $W = 4 + \gamma^2$.

3. Wedge obtained by zooming in near the origin of a quantum-length invariant SLE_κ quantum zipper: $\alpha = -2/\gamma + \gamma$, $W = 4$.

We will indicate a quantum wedge $\mathcal{W}$ parameterized by D and described by a distribution h with the notation (D, h). If we also wish to emphasize the distinguished origin (say z_1) and ∞ (say z_2) we will denote the wedge by (D, h, z_1, z_2).

Roughly, an α-**quantum cone** is a quantum surface obtained by taking $e^{\gamma h(z)}dz$ where $\gamma \in (0, 2)$ is a fixed constant and h is an instance of the GFF on the infinite cone with opening angle θ, i.e. the surface that arises by starting with $\mathbf{W}_\theta$ and then identifying its left and right sides according to Lebesgue measure. Analogous to the case of a quantum wedge, by performing a change of coordinates via the map $\psi_\theta(\widetilde{z}) = \widetilde{z}^{\theta/2\pi}$ and applying (1.3), we can represent an unscaled quantum cone in terms of the sum of an instance $\widetilde{h}$ of the whole-plane GFF plus the deterministic function $-\alpha \log|\widetilde{z}|$ where $\alpha = Q(1 - \frac{\theta}{2\pi})$. A quantum cone can be defined formally and precisely using the analog of Figure 1.9 in which the strip is replaced by the cylinder, see Section 4. As in the case of quantum wedges, there are a number of different ways of parameterizing the space of quantum cones; see Table 1.2.

We define the **weight** W of an α-quantum cone to be the number

$$W := 2\gamma(Q - \alpha). \tag{1.5}$$

Theorem 1.12 below will show that one can "glue" the two sides of a weight W quantum wedge to obtain a weight W quantum cone.

As in the case of wedges, we will indicate a quantum cone $\mathcal{C}$ parameterized by a domain D and described by a distribution h with the notation (D, h). If we also wish to emphasize the distinguished origin (say z_1) and ∞ (say z_2) we will denote the cone by (D, h, z_1, z_2).

We conclude this subsection by pointing out that the Bessel process construction as described in Figure 1.9 gives us a way to define a family of natural *infinite* measures on the space of *finite*-volume quantum disks (or spheres). Recall that for any $\delta < 2$ (which corresponds to a slope $a < 0$) one can define the **Bessel excursion measure** $\nu_\delta^{\mathrm{BES}}$ (i.e., the Itô excursion measure associated with the excursions that a Bessel process makes from 0), which is an infinite measure on the space of continuous processes X_t indexed by $[0, T]$ (for some random T) satisfying $X_0 = X_T = 0$ and $X_t > 0$ for $t \in (0, T)$. The construction of this measure is recalled in Remark 3.7.

When $\delta \in (0, 2)$, one can consider a Bessel process X_t and let ℓ_t denote the local time the processes has spent at 0 between times 0 and t. If we parameterize time by the right-continuous inverse of ℓ_t, then the excursions appear as a Poisson point process (p.p.p.) on $\mathbf{R}_+ \times \mathcal{E}$ where $\mathcal{E}$ is the space of continuous functions $\phi\colon \mathbf{R}_+ \to \mathbf{R}_+$ such that $\phi(0) = 0$ and $\phi(t) = 0$ for all $t \geq T$, some T, and it is possible to recover

the Bessel process from the p.p.p. from concatenating the countable collection of excursions. When $\delta \leq 0$, the corresponding p.p.p. is still well-defined, but it a.s. assigns, to any finite time interval, a countable collection of excursions whose lengths sum to ∞ (so that it is not possible to define the reflecting Bessel process in the same way, essentially because there are "too many small excursions"). We will discuss all of these facts in more detail in Section 3.1 and Section 3.2.

Given any Bessel excursion measure $\nu_\delta^{\mathrm{BES}}$, with $\delta < 2$, one can construct a doubly marked quantum surface using the procedure described in Figure 1.9. Observe that this surface looks like a thick quantum wedge with a value given by $-a$ (or δ value given by $4 - \delta$) near each of the two endpoints.

This suggests a way of parameterizing the family of measures on disks (those induced by the measures $\nu_\delta^{\mathrm{BES}}$ and the procedure from Figure 1.9). We define a **quantum disk of weight** W to be a sample from the infinite measure $\mathcal{M}_W$ on quantum disks induced by $\nu_\delta^{\mathrm{BES}}$ with δ chosen so that surface looks like a quantum wedge of weight W near each of its two endpoints. We define parameters α and θ similarly. A similar procedure allows us to define a **quantum sphere of weight** W to be a sample from the infinite measure $\mathcal{N}_W$ on quantum spheres induced by $\nu_\delta^{\mathrm{BES}}$ with δ chosen so that the surface looks like a weight W quantum cone near each of its two endpoints. We similarly define the parameters α and θ for quantum disks/spheres to be those of the corresponding wedges/cones. (We will describe these constructions in more detail in Section 4.4.)

Note that by definition, a thin quantum wedge of weight W (recall that the wedge being thin means $W \in (0, \frac{\gamma^2}{2}), \alpha \in (Q, Q + \frac{\gamma}{2})$) is obtained as a Poissonian concatenation of disks of weight $\widetilde{W}$, where the a corresponding to W is -1 times the a corresponding to $\widetilde{W}$. That is, $\widetilde{W} = \gamma^2 - W$, and $\widetilde{\alpha} = 2Q - \alpha$ (Table 1.1). Thus, as mentioned in Footnote 8, these marked disks locally look like thick wedges near their marked points and obey the Seiberg bound, $\widetilde{\alpha} \leq Q$.

The measure $\mathcal{M}_W$ has special significance when $W = 2$ so that $\alpha = \gamma$ and $\theta = 2\pi/(2 - \frac{\gamma^2}{2})$. The measure $\mathcal{N}_W$ has special significance when $W = 4 - \gamma^2$, so that the cone value for α is γ and $\theta = 2\pi$. In these cases, the two marked points look like "typical" points chosen from the boundary or bulk quantum measures (see e.g., Lemma 5.6 and Lemma 5.9). We sometimes use the terms **quantum disk** or **quantum sphere** (without specifying weight) and the symbols $\mathcal{M}$ and $\mathcal{M}^c$ to denote samples from the infinite measures with these special weights. See Remark 3.7 at the end of Section 3.2 for additional detail on these constructions.

One may obtain a **unit boundary length quantum disk** by sampling from $\mathcal{M}$ conditioned to have total boundary length 1. (This is now a sample from a finite measure, which can be normalized to be a probability measure.) Similarly, a **unit area quantum disk** and **unit area quantum sphere** can respectively be defined

from $\mathcal{M}$ and $\mathcal{M}^c$ in a similar way. We define a quantum disk with an arbitrary fixed boundary length (or a quantum disk or quantum sphere with a fixed area) similarly. (Alternatively, a quantum disk with arbitrary boundary length can be defined by taking the unit boundary length quantum disk and then scaling it to have the given boundary length; the same is also true in the case of the disk or sphere with fixed area.)

1.5 Conformal structure and removability

As mentioned earlier, an LQG surface can be obtained by endowing a topological surface with both a good measure and a conformal structure in a random way. (And we can imagine that these two structures are added in either order.) Given two topological disks with boundary (each endowed with a good area measure in the interior, and a good length measure on the boundary) it is a simple matter to produce a new good-measure-endowed topological surface by taking a quotient that involves gluing (all or part of) the boundaries to each other in a boundary length preserving way.

The problem of *conformally welding* two surfaces is the problem of obtaining a conformal structure on the combined surface, given the conformal structure on the individual surfaces. (See, e.g., [Bis07] for further discussion and references.) This is closely related to the problem of defining a Brownian motion (up to monotone reparameterization) on the combined surface, given the definition of a Brownian motion on each of the individual pieces. We will now briefly (and somewhat informally) describe this connection. It is well known that a conformal structure and a choice of initial point determine a Brownian diffusion process β_t (up to monotone reparameterization). Similarly, if one is given the diffusion process (for all starting points), one can recover the conformal structure in a neighborhood of a point as follows: consider any Jordan curve surrounding that point, with three marked points on the curve dividing it into three segments E_1, E_2, E_3; then for each z in the region surrounded by the curve, consider the triple (p_1, p_2, p_3) where p_i for $i = 1, 2, 3$ is the probability that the Brownian motion starting from z first hits the curve along E_i. Note that $p_1 + p_2 = p_3 = 1$. One can then "conformally map" this region to a Euclidean triangle by sending each such z to the point in the triangle such that a standard two-dimensional Brownian motion from that point has probability p_i of first hitting the triangle boundary along the ith edge. The image of β_t in the triangle will then be two-dimensional Brownian motion (up to a time change).

This recipe can be carried out for any continuous diffusion process β_t to produce a map to the triangle; however it is not true that for all diffusion processes the image process in the triangle will be a standard Brownian motion. For example, it is necessary that the stationary measure for β_t (when one allows reflection at the

boundary) is a good measure, and that β_t is reversible with respect to this measure. The diffusions of *Brownian type* — i.e., diffusions that correspond to time-changed Brownian motions w.r.t. *some* conformal structure — are a rather special subset of the set of all of the continuous diffusion processes one might produce on a topological sphere. "Conformally welding" the two conformal surfaces is equivalent to producing a continuous diffusion process of Brownian type that agrees with the Brownian motions on the individual surfaces at times when it is away from the boundary interface. To make sense of this idea, we will draw from the theory of *removability sets*, as explained below.

A compact subset K of a domain $D \subseteq \mathbf{C}$ is called (conformally) **removable** if every homeomorphism from D to D that is conformal on $D \setminus K$ is also conformal on all of D. In probabilistic language, the fact that K is removable means that once we are given the Brownian motion behavior off K, there is — among all the possible ways of extending this process to a continuous diffusion on D, involving various types of local time pushes along K, etc. — only one of Brownian type. A Jordan domain $D \subseteq \mathbf{C}$ is said to be a **Hölder domain** if any conformal transformation from $\mathbf{D}$ to D is Hölder continuous all of the way up to $\partial\mathbf{D}$. It was shown by Jones and Smirnov [JS00] that if $K \subseteq D$ is the boundary of a Hölder domain, then K is removable; it is also noted there that if a compact set K is removable as a subset of D, then it is removable in any domain containing K, including all of $\mathbf{C}$. Thus, at least for compact sets K, one can speak of removability without specifying a particular domain D.

It was further shown by Rohde and Schramm [RS05] that the following is true. Suppose that $g_t \colon \mathbf{H} \setminus \eta([0,t]) \to \mathbf{H}$ is the forward Loewner flow associated with an SLE_κ curve with $\kappa < 4$. Then for each $t \geq 0$, the map g_t^{-1} is a.s. Hölder continuous. (A more general result, proved in a different way, which implies this is also given in [MS13b, Section 8.1].) If η is an SLE_κ in $\mathbf{H}$ from 0 to 1, then the union of η and its reflection across the real axis is the boundary of a bounded Hölder domain, hence is removable by [JS00]. It follows immediately that an SLE_κ path η from 0 to ∞ is removable in $\mathbf{H}$, and that $\eta([t_1, t_2])$ is removable for any $t_1 < t_2$. In fact, we can also say the following:

Proposition 1.6. *Suppose that η is an SLE_κ curve in $\mathbf{H}$ from 0 to 1 with $\kappa \in (0,4)$. Then it is a.s. the case that for a dense set of times $t_1 < t_2$ the segment $\eta([t_1,t_2])$ is removable in the domain $\mathbf{H} \setminus \eta\big([0,t_1] \cup [t_2,\infty]\big)$.*

Proof. As explained above, we already have the removability for the overall curve from 0 to 1. If we observe the path starting from 0 (up to any stopping time) and then observe the path from 1 (up to a reverse stopping time) then the conditional law of the remaining path is that of an SLE_κ in the remaining domain [Zha08, Dub09, MS12b], which implies the result. □

Proposition 1.6 also implies the removability of random paths η that look locally like SLE_κ, such as the $\mathrm{SLE}_\kappa(\rho)$ processes with $\rho > -2$ and flow lines of the GFF. To see why, observe that for any point z on such a path, one can find times t_1 and t_2 such that $z \in \eta([t_1, t_2])$ and $\eta([t_1, t_2])$ is removable in $\mathbf{H} \setminus \eta\big([0, t_1] \cup [t_2, \infty]\big)$. It thus follows that any homeomorphism ϕ which is conformal on the complement of η will also be conformal in a neighborhood containing $\eta((t_1, t_2))$. Since this holds for any z, we find that any such map must be conformal in a neighborhood every point on η, hence conformal everywhere.

To our knowledge, it is not known in general that the union of two (non-disjoint) removable sets is removable. However, this is not a problem when one of the sets is of SLE type:

Proposition 1.7. *Suppose that $\widetilde{\eta}$ is a random segment of an SLE_κ curve η with $\kappa \in (0, 4)$ and suppose that K is removable. Then $\widetilde{\eta} \cup K$ is a.s. removable.*

Proof. Let ϕ be any homeomorphism which is conformal off $\widetilde{\eta} \cup K$. Fix $z \in \widetilde{\eta} \setminus K$. By Proposition 1.6, we can find an interval (t_1, t_2) of time such that $z \in \eta((t_1, t_2))$, $\eta([t_1, t_2])$ is removable in $\mathbf{H} \setminus \eta\big([0, t_1] \cup [t_2, \infty]\big)$, and $\eta([t_1, t_2])$ is at a positive distance from K. From this one can easily see that $\eta([t_1, t_2])$ is removable in $\mathbf{H} \setminus \big(\eta\big([0, t_1] \cup [t_2, \infty]\big) \cup K\big)$ since K has positive distance from $\eta([t_1, t_2])$. It then follows that ϕ must be conformal in a neighborhood of z. Since $z \in \widetilde{\eta} \setminus K$ was arbitrary, we have that ϕ is conformal on the complement of K, hence conformal everywhere by the removability of K. □

A similar argument implies the following:

Proposition 1.8. *A finite union of $\mathrm{SLE}_\kappa(\rho)$ curves with $\kappa \in (0, 4)$ and $\rho > -2$ or GFF flow lines in $\mathbf{H}$ or $\mathbf{C}$ is a.s. removable. The same holds for an infinite collection of compact SLE_κ segments (coupled in some way) with the property that a.s. the set of accumulation points of these intervals (i.e., the set of points any neighborhood of which intersects infinitely many segments) is discrete.*

This implies in particular that flow lines of the GFF (whole plane SLE_κ processes started at interior points) are removable.

1.6 Welding and cutting quantum wedges and cones

The current subsection and Section 1.7 present several theorems involving the "gluing together" of infinite volume objects, including quantum wedges, infinite-volume continuum random trees (c.f. Section 1.1) and infinite-volume trees of disks (c.f. Section 1.3). We include the following chart (whose entries will all be explained

Theorem	Objects to be glued	New object/new interface
1.9, 1.11	W_1-wedge and W_2-wedge	(W_1+W_2)-wedge/$\mathrm{SLE}_\kappa(W_1-2; W_2-2)$
1.12	W-wedge, self	W-cone/whole-plane $\mathrm{SLE}_\kappa(W-2)$
1.13, 1.14	coupled pair of CRTs	$2\gamma\chi$-cone/space-filling $\mathrm{SLE}_{\kappa'}$
1.17	forested W_1-, W_2-wedges	$(W_1+\gamma\chi+W_2)$-wedge/$\mathrm{SLE}_{\kappa'}(\rho_1;\rho_2)$
1.18	bi-forested W-wedge, self	$(W+\gamma\chi)$-cone/whole-plane $\mathrm{SLE}_{\kappa'}(\rho)$

later) to help the reader keep track of some of these statements. In this chart, the parameters given for the quantum cones and wedges indicate *weight*.

Note that for cones, the weight $2\gamma\chi = 4-\gamma^2$ that appears in the third row corresponds to $\alpha = \gamma$ and $\theta = 2\pi$. The value $\gamma\chi$ that appears in the last two rows corresponds to $\theta = \pi$. The so-called "forested quantum wedges" are later introduced and explored through Theorems 1.16–1.18 and Corollary 1.20. These theorems describe the structure of the pair of trees of disks produced by cutting a quantum surface with a form of $\mathrm{SLE}_{\kappa'}$ with $\kappa' \in (4,8)$, which are then related to (an infinite time version of) the pair of Lévy processes described in Figure 1.7. The values of the ρ_i and ρ in the last two rows of the table appear in the theorem statements.

Our first main result describes the welding of wedges with general positive weights. (See Figure 1.10 and Figure 1.11 for illustrations.)

Theorem 1.9 (Welding and cutting for quantum wedges)**.** *Fix $\gamma \in (0,2)$ and choose a quantum wedge $\mathcal{W}$ of weight $W > 0$, represented by $(\mathbf{H}, h, 0, \infty)$. Suppose $W = W_1 + W_2 \geq \frac{\gamma^2}{2}$ for $W_1, W_2 > 0$ and then independently choose an $\mathrm{SLE}_\kappa(\rho_1;\rho_2)$, for $\rho_i = W_i - 2$ and $\kappa = \gamma^2 \in (0,4)$, from 0 to ∞ with force points located at 0^- and 0^+. Let D_1 and D_2 denote left and right components of $\mathbf{H} \setminus \eta$. Then the quantum surfaces $\mathcal{W}_1 = (D_1, h, 0, \infty)$ (with h restricted to D_1) and $\mathcal{W}_2 = (D_2, h, 0, \infty)$ (with h restricted to D_2) are independent. Moreover, each $\mathcal{W}_i$ has the law of a quantum wedge with weight W_i.*

In the case that $W \in (0, \frac{\gamma^2}{2})$, the same statement holds except we take η to be a concatenation of independent $\mathrm{SLE}_\kappa(\rho_1;\rho_2)$ processes (one from the opening point to the closing point of each of the beads of $\mathcal{W}$ with the force points located immediately to the left and right of the opening point) and we take D_1 (resp. D_2) to be the chain of surfaces which are to the left (resp. right) of η.

Remark 1.10. We remark that this "linearity of wedge weights under gluing" (which can be extended to multiple wedges, see Figure 1.11) is pre-figured by certain results on non-intersection exponents that have appeared in the physics and math literatures. For example, suppose that on a random infinite planar triangulation of the half plane, one starts n simple random walks at far away locations and conditions on having them all reach the same single boundary point without intersecting each

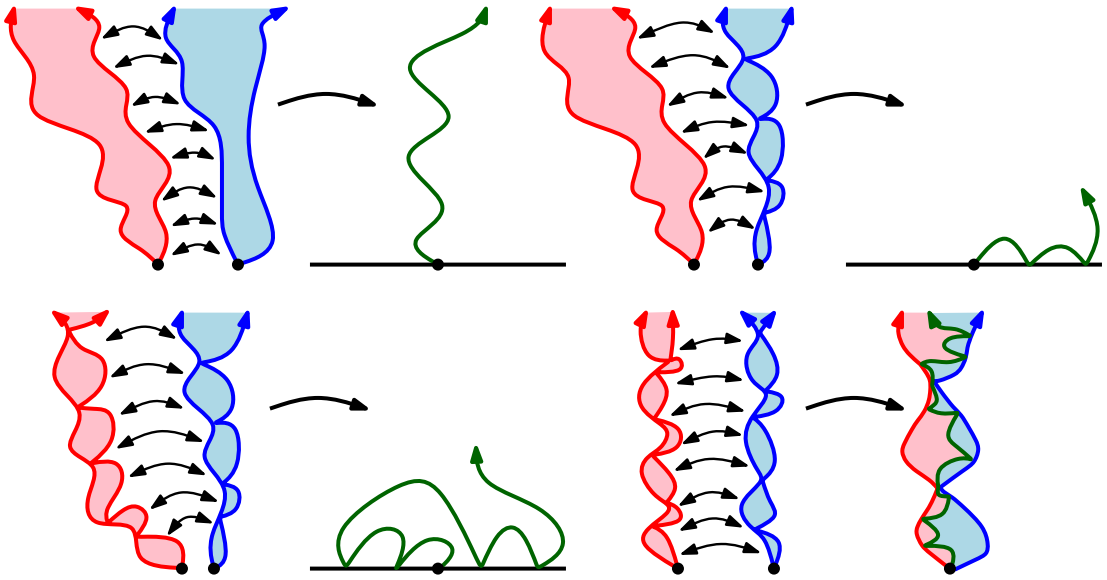

Figure 1.10: Suppose that $\mathcal{W}_1, \mathcal{W}_2$ are independent quantum wedges with respective weights $W_1, W_2 > 0$. Recall that if $W_i \geq \frac{\gamma^2}{2}$ then $\mathcal{W}_i$ is homeomorphic to $\mathbf{H}$ and if $W_i \in (0, \frac{\gamma^2}{2})$ then $\mathcal{W}_i$ consists of an ordered, countable sequence of beads each of which is topologically a disk. Illustrated are the four possible scenarios considered in Theorem 1.9. Let $W = W_1 + W_2$. **Top left:** $W_1, W_2 \geq \frac{\gamma^2}{2}$ so that both wedges are homeomorphic to $\mathbf{H}$. Their conformal welding is a wedge $\mathcal{W}$ of weight W and the interface between them is an $\mathrm{SLE}_\kappa(W_1 - 2; W_2 - 2)$ process independent of $\mathcal{W}$. **Top right:** The same is true if $W_1 \geq \frac{\gamma^2}{2}$, $W_2 \in (0, \frac{\gamma^2}{2})$. Since $W_2 \in (0, \frac{\gamma^2}{2})$, the interface intersects the right boundary of $\mathcal{W}$. **Bottom left:** The same is true if $W_1, W_2 \in (0, \frac{\gamma^2}{2})$ and $W \geq \frac{\gamma^2}{2}$. In this case, the interface intersects both the left and right boundaries of $\mathcal{W}$. **Bottom right:** If $W \in (0, \frac{\gamma^2}{2})$, the welding of $\mathcal{W}_1$ and $\mathcal{W}_2$ is still a wedge $\mathcal{W}$ of weight W. In this case, $\mathcal{W}$ is not homeomorphic to $\mathbf{H}$. Nevertheless, the interface between $\mathcal{W}_1$ and $\mathcal{W}_2$ is independently an $\mathrm{SLE}_\kappa(W_1 - 2; W_2 - 2)$ in each of the beads of $\mathcal{W}$.

other. One expects (as we will explain in Section 11) that the (infinite volume, fine mesh) scaling limit should consist of $(2n+1)$ independent quantum wedges, with n of them corresponding to a region between the left and right boundaries of a single path, and $n+1$ corresponding to a region between two paths, or between a path and the boundary. The $n+1$ of the latter type should all have weight 2 (essentially because this is the weight of a wedge obtained by zooming in at a "typical boundary measure" point, as mentioned above — see Section 11). The n wedges of the former type should all have some weight W_0 (which we do not specify for now). Thus the *total weight* of the wedge obtained by gluing these individual wedges

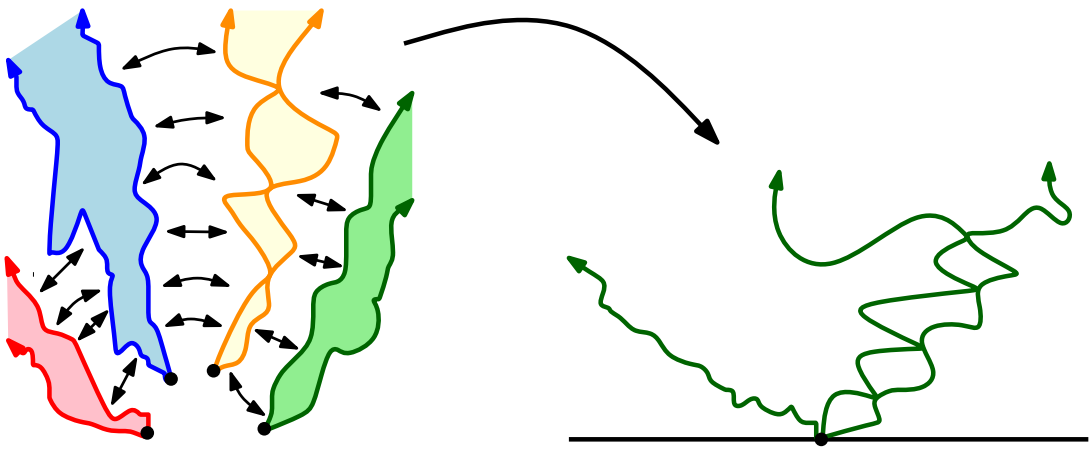

Figure 1.11: Four quantum wedges with respective weights $W_1, \dots, W_4$ conformally welded along their boundaries and conformally mapped to $\mathbf{H}$. By Proposition 8.14 (the generalization of Theorem 1.9 to the setting of a finite number of independent wedges), the resulting surface is a wedge of weight $W_1 + \cdots W_4$. In the illustration, $W_1, W_2, W_4 \geq \frac{\gamma^2}{2}$ and $W_3 \in (0, \frac{\gamma^2}{2})$. The images of the interfaces are coupled $\mathrm{SLE}_\kappa(\rho_1; \rho_2)$ processes, corresponding to rays in a so-called imaginary geometry [MS12a, MS12b, MS12c, MS13a]. Since $W_3 \in (0, \frac{\gamma^2}{2})$, the middle interface intersects the rightmost interface.

together should be $W = nW_0 + 2(n+1) = (W_0 + 2)n + 2$. In particular, this implies that $W - 2$ should be a linear function of n. Equivalently, if we take the formula $W = 2 + \gamma^2\Delta$ (from Table 1.1) this means that Δ (the so-called "boundary quantum scaling exponent" of the non-intersecting path event, see Section 11) is a linear function of n. The fact that this *should* be the case was predicted and advocated by the first co-author using properties of discrete quantum gravity models and discrete analogs of the wedge weldings discussed above [Dup98, Dup00, Dup04, Dup06]. The KPZ relation expresses that Euclidean exponents are given by a quadratic function of their quantum analogs. In particular, this suggests that an inverse quadratic function of the analogous Euclidean exponents should be a linear function of n; this latter fact was obtained (and termed the "cascade relation") in the rigorous work by Lawler and Werner on Brownian intersection exponents [LW99, LW00] (See Section 11.)

We also have the following:

Theorem 1.11. *In the construction of Theorem 1.9, both $\mathcal{W}$ and the interface η are uniquely determined by the $\mathcal{W}_i$ and may be obtained by a* conformal welding *of the right side of $\mathcal{W}_1$ with the left side of $\mathcal{W}_2$, where each is parameterized by γ-LQG boundary length.*

We will not give a separate proof of Theorem 1.11 since it follows from the same argument used to prove [She10, Theorems 1.3, 1.4] and the removability results described in Section 1.5. (The proof of [She10, Theorem 1.4] is given in [She10, Section 1.4].)

As mentioned briefly above, there is a natural generalization of Theorem 1.9 in which one cuts a quantum wedge $\mathcal{W}$ with n SLE processes (as opposed to cutting with a single path) coupled together as flow lines with varying angles of a GFF [MS12a, MS12b, MS12c, MS13a] which is independent of $\mathcal{W}$. In this case, one obtains $n+1$ independent wedges and the sum of their weights is equal to the weight of $\mathcal{W}$. This result is illustrated in Figure 1.11 and is stated precisely in Proposition 8.14. If one lets the number of paths tend to ∞ (with the spacing between the angles going to zero), then the collection of paths converges to the so-called **fan F**. (See Figures 1.2–1.5 of [MS12a] for simulations of **F**.) This is a random closed set which almost surely has zero Lebesgue measure [MS12a, Proposition 7.33]. As a consequence of Proposition 8.14, we are able to deduce (Theorem 8.17) an exact Poissonian structure of the countable collection of surface "beads" parameterized by the complement of **F**. In particular, we can interpret **F** as describing the interface that arises when one glues together a Poissonian collection of wedges with weight 0.

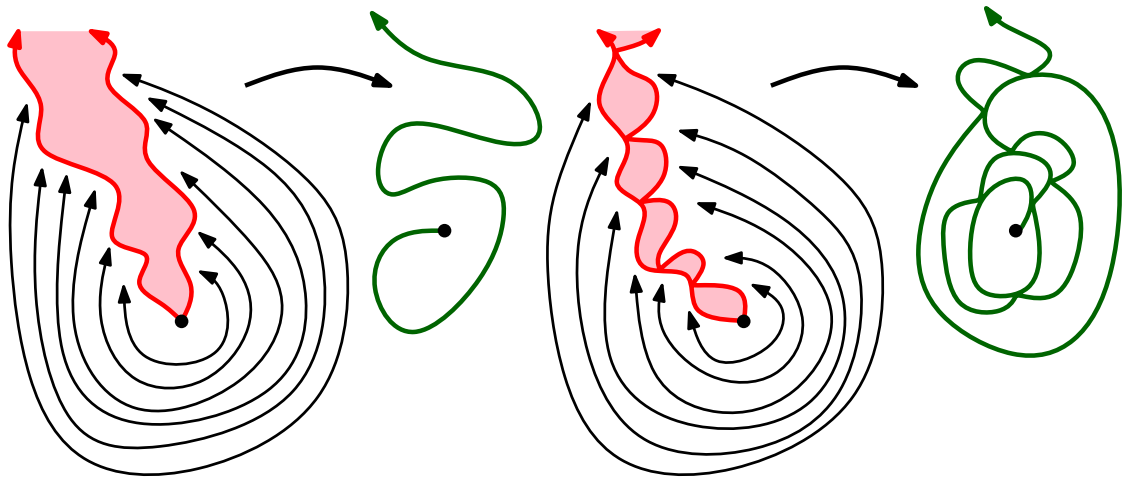

Figure 1.12: Illustration of Theorem 1.12. **Left:** A quantum wedge of weight $W \geq \frac{\gamma^2}{2}$ (hence homeomorphic to **H**). If we weld together its left and right sides according to γ-LQG boundary length, then the resulting surface is a quantum cone of the same weight W (right side) decorated with an independent whole-plane $\mathrm{SLE}_\kappa(W-2)$ process. **Right:** The same statement holds in the case that $W \in (0, \frac{\gamma^2}{2})$ so that the wedge is not homeomorphic to **H** but rather is given by a Poissonian sequence of disks; in this case, $W-2 \in (-2, \frac{\kappa}{2}-2)$ so that the $\mathrm{SLE}_\kappa(W-2)$ process is self-intersecting.

	α	W	θ	δ	a
α'	$\frac{1}{2}\alpha + \frac{1}{\gamma}$	$Q - \frac{1}{2\gamma}W$	$Q - \chi\frac{\theta}{2\pi}$	$Q + \frac{\gamma}{4}(1-\delta)$	$Q - \frac{\gamma}{4} - \frac{1}{2}a$
θ'	$\frac{\pi}{\chi}(\frac{\gamma}{2} + Q - \alpha)$	$\frac{\pi}{\chi\gamma}W$	θ	$\frac{\pi\gamma}{2\chi}(\delta - 1)$	$\frac{\pi}{\chi}(a + \frac{\gamma}{2})$
δ'	$3 + \frac{2}{\gamma}(Q - \alpha)$	$2 + \frac{2}{\gamma^2}W$	$2 + \chi\frac{2}{\gamma}\frac{\theta}{\pi}$	$\delta + 1$	$3 + \frac{2}{\gamma}a$
a'	$Q - \frac{1}{\gamma} - \frac{1}{2}\alpha$	$\frac{1}{2\gamma}W$	$\chi\frac{\theta}{2\pi}$	$\frac{\gamma}{4}(\delta - 1)$	$\frac{\gamma}{4} + \frac{1}{2}a$
ρ'	$\gamma^2 - \alpha\gamma$	$W - 2$	$\chi\gamma\frac{\theta}{\pi} - 2$	$\frac{\gamma^2}{2}(\delta - 1) - 2$	$\gamma a + \frac{\gamma^2}{2} - 2$

(a) Conversion from wedge to cone parameterizations when zipping up a quantum wedge to obtain a quantum cone.

	α'	θ'	δ'	a'	ρ'
α	$2\alpha' - \frac{2}{\gamma}$	$Q + \frac{\gamma}{2} - \chi\frac{\theta'}{\pi}$	$Q + \frac{\gamma}{2}(3 - \delta')$	$Q + \frac{\gamma}{2} - 2a'$	$\gamma - \frac{1}{\gamma}\rho'$
W	$2\gamma(Q - \alpha')$	$\gamma\chi\frac{\theta'}{\pi}$	$\frac{\gamma^2}{2}(\delta' - 2)$	$2\gamma a'$	$2 + \rho'$
θ	$\frac{2\pi}{\chi}(Q - \alpha')$	θ'	$\frac{\pi\gamma}{2\chi}(\delta' - 2)$	$\frac{2\pi}{\chi}a'$	$\frac{\pi}{\chi\gamma}(\rho' + 2)$
δ	$1 + \frac{4}{\gamma}(Q - \alpha')$	$1 + \chi\frac{2}{\gamma}\frac{\theta'}{\pi}$	$\delta' - 1$	$1 + \frac{4}{\gamma}a'$	$1 + \frac{2}{\gamma^2}(\rho' + 2)$
a	$\frac{2}{\gamma} + Q - 2\alpha'$	$\chi\frac{\theta'}{\pi} - \frac{\gamma}{2}$	$\frac{\gamma}{2}(\delta' - 3)$	$2a' - \frac{\gamma}{2}$	$\frac{1}{\gamma}(\rho' + 2) - \frac{\gamma}{2}$

(b) Conversion from cone to wedge parameterizations when cutting a quantum cone to obtain a quantum wedge.

Table 1.3: If we zip up the left and right sides of a quantum wedge according to γ-LQG boundary length, then by Theorem 1.12 we get a quantum cone decorated with an independent whole-plane $\mathrm{SLE}_\kappa(\rho)$ process, and, conversely, if we cut a quantum cone with an independent whole-plane $\mathrm{SLE}_\kappa(\rho)$ then we get a quantum wedge. **a)** Each of the entries in the first row gives a way of parameterizing the wedge and each entry in the first column gives a way of parameterizing the resulting cone. The variable ρ' refers to the ρ-value for the whole-plane $\mathrm{SLE}_\kappa(\rho)$ process which is the image of $\mathbf{R}$ under the zipping up map. Each entry of the table gives the type of cone that one gets by zipping up a wedge where the cone is described using the parameterization corresponding to the row of the entry and the wedge is described using the parameterization of the column of the entry. Note that the row corresponding to θ' is identical to the row corresponding to θ in Table 1.1. This follows because the "space of angles" in the imaginary geometry for a given wedge does not change under the zipping up operation. **b)** Each entry of the table gives the type of wedge one gets by cutting a cone with an appropriate SLE process where the cone is described using the parameterization from the column and the wedge is parameterized using the variable from the corresponding row.

Our next main result implies that a quantum cone can be constructed by identifying the left and right sides of a quantum wedge according to γ-LQG boundary length.

Theorem 1.12 (Welding and cutting for quantum cones)**.** *Fix $\gamma \in (0, 2)$, let*

$\kappa = \gamma^2 \in (0,4)$, and suppose that $\mathcal{C} = (\mathbf{C}, h, 0, \infty)$ is a quantum cone of weight $W > 0$. Let $\rho = W - 2$ and suppose that η is a whole-plane $\mathrm{SLE}_\kappa(\rho)$ process independent of $\mathcal{C}$ starting from 0. Then the quantum surface $\mathcal{W}$ described by $(\mathbf{C} \setminus \eta, h, 0, \infty)$ is a quantum wedge of weight W. Moreover, the pair consisting of $\mathcal{C}$ and η is almost surely determined by $\mathcal{W}$ and can be obtained by conformally welding the left boundary of $\mathcal{W}$ with its right boundary according to γ-LQG boundary length.

See Figure 1.12 for an illustration of Theorem 1.12. This result is stated in the case of simple $\mathrm{SLE}_\kappa(\rho)$ processes ($W \geq \frac{\gamma^2}{2}$ so that $\rho \geq \frac{\kappa}{2} - 2$) in Proposition 8.7 and in the case of self-intersecting $\mathrm{SLE}_\kappa(\rho)$ processes ($W \in (0, \frac{\gamma^2}{2})$ so that $\rho \in (-2, \frac{\kappa}{2} - 2)$) in Proposition 8.15. Moreover, in Proposition 8.16 it is explained that slicing a quantum cone with a collection of whole-plane $\mathrm{SLE}_\kappa(\rho)$ processes coupled together as flow lines of a whole-plane GFF starting from the origin [MS13a] yields a collection of independent wedges.

If we parameterize our cone in terms of α rather than W, then it follows from (1.5) that the value of ρ from Theorem 1.12 is given by

$$\rho = 2 + \gamma^2 - 2\alpha\gamma. \tag{1.6}$$

Theorem 1.12 combined with (1.4) and (1.5) tells us that zipping up the left and right sides of an α'-quantum wedge yields an α-quantum cone with

$$\alpha = \frac{\alpha'}{2} + \frac{1}{\gamma}. \tag{1.7}$$

See Table 1.3 for the conversion between several parameterizations for quantum wedges and cones when performing the welding or cutting operation from Theorem 1.12.

1.7 Matings of trees and trees of loops

1.7.1 Main result on gluing infinite volume CRTs

In this section, we describe in much greater detail the manner in which the Brownian motion pair (X_t, Y_t), as discussed in Section 1.1, encodes various objects within LQG and SLE. Here and throughout much of the rest of the paper, we will use the symbols (L_t, R_t) in place of (X_t, Y_t) in order to highlight the fact that (as we will explain) in many circumstances, L_t and R_t can be interpreted as left and right boundary lengths of the quantum surface parameterized by $\{s : s \leq t\}$, or of the quantum surface parameterized by $\{s : s \geq t\}$. We include many figures (Figures 1.13–1.22) which illustrate our most fundamental infinite volume peanosphere construction, as stated in Theorem 1.13 and Theorem 1.14 below.

Recall that space-filling $\mathrm{SLE}_{\kappa'}$ for $\kappa' \in (4,8)$ is a variant of $\mathrm{SLE}_{\kappa'}$ which fills up the components that it separates from its target point. This process was first constructed and analyzed in [MS13a]. Space-filling $\mathrm{SLE}_{\kappa'}$ for $\kappa' \geq 8$ is the same as ordinary $\mathrm{SLE}_{\kappa'}$. A precise definition of space-filling $\mathrm{SLE}_{\kappa'}$ is given in [MS13a, Section 1.2.3]; see in particular [MS13a, Figure 1.16] and the surrounding text. Many of the important properties of space-filling $\mathrm{SLE}_{\kappa'}$ are also established in [MS13a] (existence, continuity, reversibility, and its relationship to $\mathrm{CLE}_{\kappa'}$). It is also explained in [MS13a] how space-filling $\mathrm{SLE}_{\kappa'}$ can be interpreted as tracing (clockwise or counterclockwise) the outside of a (space-filling) "flow line tree" corresponding to a given instance of the Gaussian free field. In particular, if one considers the whole-plane GFF, then the corresponding path is what we will call a **whole-plane space-filling** $\mathrm{SLE}_{\kappa'}$ **from** ∞ **to** ∞.[9] Given this structure, one can also recover the non-space-filling $\mathrm{SLE}_{\kappa'}$ curves, which are called **counterflow lines** in [MS12a, MS12b, MS12c, MS13a] and studied in detail there. Theorem 1.13 describes the evolution of the left and right boundaries of a whole-plane space-filling $\mathrm{SLE}_{\kappa'}$ from ∞ to ∞ drawn on top of a quantum cone (see Figure 1.13).

Theorem 1.13. *Let $\mathcal{C} = (\mathbf{C}, h, 0, \infty)$ be a γ-quantum cone (which corresponds to $W = 4 - \gamma^2$ and $\theta = 2\pi$) together with a space-filling $\mathrm{SLE}_{\kappa'}$ process η' from ∞ to ∞ sampled independently of $\mathcal{C}$ and then reparameterized according to γ-LQG area. That is, for $s, t \in \mathbf{R}$ with $s < t$ we have that $\mu_h(\eta'([s,t])) = t - s$. Let L_t (resp. R_t) denote the change in the length of the left (resp. right) boundary of η' relative to time 0. Then (L, R) evolves as a two-dimensional Brownian motion. In the case that $\kappa' \in (4,8]$, we have (up to a non-random linear reparameterization of time) that*

$$\mathrm{var}(L_t) = t, \quad \mathrm{var}(R_t) = t, \quad \text{and} \quad \mathrm{cov}(L_t, R_t) = -\cos\left(\frac{4\pi}{\kappa'}\right) t \geq 0 \quad \text{for} \quad t \geq 0.$$

Moreover, the joint law of (h, η') is invariant under shifting by t units of (γ-LQG area) time and then recentering. That is, for each $t \in \mathbf{R}$ we have that

$$(h, \eta') \overset{d}{=} (h(\cdot - \eta'(t)), \eta'(\cdot - t) - \eta'(t)). \tag{1.8}$$

Finally, the quantum surfaces parameterized by $\eta'([0,\infty])$ and $\eta'([-\infty, 0])$ are independent quantum wedges, each with parameter $\theta = \pi$, and $W = 2 - \frac{\gamma^2}{2}$.

[9] The chordal version of space-filling $\mathrm{SLE}_{\kappa'}$ (i.e., in $\mathbf{H}$ from 0 to ∞) is discussed in detail in [MS13a]. The whole-plane version from ∞ to ∞ is not explicitly constructed and shown to be continuous in [MS13a]. However, it can be easily be constructed and shown to be continuous using chordal space-filling $\mathrm{SLE}_{\kappa'}$. To accomplish this, one first starts flow and dual flow lines of a whole-plane GFF starting from 0. If $\kappa' \geq 8$, these flow lines will partition space into two regions which are each homeomorphic to $\mathbf{H}$. In this case, a whole-plane space-filling $\mathrm{SLE}_{\kappa'}$ from ∞ to ∞ can be constructed by splicing together two chordal space-filling $\mathrm{SLE}_{\kappa'}$'s, one for each of the two regions. The first path is taken to run from ∞ to 0 and the second from 0 to ∞. If $\kappa' \in (4,8)$, then the flow and dual flow lines started from 0 will partition space into a countable collection of pockets. In this case, a whole-plane space-filling $\mathrm{SLE}_{\kappa'}$ from ∞ to ∞ can be constructed by splicing together a countable collection of chordal space-filling $\mathrm{SLE}_{\kappa'}$'s, one for each of the pockets.

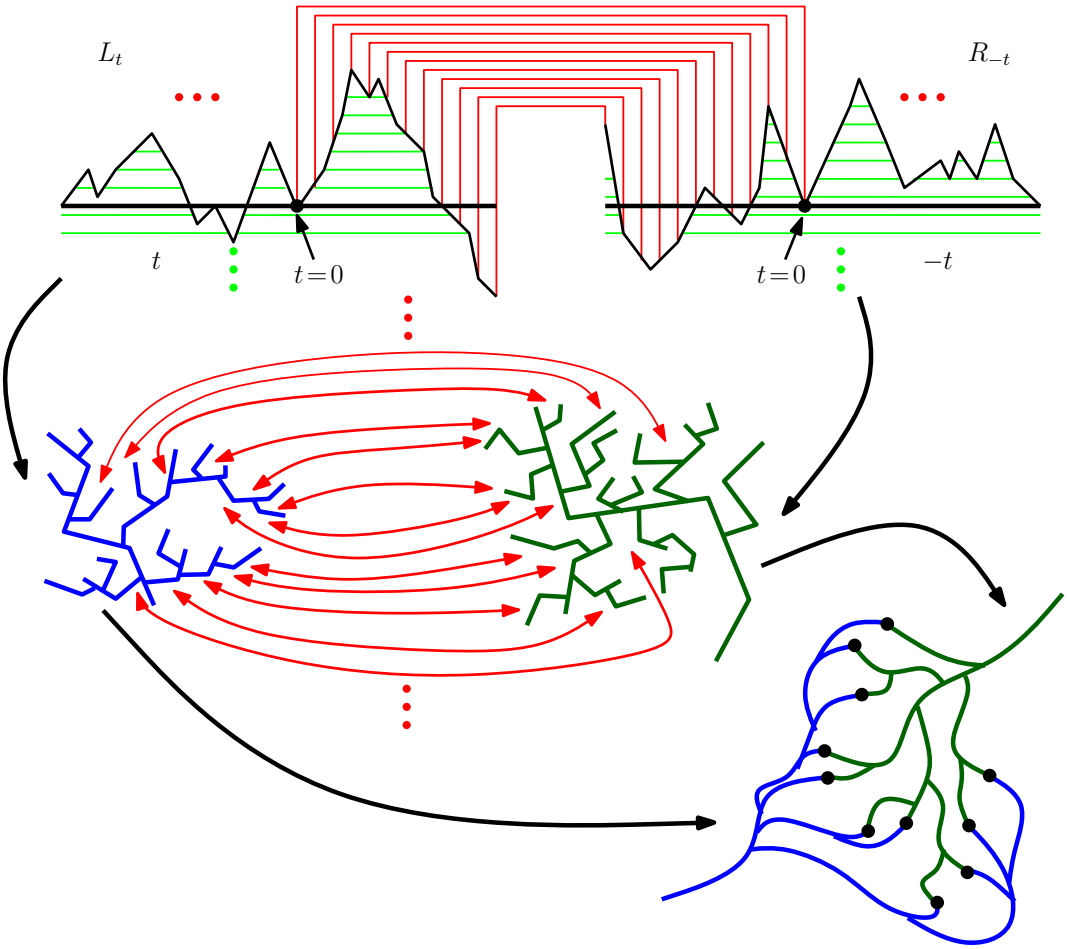

Figure 1.13: Gluing together two infinite volume space-filling trees, encoded by correlated Brownian motions L_t and R_t, produces a γ-quantum cone (i.e., $W = 4-\gamma^2$ and $\theta = 2\pi$). This cone is decorated by a space-filling $\mathrm{SLE}_{\kappa'}$ from ∞ to ∞, which in turn encodes the east-going and west-going rays of an imaginary geometry.

As we will explain in detail in Section 9, the main inputs into the proof of Theorem 1.13 are Theorem 1.9 and Theorem 1.12. (See also Figure 1.14.) Indeed, these results imply that drawing a certain pair of whole-plane $\mathrm{SLE}_\kappa(2-\kappa)$ processes coupled together as flow lines of a whole-plane GFF [MS13a] on top of an independent γ-quantum cone ($W = 4-\gamma^2$) yields a pair of independent quantum wedges of weight $2-\frac{\gamma^2}{2}$. These flow lines give the left and right boundaries of η' stopped upon hitting 0. This, combined with the invariance statement (1.8) implies that (L, R) has independent increments and it does not require much additional work to extract from this that (L, R) must be *some* two-dimensional Brownian motion. In the case that $\kappa' \in (4, 8)$, we then compute the almost sure Hausdorff dimension of the set

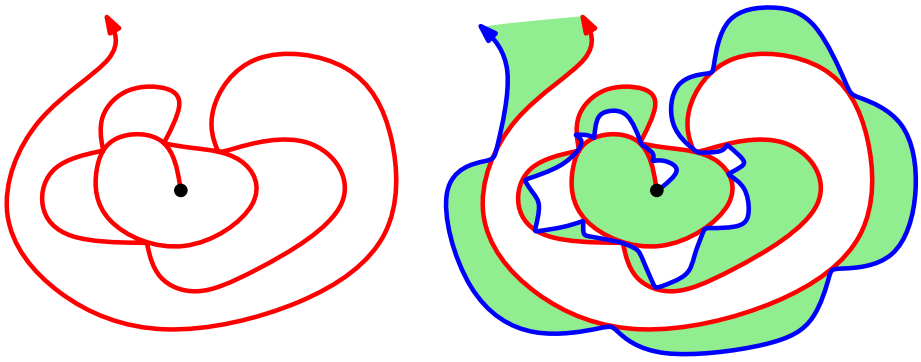

(a) (b)

Figure 1.14: Illustration of the key step in the proof of Theorem 1.13 from Theorem 1.9 and Theorem 1.12. **a)** A γ-quantum cone sliced by an independent whole-plane $\mathrm{SLE}_\kappa(\rho)$ process η_1 with $\kappa = \gamma^2$ and $\rho = 2 - \kappa$. (Whether or not η_1 is self-intersecting depends on whether $\rho \in (-2, \frac{\kappa}{2} - 2)$ or $\rho \geq \frac{\kappa}{2} - 2$.) By Theorem 1.12, the sequence of quantum surfaces corresponding to $\mathbf{C} \setminus \eta_1$ ordered according to when their boundary is first drawn by η_1 is a wedge of weight $4 - \gamma^2$. **b)** Conditional on η_1, we draw in each of the components of $\mathbf{C} \setminus \eta_1$ an independent $\mathrm{SLE}_\kappa(-\frac{\kappa}{2}; -\frac{\kappa}{2})$ process; call their concatenation η_2. By the results of [MS13a], we can view (η_1, η_2) as flow lines of a common whole-plane GFF with an angle gap of π and (η_1, η_2) give the outer boundary of a space-filling $\mathrm{SLE}_{\kappa'}$, $\kappa' = 16/\kappa$, process η' stopped upon hitting 0. Theorem 1.9 implies that the pair (η_1, η_2) divides the plane into independent wedges of weight $2 - \frac{\gamma^2}{2}$. (These correspond to the regions of $\mathbf{C}$ visited by η' before and after it visits 0 and are respectively colored green and white.) This is the key observation that leads to the statement that the γ-LQG length of the left and right boundaries of η' (when parameterized by γ-LQG area) has independent increments and, ultimately, Theorem 1.13, which states that they evolve as a certain two-dimensional Brownian motion.

of local cut times for η' (with the γ-LQG area parameterization). These local cut times turn out to correspond to so-called "cone times" for (L, R), so we are able to determine the covariance matrix for $\kappa' \in (4, 8)$ (and for the limiting case $\kappa = 8$) by matching the dimension that we find with the dimension given in the main result of [Eva85]. In Section 9, additional explanation is provided as to how this result relates to the scaling limits of discrete random planar map models [She11] described earlier. We will not identify the correlation constant for $\kappa' > 8$ here, though it is natural to guess that the formula given in Theorem 1.13 continues to hold when $\kappa' > 8$. .

Our next result is that the pair (L, R) from Theorem 1.13 almost surely determines both the space-filling $\mathrm{SLE}_{\kappa'}$ exploration path and the entire LQG surface.

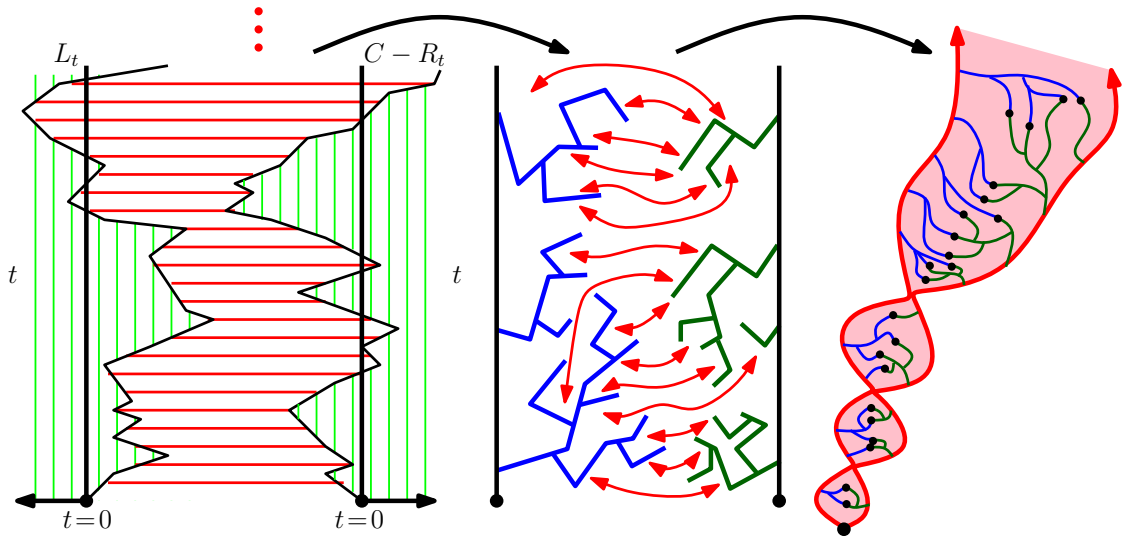

Figure 1.15: If we restrict the time in Figure 1.13 to $t \geq 0$, then the same Brownian motion encodes a $\theta = \pi$ wedge, which corresponds to $W = 2 - \frac{\gamma^2}{2}$. (Note that the vertical and horizontal axes have been swapped from what they were in Figure 1.13.) The left and right boundaries of the wedge correspond to the record minima of L_r and R_t (see also Figure 1.16, which in turn correspond to the vertical green segments that reach all the way to the bottom $t = 0$ line.

Theorem 1.14. *In the setting of Theorem 1.13, the pair (L, R) almost surely determines both η' and h (up to a rigid rotation of the complex plane about the origin).*

1.7.2 Non-space-filling counterflow lines

The peanosphere constructions are particularly interesting in the case that L_t and R_t are positively correlated, which corresponds to $\gamma \in (\sqrt{2}, 2)$. Recall that this is the range for which the corresponding $\mathrm{CLE}_{\kappa'}$ exist with $\kappa' \in (4, 8)$, where $\kappa' = 16/\gamma^2$. This is also the range in which $\mathrm{SLE}_{\kappa'}$ is itself non-space-filling and hence differs from space-filling $\mathrm{SLE}_{\kappa'}$.

Given $0 < s < t$, we say that s is an **ancestor** of t, and we write $s \prec t$, if for all $r \in (s, t]$ we have $L_r > L_s$ and $R_r > R_s$. The following facts are obvious from this definition:

1. $s \prec t$ implies $s < t$.
2. $s \prec t$ and $t \prec u$ implies $s \prec u$.

3. $s \prec t$ implies $s \prec u$ for all $u \in (s,t)$.

If s is an ancestor of any $t > s$, then s is called a **cone time** of the Brownian process. Figure 1.16 illustrates one such cone time. As the figure illustrates, the set of points that have a cone time s as an ancestor is an open set (s, s') for some s', and between s and s' the Brownian path (L_t, R_t) traces out an excursion into the quadrant $[L_s, \infty) \times [R_s, \infty)$ that begins at the corner and ends on one of the two sides. A point $t \geq 0$ is called **ancestor free** if there is no $s \in (0,t)$ that is an ancestor of t. The properties above imply that if s is ancestor free then a given $t > s$ is ancestor free if and only if t has no ancestor in (s,t). This implies that the set of ancestor free times is a regenerative process, and by scale invariance, we may conclude that it has the law of the range of a stable subordinator (which agrees in law with the zero set of a certain Bessel process, and which can be parameterized by a local time). Write $t(s)$ for the infimum of times at which this local time exceeds s (noting that $t(s)$ is necessarily an ancestor free time itself). Then we have the following:

Proposition 1.15. *The processes $L_{t(s)}$ and $R_{t(s)}$ parameterized by time s are independent totally asymmetric $\frac{\kappa'}{4}$-stable processes.*

The statement itself is a straightforward observation (it is clear from Figure 1.16 that each jump of the stable subordinator corresponds to a positive jump in precisely one of the processes $L_{t(s)}$ and $R_{t(s)}$, and that the measure on jumps has a power law distribution) but the parameter $\frac{\kappa'}{4}$ will not be identified until Section 12. As Figure 1.16 and 1.17 explain, the set of ancestor free times corresponds to the set of points in the space-filling curve from ∞ to 0 that lie on the outer boundary of the origin-containing component of the not-yet-explored region. The restriction of the path to these times is the ordinary $\text{SLE}_{\kappa'}$ counterflow line from ∞ to 0. The following list summarizes a few special subsets of the wedge parameterized by $[0, \infty)$, which are obtained by restricting to special times in $[0, \infty)$:

1. **Counterflow line from ∞ to 0:** parameterized by the set of ancestor free times t.
2. **Left (resp. right) boundary of entire wedge:** parameterized by times at which L_t (resp. R_t) attains a record minimum.
3. **Cut points of entire wedge:** times at which L_t and R_t simultaneously achieve record minima. These times also correspond to points that are ancestors of 0 w.r.t. the time reversed process (L_{-t}, R_{-t}) parameterized by $t \leq 0$. See Figure 1.17.

The processes described in Proposition 1.15 encode two so-called **Lévy trees** of disks, after the manner outlined in Figure 1.7. (Lévy trees are studied in detail in [DLG02].) The procedure for obtaining one of these trees is explained in the top row of Figure 1.18. (The later rows contain related constructions that will relevant for Theorem 1.19.) Note that in a Lévy tree there are in fact a countably infinite number of small loops along the branch connecting any two given loops (i.e., it is almost surely the case that no two loops are adjacent). Each loop comes with a well-defined boundary length, which is the magnitude of the corresponding jump in the stable Lévy process. The outer boundary of the tree of loops also comes with a natural time parameterization, which is the time of the corresponding Lévy process. Intuitively, if for some tiny ϵ one keeps track of the number of loops of size between ϵ and 2ϵ that are encountered as one traces the boundary of the tree, then that number (times an appropriate power of ϵ) is a good approximation for this natural time. A **forested line** is the object obtained by beginning with a stable Lévy process as on the top row of Figure 1.18, and then filling each of the circles illustrated on the top row of Figure 1.18 with an independent quantum disk of the given boundary length, glued onto the circle in a boundary length preserving way.

Suppose that $\mathcal{W}$ is quantum wedge of weight $W > 0$. A **forested quantum wedge of weight** W is the beaded random surface which arises by gluing the line of a forested line (i.e., an independent forest of quantum disks as constructed above where the value of α for the stable process is taken to be $\frac{\kappa'}{4} = \frac{4}{\gamma^2} \in (1, 2)$) to either the left or the right side of $\mathcal{W}$. A **doubly forested quantum wedge of weight** W is obtained by gluing an independent forested line to each of the two sides of $\mathcal{W}$. Illustrations of doubly forested wedges appear, e.g., in Figures 1.21 and 1.22.

Theorem 1.16. *Consider a quantum wedge of weight $W = 2 - \frac{\gamma^2}{2}$ (which corresponds to $\theta = \pi$) and the counterflow line from ∞ to 0 as depicted in Figure 1.17 and Figure 1.19. Then this counterflow line divides the wedge into two independent forested lines, whose boundaries are identified with one another according to the natural time parameterization of the outer boundary of the corresponding Lévy trees. Moreover, given the two forested lines, it is a.s. possible to uniquely recover the quantum wedge and the counterflow line.*

Theorem 1.16 has many variants, including Theorem 7.13 (a statement about unscaled quantum wedges) and Theorem 7.1, Theorem 7.11, and Corollary 7.12 (which involve chordal, radial, and whole-plane $\mathrm{SLE}_\kappa(\rho)$ processes, respectively).

The following theorem is one fairly easy generalization of Theorem 1.16, which can be deduced as a consequence of Theorem 1.16 and the additivity of wedges developed in Theorems 1.9 and 1.11. It states essentially that one can zip together a right-forested wedge of weight W_1 and a left-forested wedge of weight W_2 (zipping along the forested sides) in order to obtain a wedge of weight $W_1 + W_2 + 2 - \frac{\gamma^2}{2}$

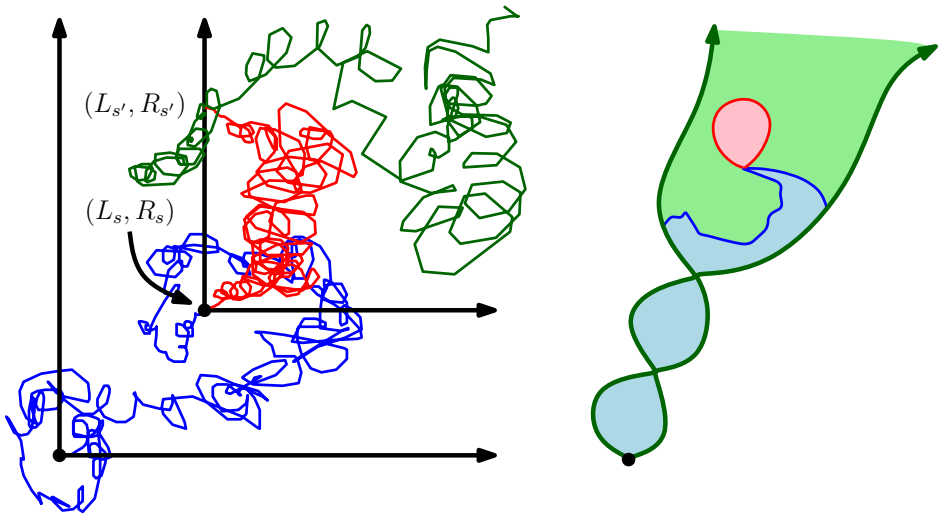

Figure 1.16: When L_t and R_t are positively correlated, we have $\gamma \in (\sqrt{2}, 2)$. In this case, there a.s. exist cone times like the time s illustrated on the left. As noted on the right, an interval of this type is "cut off" by the space-filling path from ∞ to 0 before it is filled up. (The path from ∞ to 0 fills first the green region, then the red region, then the blue region.)

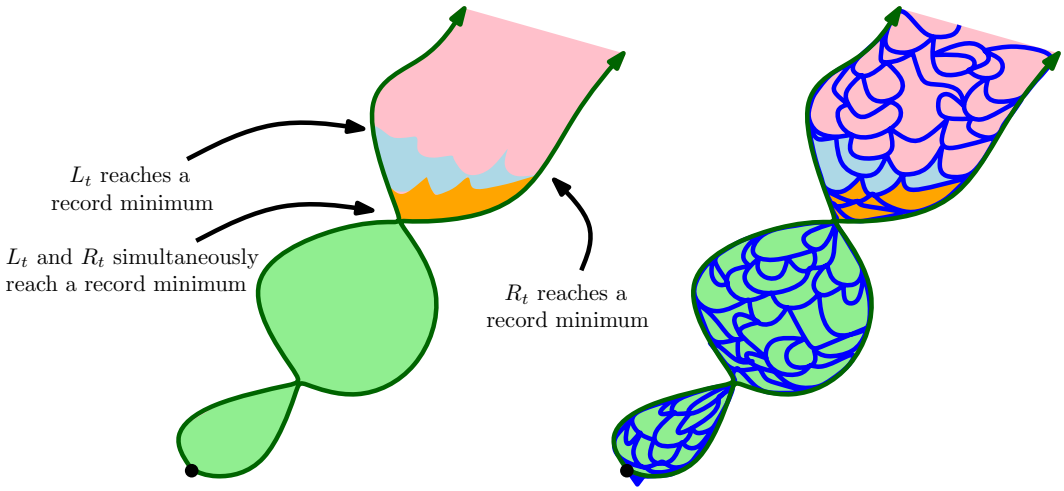

Figure 1.17: Shown on the left is a $2 - \frac{\gamma^2}{2}$ wedge. When the space-filling $\mathrm{SLE}_{\kappa'}$ process η' from 0 to ∞ hits a pinch point in the wedge, then L_t and R_t simultaneously hit a record minimum (green). When η' hits the left (resp. right) side of the wedge then L_t (resp. R_t) hits a record minimum. Shown on the right is the set of ancestor free times which corresponds to the counterflow line from ∞ to 0.

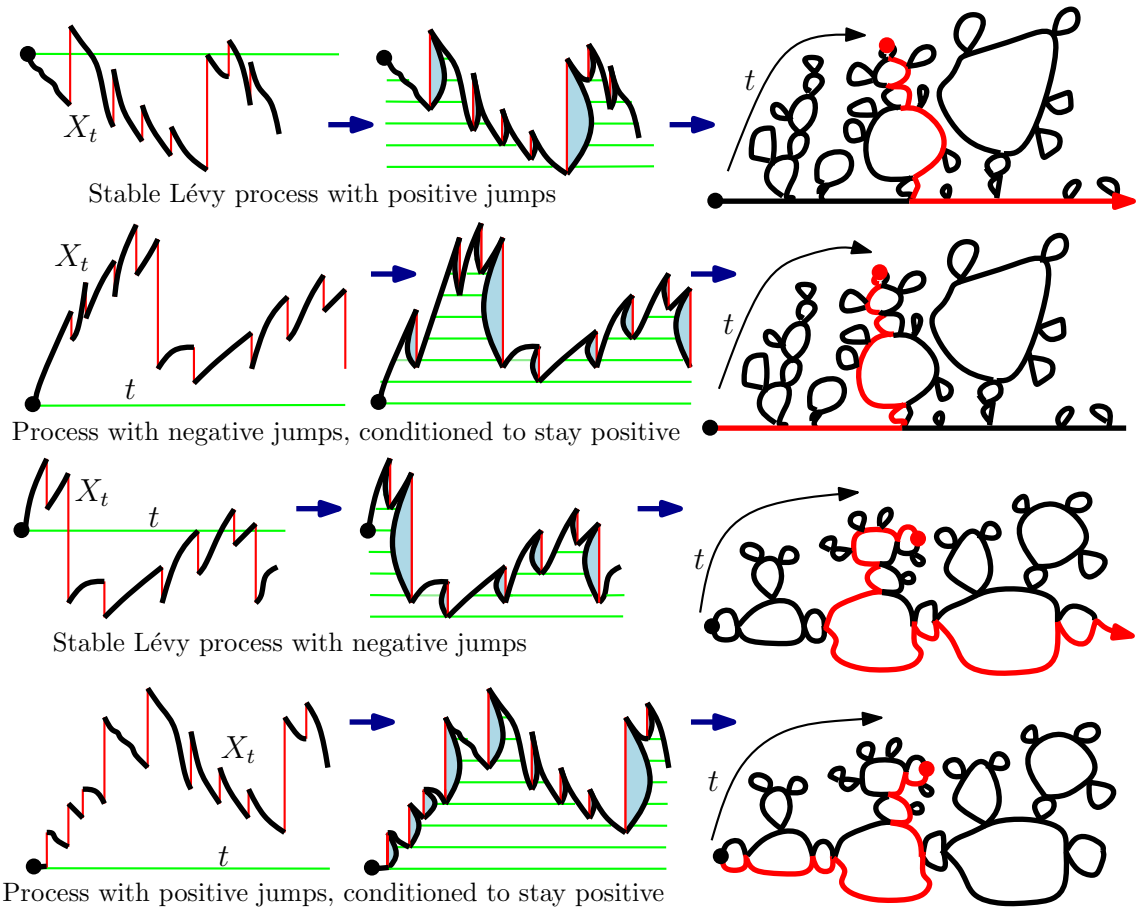

Figure 1.18: **First row:** A stable Lévy process X_t with positive jumps encodes a forested line via the procedure explained in Figure 1.7 (top right). Unmatched green segments (record minima of X_t) map to points on the line. As t increases, the red dot on right traces the forest boundary clockwise. X_t encodes the net change in length of the red path (which traces the right side of the branch of disks containing the point hit at time t, and continues right to ∞) since time 0. A jump occurs when a disk is hit for the first time, with jump size given by the boundary length of the disk. **Second row:** The same forested line corresponds to a stable Lévy process with negative jumps conditioned to stay positive. Unmatched green rays (last hitting times of X_t) map to points on the line. The value of X_t encodes the left boundary length. A jump occurs when a disk is hit for the last time. **Third row:** A stable Lévy process with negative jumps encodes a forested wedge. Unmatched green segments map to the underside of the wedge. A jump occurs when a disk is hit for the last time. **Fourth row:** The same forested wedge corresponds to a positive-jump stable Lévy process conditioned to stay positive.

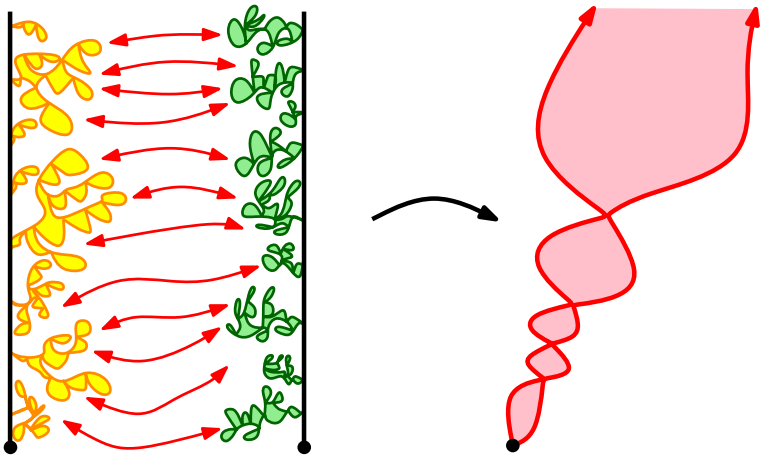

Figure 1.19: Two forested lines can be welded together according to quantum length to produce a single $\theta = \pi$ quantum wedge. Recall that $\theta = \pi$ corresponds to $W = 2 - \frac{\gamma^2}{2}$.

decorated by an appropriate $\mathrm{SLE}_{\kappa'}(\rho_1;\rho_2)$ process. We include this result in order to illustrate that general non-boundary-filling $\mathrm{SLE}_{\kappa'}(\rho_1;\rho_2)$ processes can be obtained by zipping together forested wedges.[10]

Theorem 1.17. *Fix $\gamma \in (0,2)$ and let $\kappa' = 16/\gamma^2 \in (4,\infty)$. Fix $\rho_1, \rho_2 \geq \frac{\kappa'}{2} - 4$. Let*

$$W_i = \gamma^2 - 2 + \frac{\gamma^2}{4}\rho_i \geq 0 \quad \text{for} \quad i = 1,2 \quad \text{and} \quad W = W_1 + W_2 + 2 - \tfrac{\gamma^2}{2}. \tag{1.9}$$

Let $\mathcal{W} = (\mathbf{H}, h, 0, \infty)$ be a quantum wedge of weight W and let η' be an $\mathrm{SLE}_{\kappa'}(\rho_1;\rho_2)$ process in $\mathbf{H}$ from 0 to ∞ with force points located at $0^-, 0^+$ which is independent of $\mathcal{W}$. (In the case that $W \in (0, \frac{\gamma^2}{2})$ so that $\mathcal{W}$ is not homeomorphic to $\mathbf{H}$, we take η' be to be given by a concatenation of independent $\mathrm{SLE}_{\kappa'}(\rho_1;\rho_2)$ processes: one for each of the bubbles of $\mathcal{W}$ starting at the opening point of the bubble and targeted at the terminal point.) Then the quantum surface $\mathcal{W}_1$ (resp. $\mathcal{W}_2$) which consists of those components of $\mathbf{H} \setminus \eta'$ which are to the left (resp. right) of η' is a quantum wedge of weight W_1 (resp. W_2) and the quantum surface $\mathcal{W}_3$ which is between the left and right boundaries of η' is a quantum wedge of weight $2 - \frac{\gamma^2}{2}$. (Note that $\mathcal{W}_1$ is beaded if $\rho_1 \in (\frac{\kappa'}{2} - 4, \frac{\kappa'}{2} - 2)$ and likewise $\mathcal{W}_3$ is beaded if $\rho_2 \in (\frac{\kappa'}{2} - 4, \frac{\kappa'}{2} - 2)$.) Moreover, $\mathcal{W}_1, \mathcal{W}_2, \mathcal{W}_3$ are independent.

[10] It is also natural to give a description of the structure of the surfaces cut out by an $\mathrm{SLE}_{\kappa'}(\rho_1;\rho_2)$ process, $\kappa' \in (4,8)$, drawn on top of a wedge $\mathcal{W}$ of weight W as in (1.9) when one or both of ρ_1, ρ_2 are in $(-2, \frac{\kappa'}{2} - 4)$ so that η' almost surely fills part of the domain boundary. In this case, the quantum surfaces which are completely surrounded by η' and are on its left (resp. right) side still have a tree structure. It seems, however, that these trees are not independent of each other. Describing the law of this pair of trees falls outside of the scope of this article.

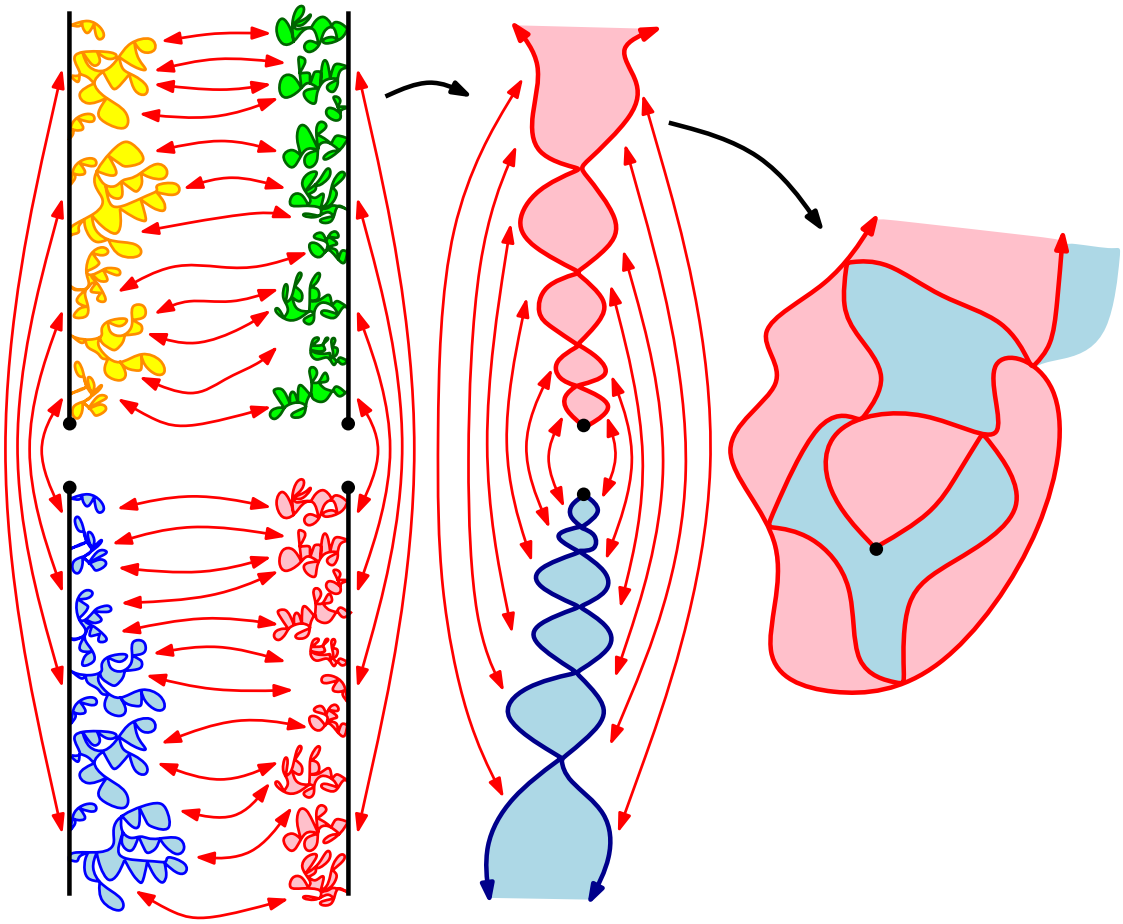

Figure 1.20: Repeating the procedure of Figure 1.19 for negative time, we can glue together four i.i.d. forested wedges to obtain the entire $\theta = 2\pi$ quantum cone. The interfaces are given by the flow line and dual flow line from 0 to ∞, and by the two counterflow lines coming from ∞ to 0 that have these paths as their boundaries.

Suppose further that $\gamma \in (\sqrt{2}, 2)$ so that $\kappa' \in (4, 8)$. Then the beaded surface $\widetilde{\mathcal{W}}_1$ (resp. $\widetilde{\mathcal{W}}_2$) which consists of those components of $\mathbf{H} \setminus \eta'$ whose boundary is drawn by the left (resp. right) side of η' is a forested wedge of weight W_1 (resp. W_2). Moreover, $\widetilde{\mathcal{W}}_1$ and $\widetilde{\mathcal{W}}_2$ are independent and, together, almost surely determine both $\mathcal{W}$ and η'.

The following is another easy consequence of Theorem 1.16, together with Theorem 1.18. It states that we can zip up *both* sides of a doubly forested wedge of general weight, as illustrated in Figure 1.21, in order to obtain a quantum cone decorated by an appropriate whole-plane $\mathrm{SLE}_{\kappa'}(\rho)$ process.

Theorem 1.18. *Fix $\gamma \in (\sqrt{2}, 2)$ and suppose that $\mathcal{C} = (\mathbf{C}, h, 0, \infty)$ is a quantum cone of weight $W \geq 2 - \frac{\gamma^2}{2}$ (so that $\theta \geq \pi$). Let $\rho = \frac{4W}{\gamma^2} - 2$ and suppose that*

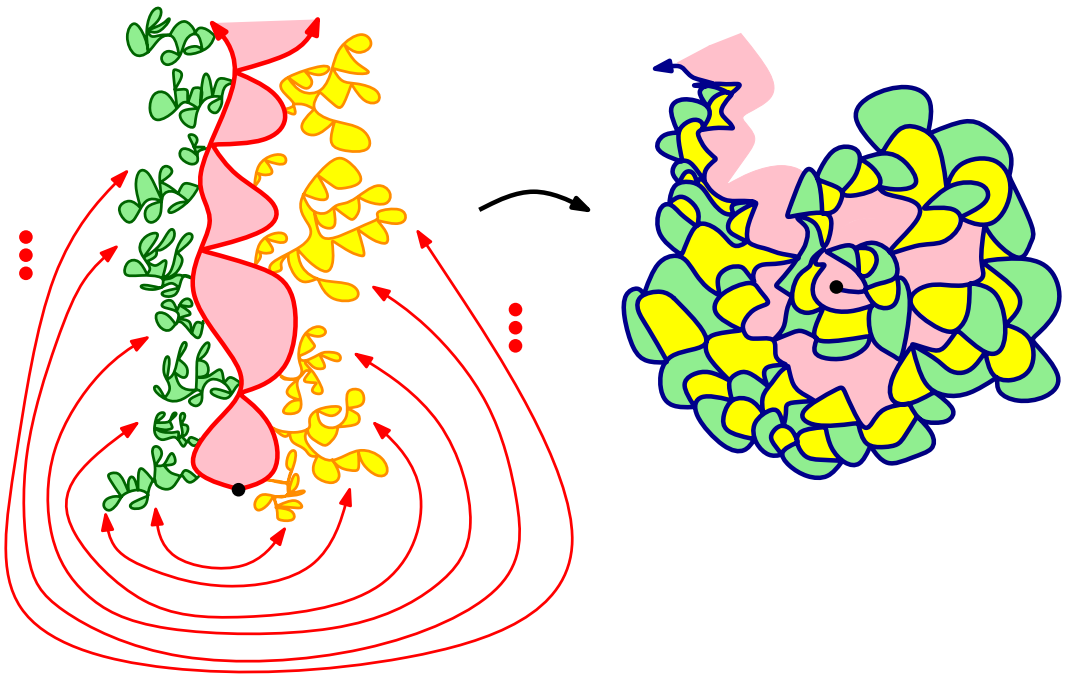

Figure 1.21: Alternatively, one can subdivide only one of the two $\theta = \pi$ wedges within a counterflow line. In this case, one has a doubly forested $\theta = \pi$ quantum wedge that zips up to become a $\theta = 2\pi$ quantum cone.

η' is a whole-plane $\mathrm{SLE}_{\kappa'}(\rho)$ *process starting from* 0 *independent of $\mathcal{C}$. Then the beaded surface $\mathcal{W}_1$ (resp. $\mathcal{W}_2$) which consists of those components of $\mathbf{C} \setminus \eta'$ which are surrounded by η' on its left (resp. right) side when viewed as a path in the universal cover of $\mathbf{C} \setminus \{0\}$ has the structure of a forested line and the (possibly beaded) surface $\mathcal{W}_3$ which consists of the remaining components of $\mathbf{C} \setminus \eta'$ is a quantum wedge of weight*

$$W - \left(2 - \frac{\gamma^2}{2}\right) = \gamma^2 - 2 + \frac{\gamma^2}{4}\rho.$$

Moreover, $\mathcal{W}_1$, $\mathcal{W}_2$, and $\mathcal{W}_3$ are independent and together almost surely determine both $\mathcal{C}$ and η'.

Observe that if we express the ρ in the statement of Theorem 1.18 in terms of κ' and α then we get

$$\rho = 2 + \kappa' - 2\alpha\sqrt{\kappa'}. \tag{1.10}$$

Note that (1.10) depends on κ' and α in the same way that (1.6) (with $\gamma^2 = \kappa$) from Theorem 1.12 depends on κ and α.

Theorem 1.19 is one of the more interesting and important consequences of Theorem 1.16. As illustrated in Figure 1.22, it implies a "quantum zipper" invariance

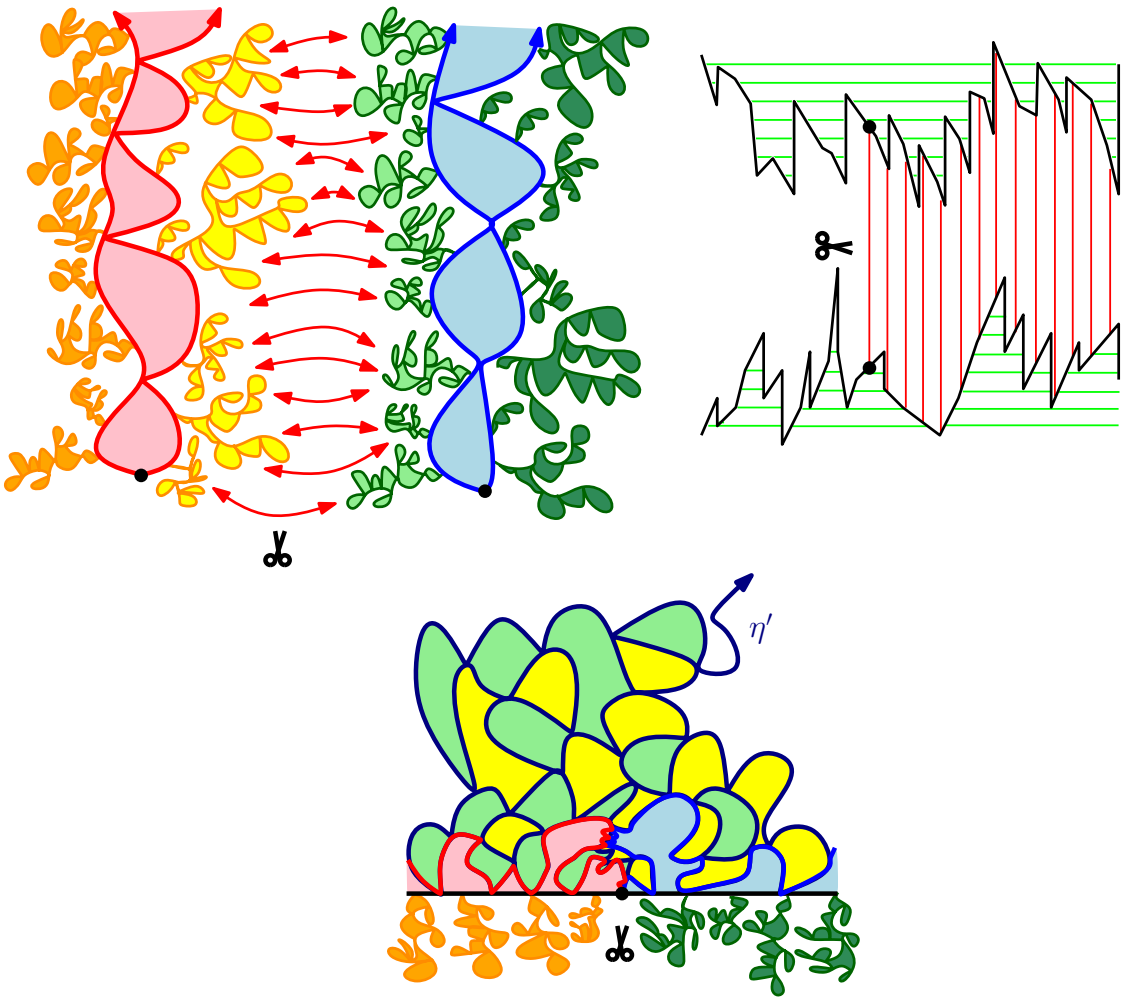

Figure 1.22: The quantum length invariant quantum zipper from [She10] involved two weight 2 quantum wedges which were zipped together on one side, and could be further zipped or unzipped; in the embedding in the upper half plane, the interface is an SLE_κ curve for $\kappa < 4$. In the analog described here for $\kappa' \in (4, 8)$ the two weight 2 quantum wedges are replaced by two doubly forested weight $(\gamma^2 - 2)$ wedges. The interface between them is a counterflow line (i.e., $\mathrm{SLE}_{\kappa'}$ curve), and once again the figure is invariant w.r.t. zipping or unzipping by a fixed amount of quantum natural time. Note that the entire collection of loops can be constructed from a pair of stable Lévy processes with negative jumps indexed by all time $\mathbf{R}$. The jumps before zero encode the loops in the two forests that have not yet been zipped up. The jumps after zero encode the loops in the upper half plane. Those jumps at times $t > 0$ at which L_t (resp. R_t) achieves a record minimum correspond to the disks that share boundary segments with the left (resp. right) real axis.

principle for $\mathrm{SLE}_{\kappa'}$ analogous to the principle established for SLE_κ in [She10].

Combining Theorem 1.16 with Theorem 1.17 leads to another notion of time parameterization for an $\mathrm{SLE}_{\kappa'}$ process η', namely the time parameterization associated with the pair of independent stable Levy processes which encode the boundary lengths of the bubbles cut off by η'. We will refer to this time-parameterization as **quantum natural time**. It is the quantum version of the so-called "natural" parameterization for SLE [LS11, LZ13, LR12], see also [DS11b]. (The quantum analog of the natural parameterization for $\kappa \in (0,4)$ is γ-LQG length and for $\kappa' \geq 8$ is γ-LQG area.) We will write $\mathfrak{q}_u$ for the function which converts from quantum natural time u to capacity time. That is, if η' is parameterized by capacity time then $\eta'(\mathfrak{q}_u)$ is parameterized by quantum natural time.

Theorem 1.19. *Fix $\gamma \in (\sqrt{2}, 2)$ and let $\mathcal{W} = (\mathbf{H}, h, 0, \infty)$ be a quantum wedge of weight $\frac{3\gamma^2}{2} - 2$ and let η' be an independent $\mathrm{SLE}_{\kappa'}$ process, $\kappa' = 16/\gamma^2 \in (4,8)$, in $\mathbf{H}$ from 0 to ∞. Then η' divides $\mathcal{W}$ into two independent forested wedges both with weight $\gamma^2 - 2$. Moreover, the joint law of (h, η') is invariant under the operation of cutting along η' until a given quantum natural time and then conformally mapping back and applying (1.3). That is, if (f_t) denotes the centered chordal Loewner flow associated with η' (with the capacity time parameterization) and $\mathfrak{q}_u$ is as above, then we have that*

$$(h, \eta') \stackrel{d}{=} (h \circ f_{\mathfrak{q}_u}^{-1} + Q \log |(f_{\mathfrak{q}_u}^{-1})'|, f_{\mathfrak{q}_u}(\eta')) \quad \text{for each} \quad u \geq 0.$$

Indeed, the entire image shown in Figure 1.22 is invariant with respect to the operation of zipping/unzipping according to quantum natural time.

If we start with the top row of Figure 1.18, and "zoom in" near a typical non-zero time, then we obtain a stable Lévy processes indexed by all of $\mathbf{R}$. We can then consider a pair of processes of this type. This is equivalent to drawing an SLE until a typical quantum time, zooming in, and "unzipping" up to the distinguished time, which produces a figure like Figure 1.22. Each of the forested lines hanging off the bottom of the image in Figure 1.22 is an independent forested line of the sort described by the top row of Figure 1.18. If we focus on the quantum wedge parameterized by the upper half plane in Figure 1.22 and then cut this wedge along the illustrated counterflow line, then we obtain a pair of forested quantum wedges, each of which corresponds, by construction, to the quantum wedge illustrated in the third line of Figure 1.18. In particular, this analysis tells us how the γ-LQG length of $\mathbf{R}_-$ and $\mathbf{R}_+$ changes when we zip and unzip the image shown in Figure 1.22.

Corollary 1.20. *In the context of Figure 1.22, the net change in the γ-LQG length of $\mathbf{R}_-$ and $\mathbf{R}_+$ as one "zips up" is given by an independent pair of totally asymmetric $\frac{\kappa'}{4}$-stable Lévy processes with positive jumps, each like the one illustrated in the*

first row of Figure 1.18. In the context of Figure 1.22, the net change in left and right boundary lengths as one "unzips" is given by an independent pair of totally asymmetric $\frac{\kappa'}{4}$-stable Lévy processes with negative jumps, each like the one illustrated in the third row of Figure 1.18.

Recall that the first row of Figure 1.18 describes a forested line. Moreover, Corollary 1.20 implies that the third row of Figure 1.18 encodes a forested wedge of weight $\gamma^2 - 2$ corresponding to (by Theorem 1.17) those bubbles which are either to the right but not surrounded by an $\mathrm{SLE}_{\kappa'}$ process (a $\gamma^2 - 2$ wedge) or those bubbles which are on the right and completely surrounded by an $\mathrm{SLE}_{\kappa'}$ process (a forested line). One can glue the former forested line to the latter forested wedge to obtain a doubly forested wedge of weight $\gamma^2 - 2$. The law of this doubly forested wedge is invariant under the operation of "sliding the tip" a fixed amount of quantum time units along the boundary of the forest. This simply corresponds to the fact that the $\frac{\kappa'}{4}$-stable Lévy process indexed by all of $\mathbf{R}$ (which encodes this doubly forested wedge) has a stationary law. The second and fourth rows of Figure 1.18 describe different ways to encode the same process. Although we will not need this point here, we remark (and leave it to the reader to check) that as one moves from right to left along the processes in either the second or fourth row, one encounters or completes disks (which correspond to jumps) at a Poisson rate, and the processes shown can be understood as stable Lévy processes conditioned to stay positive.

We next remark that it is not hard to derive analogs of Theorem 1.19 and Corollary 1.20 that involve radial and whole-plane $\mathrm{SLE}_{\kappa'}$ processes. For these variants, one considers a single doubly forested wedge of some weight, zipped up like the doubly forested wedge in Figure 1.21, so that the interface becomes the $\mathrm{SLE}_{\kappa'}(\rho)$ curve described in Theorem 1.18. We then keep track of what happens as we begin to cut with scissors along the counterflow line, starting from the origin (always conformally mapping the infinite unexplored region conformally to $\mathbf{C} \setminus \mathbf{D}$). (This is the usual setup used to construct a whole-plane $\mathrm{SLE}_{\kappa'}(\rho)$ curve.) The case in which the wedge (along which the two forested lines are added) has weight $\gamma^2 - 2$ turns out to be particularly interesting, because in this case, the disks in the wedge turn out to play (in some sense) the same role as the disks in the forests rooted on that wedge.

1.7.3 Discrete intuition

Consider the **half-planar** random planar triangulation as defined in [AS03, Ang03, AC13, AR13]. This is a simply-connected infinite planar map with an infinite boundary and a distinguished "origin" edge; it has the *domain Markov property*, which means that if we condition on any finite collection of triangles discovered by exploring from the boundary, then the conditional law of the infinite connected component of the unexplored region has the same law as the original map. (See [AR13,

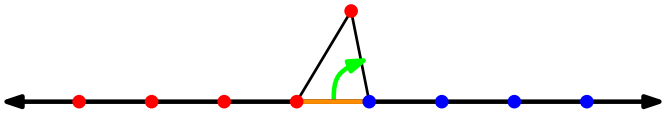

Figure 1.23: The horizontal line represents the (infinite) boundary of a domain Markov half-planar map with a marked boundary edge (orange). The boundary vertices to the left (resp. right) of this marked edge are colored red (resp. blue). The rest of the vertices in the map are colored red or blue i.i.d. with probability $\frac{1}{2}$. Shown is the first step of the percolation exploration starting from the marked edge with red (resp. blue) on the left (resp. right) side of the path. Triangles which have an edge on the boundary either have their third vertex on the boundary of the map or in the interior of the map. The triangle shown is of the latter type. By the domain Markov property, the conditional law of the map in the unbounded component given the revealed triangle is the same as the law of the original map.

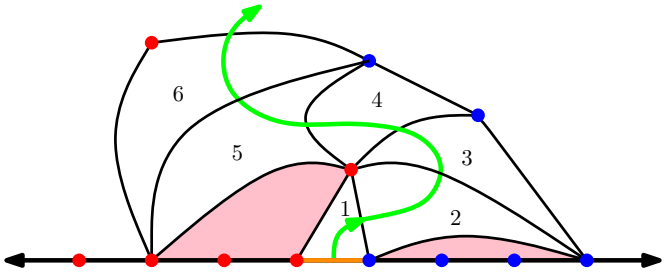

Figure 1.24: (Continuation of Figure 1.23.) Shown are five more steps of the percolation exploration (for a total of six steps). The triangles are numbered according to the order in which they are visited by the exploration path. When the exploration visits the second and fourth triangles it disconnects regions of the map from ∞; these are colored light red in the illustration. By the domain Markov property, the law of the sequence of these regions is i.i.d. Moreover, the domain Markov property implies that the incremental net changes to the left (right) boundary length are i.i.d.

Definition 1.1] for a more careful definition.) Suppose that we pick a distinguished edge on the boundary of the map and then color the vertices which are to the left (resp. right) of this edge red (resp. blue) as illustrated in Figure 1.23. We then color the remaining vertices in the map i.i.d. red or blue with equal probability $\frac{1}{2}$.

Consider the percolation exploration which starts at the marked boundary edge with red vertices on its left side and blue vertices on its right side. (See Figures 1.23–1.24.) By the domain Markov property, it follows that:

(i) The components which are cut off by the exploration form an i.i.d. sequence.

(ii) The change in the lengths of the left (resp. right) boundary of the unbounded component of the map evolve as random walks with independent increments.

Theorem 1.16 and Theorem 1.17 give the continuum analog of (i) and Corollary 1.20 gives the continuum analog of (ii).

The stable Lévy processes described in Proposition 1.15 and Corollary 1.20 for $\kappa' = 6$ are consistent with a heuristic argument made by Angel just before the statement of [Ang03, Lemma 3.1] for the scaling limit of the boundary length process associated with a percolation exploration on the uniform infinite planar triangulation. It is also consistent with [Cur13, Question 5]. The law of the boundary length process associated with the growth of a metric ball on $\sqrt{8/3}$-LQG should be related to the boundary length process associated with a percolation exploration process on $\sqrt{8/3}$-LQG via a certain time-change. In particular, if A_t denotes the boundary length process associated with the latter then the former should be given by $A_{t(s)}$ where $t(s) = \int_0^s A_u du$ (this says that the rate of growth should be proportional to boundary length, as in first passage percolation with i.i.d. exp(1) edge weights). If A is a totally asymmetric $\frac{3}{2}$-stable process conditioned to be non-negative, then $A_{t(s)}$ has the law of the time-reversal of a continuous-state branching process with branching mechanism $\psi(u) = u^{3/2}$ [Lam67]. This is consistent with a result due to Krikun [Kri05, Theorem 4] for the evolution of the length of the boundary of a metric ball as its diameter increases in the setting of the uniform infinite planar quadrangulation. This is also consistent with a calculation carried out in the continuum for the Brownian plane [CL12] recently announced by Curien and Le Gall in [Le 14, CL14].

The results described in Section 1.7 will be important ingredients for a work in progress by the second two co-authors concerning the so-called quantum Loewner evolution (QLE) [MS13b]. In particular, they allow us to define a "quantum natural time" version of QLE. Since QLE$(8/3, 0)$ is constructed by applying a certain transformation to SLE_6 (so-called "tip-rerandomization"), Theorem 1.19 gives us that the Poissonian structure of the complementary components of a QLE$(8/3, 0)$ exploration and an SLE_6 exploration of $\sqrt{8/3}$-LQG are the same. Also, Theorem 12.1 gives us that the evolution of the $\sqrt{8/3}$-LQG length of the outer boundary of a QLE$(8/3, 0)$ is the same as the corresponding boundary length process for a metric ball in the Brownian plane. Finally, Theorem 1.13 gives many distributional identities between the Poissonian structure of the complementary components of a QLE$(8/3, 0)$ and a metric ball in the Brownian plane. As a simple example, it implies that the

conditional law of the area of such a component given its boundary length is the same as in the setting of the Brownian plane.

1.8 Outline

In Section 2, we will provide some additional context for this work. Next, in Section 3, we collect some relevant facts about Bessel processes and describe some elementary but interesting symmetries enjoyed by forward and reverse $\mathrm{SLE}_\kappa(\rho)$ processes. Then in Section 4 we give an overview of the different types of GFFs that appear in this article as well a description of several different types of quantum surfaces (quantum wedges, cones, disks, and spheres). Section 5 shows how the finite volume surfaces can be constructed using limits, as mentioned in the beginning of [She10, Section 6]. Section 6 contains a brief review of the couplings between the Gaussian free field SLE that are relevant to this article. We also describe the law of the local behavior of a boundary intersecting $\mathrm{SLE}_\kappa(\rho)$ process at a time when it first cuts off a given boundary point from ∞. In Section 7 we describe the Poissonian structure of the bubbles that one encounters when cutting a γ-LQG surface along an $\mathrm{SLE}_\kappa(\rho)$ or $\mathrm{SLE}_{\kappa'}$ process; we also introduce quantum natural time. The main conformal welding results for wedges are established in Section 8. We use these results in Section 9 to show that the evolution of the left and right boundary lengths of a space-filling $\mathrm{SLE}_{\kappa'}$ process drawn on top of an LQG surface are indeed given by correlated Brownian motions (matching the continuum limit for random planar maps determined in [She11]). Section 10 then shows that the quantum surface and the space-filling $\mathrm{SLE}_{\kappa'}$ can be a.s. be recovered from the pair of Brownian motions. We then make connections between the results established here and the works of the first co-author via the KPZ formula in Section 11. In Section 12 we include additional discussion on forested wedges, trees of bubbles defined using Lévy processes, and quantum surfaces explored by $\mathrm{SLE}_{\kappa'}$ with $\kappa' \in (4, 8)$. These Lévy trees of discs (and related Lévy trees of spheres) correspond to objects constructed heuristically in the physics literature, where they are known as γ'-LQG surfaces with $\gamma'^2 \in (4, 8)$. We finish in Section 13 with a list of open questions.

2 Additional context

2.1 Conformal mating in complex dynamics

The idea of somehow stitching together a pair of trees to obtain a sphere with a conformal structure is not without precedent. There is a theory of "conformal mating" in the complex dynamics literature that in some circumstances provides a way to

obtain a conformal sphere by stitching together the Julia set of one polynomial to the Julia set of another polynomial [YZ01, Mil04, AY09, Tim10]. Milnor presents a particularly clear introduction to the theory in [Mil04] (see also Milnor's reference text on complex dynamics [Mil06]). In certain cases these Julia sets are "dendritic" like the continuum random trees described in Section 1.1, or illustrated on the left side of Figure 1.6. In such cases one obtains a space-filling curve and a measure on the sphere, much as in Section 1.1 [Mil04]. In other cases, the Julia set is the boundary of a region with non-empty interior, more like the "trees of disks" that the right side of Figure 1.6 illustrates.[11] We present a short overview of the theory (which can be skipped on a first read) in the remainder of this subsection.

Let f be a monic complex polynomial of degree $d \geq 2$. Then the *Fatou set* is defined by $\{z : \lim_{n\to\infty} f^{(n)}(z) = \infty\}$, where $f^{(n)} := f \circ f \circ \ldots \circ f$ is the n-fold composition of f. The *Julia set* $J(f)$ is the boundary of the Fatou set. The set $J(f)$ often has an interesting fractal structure. We consider only cases where $J(f)$ is connected, and we write $K = K(f)$ for the complement of the Fatou set (a.k.a., the *filling* of the Julia set). Then f is a d-to-1 conformal map from $\mathbf{C} \setminus K$ to itself that approximates the power map $z \to z^d$ near infinity. To make this point more explicit, let $\mathbf{D} \subseteq \mathbf{C}$ be the unit disk; one can show that if $\phi_K : \mathbf{C} \setminus K \to \mathbf{C} \setminus \overline{\mathbf{D}}$ is the conformal map that approximates the identity near ∞, then $f = \phi_K^{-1} \circ g \circ \phi_K$ where $g(z) = z^d$. We stress that the map $\phi_K^{-1} \circ g \circ \phi_K$ could be defined for any bounded hull K, but in general we would not expect it to be a polynomial function (which is smooth on all of $\mathbf{C}$, not just on $\mathbf{C} \setminus K$). The map f gives a surjective map from $J(f)$ to itself, which is sometimes called the *dynamics* of the Julia set $J(f)$. Also, the map ϕ_K^{-1} extends to give a surjective map from $\partial\mathbf{D}$ to $J(f)$, which provides a natural parameterization of (and measure on) $J(f)$.

The k-fold composition of f is a d^k to 1 map from $\mathbf{C} \setminus K$ to itself. Since $f^{(k)}$ is a polynomial that fixes K, it encodes a certain type of self similarity of the Julia set: a small neighborhood U of a generic point $z \in J(f)$ has d^k pre-images $U_1, \ldots, U_{d^k}$ under $f^{(k)}$, and the restrictions $U_i \cap K$ all look like $U \cap K$ (up to distortion by a polynomial map).

Suppose that $J(f_1)$ and $J(f_2)$ are connected Julia sets of polynomials f_1 and f_2, both of degree $d \geq 2$. Let σ_i be the natural parameterization mapping $\partial\mathbf{D}$ to $J(f_i)$. We let $\widetilde{J}$ be the pair $J_1 \cup J_2$ modulo the equivalence relation that identifies $\sigma_1(t)$ with $\sigma_2(t)$ when $t \in \partial\mathbf{D}$. Using Moore's theorem, it is often possible to show that $\widetilde{J}$ is topologically a sphere. Note that if each f_i induces a d to 1 map from $J(f_i)$ to itself, each of these two maps induces the same map $\psi : \widetilde{J} \to \widetilde{J}$. The interesting thing is that, in some cases, there is a unique (up to Möbius transformation) way to

[11] At the moment, an excellent gallery of related computer animations can be found on Arnaud Chéritat's webpage, illustrating both dendritic and non-dendritic matings. See also the computer images and algorithmic discussion in [BH12].

identify $\widetilde{J}$ with $\mathbf{C} \cup \{\infty\}$ in such a way that ψ becomes a rational functional. This effectively determines the conformal structure of $\widetilde{J}$.

In some sense, it is not too surprising that the requirement that ψ be rational, or even just conformal, should determine the conformal structure. A generic point in $x \in \widetilde{J}$ has d^k pre-images under $\psi^{(k)}$; thus, if the conformal structure were fixed in even one small neighborhood of x, then the requirement that ψ act conformally would fix the conformal structure in all of the d^k preimages of that neighborhood; and the union of such neighborhoods, taken over all k, can be shown to be dense and of full measure in $\widetilde{J}$.

We stress, however, that for the random trees described in Section 1.1, we do not have a nice automorphism such as ψ. Although our models are self similar *in law*, an actual instance of the peanosphere has no *exact* self-similarity of the type one encounters for Julia sets, and no natural polynomial or rational dynamics. We will need to use a different set of tools to construct what one could call a "conformal mating" in this context.

2.2 Bottlenecks, baby universes and Liouville duality

Here we remark that the idea of producing "forested wedges" and "forested lines" as trees of quantum disks is also not without precedent. In the physics literature, such objects have been heuristically described in various ways and are known as "Liouville quantum gravity with parameter $\gamma' > 2$" where $\gamma' = 4/\gamma$. (This is related to the fact that they encode $\mathrm{SLE}_{\kappa'}$ paths where $\kappa' = 16/\kappa$.) They are expected to be scaling limits of random simply connected maps with a critical number of domains cut off by small bottlenecks, as first constructed with discrete matrix models in [DDSW90, Kor92, AGBC93, Dur94, ADJ94]. (See also [JM92].)

The corresponding Liouville measure was first heuristically considered for $\gamma' > 2$ in [Kle95, KH95, KH96], in the so-called "other gravitational dressing" of the Liouville potential, or "dual branch of gravity," leading in particular to a *dual* version of the KPZ relation, extended to $\gamma' > 2$. However, the limit of the regularized Liouville bulk measure (1.1) (and of the boundary one (1.2)) actually *vanishes* for $\gamma' \geq 2$: $\lim_{\varepsilon \to 0} \varepsilon^{\gamma'^2/2} e^{\gamma' h_\varepsilon(z)} dz = 0$. This is a quite general phenomenon, first observed by Kahane in the eighties [Kah85] in the case of the so-called *Gaussian multiplicative chaos*, inspired by Mandelbrot's cascade model [Man72].

For the self-dual critical value, $\gamma = \gamma' = 2$, the Liouville measure was recently constructed and shown to be non-atomic using the so-called derivative martingale [DRSV14a, DRSV14b]. For $\gamma' > 2$, however, a precise mathematical description of Liouville duality requires additional probabilistic machinery, which we now describe.

We first recall that a forested wedge may be obtained by beginning with the tree of circles described by Figure 1.7 (if one cuts out the gray shaded regions) and then gluing the boundary of an independent quantum disk (with the given boundary length) onto each of these circles. That procedure produces something like a tree of quantum disks.

We next remark that there is a variant of this procedure that produces a "tree" of spheres (instead of a tree of disks). This tree is constructed as a quotient of the tree of circles described by Figure 1.7 (ignoring the gray filings). Recall that given a parameterized circle of length T, one can map it into the peanosphere described by an excursion of a correlated Brownian motion into the interior of a quadrant (starting and ending at the corner of the quadrant), as in Figure 1.1. Indeed this sphere may be understood as the quotient of the length T circle described by the equivalences induced by the pair of Brownian motions. If one applies a similar procedure to each of the circles in Figure 1.7 (ignoring the gray filings) one obtains a variant of the forested wedge discussed above: it is a"tree of quantum spheres" rather than a"tree of quantum disks." The individual branches of (spheres rooted at a given sphere) are sometimes called "baby universes" of *dual* parameter $\gamma = 4/\gamma'$, $\gamma < 2 < \gamma'$.

The paragraphs above (together with related discussion in introduction) comprise the first complete and fully rigorous description of these trees of disks and spheres. However, some closely related objects have been addressed mathematically (by two of the current authors, among others), as we will now explain. In the literature on these pinched surfaces, it is often natural to single out a "principal bubble" that can be conformally parameterized by a domain D in $\mathbf{C}$. One then obtains an atomic measure on that domain by replacing each tree branch rooted at a point in D by an atom whose mass is the length of the original Lévy excursion corresponding to that branch. (This is one measure of the "size" of the tree.)

Under this perspective, one way to rigorously construct the singular quantum measures $\mu_{\gamma'}$ with $\gamma' > 2$ (without developing the entire trees of disks or spheres, as we do here) has been presented in [DS09, Dup10]. It uses the dual measure μ_γ, $\gamma = 4/\gamma' < 2$, and the additional randomness of sets of point masses $\{z_i : i \in \mathbf{N}\}$ where finite amounts of quantum area $\mu_{\gamma'}(z_i)$ are *localized*. The pair $\{(\mu_{\gamma'}(z_i), z_i) : i \in \mathbf{N}\}$ is distributed as a Poisson point process (p.p.p.) $\mathcal{N}_{\gamma'}(du, dz)$ on $\mathbf{R}_+ \times D$, with intensity measure $\vartheta_\theta \otimes \mu_\gamma$, where $\vartheta_\theta(du) := u^{-1-\theta} du$ and du denotes Lebesgue measure on $\mathbf{R}_+$, with $\theta := 4/\gamma'^2 \in (0, 1)$. The quantum measure for $\gamma' > 2$ is then *purely atomic*,

$$\mu_{\gamma'}(dz) := \int_0^\infty u \, \mathcal{N}_{\gamma'}(du, dz), \quad \gamma' > 2.$$

A slightly different, but equivalent construction was proposed in the context of Gaussian multiplicative chaos [BJRV13].

2.3 Scaling exponents and KPZ

Historically, one of the major goals of the conformal field theory and quantum gravity literature has been an understanding of the scaling dimensions and exponents associated to random fractal sets. For example, one might ask for the dimension of the set of double points of an $\mathrm{SLE}_{\kappa'}$ process or the dimension of the intersection of two GFF flow lines of different angles. Similarly, one might ask for the scaling exponent associated to the probability that n independent planar Brownian motions reach a given ball of radius ϵ without intersecting each other.

All of these problems now have *rigorous* solutions in the mathematics literature. Additionally, *heuristic* solutions to most of these problems have appeared (often decades earlier) in the physics literature. We will present citations and review both literatures in Section 11.

Despite the existence of rigorous solutions, the physics arguments still have a good deal of appeal. In many cases they provide the quickest and most satisfying explanation of *why* certain dimensions and exponents are what they are. This is in particular true of the quantum gravity arguments developed by the first co-author that make use of constructions that are similar to the "wedge weldings" that appear in the current paper, along with the so-called KPZ formula (as briefly explained in Section 1.6).

In Section 11 we will revisit some of these heuristic arguments (specifically, the ones that make use of KPZ and welding ideas — we will not address the heuristic arguments based on so-called Coulomb gas techniques) and explain how they fit into the context of the current paper. We will explain how (in light of the results of the current paper) several of these arguments are now quite close to being proofs (although turning them into *actual* proofs would still require some elaboration).

The key idea is to show that the local behavior at a "quantum typical" point in a random fractal X looks like a particular type of α-quantum cone (bulk case) or α-quantum wedge (boundary case). By quantum typical, we mean a point chosen from the measure on X constructed by restricting the γ-LQG measure to the union of the set of balls of quantum mass δ that intersect X, followed by appropriate $\delta \to 0$ rescaling so that the limit is non-trivial. (We will not actually construct these measures in every case here; see [DS11b] for one approach to constructing SLE quantum measures.) As explained in [DS11a, Equation (63)], a quantum typical point in a fractal X of quantum scaling exponent Δ is a point near which the field is α-*thick* where $\alpha = \gamma(1 - \Delta)$. This means that the quantum surface near that point looks locally like an α-quantum cone (bulk case) or wedge (boundary case) [HMP10]. If we have some means of computing α, then we obtain $\Delta = 1 - \alpha/\gamma$.

The results of this paper allow us to obtain α once we know the corresponding weight W. In some cases, one can argue that near a quantum typical point, one sees a welding of a number of different types of wedges, and by summing these weights, we then

obtain W, which allows us to compute α and then Δ. The Euclidean counterparts of the quantum exponents Δ are then obtained from the celebrated Knizhnik-Polyakov-Zamolodchikov (KPZ) relation [KPZ88, DK89, Dav88, DS11a, RV11]. It relates the quantum and Euclidean (expectation) scaling exponents Δ and x of a random fractal X, sampled independently of a γ-LQG surface, as

$$x = \frac{\gamma^2}{4}\Delta^2 + \left(1 - \frac{\gamma^2}{4}\right)\Delta.$$

(See [DS11a, Theorem 1.4] for the bulk version and [DS11a, Theorem 6.1] for the boundary version.) This, in turn, should give the Euclidean dimension of X as $2-2x$ (resp. $1-x$) in the bulk (resp. on the boundary).

3 Preliminaries

This section assembles a few basic facts about local times, Bessel processes, and $\mathrm{SLE}_\kappa(\rho)$. The reader who is already well versed with these topics may be able to skim or skip much of this section, referring back as needed for reference. However, one should take note of the forward and reverse symmetries of $\mathrm{SLE}_\kappa(\rho)$ presented in Section 3.4. These are relatively straightforward observations, but they are nonetheless interesting, and we have not found them articulated elsewhere in the literature.

We begin with a discussion of the time-reversal of Markov processes using local times in Section 3.1. We recall that it is true in some generality that the *excursions* a Markov process makes away from a fixed value have a Poissonian structure when parameterized by a *local time* corresponding to that value, and we formulate a statement of the fact that this remains true when time is reversed. Next, in Section 3.2, we give a brief overview of some important properties of Bessel processes and derive a few facts about their time reversals. In Section 3.3 we recall the definition of the forward and reverse $\mathrm{SLE}_\kappa(\rho)$ processes in the chordal, radial, and whole-plane settings. Finally, in Section 3.4 we combine the results of Section 3.1 with Section 3.2 to establish the interesting forward/reverse symmetries for $\mathrm{SLE}_\kappa(\rho)$ that we mentioned above.

3.1 Reversing processes using local time

Recall that a Feller process [Kal02, Chapter 17] with semigroup P^t is said to be reversible with respect to a measure μ if for all bounded and continuous functions f, g we have that

$$\int f P^t(g) d\mu = \int g P^t(f) d\mu. \tag{3.1}$$

Since we are motivated by the study of radial and chordal SLE variants, we will be particularly interested in the case that the state space $\mathcal{X}$ is either the line $\mathbf{R}$ or unit circle $\mathbf{S}^1$. If this is the case *and* P^t admits continuous transition densities $p^t(x,y)$ with respect to Lebesgue measure *and* μ has a continuous density π with respect to Lebesgue measure, then we note that (3.1) is equivalent to

$$\pi(x)p^t(x,y) = \pi(y)p^t(y,x) \quad \text{for all} \quad x,y \in \mathcal{X}. \tag{3.2}$$

The main result of this section is the following.

Proposition 3.1. *Suppose that X is a continuous Feller process on $\mathcal{X} \in \{\mathbf{R}, \mathbf{S}^1\}$ with a family of continuous transition densities $p^t(x,y)$. Assume that X is also a semimartingale and is reversible with respect to a measure μ which has a continuous density with respect to Lebesgue measure on $\mathcal{X}$. Fix $a \in \mathcal{X}$, let ℓ be the local time of X at a, and assume that $\mathbf{P}[\ell_\infty = \infty] = 1$. For each $u > 0$, let $T_u = \inf\{t > 0 : \ell_t > u\}$ be the right-continuous inverse of ℓ. Then we have for each $u > 0$ that*

$$(X_{T_u - t} : t \in [0, T_u]) \stackrel{d}{=} (X_t : t \in [0, T_u]).$$

The reason that we assume that X is a semimartingale is that it implies [Kal02, Proposition 19.14] that the structure of the set $\{t : X_t = a\}$ is such that the Itô excursion decomposition (stated as Theorem 3.2 below) applies. Proposition 3.1 is not stated in maximal generality; the hypotheses above both fit our setting and keep the proof simple.

Assume that we have the same hypotheses as in Proposition 3.1. For each $\epsilon \geq 0$, let $\mathcal{E}(\epsilon)$ be the set of continuous functions $\phi\colon [0,T] \to \mathcal{X}$ with $T \geq \epsilon$ and $\phi(0) = \phi(T) = a$. Suppose that X is as in Proposition 3.1 and let ν be the Itô excursion measure associated with the excursions that X makes from a. That is, ν is the σ-finite measure on $\mathcal{E} = \mathcal{E}(0)$ with the following two properties:

1. For each $\epsilon > 0$, $\nu(\mathcal{E}(\epsilon)) < \infty$ and
2. The law of the sequence of excursions $(X^{j,\epsilon})$ that X makes from a with length at least ϵ (with each such excursion shifted in time so the excursions start at time 0) is distributed i.i.d. according to $\nu(\cdot \,|\, \mathcal{E}(\epsilon))$.

(See [Kal02, Chapter 19] for additional introduction to the Itô excursion measure.) Let $\mathcal{E}(0;X)$ be the set of all excursions that X makes from a (with time shifted to start from time 0). For each excursion $e \in \mathcal{E}(0;X)$, we let $\ell(e)$ be the value of ℓ at the start time of the excursion under X. We now state the Itô excursion decomposition for X. (See also [Kal02, Theorem 19.11 and Proposition 19.14].) This is the first ingredient in the proof of Proposition 3.1.

Theorem 3.2. *Let du be Lebesgue measure on $\mathbf{R}_+$ and let ν be the Itô excursion measure of X. Then the process $\{(\ell(e), e) : e \in \mathcal{E}(0; X)\}$ is distributed as a p.p.p. on $\mathbf{R}_+ \times \mathcal{E}$ with intensity measure $du \otimes \nu$.*

The equivalence of the semimartingale local time and excursion local time established in [Kal02, Proposition 19.14] is stated for processes taking values in $\mathbf{R}$, however the proof works verbatim for processes taking values in $\mathbf{S}^1$.

We emphasize that the Itô excursion decomposition itself does not require that X satisfy all of the assumptions of Proposition 3.1. These assumptions are only needed for our proof of Proposition 3.1. The next important ingredient in the proof of Proposition 3.1 is the following lemma regarding the invariance of the Itô excursion measure under time-reversal.

Lemma 3.3. *Assume that X is as in the statement of Proposition 3.1. Let ν be the Itô excursion measure of X associated with the excursions that X makes from a. Then ν is invariant under time-reversal. That is, if $\epsilon > 0$ and Y is sampled according to $\nu(\cdot \,|\, \mathcal{E}(\epsilon))$ and T is the length of Y then*

$$(Y_t : t \in [0, T]) \stackrel{d}{=} (Y_{T-t} : t \in [0, T]). \tag{3.3}$$

Proof. Let π be the density of μ with respect to Lebesgue measure on $\mathcal{X}$. By reversibility, for all $t > 0$ we then have that (recall (3.2))

$$p^t(x, y) = \frac{\pi(y)}{\pi(x)} p^t(y, x) \quad \text{for all} \quad x, y \in \mathcal{X} \quad \text{with} \quad \pi(x), \pi(y) > 0. \tag{3.4}$$

Iterating (3.4), for any $x_1, \ldots, x_{k+1} \in \mathcal{X}$ such that $\pi(x_j) > 0$ for each $1 \leq j \leq k+1$ and for any $t_1, \ldots, t_k > 0$ we have that

$$\prod_{j=1}^{k} p^{t_j}(x_j, x_{j+1}) = \prod_{j=1}^{k} \frac{\pi(x_{j+1})}{\pi(x_j)} p^{t_j}(x_{j+1}, x_j) = \frac{\pi(x_{k+1})}{\pi(x_1)} \prod_{j=1}^{k} p^{t_j}(x_{j+1}, x_j).$$

In particular, if $x_1 = x_{k+1}$, then

$$\prod_{j=1}^{k} p^{t_j}(x_j, x_{j+1}) = \prod_{j=1}^{k} p^{t_j}(x_{j+1}, x_j).$$

This implies that the conditional law of X given $X_0 = a$ and $X_t = a$ for $t > 0$ fixed is invariant under time-reversal.

Fix $\epsilon > 0$, sample Y from $\nu(\cdot \,|\, \mathcal{E}(\epsilon))$, and let T be the length of Y. We will now show that (3.3) holds. For each $\delta > 0$, let $\tau_\delta = \inf\{s \geq 0 : |Y_s - a| = \delta\}$ and let

$\sigma_\delta = \sup\{s \leq T : |Y_t - a| = \delta\}$. Let $S_\delta = \sigma_\delta - \tau_\delta$ and $Y_t^\delta = Y_{t+\tau_\delta}$ for $t \in [0, S_\delta]$. Note that $\tau_\delta \downarrow 0$ and $\sigma_\delta \uparrow T$ as $\delta \to 0$ by continuity and since $Y_t \neq a$ for $t \in (0, T)$. Consequently, it suffices to show for each $\delta > 0$ that

$$(Y_t^\delta : t \in [0, S_\delta]) \stackrel{d}{=} (Y_{S_\delta - t}^\delta : t \in [0, S_\delta]). \tag{3.5}$$

Assume for simplicity that $\mathcal{X} = \mathbf{R}$; the case that $\mathcal{X} = \mathbf{S}^1$ is analogous. Given S_δ and that $Y_t > a$ for $t \in (0, T)$, we note that we can sample from the conditional law of Y^δ by generating a sample of X with $X_0 = a + \delta$ and $X_{S_\delta} = a + \delta$ conditioned on the positive probability event that $X_t \neq a$ for $t \in [0, S_\delta]$. Since this event is invariant under time-reversal and, as explained earlier, the law of a bridge of X from $a + \delta$ to $a + \delta$ of length S_δ is also invariant under time-reversal, we get that (3.5) holds in this case. The case that $Y_t < a$ for $t \in (0, T)$ is analogous. Therefore (3.3) follows. □

Proof of Proposition 3.1. We note that we can generate a sample from the law of $X_{T_u - t}$ by sampling first the p.p.p. of excursions associated with X as in Theorem 3.2, and then running the excursions backwards starting at local time u until reaching local time 0. The result follows since Lebesgue measure is invariant under reflection and, by Lemma 3.3, the Itô excursion law for X is invariant under time-reversal. □

3.2 Bessel processes

In this section, we will recall a few facts about Bessel processes which will play an important role in this article. We direct the reader to [RY99, Chapter XI] for an in-depth overview of Bessel processes.

Fix $\delta \in \mathbf{R}$ and $x \geq 0$. The squared δ-dimensional Bessel process starting from x^2 is given by the unique strong solution to the SDE

$$dZ_t = 2\sqrt{Z_t} dB_t + \delta dt, \quad Z_0 = x^2 \tag{3.6}$$

where B is a standard Brownian motion. Following [RY99], we will denote this process by BESQ^δ (and suppress the dependency on the starting point). When $\delta > 0$, the solution to (3.6) exists for all $t \geq 0$, while 0 is an absorbing state for $\delta \leq 0$. The δ-dimensional Bessel process X_t starting from x is given by $\sqrt{Z_t}$ where Z_t is as in (3.6). Following [RY99], we will denote this process by BES^δ (and suppress the dependency on the starting point). An application of Itô's formula shows that X_t satisfies the SDE

$$dX_t = dB_t + \frac{\delta - 1}{2} \cdot \frac{1}{X_t} dt, \quad X_0 = x \tag{3.7}$$

at least at those times when $X_t \neq 0$.

There are three important ranges of δ values which determine how X interacts with 0:

1. If $\delta \geq 2$, then X_t almost surely does not hit 0 except if $X_0 = 0$ in which case $X_t \neq 0$ for all $t > 0$, so X_t in fact solves (3.7) for all times and is a semimartingale.

2. If $\delta \in (1, 2)$, then X_t hits 0 in finite time almost surely. Nevertheless, X_t satisfies (3.7) in the integrated sense for all t and is a semimartingale.

3. If $\delta \in (0, 1]$, then X_t hits 0 in finite time almost surely. In order to view X_t as a solution of (3.7) for those times when X is interacting with 0 it is necessary to introduce a principle value correction (see [RY99, Exercise 1.26, Chapter XI]). For $\delta = 1$, X_t is a semimartingale while for $\delta \in (0, 1)$ it is not.

In the case that $\delta \in (0, 2)$, X_t is instantaneously reflecting at 0. The interaction of a BES^δ with $\delta \in (0, 1]$ with 0 will not play a role in this article, so we will not delve into the technicalities associated with this regime.

We now show that a Bessel process can be viewed as a time-changed geometric Brownian motion (see [RY99, Exercise 1.28, Chapter XI]).

Proposition 3.4. *Let X_t be a BES^δ started at some positive non-zero value. Then $\log X_t$ reparameterized by its quadratic variation (and stopped the first time X_t reaches 0 or time reaches ∞) is equal in distribution to $B_t + \frac{\delta-2}{2}t$ where B is a standard Brownian motion. Conversely, if B is a standard Brownian motion and $a \in \mathbf{R}$, then $X_t = \exp(B_t + at)$ reparameterized by its quadratic variation evolves as a BES^δ with $\delta = 2a + 2$.*

Proof. Let X_t be a BES^δ. An application of Itô's formula yields that

$$d \log X_t = \frac{1}{X_t} dB_t + \frac{\delta - 2}{2X_t^2} dt. \tag{3.8}$$

Reparameterizing $\log X_t$ by its quadratic variation $ds = X_t^{-2} dt$ thus yields a standard Brownian motion plus a linear drift term $\frac{\delta-2}{2}s$. The converse statement follows from an analogous argument. □

Proposition 3.4 leads to the following important fact regarding the time-reversal of a Bessel process.

Proposition 3.5. *Fix $\delta < 2$ and $x > 0$. Suppose that X_t is a BES^δ started at $x > 0$ and let $\tau = \inf\{t \geq 0 : X_t = 0\}$. Then the time-reversal $X_{\tau - t}$ has the law of a $\mathrm{BES}^{\widetilde{\delta}}$ with*

$$\widetilde{\delta} = 4 - \delta > 2, \tag{3.9}$$

stopped at the last time that it hits x.

Note that $\delta < 2$ implies $\widetilde{\delta} > 2$ and that a $\mathrm{BES}^{\widetilde{\delta}}$ process almost surely does not hit 0.

Proof of Proposition 3.5. This follows since Proposition 3.4 implies that the time-reversal $\log X_{\tau - t}$ when parameterized by its quadratic variation evolves as a Brownian motion with linear drift $-\frac{\delta-2}{2}$. Thus $X_{\tau-t}$ evolves as a $\mathrm{BES}^{\widetilde{\delta}}$ where $\widetilde{\delta}$ satisfies $-\frac{\delta-2}{2} = \frac{\widetilde{\delta}-2}{2}$. Solving for $\widetilde{\delta}$ yields (3.9), as desired. □

We will explain in Section 3.4 how we can use the results of Section 3.1 to time-reverse a BES^{δ} with $\delta \in (0, 2)$ stopped when its local time at 0 first reaches a given value.

As a second application of Proposition 3.4, we will give a description of the law of a standard Brownian motion with negative linear drift conditioned to exceed a given positive value.

Lemma 3.6. *Let B_t be a standard Brownian motion starting from 0, fix $a < 0$, and let $X_t = B_t + at$. Fix $C > 0$ and let E_C be the event $\{\sup_{t \geq 0} X_t \geq C\}$. Then the conditional law of X given E_C can be sampled from as follows.*

1. *Sample a standard Brownian motion X^1 starting from 0 with linear drift $-a > 0$ and let τ be the first time that X^1 hits C.*
2. *Sample a standard Brownian motion X^2 starting from C with linear drift $a < 0$.*
3. *Concatenate the processes $X^1|_{[0,\tau]}$ and $X^2(\cdot - \tau)$.*

Proof. There are various ways to prove this, but we find it instructive to use the Bessel process correspondence of Proposition 3.4. (The connection to Bessel processes is actually our motivation for considering this lemma in the first place.) Let Z be given by e^{X_t} with time reparameterized by quadratic variation so that $d\langle Z \rangle_t = dt$. By Proposition 3.4, Z is a BES^{δ} with $\delta = 2a + 2$. Let τ_C (resp. τ_0) be the first time that Z hits e^C (resp. 0). Then $E_C = \{\tau_C < \tau_0\}$. Note that $Z_t^{2-\delta}$ is a local martingale for Z_t and that $Z_{\tau_C \wedge \tau_0}^{2-\delta} = e^{(2-\delta)C} \mathbf{1}_{E_C}$. By the Girsanov theorem [KS91, RY99], weighting the law of Z_t by $Z_t^{2-\delta}$ yields the law of a $\mathrm{BES}^{4-\delta}$; note that $4 - \delta = 2 - 2a > 2$. It thus follows that the law of Z conditional on E_C can be sampled from as follows.

1. Sample a Bessel process Z^1 of dimension $2 - 2a$ and let τ be the first time that Z^1 hits e^C
2. Sample a Bessel process Z^2 of dimension $2 + 2a$ starting from e^C
3. Concatenate the processes $Z^1|_{[0,\tau]}$ and $Z^2(\cdot - \tau)$

This proves the result because we can sample from the law of X given E_C by sampling from the law of Z given E_C and then taking X to be $\log Z$ reparameterized according to its quadratic variation. □

Remark 3.7. Fix $\delta \in (0,2)$ and let $\nu_\delta^{\mathrm{BES}}$ denote the Itô excursion measure associated with a BES^δ process. We can express ν_δ as follows:

1. Pick a "lifetime" t according to the σ-finite measure
$$c_\delta t^{\delta/2-2} dt \tag{3.10}$$
where c_δ is a constant which depends only on δ and dt denotes Lebesgue measure on $\mathbf{R}_+$, and then
2. Run a $\mathrm{BES}^{4-\delta}$ bridge of length t from 0 to 0.

(See [PY82] as well as the text just after [PY96, Theorem 1].)

For each $e \in \mathcal{E}$, we let e^* be the maximum value taken on by e. Suppose that Λ is a p.p.p. chosen from $du \otimes \nu_\delta^{\mathrm{BES}}$. Let $\Lambda^* = \{(u, e^*) : (u,e) \in \Lambda\}$. Then, as explained just after [PY96, Theorem 1], Λ^* is a p.p.p. on $\mathbf{R}_+ \times \mathbf{R}_+$ with intensity measure $du \otimes \nu_\delta^*$ where $\nu_\delta^*(dt) = t^{\delta-3}dt$ where dt is Lebesgue measure on $\mathbf{R}_+$. Moreover, we can use ν_δ^* to given a second description of Itô's excursion law for a BES^δ process as follows:

1. Pick t from the measure ν_δ^*, and then
2. Join back to back two independent $\mathrm{BES}^{4-\delta}$ processes starting from 0 and each run until the first time that it hits t.

Note that, although 0 is an absorbing state for a BES^δ process with $\delta \le 0$, we can still make sense of the Itô excursion measure $\nu_\delta^{\mathrm{BES}}$ for the "excursions" that such a process makes from 0 by extending the definition described above. It is just not possible to concatenate the excursions from a p.p.p. on $\mathbf{R}_+ \times \mathcal{E}$ with intensity measure $du \otimes \nu_\delta^{\mathrm{BES}}$ with $\delta \le 0$ to form a continuous process.

3.3 $\mathrm{SLE}_\kappa(\rho)$ processes

3.3.1 Chordal $\mathrm{SLE}_\kappa(\rho)$

Fix $\rho_1, \ldots, \rho_n \in \mathbf{R}$ and $x_1, \ldots, x_n \in \overline{\mathbf{H}}$. Recall from [SW05] that the SDE which drives a forward $\mathrm{SLE}_\kappa(\underline{\rho})$ process is given by

$$\begin{aligned} dW_t &= \sum_{i=1}^n \mathrm{Re}\left(\frac{-\rho_i}{f_t(x_i)}\right) dt + \sqrt{\kappa} dB_t, \\ df_t(x_i) &= \frac{2}{f_t(x_i)} dt - dW_t, \quad f_0(x_i) = x_i \quad \text{for} \quad i = 1, \ldots, n. \end{aligned} \tag{3.11}$$

The SDE for the driving process of a reverse $\mathrm{SLE}_\kappa(\underline{\rho})$ is given by

$$\begin{aligned} dW_t &= \sum_{i=1}^{n} \mathrm{Re}\left(\frac{-\rho_i}{f_t(x_i)}\right) dt + \sqrt{\kappa} dB_t, \\ df_t(x_i) &= -\frac{2}{f_t(x_i)} dt - dW_t, \quad f_0(x_i) = x_i \quad \text{for} \quad i = 1, \ldots, n. \end{aligned} \tag{3.12}$$

We will often use V^i to denote the processes $f_t(x_i)$ if we do not wish to emphasize the x_i. If there is only one force point, we will often use V to denote the process $f_t(x_1)$. Note that (3.11) and (3.12) differ only in that the force points in (3.11) evolve under the forward Loewner flow while in (3.12) they evolve under the reverse Loewner flow. In both the forward and reverse evolutions, under our convention, a positive ρ_i corresponds to a force point that pushes W_t away from itself.

The existence and uniqueness of solutions to (3.11) is discussed in detail in [MS12a, Section 2] in the case that there are only boundary force points. In particular, a precise notion of a solution to (3.11) is introduced in [MS12a, Definition 2.1] and it is shown in [MS12a, Theorem 2.1] that there exists a unique solution to (3.11) up until the **continuation threshold** is hit. This is the first time t that the sum of the weights of the force points which are immediately to the left of W_t is not more than -2 or the sum of the weights of the force points which are immediately to the right of W_t is not more than -2. Combining this result with the Girsanov theorem [KS91, RY99], one gets existence and uniqueness of solutions to (3.11) (with interior force points) until the first time that either the continuation threshold is hit or the imaginary part of one of the interior force points is equal to 0.

The arguments given in [MS12a, Section 2] also lead to existence and uniqueness results for (3.12) in the case of boundary force points. In this article, it will be important for us to consider (3.12) in the case of a force point starting infinitesimally above 0. We will establish the existence and uniqueness of such solutions in the following proposition.

Proposition 3.8. *Suppose that $\rho < \frac{\kappa}{2} + 4$. There exists a unique law on pairs (W, Z) of continuous processes such that $W_0 = Z_0 = 0$, $\mathbf{P}[\mathrm{Im}(Z_t) > 0] = 1$ for all $t > 0$, and (W, Z) solves* (3.12) *for all $t > 0$.*

In the statement of Proposition 3.8, Z_t plays the role of $f_t(x)$ in (3.12).

Proof of Proposition 3.8. Suppose that $z \in \mathbf{H}$. Then the time evolution Z of the force point associated with a centered, reverse $\mathrm{SLE}_\kappa(\rho)$ with a single force point of weight ρ starting from $z \in \overline{\mathbf{H}}$ is given by

$$dZ_t = -\frac{2}{Z_t} dt - dW_t = -\frac{2}{Z_t} dt + \mathrm{Re}\,\frac{\rho}{Z_t} dt - \sqrt{\kappa} dB_t. \tag{3.13}$$

Let $\theta_t = \arg Z_t$ and $I_t = \log \operatorname{Im} Z_t$. Now,

$$d\operatorname{Im} Z_t = -\operatorname{Im} \frac{2}{Z_t} dt,$$

so

$$dI_t = d \log \operatorname{Im} Z_t = -\frac{1}{\operatorname{Im} Z_t} \operatorname{Im} \frac{2}{Z_t} dt = \frac{2}{|Z_t|^2} dt.$$

Also,

$$\begin{aligned} d \log Z_t &= -\frac{\sqrt{\kappa}}{Z_t} dB_t + \frac{1}{Z_t} \operatorname{Re} \frac{\rho}{Z_t} dt - \frac{2 + \kappa/2}{Z_t^2} dt, \\ d\theta_t &= -\operatorname{Im} \frac{\sqrt{\kappa}}{Z_t} dB_t + \operatorname{Im} \frac{1}{Z_t} \operatorname{Re} \frac{\rho}{Z_t} dt - \operatorname{Im} \frac{2 + \kappa/2}{Z_t^2} dt. \end{aligned}$$

If we reparameterize time by setting $ds = |Z_t|^{-2} dt$, then we have $dI_{t(s)} = 2ds$ and for a Brownian motion $\widehat{B}_s$ we have $d\widehat{B}_s := dB_t / |Z_t|$. We then have that,

$$d\theta_{t(s)} = \sqrt{\kappa} \sin \theta_{t(s)} d\widehat{B}_s + \left(2 + \frac{\kappa}{2} - \frac{\rho}{2}\right) \sin(2\theta_{t(s)}) ds. \tag{3.14}$$

It is easy to see from that if we take $z = i\epsilon$ then the law of $(I_{t(s)}, \theta_{t(s)})$ converges weakly with respect to the topology of local uniform convergence as $\epsilon \to 0$. Indeed, to see this we let μ be the measure on $[0, \pi]$ given by

$$\mu(d\theta) = \sin^a(\theta) d\theta \quad \text{where} \quad a = \frac{8 - 2\rho}{\kappa} \tag{3.15}$$

and $d\theta$ denotes Lebesgue measure. By noting that the generator for SDE (3.14) is self-adjoint with respect to the space $L^2([0, \pi], \mu)$, it follows that μ gives a reversible measure for (3.14). (The equivalence between reversibility and the generator being self-adjoint is given, for example, in [Lig05, Proposition 5.3].) Note, in particular, that $a > -1$ provided $\rho < \frac{\kappa}{2} + 4$. In this case, μ (after normalization) gives the unique stationary distribution to (3.14) to which any solution converges exponentially fast uniformly in the location of the starting point. This proves the existence component of the proposition since to sample (W, Z) we can first sample the infinite time solution $(I_{t(s)}, \theta_{t(s)})$ to the dynamics above and then generate (W, Z) from $(I_{t(s)}, \theta_{t(s)})$ by inverting the time change. Uniqueness follows similarly (we can couple any two solutions (W, Z) and $(\widetilde{W}, \widetilde{Z})$ together onto a common probability space so that in each unit of $t(s)$ time there is a uniformly positive chance that the solutions will coalesce and then stay together). □

Suppose that W is a solution to (3.12). Then the centered reverse chordal $\mathrm{SLE}_\kappa(\underline{\rho})$ process is given by the family of conformal maps (f_t) which solve the SDE:

$$df_t(z) = -\frac{2}{f_t(z)} dt - dW_t, \quad f_0(z) = z. \tag{3.16}$$

In some cases, it will be convenient to refer to the (uncentered) reverse $\mathrm{SLE}_\kappa(\underline{\rho})$ Loewner flow. This is given by the family of conformal maps (g_t) which solve the ODE

$$dg_t(z) = -\frac{2}{g_t(z) - W_t}dt, \quad g_0(z) = z. \tag{3.17}$$

That is, $g_t = f_t + W_t$. The force points for the uncentered flow have the same relationship with the force points of the centered flow.

The centered (resp. uncentered) forward chordal $\mathrm{SLE}_\kappa(\underline{\rho})$ evolution is defined in the same way except the minus sign before $2/f_t(z)$ (resp. $2/(g_t(z) - W_t)$) in (3.16) (resp. (3.17)) is not present in the forward case.

In the special case of a single force point $x \in \mathbf{R}$, (3.16) evaluated at x takes the form

$$df_t(x) = \frac{-2}{f_t(x)}dt - dW_t = \frac{-2+\rho}{f_t(x)}dt - \sqrt{\kappa}dB_t. \tag{3.18}$$

Comparing with (3.7), we see that $f_t(x)/\sqrt{\kappa}$ evolves as a BES^δ where $(\delta - 1)/2 = (\rho - 2)/\kappa$, i.e.,

$$\delta = 1 + \frac{2(\rho - 2)}{\kappa}. \tag{3.19}$$

In particular, the first time t that $f_t(x) = 0$ is finite almost surely if and only if $\rho < \frac{\kappa}{2} + 2$ so that $\delta < 2$. By combining this with Proposition 3.8, we see that if $\rho < \frac{\kappa}{2} + 2$ then we can always "continue" such a reverse $\mathrm{SLE}_\kappa(\rho)$ Loewner flow when the force point hits 0 by mapping it into the interior. If, in addition, $\rho > -2 - \frac{\kappa}{2}$ so that $\delta \in (0, 2)$, then we can also "continue" a reverse $\mathrm{SLE}_\kappa(\rho)$ Loewner flow when the force point hits 0 by reflecting it off 0 in $\mathbf{R}$. We will consider both types of continuations in this article.

Similarly, if (f_t) corresponds to a centered forward Loewner flow with a single force point of weight ρ located at x, then $f_t(x)/\sqrt{\kappa}$ evolves as a BES^δ where

$$\delta = 1 + \frac{2(\rho + 2)}{\kappa}. \tag{3.20}$$

The reason for the difference from (3.19) can be seen by considering the case $\rho = 0$. In the reverse process, the Loewner drift is pulling $f_t(x)$ toward the origin, while in the forward process the Loewner drift is pushing $f_t(x)$ away from the origin. In both cases ρ indicates a quantity of additional force pushing $f_t(x)$ away from the origin.

3.3.2 Radial and whole-plane $\mathrm{SLE}_\kappa(\rho)$

Let

$$\Psi(u, z) = \frac{u + z}{u - z} \quad \text{and} \quad \Phi(u, z) = z\Psi(u, z).$$

A radial SLE_κ in $\mathbf{D}$ targeted at 0 is the random growth process (K_t) in $\mathbf{D}$ starting from a point on $\partial\mathbf{D}$ growing towards 0 which is described by the random family of conformal maps (g_t) which solve the radial Loewner equation:

$$\partial_t g_t(z) = \Phi(U_t, g_t(z)), \quad g_0(z) = z. \tag{3.21}$$

Here, $U_t = e^{i\sqrt{\kappa}B_t}$ where B_t is a standard Brownian motion; U is referred to as the driving function for the radial Loewner evolution. The set K_t is the complement of the domain of g_t in $\mathbf{D}$ and g_t is the unique conformal transformation $\mathbf{D} \setminus K_t \to \mathbf{D}$ fixing 0 with $g_t'(0) > 0$. Time is parameterized by the logarithmic conformal radius as viewed from 0 so that $\log g_t'(0) = t$ for all $t \geq 0$.

As in the chordal setting, radial $\mathrm{SLE}_\kappa(\rho)$ is a generalization of radial SLE in which one keeps track of one extra marked point. We say that a pair of processes (U, V), each of which takes values in $\mathbf{S}^1$, solves the radial $\mathrm{SLE}_\kappa(\rho)$ equation for $\rho \in \mathbf{R}$ with a single boundary force point of weight ρ provided that

$$\begin{aligned} dU_t &= -\frac{\kappa}{2}U_t dt + i\sqrt{\kappa}U_t dB_t + \frac{\rho}{2}\Psi(V_t, U_t)dt \\ dV_t &= \Psi(U_t, V_t)dt. \end{aligned} \tag{3.22}$$

A radial $\mathrm{SLE}_\kappa(\rho)$ is the growth process corresponding to the solution (g_t) of (3.21) when U is taken to be as in (3.22). It is explained in [MS13a, Section 2.1.2] that (3.22) has a unique solution which exists for all time provided $\rho > -2$.

It will often be useful to consider the SDE

$$d\theta_t = \frac{\rho+2}{2}\cot\left(\frac{\theta_t}{2}\right)dt + \sqrt{\kappa}dB_t \tag{3.23}$$

where B is a standard Brownian motion. This SDE can be derived formally by taking a solution (U, V) to (3.22) and then setting $\theta_t = \arg U_t - \arg V_t$ (see [She09, Equation 4.1] for the case $\rho = \kappa - 6$).

Reverse radial SLE_κ is described in terms of the family of conformal maps (g_t) which solve the reverse radial Loewner equation

$$\partial_t g_t(z) = -\Phi(U_t, g_t(z)), \quad g_0(z) = z \tag{3.24}$$

where $U_t = e^{i\sqrt{\kappa}B_t}$ and B is a standard Brownian motion.

Reverse radial $\mathrm{SLE}_\kappa(\rho)$ is a variant of reverse radial SLE_κ in which one keeps track of an extra marked point on $\partial\mathbf{D}$. It is defined in an analogous way to reverse radial SLE_κ except the driving function U_t is taken to be a solution to the SDE:

$$\begin{aligned} dU_t &= -\frac{\kappa}{2}U_t dt + i\sqrt{\kappa}U_t dB_t + \frac{\rho}{2}\Phi(V_t, U_t)dt \\ dV_t &= -\Phi(U_t, V_t)dt. \end{aligned} \tag{3.25}$$

Observe that when $\rho = 0$ this is the same as the driving SDE for ordinary reverse radial SLE_κ.

Whole-plane SLE is a variant of SLE_κ which describes a random growth process K_t where, for each $t \in \mathbf{R}$, $K_t \subseteq \mathbf{C}$ is compact with $\mathbf{C}_t = \mathbf{C} \setminus K_t$ simply connected (viewed as a subset of the Riemann sphere). For each t, we let $g_t \colon \mathbf{C}_t \to \mathbf{C} \setminus \mathbf{D}$ be the unique conformal transformation with $g_t(\infty) = \infty$ and $g_t'(\infty) > 0$. Then g_t solves the whole-plane Loewner equation

$$\partial_t g_t = \Phi(U_t, g_t(z)), \quad g_0(z) = z. \tag{3.26}$$

Here, $U_t = e^{i\sqrt{\kappa}B_t}$ where B_t is a two-sided standard Brownian motion. Equivalently, U is given by the time-stationary solution to (3.22) with $\rho = 0$. Note that (3.26) is the same as (3.21). In fact, for any $s \in \mathbf{R}$, the growth process $2/g_s(K_t \setminus K_s)$ for $s \geq t$ from $\partial\mathbf{D}$ to 0 is a radial SLE_κ process in $\mathbf{D}$. Thus, whole-plane SLE can be thought of as a bi-infinite time version of radial SLE. Whole-plane $\mathrm{SLE}_\kappa(\rho)$ is the growth process associated with (3.26) where U is taken to be the time-stationary solution of (3.21) (see the discussion in [MS13a, Section 2] for more on the existence and convergence to the time-stationary solution to (3.21)).

If (g_t) is the Loewner flow associated with a forward or reverse radial $\mathrm{SLE}_\kappa(\underline{\rho})$ or a whole-plane $\mathrm{SLE}_\kappa(\rho)$ with driving function U_t, then $f_t = U_t^{-1} g_t$ gives the centered Loewner flow.

The continuity of radial and whole-plane SLE_κ for $\kappa \neq 8$ was proved by Rohde and Schramm [RS05] and for $\kappa = 8$ follows by work of Lawler, Schramm, and Werner [LSW04]. The transience of radial and whole-plane SLE_κ was proved by Lawler [Law13]. The continuity and transience of radial and whole-plane $\mathrm{SLE}_\kappa(\rho)$ for $\rho > -2$ is proved in [MS13a].

3.4 Forward/reverse symmetries for $\mathrm{SLE}_\kappa(\rho)$ processes

In this section, we are going to establish several types of forward/reverse $\mathrm{SLE}_\kappa(\rho)$ symmetries. The first of these was also used in [She10] and justified there using the same argument we present below. See also Figure 3.1a for an illustration.

Proposition 3.9. *Suppose that $(\widetilde{f}_t)$ is the centered reverse Loewner flow associated with an $\mathrm{SLE}_\kappa(\widetilde{\rho})$ process with a single force point of weight $\widetilde{\rho} < \frac{\kappa}{2} + 2$ located at $x > 0$. Let $\widetilde{\tau} = \inf\{t \geq 0 : \widetilde{f}_t(x) = 0\}$ and let*

$$\rho = \kappa - \widetilde{\rho}. \tag{3.27}$$

Then $\widetilde{f}_{\widetilde{\tau}}$ maps $\mathbf{H}$ to $\mathbf{H} \setminus \eta_{\widetilde{\tau}}$ where $\eta_{\widetilde{\tau}}$ has the law of the initial segment of a forward $\mathrm{SLE}_\kappa(\rho)$ with a single boundary force point located at 0^+ of weight ρ stopped at some almost surely positive time τ. In particular, if $\widetilde{\rho} = \kappa$, then $\eta_{\widetilde{\tau}}$ has the law of an ordinary SLE_κ stopped at an almost surely positive time τ.

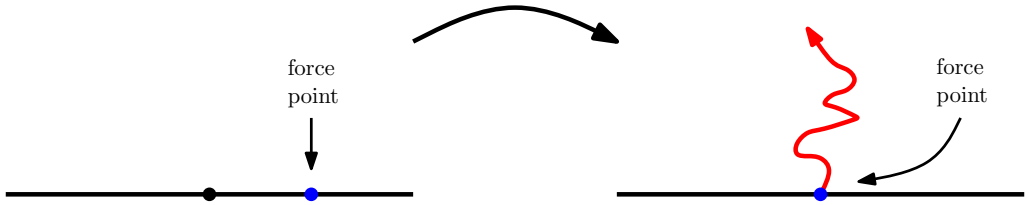

(a) Zipping up until the force point reaches the origin.

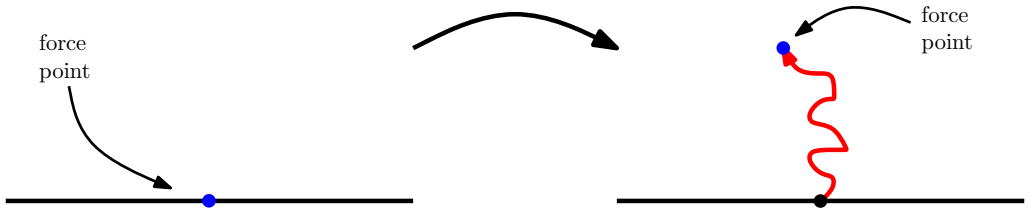

(b) Zipping a force point at the origin into the interior.

Figure 3.1: Two types of forward/reverse symmetry for $\mathrm{SLE}_\kappa(\rho)$. In each case, one can generate the path on the right either by starting with the scenario on the left and zipping up (via reverse $\mathrm{SLE}_\kappa(\widetilde{\rho})$ with the force point as shown) or starting with the scenario on the right and unzipping (i.e., drawing the path on the right as a forward $\mathrm{SLE}_\kappa(\rho)$ with the force point as shown). In the top setting (see Proposition 3.9), we have $\rho = \kappa - \widetilde{\rho}$. In the bottom setting (see Proposition 3.10), we have $\rho = \widetilde{\rho} - 8$.

We note that the time τ is not a stopping time for the filtration generated by the forward $\mathrm{SLE}_\kappa(\rho)$ process in the statement of Proposition 3.9. As we will see in the proof, it is given by the *last* time that the centered forward Loewner flow sends 0^+ to x. Note that the assumption $\widetilde{\rho} < \frac{\kappa}{2} + 2$ implies that $\mathbf{P}[\widetilde{\tau} < \infty] = 1$ in the statement of Proposition 3.9. It also implies that ρ from (3.27) satisfies $\rho > \frac{\kappa}{2} - 2$ and recall that $\frac{\kappa}{2} - 2$ is the critical threshold at or above which forward $\mathrm{SLE}_\kappa(\rho)$ almost surely does not hit its force point.

Proof of Proposition 3.9. Let (W, V) (resp. $(\widetilde{W}, \widetilde{V})$) be the driving process associated with a forward (resp. reverse) $\mathrm{SLE}_\kappa(\rho)$ (resp. $\mathrm{SLE}_\kappa(\widetilde{\rho})$) process with a single boundary force point of weight ρ (resp. $\widetilde{\rho}$) located at 0^+ (resp. $x > 0$). Here, we assume that V (resp. $\widetilde{V}$) is the process which gives the location of the force point for the uncentered Loewner flow. Then we know that $\kappa^{-1/2}(V - W)$ evolves as a BES^δ where δ is as in (3.20). Similarly, $\kappa^{-1/2}(\widetilde{V} - \widetilde{W})$ evolves as a $\mathrm{BES}^{\widetilde{\delta}}$ where $\widetilde{\delta}$ is as in (3.19). Combining (3.19) and (3.20) with (3.9) of Proposition 3.5 gives the relationship

between ρ and $\widetilde{\rho}$. Namely,

$$1 + \frac{2(\rho+2)}{\kappa} = 4 - \left(1 + \frac{2(\widetilde{\rho}-2)}{\kappa}\right),$$

so that ρ and $\widetilde{\rho}$ satisfy the relationship (3.27). This implies that we can couple together (W, V) and $(\widetilde{W}, \widetilde{V})$ such that if we let $\widetilde{\tau} = \inf\{t \geq 0 : \widetilde{V}_t - \widetilde{W}_t = 0\}$ then

$$V_t - W_t = \widetilde{V}_{\widetilde{\tau}-t} - \widetilde{W}_{\widetilde{\tau}-t} \quad \text{for all} \quad t \in [0, \widetilde{\tau}]. \tag{3.28}$$

Under this coupling, we have for all $t \in [0, \widetilde{\tau}]$ that

$$\begin{aligned}
W_t &= V_t + (W_t - V_t) \\
&= \int_0^t \frac{2}{V_s - W_s} ds + (W_t - V_t) \quad \text{(definition of } V\text{)} \\
&= \int_0^t \frac{2}{\widetilde{V}_{\widetilde{\tau}-s} - \widetilde{W}_{\widetilde{\tau}-s}} ds + (\widetilde{W}_{\widetilde{\tau}-t} - \widetilde{V}_{\widetilde{\tau}-t}) \quad \text{(by (3.28))} \\
&= \int_{\widetilde{\tau}-t}^{\widetilde{\tau}} \frac{2}{\widetilde{V}_s - \widetilde{W}_s} ds + (\widetilde{W}_{\widetilde{\tau}-t} - \widetilde{V}_{\widetilde{\tau}-t}) \\
&= \int_0^{\widetilde{\tau}} \frac{2}{\widetilde{V}_s - \widetilde{W}_s} ds - \int_0^{\widetilde{\tau}-t} \frac{2}{\widetilde{V}_s - \widetilde{W}_s} ds + (\widetilde{W}_{\widetilde{\tau}-t} - \widetilde{V}_{\widetilde{\tau}-t}) \\
&= \widetilde{V}_{\widetilde{\tau}-t} - \widetilde{V}_{\widetilde{\tau}} + (\widetilde{W}_{\widetilde{\tau}-t} - \widetilde{V}_{\widetilde{\tau}-t}) \quad \text{(definition of } \widetilde{V}\text{)} \\
&= \widetilde{W}_{\widetilde{\tau}-t} - \widetilde{V}_{\widetilde{\tau}} = \widetilde{W}_{\widetilde{\tau}-t} - \widetilde{W}_{\widetilde{\tau}}.
\end{aligned} \tag{3.29}$$

In the last step, we used that $\widetilde{V}_{\widetilde{\tau}} - \widetilde{W}_{\widetilde{\tau}} = 0$. Since $\widetilde{W}_0 = 0$, we in particular have that

$$W_{\widetilde{\tau}} = -\widetilde{W}_{\widetilde{\tau}}. \tag{3.30}$$

Let (g_t) (resp. $\widetilde{g}_t$) be the forward (resp. reverse) Loewner flow driven by W (resp. $\widetilde{W}$). We also let (f_t) (resp. $(\widetilde{f}_t)$) be the centered forward (resp. reverse) Loewner flow driven by W (resp. $\widetilde{W}$). Let

$$\varphi_t(z) = g_t(\widetilde{g}_{\widetilde{\tau}}(z) - \widetilde{W}_{\widetilde{\tau}}) + \widetilde{W}_{\widetilde{\tau}} = g_t(\widetilde{f}_{\widetilde{\tau}}(z)) - W_{\widetilde{\tau}}. \tag{3.31}$$

(The second equality uses (3.30).) Note that

$$\varphi_{\widetilde{\tau}}(z) = f_{\widetilde{\tau}}(\widetilde{f}_{\widetilde{\tau}}(z)). \tag{3.32}$$

We have that

$$\varphi_t(z) = \widetilde{g}_{\widetilde{\tau}}(z) + \int_0^t \frac{2}{g_s(\widetilde{f}_{\widetilde{\tau}}(z)) - W_s} ds \quad \text{(definition of } \varphi_t \text{ and } g_t\text{)}$$

$$= \widetilde{g}_{\widetilde{\tau}}(z) + \int_0^t \frac{2}{\varphi_s(z) - (W_s + \widetilde{W}_{\widetilde{\tau}})} ds \quad \text{(definition of } \varphi_t\text{)}$$
$$= \widetilde{g}_{\widetilde{\tau}}(z) + \int_0^t \frac{2}{\varphi_s(z) - \widetilde{W}_{\widetilde{\tau}-s}} ds \quad \text{(by (3.29))}.$$

Since $\widetilde{g}_{\widetilde{\tau}-t}$ satisfies the same equation, we must have that

$$f_{\widetilde{\tau}}(\widetilde{f}_{\widetilde{\tau}}(z)) = \varphi_{\widetilde{\tau}}(z) = \widetilde{g}_0(z) = z, \tag{3.33}$$

as desired.

Therefore $\widetilde{f}_{\widetilde{\tau}}$ maps $\mathbf{H}$ to $\mathbf{H} \setminus \eta_{\widetilde{\tau}}$ where $\eta_{\widetilde{\tau}}$ has the law of an initial segment of a forward $\mathrm{SLE}_\kappa(\rho)$, as desired. □

The correspondence between ρ and $\widetilde{\rho}$ derived in Proposition 3.9 takes a rather different form if we consider an interior force point instead of a point on $\mathbf{R}$. See the bottom part of Figure 3.1b for an illustration.

Proposition 3.10. *Fix $\widetilde{\rho} < \frac{\kappa}{2} + 4$. Suppose that $(\widetilde{f}_t)$ is the centered reverse Loewner flow associated with an $\mathrm{SLE}_\kappa(\widetilde{\rho})$ process with a single interior force point located infinitesimally above 0. Let $\rho = \widetilde{\rho} - 8$ and let $\widetilde{Z}_t$ denote the evolution of the force point under $\widetilde{f}_t$. For each $r > 0$, let $\widetilde{\tau}_r = \inf\{t > 0 : \mathrm{Im}(\widetilde{Z}_t) = r\}$. The law of $\mathbf{H} \setminus \widetilde{f}_{\widetilde{\tau}_r}(\mathbf{H}) = \eta_{\widetilde{\tau}_r}$ given $\widetilde{Z}_{\widetilde{\tau}_r}$ is that of a forward $\mathrm{SLE}_\kappa(\rho)$ process with a single interior force point of weight ρ located at $\widetilde{Z}_{\widetilde{\tau}_r}$.*

Proof. Repeating the calculations in the proof of Proposition 3.8 using forward $\mathrm{SLE}_\kappa(\rho)$ instead of reverse $\mathrm{SLE}_\kappa(\widetilde{\rho})$ yields

$$d\theta_{t(s)} = \sqrt{\kappa} \sin\theta_{t(s)} d\widehat{B}_s + \left(-2 + \frac{\kappa}{2} - \frac{\rho}{2}\right) \sin(2\theta_{t(s)}) ds, \tag{3.34}$$

and $dI_{t(s)} = -2ds$. We conclude that if we take $\rho = \widetilde{\rho} - 8$, then (3.34) and (3.14) are the same.

By the reversibility of (3.14) and (3.34), this implies that the following is true. Suppose that we fix $r > 0$ and then

1. Sample $Z_r = X + ir$ so that $\arg(Z_r)$ is given by the stationary measure for (3.14),(3.34) as described in (3.15) in the proof of Proposition 3.8.
2. Sample a centered forward $\mathrm{SLE}_\kappa(\rho)$ process (f_t) with a single interior force point of weight ρ located at Z_r.

Then the evolution of $f_t(Z_r)$ considered in the time-interval from 0 to $\inf\{t \geq 0 : \mathrm{Im}(f_t(Z_r)) = 0\}$ has the same law as $\widetilde{Z}_{\widetilde{\tau}_r - t}$ for $t \in [0, \widetilde{\tau}_r]$. Therefore the result follows from the argument given at the end of the proof of Proposition 3.9. □

Our next two forward/reverse symmetry results describe how one can sample the range of a boundary-intersecting forward $\mathrm{SLE}_\kappa(\rho)$ using a reverse Loewner flow in both the chordal and radial settings.

Proposition 3.11. *Fix $\kappa > 0$, $\rho \in (-2, \frac{\kappa}{2} - 2)$, and let $\widetilde{\rho} = \rho + 4$. Let (W, V) (resp. $(\widetilde{W}, \widetilde{V})$) be the driving process associated with a forward (resp. reverse) $\mathrm{SLE}_\kappa(\rho)$ (resp. $\mathrm{SLE}_\kappa(\widetilde{\rho})$) process in $\mathbf{H}$ from 0 to ∞ with a single boundary force point of weight ρ (resp. $\widetilde{\rho}$) located at 0^+. Let (f_t) (resp. $(\widetilde{f}_t)$) denote the centered forward (resp. reverse) Loewner flow driven by W (resp. $\widetilde{W}$). Let ℓ (resp. $\widetilde{\ell}$) denote the local time of the Bessel process $\kappa^{-1/2}(V - W)$ (resp. $\kappa^{-1/2}(\widetilde{V} - \widetilde{W})$) at 0 and denote by T (resp. $\widetilde{T}$) the right continuous inverse of ℓ (resp. $\widetilde{\ell}$). For each $u > 0$, we have that $f_{T_u}^{-1} \overset{d}{=} \widetilde{f}_{\widetilde{T}_u}$.*

We first note that a BES^δ with $\delta > 1$ is a continuous semimartingale, a Feller process, and has continuous transition densities [RY99, Chapter XI]. Such a Bessel process is reversible with respect to the measure $x^{\delta-1}dx$ where dx denotes Lebesgue measure on $\mathbf{R}_+$. This is a generalization of the observation that Brownian motion is reversible with respect to Lebesgue measure on $\mathbf{R}$. To see this, one notes that the generator for a Bessel process is self-adjoint with respect to the L^2 space induced by the measure $x^{\delta-1}dx$ on $\mathbf{R}_+$. (Recall [Lig05, Proposition 5.2] as before.)

Proof of Proposition 3.11. Recall from (3.20) that $\kappa^{-1/2}(V_t - W_t)$ is a BES^δ with $\delta = 1 + 2(\rho+2)/\kappa$ and from (3.19) $\kappa^{-1/2}(\widetilde{V}_t - \widetilde{W}_t)$ is a $\mathrm{BES}^{\widetilde{\delta}}$ with $\widetilde{\delta} = 1 + 2(\widetilde{\rho} - 2)/\kappa$. By the choice of ρ and $\widetilde{\rho}$, we have that $\delta = \widetilde{\delta}$. Consequently, Proposition 3.1 tells us that we can couple (W, V) and $(\widetilde{W}, \widetilde{V})$ together so that

$$T_u = \widetilde{T}_u \quad \text{and} \quad W_{T_u - t} - V_{T_u - t} = \widetilde{W}_t - \widetilde{V}_t \quad \text{for} \quad t \in [0, T_u]. \tag{3.35}$$

The result thus follows from the argument given at the end of Proposition 3.9. □

We now give the analog of Proposition 3.11 in the setting of radial $\mathrm{SLE}_\kappa(\rho)$.

Proposition 3.12. *Fix $\kappa > 0$, $\rho \in (-2, \frac{\kappa}{2} - 2)$, and let $\widetilde{\rho} = \rho + 4$. Let (W, V) (resp. $(\widetilde{W}, \widetilde{V})$) be the driving process associated with a forward (resp. reverse) radial $\mathrm{SLE}_\kappa(\rho)$ (resp. $\mathrm{SLE}_\kappa(\widetilde{\rho})$) process in $\mathbf{D}$ from 1 to 0 with a single boundary force point of weight ρ (resp. $\widetilde{\rho}$) located at 1^+. Let (f_t) (resp. $(\widetilde{f}_t)$) denote the centered forward (resp. reverse) radial Loewner flow driven by W (resp. $\widetilde{W}$). Let ℓ (resp. $\widetilde{\ell}$) denote the local time of V_t/W_t (resp. $\widetilde{V}_t/\widetilde{W}_t$) at 1 and denote by T (resp. $\widetilde{T}$) the right continuous inverse of ℓ (resp. $\widetilde{\ell}$). For each $u > 0$, we have that $f_{T_u}^{-1} \overset{d}{=} \widetilde{f}_{\widetilde{T}_u}$.*

The proof of Proposition 3.12 is analogous to Proposition 3.11. The one point that we will explain is why we can apply Proposition 3.1 to justify time-reversing the driving process. First, we write $V_t/W_t = e^{i\theta_t}$ where θ_t is as in (3.23). We note that we can view θ_t as being a time-change of the solution to the SDE

$$d\phi_t = \frac{\delta - 1}{4} \cot\left(\frac{\phi_t}{2}\right) dt + dB_t \tag{3.36}$$

with $\delta = 1 + 2(\rho + 2)/\kappa$. This is the same relationship between δ, κ, and ρ as in the case of forward chordal $\mathrm{SLE}_\kappa(\rho)$ given in (3.20). Note that ϕ_t a semi-martingale for $\delta > 1$ since, by the Girsanov theorem, its law is absolutely continuous with respect to that of a BES^δ with $\delta > 1$ when it is interacting with either 0 or 2π. It is similarly a time-homogeneous Markov process with continuous transition densities. Moreover, it is reversible with respect to the measure $\sin(x/2)^{\delta-1}dx$ where dx denotes Lebesgue measure on $[0, 2\pi]$. To see this, we note that the generator of ϕ_t is self-adjoint with respect to the L^2 space associated with the measure $\sin(x/2)^{\delta-1}dx$ on $[0, 2\pi]$ (recall [Lig05, Proposition 5.2] as before).

4 Quantum surfaces

The purpose of this section is to give a careful definition of the different types of quantum surfaces which will arise in this article as introduced in Section 1.4: quantum wedges, cones, disks, and spheres. We will begin in Section 4.1 with a brief introduction to the various types of GFFs which will be important for this article. We continue in Section 4.2 with the definition of a so-called "thick" wedge. This is a surface which is homeomorphic to $\mathbf{H}$. We will then give the definition of a quantum cone in Section 4.3. This is a surface which is homeomorphic to $\mathbf{C}$. This section will be largely parallel with Section 4.2. We will then give our first definition of a "thin" wedge in Section 4.4 (we will give another construction in Section 8). This will describe an ordered sequence of surfaces each of which is homeomorphic to $\mathbf{D}$.

4.1 Gaussian free fields

We are now going to summarize the properties of the GFF which will be important for this article. We direct the reader to [She07] for a detailed introduction in addition to [She10, Section 3] and [MS13a, Section 2.2] for some additional discussion of the whole-plane and free boundary GFFs.

4.1.1 Dirichlet inner product

Suppose that $D \subseteq \mathbf{C}$ is a domain. Let $C_0^\infty(D)$ denote the set of C^∞ functions which are compactly supported in D. The **Dirichlet inner product** is defined by

$$(f,g)_\nabla = \frac{1}{2\pi}\int_D \nabla f(x)\cdot\nabla g(x)dx \quad \text{for} \quad f,g \in C_0^\infty(D). \tag{4.1}$$

More generally, (4.1) makes sense for $f, g \in C^\infty$ with L^2 gradients.

4.1.2 Distributions

We view $C_0^\infty(D)$ as a space of test functions and equip it with the topology where a sequence (ϕ_k) in $C_0^\infty(D)$ satisfies $\phi_k \to 0$ if and only if there exists a compact set $K \subseteq D$ such that the support of ϕ_k is contained in K for every $k \in \mathbf{N}$ and ϕ_k as well as all of its derivatives converge uniformly to zero as $k \to \infty$. A **distribution** on D is a continuous linear functional on $C_0^\infty(D)$ with respect to the aforementioned topology. A **modulo additive constant distribution** on D is a continuous linear functional which is defined on the subspace of functions $f \in C_0^\infty(D)$ with $\int_D f(x)dx = 0$ with the same topology.

4.1.3 GFF with Dirichlet and mixed boundary conditions

Assume that $D \subseteq \mathbf{C}$ is a domain with **harmonically non-trivial** boundary. This means that the harmonic measure of ∂D is positive as seen from any point in D. We let $H_0(D)$ be the Hilbert-space closure of $C_0^\infty(D)$ with respect to the Dirichlet inner product (4.1). The GFF h on D with zero Dirichlet boundary conditions can be expressed as a random linear combination of an $(\cdot,\cdot)_\nabla$-orthonormal basis (f_n) of $H_0(D)$:

$$h = \sum_n \alpha_n f_n, \quad (\alpha_n) \quad \text{i.i.d.} \quad N(0,1). \tag{4.2}$$

Although this expansion of h does not converge in $H_0(D)$, it does converge almost surely in the space of distributions or (when D is bounded) in the fractional Sobolev space $H^{-\epsilon}(D)$ for each $\epsilon > 0$ (see [She07, Proposition 2.7] and the discussion thereafter). If $f, g \in C_0^\infty(D)$ then an integration by parts gives $(f,g)_\nabla = -(2\pi)^{-1}(f,\Delta g)$. Using this, we define

$$(h,f)_\nabla = -\frac{1}{2\pi}(h,\Delta f) \quad \text{for} \quad f \in C_0^\infty(D).$$

Observe that $(h,f)_\nabla$ is a Gaussian random variable with mean zero and variance $(f,f)_\nabla$. Hence h induces a map $C_0^\infty(D) \to \mathcal{G}$, $\mathcal{G}$ a Gaussian Hilbert space, that

preserves the Dirichlet inner product. This map extends uniquely to $H_0(D)$ and allows us to make sense of $(h, f)_\nabla$ for all $f \in H_0(D)$ and, moreover,

$$\operatorname{cov}((h, f)_\nabla, (h, g)_\nabla) = (f, g)_\nabla \quad \text{for all} \quad f, g \in H_0(D).$$

More generally, suppose that $D \subseteq \mathbf{C}$ is a domain and $\partial D = \partial^{\mathrm{D}} \cup \partial^{\mathrm{F}}$ where $\partial^{\mathrm{D}} \cap \partial^{\mathrm{F}} = \emptyset$. We also assume that the harmonic measure of ∂^{D} is positive as seen from any point $z \in D$. The GFF on D with Dirichlet (resp. free) boundary conditions on ∂^{D} (resp. ∂^{F}) is constructed using a series expansion as in (4.2) except the space $H_0(D)$ is replaced with the Hilbert space closure with respect to $(\cdot, \cdot)_\nabla$ of the subspace of functions in $C^\infty(D)$ which have an L^2 gradient and vanish on ∂^{D}. The aforementioned facts for the GFF with only Dirichlet boundary conditions also hold verbatim for the GFF with mixed Dirichlet/free boundary conditions. See also [DS11a, Section 6.2] for some additional discussion of the GFF with mixed boundary conditions.

4.1.4 GFF with free boundary conditions

The GFF with free boundary conditions on $D \subseteq \mathbf{C}$ with harmonically non-trivial boundary is constructed using a series expansion as in (4.2) except we replace $H_0(D)$ with the Hilbert space closure $H(D)$ of the subspace of functions $f \in C^\infty(D)$ with $\|f\|_\nabla^2 := (f, f)_\nabla < \infty$ with respect to the Dirichlet inner product (4.1). Since the constant functions are elements of $C^\infty(D)$ but have $\|\cdot\|_\nabla$-norm zero, in order to make sense of this object, we will work in the space of distributions modulo additive constant. As in the case of the ordinary GFF, it is not difficult to see that the series converges almost surely in this space. As in Section 4.1.3, we can view $(h, f)_\nabla$ for $f \in H(D)$ as a Gaussian Hilbert space where

$$\operatorname{cov}((h, f)_\nabla, (h, g)_\nabla) = (f, g)_\nabla \quad \text{for all} \quad f, g \in H(D).$$

Note that we do not need to restrict to mean zero test functions here due to the presence of gradients.

The whole-plane GFF is constructed in the same manner except with $D = \mathbf{C}$. In particular, like the free boundary GFF, the whole-plane GFF is only defined modulo a global additive constant. See [She10, Section 3] and [MS13a, Section 2.2] for additional discussion of the whole-plane GFF.

4.1.5 Circle averages and Brownian motion

Suppose that h is a GFF on a domain $D \subseteq \mathbf{C}$ (with any type of boundary conditions or a whole-plane GFF if $D = \mathbf{C}$). For each $\epsilon > 0$, we let $h_\epsilon(z)$ be the average of

h on $\partial B(z,\epsilon)$. As explained in [DS11a, Proposition 3.1], the circle average process $(z,\epsilon) \mapsto h_\epsilon(z)$ has a modification which is Hölder continuous jointly in z and ϵ. In particular, $h_\epsilon(z)$ is defined for all (z,ϵ) pairs simultaneously almost surely. When h is only defined up to a global additive constant, then so is h_ϵ. In this case, differences of averages such as $h_\epsilon(z) - h_\delta(w)$ for $z, w \in D$ have well-defined values. For fixed $z \in D$, $h_{e^{-t}}(z)$ evolves as a standard Brownian motion for all t sufficiently large so that $B(z, e^{-t}) \subseteq D$ [DS11a, Proposition 3.3]. If h has free boundary conditions, L is a linear segment of ∂D, and $z \in L$, then $h_{e^{-t}}(z)$ evolves as $\sqrt{2}$ times a standard Brownian motion for all t sufficiently large so that $B(z, e^{-t}) \cap \partial D = B(z, e^{-t}) \cap L \neq \emptyset$ (see the discussion in [DS11a, Section 6]).

Due to the following orthogonal decomposition for $H(\mathbf{H})$ it is often convenient to take $D = \mathbf{H}$. (As we explain momentarily, this leads to a two-step procedure for sampling a free-boundary GFF which will be important when we give the definition of a quantum wedge.)

Lemma 4.1. *Let $\mathcal{H}_1(\mathbf{H})$ be the subspace of $H(\mathbf{H})$ which consists of functions which are radially symmetric about the origin and let $\mathcal{H}_2$ be the subspace of $H(\mathbf{H})$ which consists of functions which have mean zero about all circles centered at the origin. Then $\mathcal{H}_1(\mathbf{H})$ and $\mathcal{H}_2(\mathbf{H})$ give an orthogonal decomposition of $H(\mathbf{H})$.*

Proof. If $f \in H(\mathbf{H})$ then we can let f_1 be the function which on a given circle $\partial B(0,r) \cap \mathbf{H}$ is given by the average of f on $\partial B(0,r) \cap \mathbf{H}$ and let $f_2 = f - f_1$. Then $f = f_1 + f_2$, $f_1 \in \mathcal{H}_1(\mathbf{H})$, and $f_2 \in \mathcal{H}_2(\mathbf{H})$. Consequently, $H(\mathbf{H}) = \mathcal{H}_1(\mathbf{H}) \oplus \mathcal{H}_2(\mathbf{H})$. To see that the sum is orthogonal, for $f_1 \in \mathcal{H}_1(\mathbf{H})$ and $f_2 \in \mathcal{H}_2(\mathbf{H})$ one computes $(f_1, f_2)_\nabla$ by putting ∇f_1 and ∇f_2 into polar coordinates. In particular, the normal derivative of f_1 at $z \in \mathbf{H}$ depends only on $|z|$ while the mean of the normal derivative of f_2 on $\partial B(0,r) \cap \mathbf{H}$ is 0 for each $r > 0$. Thus the mean of the product of the normal derivatives of f_1 and f_2 on $\partial B(0,r) \cap \mathbf{H}$ is equal to 0 for each $r > 0$. Similarly, the tangential derivative of f_1 on $\partial B(0,r) \cap \mathbf{H}$ is 0 for each $r > 0$ so the mean of the product of the tangential derivatives of f_1 and f_2 is equal to 0. □

Lemma 4.1 implies that we can sample a free boundary GFF on $\mathbf{H}$ in two steps:

1. Sample its projection onto $\mathcal{H}_1(\mathbf{H})$ to be given by the function whose common value on $\partial B(0, e^{-t}) \cap \mathbf{H}$ is given by B_{2t} where B is a two-sided standard Brownian motion with $B_0 = 0$.
2. Sample its projection onto $\mathcal{H}_2(\mathbf{H})$ independently by taking it to be $\sum_n \alpha_n f_n$ where (f_n) is an orthonormal basis of $\mathcal{H}_2(\mathbf{H})$ and (α_n) is a sequence of i.i.d. $N(0,1)$ random variables.

We note that normalizing so that $B_0 = 0$ fixes the additive constant for the field so that its average on $\partial \mathbf{D} \cap \mathbf{H}$ is equal to 0.

4.1.6 GFFs on strips and cylinders

In many places in this article it will be convenient to work on the infinite strip $\mathcal{S} = \mathbf{R} \times [0, \pi]$. Suppose that h is a free boundary GFF on $\mathcal{S}$. Let $\psi \colon \mathcal{S} \to \mathbf{H}$ be the conformal transformation given by $z \mapsto -e^{-z}$. Then $\widetilde{h} = h \circ \psi^{-1}$ is a free boundary GFF on $\mathbf{H}$; let $\widetilde{h}_\epsilon(z)$ be the circle average process associated with $\widetilde{h}$. Note ψ maps the vertical line $u + [0, i\pi]$ to the half-circle $\partial B(0, e^{-u}) \cap \mathbf{H}$. Since $\widetilde{h}_{e^{-t}}(0)$ evolves as $\sqrt{2}$ times a standard Brownian motion, it follows that the average of h on $u + [0, i\pi]$ evolves as $\sqrt{2}$ times a standard Brownian motion in u.

In analogy with Lemma 4.1, we have the following orthogonal decomposition for $H(\mathcal{S})$:

Lemma 4.2. *Let $\mathcal{H}_1(\mathcal{S})$ be the subspace of $H(\mathcal{S})$ which consists of functions which are constant on vertical lines of the form $u + [0, i\pi]$ for $u \in \mathbf{R}$ and let $\mathcal{H}_2(\mathcal{S})$ be the subspace of $H(\mathcal{S})$ which consists of functions which have mean zero on all such vertical lines. Then $\mathcal{H}_1(\mathcal{S})$ and $\mathcal{H}_2(\mathcal{S})$ give an orthogonal decomposition of $H(\mathcal{S})$.*

Proof. This follows from the same argument as in the proof of Lemma 4.1. Alternatively, the result can be deduced from Lemma 4.1 using the conformal invariance of the Dirichlet inner product and the map ψ defined above. □

In analogy with the case of a free boundary GFF on $\mathbf{H}$, we can use Lemma 4.2 to sample a free boundary GFF on $\mathcal{S}$ in two steps by first sampling the Brownian motion which determines its averages on vertical lines and then sampling independently its orthogonal projection onto $\mathcal{H}_2(\mathcal{S})$. We can fix the additive constant for h through its projection onto $\mathcal{H}_1(\mathcal{S})$. This will be useful in Section 4.4 below where we will want to sample a Poissonian collection of fields on $\mathcal{S}$.

It is also natural to consider the GFF on the infinite cylinder $\mathcal{Q} = \mathbf{R} \times [0, 2\pi]$ (with the lines $\mathbf{R} \times \{0\}$ and $\mathbf{R} \times \{2\pi\}$ identified). We can decompose each $\phi \in H(\mathcal{Q})$ into an even component ϕ_1 (with $\phi_1(x, \theta) = \phi_1(x, -\theta)$) and an odd component ϕ_2 (with $\phi_2(x, \theta) = -\phi_2(x, -\theta)$). Observe that each of these components is determined by its values on $\mathbf{R} \times [0, \pi)$. The even component of h can be viewed as a GFF with free boundary conditions on $\mathrm{Im}(z) \in \{0, \pi\}$ and the odd component of h can be viewed as a GFF with zero boundary conditions. (See the discussion of the odd/even decomposition in [She10, Section 3].)

4.2 Thick quantum wedges

We will now give a precise description of a quantum wedge. In this section, we will focus on the case of a wedge which is homeomorphic to $\mathbf{H}$ and will refer to such

a wedge as being "thick." In Section 4.4, we will give the definition of a quantum wedge which is "thin" (i.e., not homeomorphic to $\mathbf{H}$). The contents of this section are similar to that of [She10, Section 1.6], however the presentation here is somewhat different.

Fix a proper simply connected domain $\widetilde{D} \subseteq \mathbf{C}$. Suppose that we have a quantum surface represented by $(\widetilde{D}, \widetilde{h})$ with two distinct marked boundary points. Then we can apply the change of coordinates formula (1.3) to represent the surface as $(\mathbf{H}, h, 0, \infty)$ for some h and the two marked points are taken to be 0 and ∞. We will focus on the case that there is almost surely a finite amount of both μ_h and ν_h mass in each bounded neighborhood of the origin and infinite mass in each neighborhood of ∞. We will refer to such a surface as **half-plane-like** since it has a distinguished point of "infinity" whose neighborhoods have an infinite amount of area and boundary length and a distinguished "origin," sufficiently small neighborhoods of which have a finite amount of area and boundary length. In general, we will refer to a surface with two distinguished boundary points as being **doubly marked**.

Note that the h which describes the surface is canonical except that it has one free parameter corresponding to constant rescalings of $\mathbf{H}$. We can fix this parameter by requiring that $\mu_h(\mathbf{D} \cap \mathbf{H}) = 1$. (Note that there almost surely exists such a rescaling because the amount of mass near 0 is finite, the amount of mass near ∞ is infinite, μ_h does not have atoms, and $\mu_h(\mathbf{D} \cap \mathbf{H})$ is a continuous function of the rescaling.) Extending μ_h to be zero on $\mathbf{C} \setminus \mathbf{H}$, we can write this more compactly as $\mu_h(\mathbf{D}) = 1$. We will call the h for which $\mu_h(\mathbf{D}) = 1$ the **canonical description** of the doubly marked quantum surface.

Remark 4.3. In many places in this article (e.g., Definition 4.4 below) we will consider processes of the form $B_t + at$ where B is a standard Brownian motion with $B_0 \geq 0$ and $a > 0$ *conditioned* on the event that $B_t + at > 0$ for all $t > 0$. If $B_0 > 0$, then this is a positive probability event so there is no difficulty in making sense of this process. In the case that $B_0 = 0$, however, we are conditioning on an event which occurs with zero probability. We can make sense of this process by first sampling a Brownian motion $\widetilde{B}$ with $\widetilde{B}_0 = 0$, letting τ be the last time that $\widetilde{B}_t + at$ hits 0 (this time is almost surely finite due to the positive drift), and then taking $B_t + at = \widetilde{B}_{t+\tau} + a(t + \tau)$.

In the case that $a = 0$ we can make sense of $B_t + at = B_t$, $B_0 = 0$, conditioned to be positive for all $t > 0$ using Bessel processes. Namely, Proposition 3.4 implies that B_t is given by $\log X_t$, X_t a BES^2 process, reparameterized to have quadratic variation dt. Suppose that $X_0 = 0$ and τ is the first time that X hits 1. Then the time-reversal $-\log X_{\tau - t}$ starts from 0 and does not subsequently hit 0. We interpret this process parameterized to have quadratic variation dt as corresponding to B_t, $B_0 = 0$, conditioned to be positive for all $t > 0$. (We can similarly use Bessel processes for the $a > 0$ case.)

Definition 4.4. Fix $\alpha \leq Q$. An **α-quantum wedge** is the doubly marked quantum surface (when parameterized by $\mathbf{H}$) described by the distribution h on $\mathbf{H}$ whose law can be sampled from as follows. Let A_s be the process defined for $s \in \mathbf{R}$ such that

1. For $s > 0$, $A_s = B_{2s} + \alpha s$ where B is a standard Brownian motion with $B_0 = 0$ and
2. For $s < 0$, $A_s = \widehat{B}_{-2s} + \alpha s$ where $\widehat{B}$ is a standard Brownian motion with $\widehat{B}_0 = 0$ conditioned so that $\widehat{B}_{2t} + (Q - \alpha)t > 0$ for all $t > 0$.

Let $\mathcal{H}_1(\mathbf{H})$ and $\mathcal{H}_2(\mathbf{H})$ be as in the statement of Lemma 4.1. Then h is the field with projection onto $\mathcal{H}_1(\mathbf{H})$ given by the function whose common value on $\partial B(0, e^{-s}) \cap \mathbf{H}$ is equal to A_s for each $s \in \mathbf{R}$ and with projection onto $\mathcal{H}_2(\mathbf{H})$ given by the corresponding projection of a free boundary GFF on $\mathbf{H}$. That is, the projection of h onto $\mathcal{H}_2(\mathbf{H})$ is given by $\sum_n \alpha_n f_n$ where (f_n) is an orthonormal basis of $\mathcal{H}_2(\mathbf{H})$ and (α_n) is an i.i.d. $N(0,1)$ sequence.

As mentioned in Table 1.1, there are many different variables that one can use to parameterize the space of quantum wedges. In this article, we will mainly use α (multiple of log singularity at the origin) and weight W (as defined in (1.4)). Note that the constraint $\alpha \leq Q$ corresponds to $W \geq \frac{\gamma^2}{2}$.

Note that if $(\mathbf{H}, h, 0, \infty)$ is an α-quantum wedge with h as in Definition 4.4, then the law of h restricted to $\mathbf{D} \cap \mathbf{H}$ is the same as the law of $\widetilde{h} - \alpha \log|\cdot|$ where $\widetilde{h}$ is a free boundary GFF on $\mathbf{H}$ with the additive constant fixed so that its average on $\partial\mathbf{D} \cap \mathbf{H}$ is equal to 0.

Remark 4.5. As we will see in Section 4.4, it is also natural to parameterize an α-quantum wedge by the strip $\mathcal{S}$. Note that if we start with a surface parameterized by $\mathbf{H}$ and we change coordinates using $z \mapsto \log(z)$ to parameterize it by $\mathcal{S}$, then applying (1.3) involves subtracting the function $Q\mathrm{Re}(z)$. Suppose that $\mathcal{H}_1(\mathcal{S}), \mathcal{H}_2(\mathcal{S})$ are as in Lemma 4.2. It thus follows that we can sample from the law of a distribution h which represents an α-quantum wedge parameterized by $\mathcal{S}$ by sampling its projection onto $\mathcal{H}_1(\mathcal{S})$ from the law of the function whose common value on $u + [0, i\pi]$ is $\widetilde{A}_u$ where:

1. For $u > 0$, $\widetilde{A}_u = B_{2u} + (\alpha - Q)u$ where B is a standard Brownian motion with $B_0 = 0$ and
2. For $u < 0$, $\widetilde{A}_u = \widehat{B}_{-2u} + (\alpha - Q)u$ where $\widehat{B}$ is a standard Brownian motion with $\widehat{B}_0 = 0$ conditioned so that $\widehat{B}_{2t} + (Q - \alpha)t > 0$ for all $t > 0$.

The projection of h onto $\mathcal{H}_2(\mathcal{S})$ can be sampled from independently from the law of the corresponding projection of a free boundary GFF on $\mathcal{S}$. (We note that this is opposite of the illustration in Figure 1.9; one can transform from the above to Figure 1.9 by swapping the roles of $\pm\infty$.)

We note that by Proposition 3.4, the construction of a quantum wedge described in Remark 4.5 is equivalent to the definition described in Figure 1.9.

We are now going to show that the law of a quantum wedge is invariant under the operation of multiplying its area by a constant. The proof of this result will also provide some additional motivation for the definition of a quantum wedge. We say that a sequence of doubly marked quantum surfaces $(\mathbf{H}, h_n, 0, \infty)$ converges to the doubly marked surface $(\mathbf{H}, h, 0, \infty)$ if the corresponding measures μ_{h_n} associated with the canonical description of $(\mathbf{H}, h_n, 0, \infty)$ converge weakly to the measure μ_h associated with the canonical description of $(\mathbf{H}, h, 0, \infty)$.

Note that if (D, h) is a quantum surface and $C \in \mathbf{R}$ is a constant then replacing h with $h + C/\gamma$ corresponds to multiplying the μ_h area of D by e^C.

Proposition 4.6. *Fix $\alpha \leq Q$. Then the following hold:*

(i) The law of an α-quantum wedge is invariant under the operation of multiplying its area by a constant. That is, if $(\mathbf{H}, h, 0, \infty)$ is a canonical description of an α-quantum wedge, we fix $C \in \mathbf{R}$, and then let $(\mathbf{H}, \widetilde{h})$ be a canonical description of $(\mathbf{H}, h + C/\gamma, 0, \infty)$, then $(\mathbf{H}, h, 0, \infty) \overset{d}{=} (\mathbf{H}, \widetilde{h}, 0, \infty)$.

(ii) Suppose that $\widetilde{h}$ is a free boundary GFF on $\mathbf{H}$ and let $h = \widetilde{h} - \alpha \log|\cdot|$. Then the quantum surfaces $(\mathbf{H}, h + C/\gamma, 0, \infty)$ converge in law (w.r.t. the topology of convergence of doubly-marked quantum surfaces) as $C \to \infty$ to an α-quantum wedge.

Proof. The proofs of both parts of the proposition are explained in the text of [She10, Section 1.6]. For the convenience of the reader, we are going to provide a self-contained treatment here. Let $h = \widetilde{h} - \alpha \log|\cdot|$ where $\widetilde{h}$ is a free boundary GFF on $\mathbf{H}$ and $\alpha \leq Q$. For each $\epsilon > 0$ and $z \in \overline{\mathbf{H}}$, we let $h_\epsilon(z)$ be the average of h on $\partial B(z, \epsilon) \cap \mathbf{H}$. We can fix the additive constant for h by taking $h_1(0) = 0$. Then $h_{e^{-t}}(0)$ for $t > 0$ evolves as $B_{2t} + \alpha t$ where B is a standard Brownian motion; for $t < 0$, it evolves as $\widehat{B}_{-2t} + \alpha t$ where $\widehat{B}$ is a standard Brownian motion.

We can multiply the surface area as measured by μ_h by a constant e^C for $C \in \mathbf{R}$ by replacing h with $h + C/\gamma$. By (1.3), rescaling by the constant factor a involves replacing $\widetilde{h}$ with $\widetilde{h} - Q \log a$ where $\widetilde{h}$ is a free boundary GFF on $\mathbf{H}$. This, in turn, is

the same (in law) as adding $-Q \log a$ to h. Assume that $C > 0$ so that $e^C > 1$ and let

$$\epsilon_0 = \sup \{\epsilon \in [0,1] : h_\epsilon(0) + Q \log \epsilon + C/\gamma = 0\} .$$

That is, ϵ_0 gives the largest value of $\epsilon \in [0,1]$ such that if we add C/γ to h and then rescale by ϵ^{-1} so that $B(0,\epsilon)$ is mapped to $B(0,1)$ then the average of the rescaled field on $\partial \mathbf{D} \cap \mathbf{H}$ is equal to 0. We note that for each $C > 0$ there almost surely exists such an $\epsilon \in [0,1]$ since $h_{e^{-t}}(0) - Qt + C/\gamma$ for $t \geq 0$ evolves as a Brownian motion with either negative or zero drift (recall $\alpha \leq Q$) and starts from a positive value.

Assume that we have replaced h with the field which arises by rescaling by ϵ_0^{-1}, applying (1.3), and adding C/γ. Then we have that:

1. For $t > 0$, $h_{e^{-t}}(0)$ evolves as $B_{2t} + \alpha t$ where B is a standard Brownian motion.
2. For $t \in [\log \epsilon_0, 0]$, $h_{e^{-t}}(0) - Qt$ evolves as $\widehat{B}_{-2t} + (\alpha - Q)t$ conditioned on being positive in $[\log \epsilon_0, 0)$ where $\widehat{B}$ is a standard Brownian motion and conditioned to take the value C/γ for $t = \log \epsilon_0$. Equivalently, $h_{e^{-t}}(0)$ evolves as $\widehat{B}_{-2t} + \alpha t$ conditioned on being larger than Qt for $t \in [\log \epsilon_0, 0)$ and conditioned so that $h_{\epsilon_0^{-1}}(0) = C/\gamma + Q \log \epsilon_0$.
3. For $t < \log \epsilon_0$, $h_{e^{-t}}(0)$ (with t decreasing) evolves as $\widetilde{B}_{-2t} + \alpha t$ where $\widetilde{B}$ is a standard Brownian motion (with no conditioning).

It is therefore easy to see that if we take a limit as $C \to \infty$, then the law of $\epsilon \mapsto h_\epsilon(0)$ (i.e., the projection of h onto $\mathcal{H}_1(\mathbf{H})$) converges weakly with respect to the topology of local uniform convergence to the law of $\epsilon \mapsto A_{\log \epsilon^{-1}}$ where A_s is as in Definition 4.4. On the other hand, this rescaling procedure does not affect the projection of h onto the subspace $\mathcal{H}_2(\mathbf{H})$. This proves part (ii).

Part (i) also follows from this argument because if we fix $u > 0$ and take $C' = C + u$, the law of the canonical descriptions of the surfaces associated with the field with area rescaled by e^C and the field with area rescaled by $e^{C'}$ will have the same limit as $C \to \infty$ (with u fixed). □

We finish with the following characterization of an α-quantum wedge which will be useful later in the article. (This characterization, along with its companion Proposition 4.12 for quantum cones, may seem trivial. However, both results will be useful for showing that certain surfaces are α-quantum wedges or cones which at first glance may not appear to be so.)

Proposition 4.7. *Fix $\alpha \leq Q$ and suppose that $(\mathbf{H}, h, 0, \infty)$ is a canonical description of a quantum surface parameterized by $\mathbf{H}$ such that the following hold:*

(i) *The law of* $(\mathbf{H}, h, 0, \infty)$ *(as a quantum surface) is invariant under the operation of multiplying its area by a constant. That is, if we fix* $C \in \mathbf{R}$*, and then let* $(\mathbf{H}, \widetilde{h}, 0, \infty)$ *be a canonical description of* $(\mathbf{H}, h + C/\gamma, 0, \infty)$*, then* $(\mathbf{H}, h, 0, \infty) \stackrel{d}{=} (\mathbf{H}, \widetilde{h}, 0, \infty)$*.*

(ii) *The total variation distance between the law of* $(\mathbf{H}, h, 0, \infty)$ *restricted to* $B(0, r)$ *and the law of an* α*-quantum wedge* $(\mathbf{H}, h_\alpha, 0, \infty)$ *restricted to* $B(0, r)$ *tends to* 0 *as* $r \to 0$*.*

Then $(\mathbf{H}, h, 0, \infty)$ *has the law of an* α*-quantum wedge.*

Proof. Observe that if $R, \epsilon > 0$ are fixed then there exists $C_0 > 0$ such that for all $C \geq C_0$ we can couple together the canonical description of $(\mathbf{H}, h + C/\gamma, 0, \infty)$ with the canonical description of $(\mathbf{H}, h_\alpha + C/\gamma, 0, \infty)$ in $B(0, R)$ so that they agree with probability at least $1 - \epsilon$. Thus sending $C \to \infty$ yields an asymptotic coupling where both surfaces are agree with probability 1. The claim then follows since the laws of both surfaces are invariant under the operation of multiplying their area by a constant. □

4.3 Quantum cones

We are now going to give a precise description of a quantum cone. This will be a surface homeomorphic to $\mathbf{C}$ with a marked interior point and will be derived from the whole-plane GFF. Like quantum wedges, quantum cones are also doubly marked where the marked interior point plays the role of the origin and ∞ plays the role of the marked point whose neighborhoods have infinite mass. The discussion will be largely parallel with that given in Section 4.2. In order to give the definition of a quantum cone, we first need to record the whole-plane analog of Lemma 4.1.

Lemma 4.8. *Let* $\mathcal{H}_1(\mathbf{C})$ *be the subspace of* $H(\mathbf{C})$ *which consists of functions which are radially symmetric about the origin and let* $\mathcal{H}_2(\mathbf{C})$ *be the subspace of* $H(\mathbf{C})$ *which consists of functions which have mean zero about all circles centered at the origin. Then* $\mathcal{H}_1(\mathbf{C})$ *and* $\mathcal{H}_2(\mathbf{C})$ *give an orthogonal decomposition of* $H(\mathbf{C})$*.*

Proof. This is proved in the same manner as Lemma 4.1. □

Definition 4.9. Fix $\alpha < Q$. An **α-quantum cone** is the doubly marked quantum surface (when parameterized by $\mathbf{C}$) described by the distribution h on $\mathbf{C}$ whose law can be sampled from as follows. Let A_s be as in Definition 4.4 except with B_{2s} and $\widehat{B}_{2s}$ replaced by B_s and $\widehat{B}_s$. Let $\mathcal{H}_1(\mathbf{C})$ and $\mathcal{H}_2(\mathbf{C})$ be as in the statement of Lemma 4.8. Then h is the field with projection onto $\mathcal{H}_1(\mathbf{C})$ given by the function

whose common value on $\partial B(0, e^{-s})$ is equal to A_s for each $s \in \mathbf{R}$ and with projection onto $\mathcal{H}_2(\mathbf{C})$ is given by the corresponding projection of a whole-plane GFF. That is, the projection of h onto $\mathcal{H}_2(\mathbf{C})$ given by $\sum_n \alpha_n f_n$ where (f_n) is an orthonormal basis of $\mathcal{H}_2(\mathbf{C})$ and (α_n) is an i.i.d. $N(0,1)$ sequence.

Note that if $(\mathbf{C}, h, 0, \infty)$ is an α-quantum cone with h as in Definition 4.9, then the law of h restricted to $\mathbf{D}$ is the same as the law of $\widetilde{h} - \alpha \log|\cdot|$ where $\widetilde{h}$ is a whole-plane GFF with the additive constant fixed so that its average on $\partial\mathbf{D}$ is equal to 0.

As mentioned in Table 1.2, there are many different variables that one can use to parameterize the space of quantum cones. In this article, we will mainly use α (multiple of log singularity at the origin) and weight W (as defined in (1.5)). Note that the constraint $\alpha < Q$ corresponds to $W > 0$.

Remark 4.10. As we will see in Section 4.4, it is also natural to parameterize an α-quantum cone by the infinite cylinder $\mathcal{Q}$. Note that if we start with a surface parameterized by $\mathbf{C}$ and we change coordinates using $z \mapsto \log(z)$ to parameterize it by $\mathcal{Q}$, then applying (1.3) involves subtracting the function $Q\mathrm{Re}(z)$. Suppose that $\mathcal{H}_1(\mathcal{Q}), \mathcal{H}_2(\mathcal{Q})$ are as in Lemma 4.2 (with $\mathcal{Q}$ in place of $\mathcal{S}$). It thus follows that we can sample from the law of a distribution h which represents an α-quantum cone parameterized by $\mathcal{Q}$ by sampling its projection onto $\mathcal{H}_1(\mathcal{Q})$ from the law of the function whose common value on $u + [0, 2\pi i]$ is $\widetilde{A}_u$ where:

1. For $u > 0$, $\widetilde{A}_u = B_u + (\alpha - Q)u$ where B is a standard Brownian motion with $B_0 = 0$ and
2. For $u < 0$, $\widetilde{A}_u = \widehat{B}_{-u} + (\alpha - Q)u$ where $\widehat{B}$ is a standard Brownian motion with $\widehat{B}_0 = 0$ conditioned so that $\widehat{B}_t + (Q - \alpha)t > 0$ for all $t > 0$.

The projection of h onto $\mathcal{H}_2(\mathcal{Q})$ can be sampled from independently from the law of the corresponding projection of a GFF on $\mathcal{Q}$.

We next record the analog of Proposition 4.6.

Proposition 4.11. *Fix $\alpha < Q$. Then the following hold:*

(i) The law of an α-quantum cone is invariant under the operation of multiplying its area by a constant. That is, if $(\mathbf{C}, h, 0, \infty)$ is a canonical description of an α-quantum cone, we fix $C \in \mathbf{R}$, and then let $(\mathbf{C}, \widetilde{h}, 0, \infty)$ be a canonical description of $(\mathbf{C}, h + C/\gamma, 0, \infty)$, then $(\mathbf{C}, h, 0, \infty) \overset{d}{=} (\mathbf{C}, \widetilde{h}, 0, \infty)$.

(ii) Suppose that $D \subseteq \mathbf{C}$ is a domain with $0 \in D$ and that $\widetilde{h}$ is a GFF on D with any type of boundary conditions if $D \neq \mathbf{C}$ or a whole-plane GFF if $D = \mathbf{C}$. Let $h = \widetilde{h} - \alpha \log|\cdot|$. Then the quantum surfaces $(\mathbf{C}, h + C/\gamma, 0, \infty)$ converge in law (w.r.t. the topology of convergence of doubly-marked quantum surfaces) as $C \to \infty$ to an α-quantum cone.

Proof. Both parts follow from the same proof as given in Proposition 4.6. □

We also have the following analog of Proposition 4.7.

Proposition 4.12. *Fix $\alpha < Q$ and suppose that $(\mathbf{C}, h, 0, \infty)$ is a canonical description of a quantum surface parameterized by $\mathbf{C}$ such that the following hold:*

(i) The law of $(\mathbf{C}, h, 0, \infty)$ (as a quantum surface) is invariant under the operation of multiplying its area by a constant. That is, if we fix $C \in \mathbf{R}$, and then let $(\mathbf{C}, \widetilde{h}, 0, \infty)$ be a canonical description of $(\mathbf{C}, h + C/\gamma, 0, \infty)$, then $(\mathbf{C}, h, 0, \infty) \overset{d}{=} (\mathbf{C}, \widetilde{h}, 0, \infty)$.

(ii) The total variation distance between the law of $(\mathbf{C}, h, 0, \infty)$ restricted to $B(0, r)$ and the law of an α-quantum cone $(\mathbf{C}, h_\alpha, 0, \infty)$ restricted to $B(0, r)$ tends to 0 as $r \to 0$.

Then $(\mathbf{C}, h, 0, \infty)$ has the law of an α-quantum cone.

Proof. This follows from the same argument given in the proof of Proposition 4.7. □

4.4 Encoding surfaces using Bessel processes

We are now going to explain how to encode a quantum wedge using a Bessel process (as will be clear from the following discussion, one can similarly encode a quantum cone using a Bessel process). This perspective will allow us to give the definition of a thin quantum wedge (i.e., not homeomorphic to $\mathbf{H}$). Note that if we conformally map the sum of a free boundary GFF on $\mathbf{H}$ and a multiple of the log function to $\mathcal{S}$, then the result is the sum of a GFF on $\mathcal{S}$ with free boundary conditions and a linear function. In this case, the projection X of the resulting field onto $\mathcal{H}_1(\mathcal{S})$ as in Lemma 4.2 evolves as a Brownian motion with a given linear drift. That is, we can write $X_t = B_{2t} + at$ where $a \in \mathbf{R}$ and B is a standard Brownian motion.

Fix $\gamma \in (0, 2)$ and consider a γ-LQG surface parameterized by such a distribution h on $\mathcal{S}$. Write $Z_t = \exp(\frac{\gamma}{2} X_t)$. By Itô's formula,

$$d\langle Z \rangle_t = \frac{\gamma^2}{2} Z_t^2 dt.$$

By [DS11a, Proposition 1.2], we have that the conditional expectation of the quantum mass of the surface given X is given by

$$\int_{-\infty}^{\infty} \exp(\gamma X_t)\, dt = \frac{2}{\gamma^2} \int_{-\infty}^{\infty} d\langle Z \rangle_t = \frac{2}{\gamma^2} \langle Z \rangle_\infty. \tag{4.3}$$

By Proposition 3.4, we see that if we reparameterize Z by its quadratic variation then it evolves as a BES^δ with

$$\delta = 2 + \frac{2a}{\gamma}. \tag{4.4}$$

Equivalently,

$$a = \frac{\gamma}{2}(\delta - 2). \tag{4.5}$$

Recalling the phases described in Section 3.2, we note that:

1. If $a \geq 0$, then $\delta \geq 2$. This implies that Z — if started at zero —almost surely does not hit zero in the future.
2. If $a \in (-\gamma, 0)$, then $\delta \in (0, 2)$. This implies that we can view Z as a process which is defined for all times and is instantaneously reflecting at 0.

In the former case, we can associate with Z a single quantum wedge where the projection of the field onto $\mathcal{H}_1(\mathcal{S})$ is determined by Z by reparameterizing $2\gamma^{-1} \log Z$ to have quadratic variation given by $2dt$. In the latter case, each excursion of Z from 0 can be associated with a (finite area) quantum surface, which we can view as being parameterized by $\mathcal{S}$. Using the change of coordinates formula (with the map $\mathcal{S} \to \mathbf{H}$ given by $z \mapsto e^z$), this corresponds to a quantum wedge with $\alpha = Q - a$. We will now use this construction to give a definition of a quantum wedge with $\alpha \in (Q, Q + \frac{\gamma}{2})$.

Definition 4.13. Fix $\alpha \in (Q, Q + \frac{\gamma}{2})$. An **$\alpha$-quantum wedge** is the law on (ordered) sequences of surfaces which can be sampled from as follows. Let

$$\delta = 2 + \frac{2(Q - \alpha)}{\gamma} = 3 + \frac{4 - 2\alpha\gamma}{\gamma^2} \tag{4.6}$$

(note that $\delta \in (1, 2)$) and let Y be a BES^δ. Let $\mathcal{H}_1(\mathcal{S})$, $\mathcal{H}_2(\mathcal{S})$ be as in the statement of Lemma 4.2. Sample a countable collection of distribution valued random variables h_e on $\mathcal{S}$ indexed by the excursions e of Y from 0 where the projection of h_e onto $\mathcal{H}_1(\mathcal{S})$ is given by reparameterizing $2\gamma^{-1} \log(e)$ to have quadratic variation $2dt$ and the projection of h_e onto $\mathcal{H}_2(\mathcal{S})$ is sampled independently according to the law of the corresponding projection of a free boundary GFF on $\mathcal{S}$.

Remark 4.14. Note that the length of a given excursion e of Y from 0 as in Definition 4.13 is equal to a non-random constant times the conditional expectation of the quantum mass of the quantum surface described by h_e given e (recall (4.3)).

We will see in Section 7 and Section 8 that the manner in which we string together a sequence of quantum disks in Definition 4.13 using a Bessel process is natural in the context of quantum wedges. In particular, we will show that the beaded surface which arises by slicing a thick wedge with an independent boundary intersecting $\mathrm{SLE}_\kappa(\rho_1;\rho_2)$ process yields a thin wedge as defined in Definition 4.13.

Remark 4.15. Some critical values for the Bessel process occur when $\delta \in \{0,1,2\}$. As explained in Section 3.2, these respectively correspond to when 0 is an absorbing state, the critical value below which the process fails to be a semimartingale when it is interacting with 0, and the critical value at or above which the process never hits 0. These respectively correspond to

$$a \in \left\{-\gamma, -\frac{\gamma}{2}, 0\right\},$$

which in turn correspond to

$$\alpha \in \left\{\gamma + Q, \frac{\gamma}{2} + Q, Q\right\} = \left\{\frac{3\gamma}{2} + \frac{2}{\gamma}, \gamma + \frac{2}{\gamma}, \frac{\gamma}{2} + \frac{2}{\gamma}\right\},$$

and

$$W \in \left\{-\frac{\gamma^2}{2}, 0, \frac{\gamma^2}{2}\right\}.$$

It is also natural to encode an α-quantum wedge using a Bessel process $\widehat{Y}$ so that the length of each excursion of $\widehat{Y}$ from 0 corresponds to a non-random constant times the γ-LQG mass of the corresponding bubble (rather than a conditional expectation). We will now explain why this is possible and why the dimension of the Bessel process is the same as in (4.6).

Proposition 4.16. *Fix $\alpha \in (Q, Q + \frac{\gamma}{2})$ and suppose that $\mathcal{W}$ is an α-quantum wedge. There exists a Bessel process $\widehat{Y}$ with dimension δ as in Definition 4.4 such that the ordered excursions of $\widehat{Y}$ from 0 are in correspondence with the ordered excursions of Y from 0 and the length of an excursion of the former is equal to the area of the surface which corresponds to the latter.*

We will need two preparatory lemmas to prove Proposition 4.16. We begin with the following basic observation about p.p.p.'s.

Lemma 4.17. *Suppose that Λ is a p.p.p. on $\mathbf{R}_+ \times \mathbf{R}_+ \times \mathbf{R}_+$ chosen with intensity measure $du \otimes t^\alpha dt \otimes \mu$ where μ is a probability measure on $\mathbf{R}_+$ and both du and dt denote Lebesgue measure on $\mathbf{R}_+$. Assume that $c = \mathbf{E}[U^{-\alpha-1}] < \infty$ for $X \sim \mu$. Then $\{(u, Ue) : (u, e, U) \in \Lambda\}$ is a p.p.p. on $\mathbf{R}_+ \times \mathbf{R}_+$ with intensity measure $c(du \otimes t^\alpha dt)$.*

Proof. Let ν the law of $\log U$ for $U \sim \mu$. Applying a change of variables using the log function, the density $t^\alpha dt$ becomes $e^{(\alpha+1)t}dt$. The convolution of this density with ν is given by:

$$\int_{\mathbf{R}} e^{(\alpha+1)(t-s)} d\nu(s) = e^{(\alpha+1)t}\mathbf{E}[U^{-\alpha-1}],$$

which implies the lemma. □

Lemma 4.18. *Fix $a < 0$ and suppose that h is a random distribution on $\mathcal{S}$ such that*

(i) Its projection onto $\mathcal{H}_1(\mathcal{S})$ is given by $X_u = B_{2u} + au$ for $u \geq 0$ and $X_u = \widehat{B}_{-2u} - au$ for $u < 0$ where $B, \widehat{B}$ are independent standard Brownian motions with $B_0 = \widehat{B}_0 = 0$ conditioned so that $X_u \leq 0$ for all $u \in \mathbf{R}$.

(ii) Its projection onto $\mathcal{H}_2(\mathcal{S})$ is given independently by the corresponding projection of a free boundary GFF on $\mathcal{S}$.

Then both $\mathbf{E}[\nu_h(\partial\mathcal{S})] < \infty$ and $\mathbf{E}[\mu_h(\mathcal{S})] < \infty$.

Proof. We will give the proof that $\mathbf{E}[\mu_h(\mathcal{S})] < \infty$; that $\mathbf{E}[\nu_h(\partial\mathcal{S})] < \infty$ follows from the same argument.

We note that by [DS11a, Proposition 1.2] we have that the conditional expectation of $\mu_h(\mathcal{S})$ given X is equal to $\int_{\mathbf{R}} e^{\gamma X_u} du$. By symmetry, it suffices to show that $\mathbf{E}\int_0^\infty e^{\gamma X_u} du < \infty$. Assume momentarily that $X_0 = -1$. Then $X_u = B_{2u} + au$ conditioned on the positive probability event that $B_{2u} + au < 0$ for all $u \geq 0$. Let $C < \infty$ be given by the reciprocal of the probability of this event. For each $u \geq 0$, we let $E_u = \{B_{2u} + au \leq 0\}$ and $F_u = \{B_{2u} + au \geq \frac{1}{2}au\}$. We then have that

$$\begin{aligned}\mathbf{E}\int_0^\infty e^{\gamma X_u} du &\leq C\int_0^\infty \mathbf{E}\left[e^{\gamma(B_{2u}+au)}\mathbf{1}_{E_u}\right] du \\ &\leq C\int_0^\infty \mathbf{P}[F_u] + e^{\gamma au/2} du.\end{aligned}$$

In the second equality, we used that the integrand is bounded by 1 on E_u. It is easy to see from standard Gaussian tail estimates that $\mathbf{P}[F_u]$ is integrable on $\mathbf{R}_+$ so that the integral above is finite. The case that $X_0 = 0$ follows from the case that $X_0 = -1$ by noting that the first hitting time of -1 by X has an exponential tail and X is Markovian. □

Proof of Proposition 4.16. We can think of sampling the Bessel process Y in Definition 4.13 by first sampling a p.p.p. Λ^* according to $du \otimes \nu_\delta^*$ (where du is Lebesgue measure on $\mathbf{R}_+$ and ν_δ^* is in Remark 3.7) and then sampling Y by associating with

each $(u, e^*) \in \Lambda^*$ a BES^δ excursion from 0 to 0 whose maximum value is given by e^* (this law can be constructed using $\mathrm{BES}^{4-\delta}$ processes as described in Remark 3.7). Note that the total mass of the bubble corresponding to a given (u, e^*) is given by $(e^*)^2 U_e$ where the U_e are i.i.d. random variables indexed by the excursions of Y from 0. By the discussion just after (3.10), we note that $\{(u, (e^*)^2) : (u, e^*) \in \Lambda^*\}$ is a p.p.p. on $\mathbf{R}_+ \times \mathbf{R}_+$ with intensity measure proportional to $du \otimes t^{\delta/2-2} dt$ where dt denotes Lebesgue measure on $\mathbf{R}_+$. Moreover, the law of U_e is given by the law of the γ-LQG mass associated with the law on distributions on $\mathcal{S}$ described in the statement of Lemma 4.18 with $a = Q - \alpha$ (this follows from Proposition 3.4 and Proposition 3.5). In particular, we have that $\mathbf{E}[(\mu_h(\mathcal{S}))^{1-\delta/2}] < \infty$ since $\delta \in (0, 2)$. The result is thus a consequence of Lemma 4.17. □

We will now describe how to extend the definition of an α-quantum wedge with $\alpha \in (Q, Q + \frac{\gamma}{2})$ to other Poissonian families of surfaces.

Definition 4.19. For each $\delta, b \in \mathbf{R}$ we let $\mathcal{M}_\delta^b$ be the measure on quantum surfaces parameterized by $\mathcal{S}$ described by a distribution h which is defined as follows:

1. Pick e from $\nu_\delta^{\mathrm{BES}}$ and then take the projection of h onto $\mathcal{H}_1(\mathcal{S})$ to be given by parameterizing $b \log(e)$ to have quadratic variation $2du$.
2. Take the projection of h onto $\mathcal{H}_2(\mathcal{S})$ to be given independently by the corresponding projection of a free boundary GFF onto $\mathcal{H}_2(\mathcal{S})$.

We will very often consider p.p.p.'s with intensity measure of the form $du \otimes \mathcal{M}_\delta^b$ where du denotes Lebesgue on $\mathbf{R}_+$. Note that an α-quantum wedge corresponds to a p.p.p. sampled from $du \otimes \mathcal{M}_\delta^{2\gamma^{-1}}$ where δ is determined by α using (4.6).

We will momentarily given the definitions of the unit area and unit boundary length quantum disks using the measures $\mathcal{M}_\delta^b$. We will also given the definition of the unit area quantum sphere using the following variant of $\mathcal{M}_\delta^b$ (it is a measure on distributions on $\mathcal{Q}$ rather than $\mathcal{S}$).

Definition 4.20. For each $\delta, b \in \mathbf{R}$ we let $\mathcal{N}_\delta^b$ be the measure on surfaces parameterized by $\mathcal{Q}$ described by a distribution h which is defined as follows:

1. Pick e from $\nu_\delta^{\mathrm{BES}}$ and then take the projection of h onto $\mathcal{H}_1(\mathcal{Q})$ to be given by parameterizing $b \log(e)$ to have quadratic variation du.
2. Take the projection of h onto $\mathcal{H}_2(\mathcal{Q})$ to be given independently by the corresponding projection of a GFF onto $\mathcal{H}_2(\mathcal{Q})$.

Definition 4.21. (i) The **unit area quantum disk** is the law on quantum surfaces given by $(\nu_h(\partial\mathcal{S}))^{-1} d\mathcal{M}_\delta^{2\gamma^{-1}}(h)$ with $\delta = 3 - \frac{4}{\gamma^2}$ conditional on $\mu_h(\mathcal{S}) = 1$. (Note that this is also the same as the conditional law of $(\nu_h(\partial\mathcal{S}))^{-1} d\mathcal{M}_{\delta'}^{4\gamma^{-1}}(h)$ given $\mu_h(\mathcal{S}) = 1$ where $\delta' = 4 - \frac{8}{\gamma^2}$.)

(ii) The **unit boundary length quantum disk** is the law on quantum surfaces given by $\mathcal{M}_\delta^{2\gamma^{-1}}(h)$ with $\delta = 3 - \frac{4}{\gamma^2}$ conditional on $\nu_h(\partial\mathcal{S}) = 1$. (Note that this is also the same as the conditional law of $\mathcal{M}_{\delta'}^{4\gamma^{-1}}(h)$ given $\nu_h(\mathcal{S}) = 1$ where $\delta' = 4 - \frac{8}{\gamma^2}$.)

(iii) The **unit area quantum sphere** is the law on quantum surfaces given by $\mathcal{N}_\delta^{2\gamma^{-1}}$ with $\delta = 4 - \frac{8}{\gamma^2}$ conditional on $\mu_h(\mathcal{Q}) = 1$.

Remark 4.22. In Section 5, we will show that each of the laws on finite volume surfaces from Definition 4.21 can be constructed using a limiting procedure. We will explain in Section 7.3 that the laws of the unit area and boundary length quantum disks can be used to describe the structure of the bubbles which are cut out from a $\frac{3\gamma^2}{2} - 2$ quantum wedge by an independent $\mathrm{SLE}_{\kappa'}$ process, $\kappa' \in (4, 8)$. We will also explain in Remark 12.5 that the unit area and boundary length quantum disks can be constructed from a certain excursion measure which is naturally associated with the cone times of a 2-dimensional Brownian motion. (Altogether, there will be four different constructions of these objects in this article.) Finally, we show in Section 12 that the law of the unit area quantum sphere can be used in conjunction with Lévy trees to construct the γ-LQG surfaces with $\gamma^2 \in (4, 8)$.

Remark 4.23. Using the notation for infinite measures on quantum disks and spheres introduced in Section 1.4, we have that $\mathcal{M}_\delta^b = \mathcal{M}_W$ where

$$W = \frac{\gamma}{2b}(4 - 2\delta + b\gamma). \tag{4.7}$$

In particular, if we plug in the values $b = 2\gamma^{-1}$ and $\delta = 3 - \frac{4}{\gamma^2}$ into (4.7), we get that $W = 2$ as claimed in Section 1.4. We also have that $\mathcal{N}_\delta^b = \mathcal{N}_W$ where

$$W = \frac{\gamma(2 - \delta)}{b}. \tag{4.8}$$

In particular, if we plug in the values $b = 2\gamma^{-1}$ and $\delta = 4 - \frac{8}{\gamma^2}$ into (4.8), we get that $W = 4 - \gamma^2$ as claimed in Section 1.4.

We finish this subsection by giving a version of Proposition 4.16 which holds for p.p.p.'s of quantum surfaces sampled using the measures $\mathcal{M}_\delta^b$ and $\mathcal{N}_\delta^b$. (As we will see in Section 7.3, this result will be useful for relating the structure of the bubbles cut out by an $\mathrm{SLE}_{\kappa'}$ process from certain types of quantum surfaces to the unit area and unit boundary length quantum disks.)

Proposition 4.24. *Fix $\delta, \gamma \in (0, 2)$. There exists constants $c_1, c_2, c_3 > 0$ such that the following is true.*

(i) If Λ is a p.p.p. with intensity measure $du \otimes \mathcal{M}_\delta^{2\gamma^{-1}}$, then $\{(u, \mu_h(\mathcal{S})) : (u, h) \in \Lambda\}$ is a p.p.p. with intensity measure $c_1 du \otimes t^{\delta/2-2} dt$.

(ii) If Λ is a p.p.p. with intensity measure $du \otimes \mathcal{N}_\delta^{2\gamma^{-1}}$, then $\{(u, \mu_h(\mathcal{Q})) : (u,h) \in \Lambda\}$ is a p.p.p. with intensity measure $c_2 du \otimes t^{\delta/2-2} dt$.

(iii) If Λ is a p.p.p. with intensity measure $du \otimes \mathcal{M}_\delta^{4\gamma^{-1}}$ then $\{(u, \nu_h(\partial\mathcal{S})) : (u,h) \in \Lambda\}$ is a p.p.p. with intensity measure $c_3 du \otimes t^{\delta/2-2} dt$.

Proof. This is established in the same manner as Proposition 4.16. □

5 Quantum disks and spheres as limits

We are now going to show that the unit area and boundary length quantum disks and the unit area sphere as defined in Definition 4.21 can be constructed using a limiting procedure. (Recall from Remark 4.22 that we will give multiple equivalent constructions of each of the finite volume surfaces.) Throughout, we let $\mathcal{S}_+ = \mathbf{R}_+ \times [0,\pi]$ and $\mathcal{Q}_+ = \mathbf{R}_+ \times [0, 2\pi]$ with $\mathbf{R}_+ \times \{0\}$ and $\mathbf{R}_+ \times \{2\pi\}$ identified.

5.1 Unit area quantum disk

We begin with the case of unit area disks.

Proposition 5.1. *Fix a smooth, bounded domain D whose boundary contains a linear segment L. Let h be a GFF on D with free boundary conditions on L and zero boundary conditions on $\partial D \setminus L$. Fix $C, \epsilon > 0$ and condition on $\{C \leq \mu_h(D) \leq C(1+\epsilon)\}$. Let $\widehat{h} = h - (\log C)/\gamma$ so that $1 \leq \mu_{\widehat{h}}(D) \leq 1+\epsilon$. Then the law of $(D, \widehat{h})$ (viewed as a quantum surface) converges weakly to the law of the unit area quantum disk as in Definition 4.21 when we take a limit first as $C \to \infty$ and then as $\epsilon \to 0$. In particular, the limiting law does not depend on D or L.*

The idea to prove Proposition 5.1 is to consider the law of h weighted by $\nu_h(L)$ (i.e., $\nu_h(L)dh$). As we will explain in Lemma 5.6, sampling from this law is equivalent to first sampling from the (unweighted) law of h and then adding to it a certain log singularity at a point chosen uniformly from Lebesgue measure on L. We will then apply a change of coordinates from D to $\mathcal{S}$ with this extra marked point sent to $+\infty$ and the two endpoints of L sent to 0 and $i\pi$. We will argue that (Lemma 5.5) conditioning the area to be large is equivalent to conditioning the projection of the field onto $\mathcal{H}_1(\mathcal{S})$ from Lemma 4.2 to take on a large value and that this large value is realized along a line $u + [0, i\pi]$ with u large. We then find that (Lemma 5.3) if we horizontally translate so that this line segment is sent to $[0, i\pi]$ then the law of the random field which describes the surface converges to a limiting law as we take a limit as the area tends to ∞ (while renormalizing). The result then follows by

unweighting the resulting law by its boundary length. A similar procedure will lead to the construction of the unit boundary length quantum disk (Proposition 5.10) and the unit area quantum sphere (Proposition 5.13).

Lemma 5.2. *Suppose that $f : \mathcal{S}_+ \to \mathbf{R}$ is a function which is harmonic in $\mathcal{S}_+$ with Neumann boundary conditions on $\mathcal{S}_+ \setminus [0, i\pi]$ and Dirichlet boundary conditions on $[0, i\pi]$. Then the limit*

$$\lim_{\mathrm{Re}(z)\to\infty} f(z) \tag{5.1}$$

exists and is given by the average $\overline{f}$ of f on $[0, i\pi]$. That is, for every $\epsilon > 0$ there exists $R \geq 0$ such that $\sup_{\mathrm{Re}(z)\geq R} |f(z) - \overline{f}| \leq \epsilon$.

Proof. Let F be the harmonic function which is defined on $\{z \in \mathbf{C} : \mathrm{Re}(z) \geq 0\} = -i\mathbf{H}$ whose boundary conditions on the imaginary axis are given by first extending the boundary conditions of f from $[0, \pi i]$ to $[0, 2\pi i]$ by reflection and then to all of $i\mathbf{R}$ periodically. Then the restriction of F to $\mathcal{S}_+$ is equal to f. From the explicit form of the Poisson kernel on $-i\mathbf{H}$, it is clear that $\lim_{\mathrm{Re}(z)\to\infty} F(z)$ exists in the sense described in the lemma statement. □

Lemma 5.3. *Suppose that h is a GFF on $\mathcal{S}$ with free boundary conditions on $\partial\mathcal{S}_+ \setminus [0, i\pi]$ and zero boundary conditions on $\partial\mathcal{S} \setminus \partial\mathcal{S}_+$. Let F be a function which is harmonic in $\mathcal{S}_+$ with Dirichlet boundary conditions on $[0, i\pi]$ and Neumann boundary conditions on $\partial\mathcal{S}_+ \setminus [0, i\pi]$. (In particular, F has Neumann boundary conditions at $+\infty$.) Fix $a > 0$. For each $u \geq 0$, let X_u be given by the average of $h + F - a\mathrm{Re}(z)$ on $u + [0, i\pi]$. For each $C > 0$, let $\tau_C = \inf\{u \geq 0 : X_u \geq C\}$ and let $E_C = \{\tau_C < \infty\}$. On E_C, let $\widetilde{h}$ be the field which is given by precomposing $h + F - a\mathrm{Re}(z) - C$ with the horizontal translation $z \mapsto z + \tau_C$. Then the conditional law of $\widetilde{h}$ given E_C converges weakly as $C \to \infty$. With $\mathcal{H}_1(\mathcal{S})$ and $\mathcal{H}_2(\mathcal{S})$ as in Lemma 4.2, the limit law can be sampled from by:*

(i) Taking its projection $\widetilde{X}_u$ onto $\mathcal{H}_1(\mathcal{S})$ to be given by $B_{2u} - au$ for $u \geq 0$ where B is a standard Brownian motion with $B_0 = 0$ and to be given by $\widehat{B}_{-2u} + au$ for $u < 0$ where $\widehat{B}$ is a standard Brownian motion with $\widehat{B}_0 = 0$ conditioned so that $\widehat{B}_{-2u} + au < 0$ for all $u < 0$.

(ii) Independently sampling its projection onto $\mathcal{H}_2(\mathcal{S})$ from the law of the corresponding projection of a free boundary GFF on $\mathcal{S}$.

Proof. Let τ_C be as in the statement and let Y have the law of X given E_C. To prove the result, it suffices to show that:

(I) For each $N \geq 0$ we have that $\mathbf{P}[\tau_C \geq N \,|\, E_C] \to 1$ as $C \to \infty$ and

(II) The law of $Y - C$ with time translated by τ_C (so that it first hits 0 at time $u = 0$) converges to the limit described in (i) above.

Indeed, note that (I) combined with Lemma 5.2 implies that the law of the projection onto $\mathcal{H}_2(\mathcal{S})$ of $h + F - a\mathrm{Re}(z) - C$ precomposed with $z \mapsto z + \tau_C$ converges weakly to the law of the corresponding projection of a free boundary GFF on $\mathcal{S}$.

Note that since F is harmonic on $\mathcal{S}_+$ with Dirichlet boundary conditions on $[0, i\pi]$ and Neumann boundary conditions on $\partial\mathcal{S}_+ \setminus [0, i\pi]$, it follows that its average on each vertical line $u + [0, i\pi]$ is the same. It thus follows that X is a Brownian motion with linear drift, so that the law of Y is given by Lemma 3.6. It is therefore clear from Lemma 3.6 that both (I) and (II) hold. □

Lemma 5.4. *Suppose that h is a GFF on $\mathcal{S}_+$ with free boundary conditions on $\partial\mathcal{S}_+ \setminus [0, i\pi]$ and Dirichlet boundary conditions on $[0, i\pi]$, let $\widetilde{h}$ be the projection of h onto $\mathcal{H}_2(\mathcal{S}_+)$, and let $\mu_{\widetilde{h}}$ be the γ-LQG measure associated with $\widetilde{h}$. For each $p \in (0, 2/\gamma^2)$ there exists a constant $c_p < \infty$ such that*

$$\mathbf{E}\left[\left(\mu_{\widetilde{h}}([u, u+1] \times [0, \pi])\right)^p\right] < c_p. \tag{5.2}$$

If h is instead a GFF on $\mathcal{Q}_+$ with Dirichlet boundary conditions then the same holds for each $p \in (0, 4/\gamma^2)$.

Proof. Fix $R > 1$ and suppose that h is a GFF on $B(0, R) \cap \mathbf{H}$ with Dirichlet boundary conditions on $\mathbf{H} \cap \partial B(0, R)$ and free boundary conditions on $[-R, R]$ and let $\widetilde{h}$ be the projection of h onto $\mathcal{H}_2(B(0, R) \cap \mathbf{H})$. By applying a change of coordinates, it suffices to show that $\mu_{\widetilde{h}}(\mathbf{D} \cap \mathbf{H})$ has a finite pth moment for each fixed $p \in (0, 2/\gamma^2)$ which is uniform in R. By the odd-even decomposition for the GFF (see [DS11a, Section 6.2] and [She10, Section 3.2]), we know that we can write $\widetilde{h}$ as the corresponding projection of the even part of a GFF $h^\dagger$ on $B(0, R)$ with Dirichlet boundary conditions. It therefore follows that the covariance function for $\widetilde{h}$ is dominated by twice the covariance function for the corresponding projection of $h^\dagger$. By [RV10, Proposition 3.5], the associated γ-LQG measure has a finite pth moment for all $p \in (0, 4/\gamma^2)$. Therefore the result follows in this case by applying [Kah86, Theorem 2].

The case of a GFF on $\mathcal{Q}_+$ with Dirichlet boundary conditions is proved similarly. □

Lemma 5.5. *Fix $a \in (0, 2/\gamma)$ and suppose that $h = \widetilde{h} - a\mathrm{Re}(z)$ where $\widetilde{h}$ is a GFF on $\mathcal{S}_+$ with free boundary conditions on $\partial\mathcal{S}_+ \setminus [0, i\pi]$ and on $[0, iu]$, some $u \in [0, \pi)$, and Dirichlet boundary conditions on $(u, i\pi]$. Let X be the projection of h onto $\mathcal{H}_1(\mathcal{S})$ from Lemma 4.2. For each $C, \epsilon > 0$ and $\beta > 1$ we let*

$$\begin{aligned} E_{C,\epsilon} &= \{C \leq \mu_h(\mathcal{S}_+) \leq C(1+\epsilon)\} \quad \text{and} \\ E'_{C,\beta} &= \left\{\sup_{u \geq 0} X_u \geq \gamma^{-1} \log\left(\frac{C}{\beta}\right)\right\}. \end{aligned} \tag{5.3}$$

We have both

$$\mathbf{P}[E'_{C,\beta} \,|\, E_{C,\epsilon}] \to 1 \quad \textit{as} \quad \beta \to \infty \quad \textit{uniformly in} \quad C \quad \textit{and} \tag{5.4}$$

$$\mathbf{P}[E_{C,\epsilon} \,|\, E'_{C,\beta}] > 0 \quad \textit{uniformly in} \quad C \quad \textit{for} \quad \epsilon, \beta \quad \textit{fixed.} \tag{5.5}$$

The same likewise holds if we replace $\mathcal{S}_+$ with $\mathcal{Q}_+$ and take h to be a GFF on $\mathcal{Q}_+$ with Dirichlet boundary conditions.

Proof. We note that (5.5) is obvious from the definition of μ_h. Hence we will only give the proof of (5.4).

Note that $X_u = B_{2u} - au$ where B is a standard Brownian motion. Let

$$M = \sup_{u \geq 0} e^{\gamma X_u}.$$

We claim that

$$\mathbf{P}[M \geq C] \asymp C^{-a/\gamma}. \tag{5.6}$$

Indeed, this can be seen by using that $Z_t = e^{\gamma X_t}$ reparameterized according to its quadratic variation is a Bessel process of dimension $2 - a/\gamma$ (Proposition 3.4) and that $Z_t^{2-\delta}$ is a martingale (recall the proof of Lemma 3.6). By (5.5) and (5.6) , it thus follows that

$$\mathbf{P}[E_{C,\epsilon}] \gtrsim C^{-a/\gamma}. \tag{5.7}$$

Thus to prove (5.4) it suffices to show that for each $\delta > 0$ there exists $\beta_0 > 0$ such that $\beta \geq \beta_0$ implies that $\mathbf{P}[E_{C,\epsilon} \cap (E'_{C,\beta})^c] \leq \delta C^{-a/\gamma}$.

Let $N = \mu_h(\mathcal{S})$. For each $j \in \mathbf{N}_0$, we define events

$$Q_j = \left\{ \frac{N}{M} \geq \beta e^{j+1} \right\}, \quad R_j = \left\{ \frac{C}{\beta} e^{-j-1} \leq M \leq \frac{C}{\beta} e^{-j} \right\}, \quad \text{and} \quad P_j = Q_j \cap R_j.$$

Let $\widetilde{h}$ be the projection of h onto $\mathcal{H}_2(\mathcal{S}_+)$. For each $j \geq 0$, we let $\widetilde{N}_j$ be the γ-LQG mass assigned to $[j, j+1] \times [0, \pi]$ by $\widetilde{h}$ and we let j^* be the value of $u \in [j, j+1]$ which maximizes $B_{2u} - au$. Fix $\epsilon \geq 0$ such that $a' = a - \epsilon > 0$. Then we have that

$$N \leq \sum_{j=0}^{\infty} e^{\gamma(B_{2j^*} - aj^*)} \widetilde{N}_j \leq \sum_{j=0}^{\infty} e^{-\gamma \epsilon j} \times e^{\gamma(B_{2j^*} - a'j^*)} \widetilde{N}_j.$$

By Jensen's inequality there exists $c_0 > 0$ depending only on ϵ such that

$$N^p \leq c_0 \sum_{j=0}^{\infty} e^{-\gamma \epsilon j} e^{p\gamma(B_{2j^*} - a'j^*)} \widetilde{N}_j^p \quad \text{for all} \quad p > 1$$

provided we take $\epsilon > 0$. The same likewise holds for $p \in (0,1]$ provided we take $\epsilon = 0$. Lemma 5.4 implies that $\mathbf{E}[\widetilde{N}_j^p] < \infty$ uniformly in j provided $p \in (0, 2/\gamma^2)$. Since the $\widetilde{N}_j$ are independent of B, it is thus easy to see that

$$\mathbf{E}\left[\left(\frac{N}{M}\right)^p \mid M\right] \asymp 1 \quad \text{and} \quad \mathbf{E}\left[\left(\frac{N}{M}\right)^p\right] < \infty \quad \text{for all} \quad p \in (0, 2/\gamma^2). \tag{5.8}$$

Fix $p \in (a/\gamma, 2/\gamma^2)$. Using (5.8), Markov's inequality for N/M and (5.6) respectively imply that

$$\mathbf{P}[Q_j] \lesssim \beta^{-p} e^{-pj}, \quad \mathbf{P}[Q_j \mid R_j] \lesssim \beta^{-p} e^{-pj}, \quad \text{and} \quad \mathbf{P}[R_j] \lesssim \beta^{a/\gamma} C^{-a/\gamma} e^{aj/\gamma}.$$

We have that,

$$\begin{aligned}
\mathbf{P}[N \geq C,\ M \leq C/\beta] &\leq \sum_{j=0}^{\infty} \mathbf{P}[P_j] \leq \sum_{j=0}^{\infty} \mathbf{P}[Q_j \mid R_j]\mathbf{P}[R_j] \\
&\lesssim \beta^{a/\gamma} C^{-a/\gamma} \sum_{j=0}^{\infty} e^{aj/\gamma} \times \beta^{-p} e^{-pj} \\
&\lesssim \beta^{a/\gamma - p} C^{-a/\gamma} \quad (\text{since } p \in (a/\gamma, 2/\gamma^2)).
\end{aligned}$$

Combining with (5.7) proves (5.4).

Minor modifications to the above argument also give the result in the case that h is a GFF with Dirichlet boundary conditions on $\mathcal{Q}_+$. In particular, in this case $X_t = B_u - au$ where B is a standard Brownian motion. This changes the exponent in (5.6) from $-a/\gamma$ to $-2a/\gamma$. The result still holds for all $a \in (0, 2/\gamma)$ because the range of p values for which (5.8) holds is $p \in (0, 4/\gamma^2)$. □

We will now describe the law of a GFF h weighted by its ν_h mass. (Versions of this idea are also present in [DS11a, Section 6], [She10], and [MS13b, Section 4.4].)

For a simply connected domain $D \subseteq \mathbf{C}$ and $z \in D$, we let $\mathrm{CR}(z; D)$ denote the conformal radius of $z \in D$. That is, $\mathrm{CR}(z; D) = \varphi'(0)$ where $\varphi \colon \mathbf{D} \to D$ is the unique conformal transformation with $\varphi(0) = z$ and $\varphi'(0) > 0$.

Lemma 5.6. *Suppose that h is a GFF on a simply connected domain D whose boundary contains a linear segment L. Let dh denote the law of a GFF on D with free boundary conditions on L and Dirichlet boundary conditions on $\partial D \setminus L$. A sample from the law $\nu_h(L)dh$ can be produced by:*

1. *Sampling h according to its (unweighted) law.*

2. *Picking $z_0 \in L$ according to the measure $\mathrm{CR}(z; D^\dagger)^{\gamma^2/4} dz$ where dz is Lebesgue measure on L, $D^\dagger = D \cup \overline{D}$, and $\overline{D}$ is the reflection of D across L, independently of h and then adding to h the function $z \mapsto \frac{\gamma}{2} G(z_0, z)$ where G is the Green's function on D with Neumann (resp. Dirichlet) boundary conditions on L (resp. $\partial D \setminus L$).*

Proof. For each $\epsilon > 0$ and $z \in \overline{D}$, we let $h_\epsilon(z)$ be the average of h on $D \cap \partial B(z, \epsilon)$. Consider the law $\epsilon^{\gamma^2/4} \exp(\frac{\gamma}{2} h_\epsilon(u)) dh du$ where du is Lebesgue measure on L. As explained in [DS11a, Section 6.2], we note that we can write h as the even part of a GFF $h^\dagger$ on $D^\dagger$ on with Dirichlet boundary conditions. This in particular means that for $u \in L$ we have that with $h^\dagger_\epsilon(u)$ the average of $h^\dagger$ on $\partial B(u, \epsilon)$ with $B(u, \epsilon) \subseteq D^\dagger$ we have that

$$h_\epsilon(u) = \frac{1}{\sqrt{2}} \cdot 2 h^\dagger_\epsilon(u) = \sqrt{2} h^\dagger_\epsilon(u)$$

(see also [She10, Section 3.2]). Consequently, using [DS11a, Proposition 3.2] the marginal law of u is given by

$$\epsilon^{\gamma^2/4} \int e^{\gamma h^\dagger_\epsilon(u)/\sqrt{2}} dh^\dagger = \mathrm{CR}(u; D^\dagger)^{\gamma^2/4}.$$

Under this law, the conditional law of h given u is given by $\exp(\frac{\gamma}{2} h_\epsilon(u)) dh$. For $z \in \overline{D}$ we let ρ^z_ϵ be the uniform measure on $D \cap \partial B(z, \epsilon)$ and let

$$\xi^z_\epsilon(y) = -2 \log \max(|z - y|, \epsilon) - \widetilde{G}_{z,\epsilon}(y)$$

where $\widetilde{G}_{z,\epsilon}$ is given by the function which is harmonic in D with Neumann boundary conditions on L and with Dirichlet boundary values given by $y \mapsto -2 \log \max(|z-y|, \epsilon)$ on $\partial D \setminus L$. For $u \in L$, we note that $\Delta \xi^z_\epsilon(u) = -2\pi \rho^z_\epsilon(u)$ for all $\epsilon > 0$ sufficiently small so that $\partial B(u, \epsilon) \cap \partial D \subseteq L$. Moreover, we have that

$$\begin{aligned} h_\epsilon(u) &= \int_D h(y) \rho^u_\epsilon(y) dy = -\frac{1}{2\pi} \int_D h(y) \Delta \xi^u_\epsilon(y) dy \\ &= \frac{1}{2\pi} \int_D \nabla h(y) \cdot \nabla \xi^u_\epsilon(y) dy = (h, \xi^u_\epsilon)_\nabla \end{aligned}$$

for all $\epsilon > 0$ sufficiently small. Now, the marginal law of h under the weighted law $\exp(\frac{\gamma}{2}(h, \xi^u_\epsilon)_\nabla) dh$ can be sampled from by sampling h according to its unweighted law and then adding to it $\frac{\gamma}{2} \xi^u_\epsilon$. The result follows because $\xi^u_\epsilon \to G(u, \cdot)$ for $u \in L$ and $\epsilon^{\gamma^2/4} \exp(\frac{\gamma}{2} h_\epsilon(u)) du \to \nu_h$ as $\epsilon \to 0$. □

Proof of Proposition 5.1. We are first going to prove the result with h sampled from the law $\nu_h(L) dh$ as in Lemma 5.6 in place of the unweighted law dh.

Let G be the Green's function on D with Neumann (resp. Dirichlet) boundary conditions on L (resp. $\partial D \setminus L$). By Lemma 5.6, we know that we can produce a sample of h from $\nu_h(L)dh$ by first sampling $\widehat{h}$ according to the law dh and then taking $h = \widehat{h} + \frac{\gamma}{2}G(u_0, \cdot)$ where $u_0 \in L$ is chosen independently of $\widehat{h}$ from the measure $\mathrm{CR}(z; D^\dagger)^{\gamma^2/4}dz$ where dz is Lebesgue measure on L (as in the statement of Lemma 5.6). Let x_0 (resp. y_0) be the two endpoints of L. Let $\psi \colon D \to \mathcal{S}$ be the unique conformal transformation with $\psi(u_0) = +\infty$, $\psi(x_0) = 0$, and $\psi(y_0) = \pi i$. Then $h \circ \psi^{-1} + Q \log |(\psi^{-1})'|$ can be written as $\widetilde{h} + F + (\gamma - Q)\mathrm{Re}(z)$ where $\widetilde{h}$ and F are as in the statement of Lemma 5.3. (The terms F and $-Q\mathrm{Re}(z)$ come from the coordinate change term $Q \log |(\psi^{-1})'|$ and the term $\gamma \mathrm{Re}(z)$ comes because $G(u_0, \cdot)$ behaves like $-2 \log |u_0 - \cdot|$ near u_0.)

Let $\widetilde{X}_u$ be the projection of $\widetilde{h} + F + (\gamma - Q)\mathrm{Re}(z)$ onto $\mathcal{H}_1(\mathcal{S})$. For $C, \epsilon > 0$ and $\beta > 1$, we let $E_{C,\epsilon}$ and $E'_{C,\beta}$ be as in Lemma 5.5 (note that $Q - \gamma = 2/\gamma - \gamma/2 \in (0, 2/\gamma)$). Note that (5.4) implies that for each $\delta > 0$ there exists β_0 such that $\beta \geq \beta_0$ implies that the total variation distance between the law of $\widetilde{h} - \gamma^{-1} \log C$ given $E_{C,\epsilon}$ and $\widetilde{h} - \gamma^{-1} \log C$ given $E'_{C,\beta} \cap E_{C,\epsilon}$ is at most $\delta > 0$. Thus by (5.5), to prove the existence of the limit of the law of $\widetilde{h} - \gamma^{-1} \log C$ given $E_{C,\epsilon}$ as $C \to \infty$ it suffices to prove the existence of the limit of the law of $\widetilde{h} - \gamma^{-1} \log C$ given $E'_{C,\beta}$ as $C \to \infty$ for each $\beta > 1$. Lemma 5.3 implies that the law of $\widetilde{h} - \gamma^{-1} \log C$ given $E'_{C,\beta}$ with the horizontal translation fixed so that $\widetilde{X}$ first hits $\gamma^{-1} \log(C/\beta)$ at $u = 0$ converges to a limit as $C \to \infty$ which does not depend on our initial choices.

We can describe the limiting law explicitly as follows. Using Proposition 3.4, it follows that the limiting law as $C \to \infty$ for $\widetilde{h} - \gamma^{-1} \log C$ is given by $\mathcal{M}_\delta^{2\gamma^{-1}}$ (as described in the statement of the present proposition with $\delta = 3 - \frac{4}{\gamma^2}$) conditioned on both

1. The supremum of the projection onto $\mathcal{H}_1(\mathcal{S})$ is at least $-\gamma^{-1} \log \beta$ and
2. The γ-LQG area is between 1 and $1 + \epsilon$.

(Note that this describes a probability measure since this set has positive and finite $\mathcal{M}_\delta^{2\gamma^{-1}}$-mass.) Sending $\beta \to \infty$ and $\epsilon \to 0$ we see that the limiting law when we have weighted by γ-LQG boundary length is given by $\mathcal{M}_\delta^{2\gamma^{-1}}$ conditioned on $\mu_h(\mathcal{S}) = 1$. The result follows by unweighting by γ-LQG boundary length. □

We are now going to deduce from the proof of Proposition 5.13 a certain symmetry property for the unit area quantum disk which is not immediately obvious from Definition 4.21.

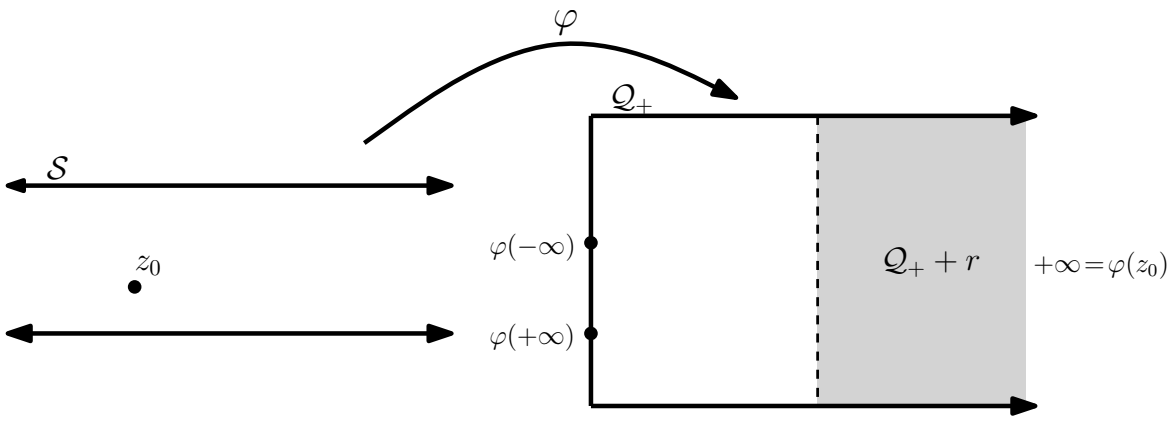

Figure 5.1: Shown on the left is a unit area quantum disk parameterized by $\mathcal{S}$, z_0 a point picked in $\mathcal{S}$ uniformly from the quantum measure, and $\varphi\colon \mathcal{S} \to \mathcal{Q}_+$ the unique conformal map with $\varphi(z_0) = +\infty$ and $\varphi'(z_0) > 0$. Proposition 5.8 implies that the conditional law of the surface on the right given the field values in $\mathcal{Q}_+ + r$, $r > 0$ fixed, is given by that of a GFF in $[0, r] \times [0, 2\pi] \subseteq \mathcal{Q}_+$ with Dirichlet (resp. free) boundary conditions on $\partial\mathcal{Q}_+ + r$ (resp. $\partial\mathcal{Q}_+$) weighted by the quantum boundary length of $\partial\mathcal{Q}_+$ conditioned on the total area being equal to 1.

Proposition 5.7. *Suppose that $(\mathcal{S}, h)$ has the law of a unit area quantum disk with the embedding into $\mathcal{S}$ as described in Definition 4.21. Conditional on $\mathcal{S}$, the points which correspond to $-\infty$ and $+\infty$ are uniformly and independently distributed according to the quantum boundary measure.*

Proof. It follows from the proof of Proposition 5.1 that the point which corresponds to $+\infty$ is uniformly distributed according to the quantum boundary measure. Moreover, the proof of Proposition 5.1 implies that this holds conditionally on the location of the point which corresponds to $-\infty$. By the symmetry of the construction given in Definition 4.21, it follows that $-\infty$ is also uniformly distributed according to the quantum boundary measure. Combining implies the result. □

We are now going to explain a variant of the proof of Proposition 5.1 which yields the following useful resampling property for the unit area quantum disk.

Proposition 5.8. *Suppose that $D \subseteq \mathbf{C}$ is a simply-connected domain and h is such that (D, h) has the law of a unit area quantum disk. Pick $z \in D$ uniformly at random from the quantum measure associated with h, let $\varphi\colon D \to \mathcal{Q}_+$ be the unique conformal transformation with $\varphi(z) = +\infty$ and $\varphi'(z) > 0$, and let $\widetilde{h} = h \circ \varphi^{-1} + Q \log |(\varphi^{-1})'|$. For each $r > 0$, let $\mathcal{F}_r$ be the σ-algebra generated by the restriction of h to $\mathcal{Q}_+ + r$. Then the conditional law of h given $\mathcal{F}_r$ is that of a GFF on $[0, r] \times [0, 2\pi] \subseteq \mathcal{Q}_+$ with*

free boundary conditions on $\partial\mathcal{Q}_+$ and Dirichlet boundary conditions given by h on $\partial(\mathcal{Q}_+ + r)$ weighted by $\nu_h(\partial\mathcal{Q}_+)$ conditioned on the total area being equal to 1.

See Figure 5.1 for an illustration of the setup of Proposition 5.8. To give the proof of Proposition 5.8, we need the following analog of Lemma 5.6 (see also [DS11a, Section 3.3]). This lemma will also be useful to us later when we construct the unit area quantum sphere as a limit in Section 5.3 below.

Lemma 5.9. *Suppose that h is a GFF on a bounded, simply connected domain D with Dirichlet boundary conditions. Let dh denote the law of h and consider the law $\mu_h(D)dh$. A sample from the law $\mu_h(D)dh$ can be produced by:*

1. *Sampling h according to its (unweighted) law.*
2. *Picking $z_0 \in D$ according to the measure $\mathrm{CR}(z;D)^{\gamma^2/2}dz$ where dz denotes Lebesgue measure on D independently of h and then adding to h the function $z \mapsto \gamma G(z_0, z)$ where G is the Green's function on D with Dirichlet boundary conditions.*

The same likewise holds if $\partial D = \partial^{\mathrm{F}} \cup \partial^{\mathrm{D}}$ is a disjoint union with $\partial^{\mathrm{F}}, \partial^{\mathrm{D}} \neq \emptyset$ and h is a GFF on D with Dirichlet (resp. free) boundary conditions on ∂^{D} (resp. ∂^{F}) where we take G to be the Green's function on D with Dirichlet (resp. Neumann) boundary conditions on ∂^{D} (resp. ∂^{F}) and $C(z;D)$ in the density for the law of $z_0 \in D$ is replaced by the function $\lim_{y\to z} \exp(G(y,z) + \log|y-z|)$. (In this case, $\mu_h(D)dh$ may be an infinite measure).

Proof. We are going to give the proof in the case of Dirichlet boundary conditions; the proof in the case of mixed boundary conditions follows from the same argument.

For each $\epsilon > 0$, we let h_ϵ be the circle average process associated with h. Consider the measure $\epsilon^{\gamma^2/2}\exp(\gamma h_\epsilon(u))dhdu$ where du is Lebesgue measure on D. By [DS11a, Proposition 3.2], we note that the density of the marginal law of u with respect to Lebesgue measure is given by

$$\epsilon^{\gamma^2/2}\int e^{\gamma h_\epsilon(u)}dh = \mathrm{CR}(u;D)^{\gamma^2/2}$$

provided $B(u,\epsilon) \subseteq D$. Moreover, the law of h under this weighting converges as $\epsilon \to 0$ to the same law as $\mu_h(D)dh$. Using the former law, the conditional law of h given u is given by $\exp(\gamma h_\epsilon(u))dh$. Let ρ_ϵ^z be the uniform measure on $\partial B(z,\epsilon)$ and let

$$\xi_\epsilon^z(y) = -\log\max(|z-y|,\epsilon) - \widetilde{G}_{z,\epsilon}(y)$$

where $\widetilde{G}_{z,\epsilon}$ is given by the harmonic extension of $y \mapsto -\log\max(|z-y|,\epsilon)$ from ∂D to D. Note that $\Delta\xi^z_\epsilon(y) = -2\pi\rho^z_\epsilon(y)$. Moreover, we have that

$$\begin{aligned} h_\epsilon(u) &= \int_D h(y)\rho^u_\epsilon(y)dy = -\frac{1}{2\pi}\int_D h(y)\Delta\xi^u_\epsilon(y)dy \\ &= \frac{1}{2\pi}\int_D \nabla h(y)\cdot\nabla\xi^u_\epsilon(y)dy = (h,\xi^u_\epsilon)_\nabla. \end{aligned}$$

Now, the marginal law of h under the weighting $\exp(\gamma(h,\xi^u_\epsilon)_\nabla)dh$ is given by taking the law of h and then adding to it $\gamma\xi^u_\epsilon$. The result follows because $\xi^u_\epsilon \to G(u,\cdot)$ as $\epsilon \to 0$. □

Proof of Proposition 5.8. We are going to deduce the result from the proof of Proposition 5.13.

We first suppose that (D,h) is as in the statement of Proposition 5.13. Let G be the Green's function for Δ on D with Dirichlet (resp. Neumann) boundary conditions on $\partial D \setminus L$ (resp. L). By Lemma 5.6, we know that we can produce a sample from the law of $\nu_h(L)dh$ by first producing a sample of $\widehat{h}$ from the law dh and then taking $\widetilde{h} = \widehat{h} + \frac{\gamma}{2}G(u_0,\cdot)$ where u_0 is picked from the measure $\mathrm{CR}(z;D^\dagger)^{\gamma^2/4}dz$, dz Lebesgue measure on L, and $D^\dagger = D \cup \overline{D}$. Fix a neighborhood $U \subseteq L$ of u_0. Lemma 5.9 implies that we can produce a sample from the conditional law of $\widetilde{h}$ given its values on U and weighted by $\mu_{\widetilde{h}}(D)$ by first picking $z_0 \in D$ according to the measure $(f(z))^{\gamma^2/2}dz$ and then adding $\gamma\widetilde{G}(z_0,z)$ to the field where $\widetilde{G}$ is the Green's function on D with Dirichlet boundary values on $(\partial D \setminus L) \cup U$ and Neumann boundary conditions on $L \setminus U$ and $f(z) = \lim_{y\to z}\exp(\widetilde{G}(y,z) + \log|y-z|)$.

Let x, y be the two endpoints of L and let φ be the unique conformal map $D \to \mathcal{S}_+$ which takes x to 0, y to $i\pi$, and u_0 to $+\infty$. We then let r_0 be such that the real part of $\varphi(z_0) + r_0$ is equal to 0 and then let $\widetilde{\varphi} = \varphi + r_0$ and $\breve{h} = \widetilde{h} \circ \widetilde{\varphi}^{-1} + Q\log|(\widetilde{\varphi}^{-1})'|$.

It follows from the proof of Proposition 5.1 that the limit of the law of $(\mathcal{S}_+ - r_0, \widetilde{h} - (\log C)/\gamma)$ conditioned on $C \le \mu_{\widetilde{h}}(\mathcal{S}_+ - r_0) \le C(1+\epsilon)$ converges when we take a limit as $C \to \infty$ and then $\epsilon \to 0$ to the law of the unit area quantum disk weighted by its quantum boundary length. Thus the above tells us how to resample the law of the unit area quantum disk weighted by its quantum boundary length once we have picked a uniformly random point from the quantum area measure and we have fixed its values in a neighborhood U of $\pm\infty$ in $\partial\mathcal{S}$. Namely, the conditional law is given by that of a GFF in $\mathcal{S}$ with free boundary conditions along $\partial\mathcal{S} \setminus U$ and Dirichlet boundary conditions along ∂U plus $\gamma G(w_0,\cdot)$ where G is the Green's function on $\mathcal{S}$ with Neumann (resp. Dirichlet) boundary conditions on $\partial\mathcal{S} \setminus U$ (resp. $\partial U \cap \mathcal{S}$) conditioned on the total mass being equal to 1.

Suppose that $(\mathcal{S},h)$ has the law of a unit area quantum disk weighted by its boundary length, w_0 is chosen uniformly from the quantum area measure, and that $\varphi\colon \mathcal{S} \to \mathcal{Q}_+$

is the unique conformal map with $\varphi(w_0) = +\infty$ and $\varphi'(w_0) > 0$. Then with $\widetilde{h} = h \circ \varphi^{-1} + Q \log |(\varphi^{-1})'|$ we have that $(\mathcal{Q}_+, \widetilde{h})$ has the law of a unit area quantum disk weighted by its quantum boundary length. Suppose that $a_0, b_0 \in \partial\mathcal{Q}_+$ are picked uniformly and independently from the quantum boundary measure. Proposition 5.7 combined with the above implies that if $r > 0$ is fixed, then the conditional law of $\widetilde{h}$ in $[0, r] \times [0, 2\pi]$ given its values in $\mathcal{Q}_+ + r$ and in a neighborhood U of a_0, b_0 in $\partial\mathcal{Q}_+$ is that of a GFF with free (resp. Dirichlet) boundary conditions on $\partial\mathcal{Q}_+ \setminus U$ (resp. $U \cup \partial(\mathcal{Q}_+ + r)$) conditioned on the total area being equal to 1. By taking a limit as the size of U tends to 0, we see from Lemma 5.6 that the conditional law of h given $\mathcal{F}_r$ is that of a GFF weighted by the square of its boundary length on $\partial\mathcal{Q}_+$. Unweighting by the boundary length of $\partial\mathcal{Q}_+$ proves the result. □

5.2 Unit boundary length quantum disk

We next construct the unit boundary length quantum disk using a limiting procedure similar to that described in Proposition 5.1.

Proposition 5.10. *Fix a smooth, bounded domain D with a linear segment L of ∂D. Let h be a GFF on D with free boundary conditions on L and zero boundary conditions on $\partial D \setminus L$. Fix $C, \epsilon > 0$ and condition on $\{\sqrt{C} \le \nu_h(L) \le \sqrt{C}(1+\epsilon)\}$. Let $\widehat{h} = h - \gamma^{-1} \log C$ so that $1 \le \nu_{\widehat{h}}(L) \le 1 + \epsilon$. Then the law of $(D, \widehat{h})$ (viewed as a quantum surface) converges weakly to the law of the unit boundary length quantum disk as in Definition 4.21 when we take a limit first as $C \to \infty$ and then as $\epsilon \to 0$. In particular, the limiting law does not depend on D or L.*

Proof. As in the proof of Proposition 5.1, we consider the law of $\nu_h(L)dh$ in place of h. We then let $\widetilde{h}$ and $\widetilde{X}$ be as in the proof of Proposition 5.1. For each $C, \epsilon > 0$ and $\beta > 1$, we define events

$$\begin{aligned} E_{C,\epsilon} &= \{\sqrt{C} \le \nu_{\widetilde{h}}(\partial\mathcal{S}) \le \sqrt{C}(1+\epsilon)\} \quad \text{and} \\ E'_{C,\beta} &= \left\{ \sup_{u \ge 0} \widetilde{X}_u \ge \gamma^{-1} \log\left(\frac{C}{\beta}\right) \right\}. \end{aligned} \tag{5.9}$$

The same argument as in the proof of Lemma 5.5 implies that we have both

$$\mathbf{P}[E'_{C,\beta} \,|\, E_{C,\epsilon}] \to 1 \quad \text{as} \quad \beta \to \infty \quad \text{uniformly in} \quad C \quad \text{and} \tag{5.10}$$

$$\mathbf{P}[E_{C,\epsilon} \,|\, E'_{C,\beta}] > 0 \quad \text{uniformly in} \quad C \quad \text{for} \quad \beta > 1 \quad \text{fixed.} \tag{5.11}$$

Thus, as in the proof of Proposition 5.1, it suffices to prove the existence of the limit of the law of $\widetilde{h} - \gamma^{-1} \log C$ given $E'_{C,\beta}$ with the horizontal translation taken so that $\widetilde{X}$ first hits $\gamma^{-1} \log(C/\beta)$ at $u = 0$. This, in turn, follows from Lemma 5.3. The limiting law is identified in the same manner as in the proof of Proposition 5.1. □

We also have the following analog of Proposition 5.7 for the unit boundary length quantum disk.

Proposition 5.11. *Suppose that $(\mathcal{S}, h)$ has the law of a unit boundary length quantum disk with the embedding into $\mathcal{S}$ as described in Definition 4.21. Conditional on $\mathcal{S}$, the points which correspond to $-\infty$ and $+\infty$ are uniformly and independently distributed according to the quantum boundary measure.*

Proof. This follows from the same argument used to prove Proposition 5.7. □

Proposition 5.12. *Suppose that $D \subseteq \mathbf{C}$ is a simply connected domain and h is such that (D, h) has the law of a unit boundary length quantum disk. Pick $z \in D$ uniformly at random from the quantum measure associated with h, let $\varphi \colon D \to \mathcal{Q}_+$ be the unique conformal transformation with $\varphi(z) = +\infty$ and $\varphi'(z) > 0$, and let $\widetilde{h} = h \circ \varphi^{-1} + Q \log |(\varphi^{-1})'|$. For each $r > 0$, let $\mathcal{F}_r$ be the σ-algebra generated by the restriction of h to $\mathcal{Q}_+ + r$. Then the conditional law of h given $\mathcal{F}_r$ is that of a GFF on $[0, r] \times [0, 2\pi] \subseteq \mathcal{Q}_+$ with free boundary conditions on $\partial\mathcal{Q}_+$ and Dirichlet boundary conditions given by those of h on $\partial(\mathcal{Q}_+ + r)$ conditioned on the quantum boundary length of $\partial\mathcal{Q}_+$ being equal to 1.*

Proof. This follows from the same argument used to prove Proposition 5.8. □

5.3 Unit area quantum sphere

We now turn to the case of the unit area quantum sphere.

Proposition 5.13. *Fix a smooth, bounded domain D. Let h be a GFF on D with zero boundary conditions. Fix $C, \epsilon > 0$ and condition on $\{C \leq \mu_h(D) \leq C(1+\epsilon)\}$. Let $\widehat{h} = h - \gamma^{-1} \log C$ so that $1 \leq \mu_{\widehat{h}}(D) \leq 1 + \epsilon$. Then the law of $(D, \widehat{h})$ (viewed as a quantum surface) converges weakly to the law of the unit area quantum sphere as in Definition 4.21 when we take a limit first as $C \to \infty$ and then as $\epsilon \to 0$. In particular, the limiting law does not depend on D.*

Before proving Proposition 5.13, we need to collect the following analog of Lemma 5.3.

Lemma 5.14. *Suppose that h is a GFF on $\mathcal{Q}_+$ with zero boundary conditions and let F be a function which is harmonic on $\mathcal{Q}_+$. Fix $a > 0$ and for each $u > 0$ we let X_u be the average of $h + F - a\mathrm{Re}(z)$ on $u + [0, 2\pi i]$. For each $C > 0$, let $\tau_C = \inf\{u \geq 0 : X_u \geq C\}$ and let $E_C = \{\tau_C < \infty\}$. On E_C, we let $\widetilde{h}$ be given by precomposing $h + F - a\mathrm{Re}(z) - C$ with the horizontal translation $z \mapsto z + \tau_C$. Then the conditional law of $\widetilde{h}$ given E_C converges as $C \to \infty$. Moreover, the limit law can be sampled from by:*

(i) Taking its projection $\widetilde{X}_u$ onto $\mathcal{H}_1(\mathcal{Q})$ to be given by $B_u - au$ for $u \geq 0$ where B is a standard Brownian motion with $B_0 = 0$ and to be given by $\widehat{B}_{-u} + au$ for $u < 0$ where $\widehat{B}$ is a standard Brownian motion with $\widehat{B}_0 = 0$ conditioned so that $\widehat{B}_{-u} + au < 0$ for all $u < 0$.

(ii) Independently sampling its projection onto $\mathcal{H}_2(\mathcal{Q})$ according to the law of the corresponding projection of the GFF on $\mathcal{Q}$.

Proof. We omit the details since it is very similar to the proof of Lemma 5.3. □

Proof of Proposition 5.13. The proof is similar to the proof of Proposition 5.1. We consider the law $\mu_h(D)dh$ in place of the law h.

By Lemma 5.9, we can produce a sample of h from $\mu_h(D)dh$ by first sampling $\widehat{h}$ according to the law of dh and then taking $h = \widehat{h} + \gamma G(z_0, \cdot)$ where $z_0 \in D$ is chosen uniformly from Lebesgue measure independently of $\widehat{h}$. We let $\psi \colon D \to \mathcal{Q}_+$ be the unique conformal transformation with $\psi(z_0) = +\infty$ and $\psi'(z_0) > 0$. Consider the field $\widetilde{h} = h \circ \psi^{-1} + Q \log |(\psi^{-1})'|$ on $\mathcal{Q}_+$. Note that $\widetilde{h}$ is given by a GFF on $\mathcal{Q}_+$ with Dirichlet boundary conditions plus the function $(\gamma - Q)\mathrm{Re}(z)$. We let $\widetilde{X}_u$ be the projection of $\widetilde{h}$ onto $\mathcal{H}_1(\mathcal{Q}_+)$ as in Lemma 4.2. As in the proof of Proposition 5.1, for $C, \epsilon > 0$ and $\beta > 1$ we define events

$$\begin{aligned} E_{C,\epsilon} &= \left\{ C \leq \mu_{\widetilde{h}}(\mathcal{Q}_+) \leq C(1+\epsilon) \right\} \quad \text{and} \\ E'_{C,\beta} &= \left\{ \sup_{u \geq 0} \widetilde{X}_u \geq \gamma^{-1} \log \left(\frac{C}{\beta} \right) \right\}. \end{aligned} \tag{5.12}$$

Therefore the result follows by arguing as in Proposition 5.1 using Lemma 5.14 in place of Lemma 5.3. □

We finish this section with the following analog of Proposition 5.7 and Proposition 5.11 for the unit area sphere.

Proposition 5.15. *Suppose that $\mathcal{S} = (\mathcal{Q}, h)$ is a unit area quantum sphere embedded into $\mathcal{Q}$ as in Definition 4.21. Conditional on $\mathcal{S}$, the points which correspond to $-\infty$ and $+\infty$ are distributed independently and uniformly from the quantum area measure.*

Proof. This follows from the same argument used to prove Proposition 5.7 and Proposition 5.11. □

Proposition 5.16. *Suppose that $(\mathcal{Q}, h)$ has the law of the unit area sphere embedded into $\mathcal{Q}$ as in Definition 4.21. Assume that $z \in \mathcal{Q}$ is picked uniformly from the quantum measure and let $\widetilde{h} = h(\cdot - z)$ (so that $(\mathcal{Q}, \widetilde{h})$ has the law of the unit area sphere with a fixed embedding because we have chosen the locations of three points). Fix a bounded domain $U \subseteq \mathcal{Q}$ containing 0. Let G be the Green's function on U with Dirichlet boundary conditions. Then the conditional law of h in U given its values in $\mathcal{Q} \setminus U$ is that of a GFF in U with the given boundary conditions on ∂U plus $\gamma G(0, \cdot)$ conditioned so that the total area is equal to 1.*

Proof. This follows from the same argument used to prove Proposition 5.12 and Proposition 5.8. □

We remark that a statement similar to Proposition 5.16 also appears in [AHS15], which proves the equivalence of the unit area quantum sphere with another construction given in [DKRV14].

6 SLE/GFF couplings

In this section, we will describe the reverse (Section 6.1) and forward (Section 6.2) couplings of SLE with the GFF. As an application of the latter, in Section 6.3 we will give the conditional law of the excursion of a boundary intersecting $\mathrm{SLE}_\kappa(\rho)$ process in $\mathbf{H}$ with $\kappa \in (0, 4)$ which separates a given boundary point u from ∞ given the realization of the path before (resp. after) the start (resp. end) of the excursion.

6.1 Reverse coupling

Throughout, we fix $\kappa > 0$, let $\gamma = \min(\sqrt{\kappa}, 4/\sqrt{\kappa})$, and $Q = \frac{2}{\gamma} + \frac{\gamma}{2}$. Let

$$G(y, z) = -\log|y - z| - \log|y - \overline{z}| \tag{6.1}$$

denote the Neumann Green's function on $\mathbf{H}$. For a given reverse Loewner flow (f_t) (which will be clear from the context), we let $G_t(y, z) = G(f_t(y), f_t(z))$,

$$\mathfrak{h}_0(z) = \frac{2}{\sqrt{\kappa}} \log|z|, \quad \text{and} \quad \mathfrak{h}_t(z) = \mathfrak{h}_0(f_t(z)) + Q \log|f_t'(z)|.$$

The following is a version of [She10, Theorem 4.5].

Theorem 6.1. *Fix $\kappa > 0$, $\rho_1, \ldots, \rho_k \in \mathbf{R}$, and $x_1, \ldots, x_k \in \overline{\mathbf{H}}$. Suppose that W solves the reverse $\mathrm{SLE}_\kappa(\underline{\rho})$ SDE (3.12) with force points located at $x_1, \ldots, x_k$ of weight $\rho_1, \ldots, \rho_k$, respectively, and let (f_t) be the centered reverse Loewner evolution driven by W. For each $t \geq 0$, let*

$$\widehat{\mathfrak{h}}_t(z) = \mathfrak{h}_t(z) + \frac{1}{2\sqrt{\kappa}} \sum_{j=1}^{k} \rho_j G_t(x_j, z)$$

and let h be an instance of the free boundary GFF on $\mathbf{H}$ independent of W. Suppose that τ is an almost surely finite stopping time for the filtration generated by the Brownian motion which drives W that occurs at or before the continuation threshold for W is reached. Then

$$\widehat{\mathfrak{h}}_0 + h \stackrel{d}{=} \widehat{\mathfrak{h}}_\tau + h \circ f_\tau$$

where the left and right sides are viewed as modulo additive constant distributions.

The statement of Theorem 6.1 differs from that of [She10, Theorem 4.5] in two ways:

1. We only work with a finite, discrete set of force points. In particular, we do not include the possibility of having a continuum of force points.
2. The coupling is stated and proved even after the force points have interacted with the driving function.

The proof of Theorem 6.1 is similar to that of [She10, Theorem 4.5], but we will provide it for completeness. The proof below closely follows the presentation of the radial version of this theorem given in [MS13b, Section 5].

Lemma 6.2. *For each $y, z \in \mathbf{H}$ distinct, we have that*

$$dG_t(y, z) = -\mathrm{Re}\frac{2}{f_t(y)}\mathrm{Re}\frac{2}{f_t(z)}dt. \tag{6.2}$$

For each $z \in \mathbf{H}$, we have that

$$d\widehat{\mathfrak{h}}_t(z) = -\mathrm{Re}\frac{2}{f_t(z)}dB_t. \tag{6.3}$$

Proof. Applications of Itô's formula imply that

$$d\log(f_t(y) - f_t(z)) = \frac{2dt}{f_t(y)f_t(z)} \quad \text{and}$$
$$d\log(f_t(y) - \overline{f_t(z)}) = \frac{2dt}{f_t(y)\overline{f_t(z)}}.$$

Adding these up, multiplying by -1, and then taking real parts yields (6.2). See the proof of [She10, Theorem 1.2] for a similar calculation (though for the forward rather than reverse coupling).

For (6.3), we first note by several applications of Itô's formula that:

$$\begin{aligned} df_t(z) &= \left(-\frac{2}{f_t(z)} + \sum_{j=1}^{k} \mathrm{Re}\frac{\rho_j}{f_t(x_j)} \right) dt - \sqrt{\kappa} dB_t, \\ d\log f_t(z) &= \left(-\frac{4+\kappa}{2f_t^2(z)} + \frac{1}{f_t(z)} \sum_{j=1}^{k} \mathrm{Re}\frac{\rho_j}{f_t(x_j)} \right) dt - \frac{\sqrt{\kappa}}{f_t(z)} dB_t, \\ df_t'(z) &= \frac{2f_t'(z)}{f_t^2(z)} dt, \quad \text{and} \quad d\log f_t'(z) = \frac{2}{f_t^2(z)} dt. \end{aligned}$$

Taking real parts and adding up (and using (6.2)) yields (6.3). □

Lemma 6.3. *For each $t \geq 0$, $\widehat{\mathfrak{h}}_t + h \circ f_t$ almost surely takes values in the space of modulo additive constant distributions. Suppose that $\phi \in C_0^\infty(\mathbf{H})$ with $\int_{\mathbf{H}} \phi(z) dz = 0$. Then both $(\widehat{\mathfrak{h}}_t + h \circ f_t, \phi)$ and $(\widehat{\mathfrak{h}}_t, \phi)$ are almost surely continuous in t and the latter is a square-integrable martingale.*

Proof. We first note that it is clear that $h \circ f_t$ takes values in the space of distributions modulo additive constant and that $(h \circ f_t, \rho)$ is almost surely continuous in t from how it is defined. This leaves us to deal with $\widehat{\mathfrak{h}}_t$. It follows from (6.3) of Lemma 6.2 that for each fixed $z \in \mathbf{H}$ we have

$$d\langle \widehat{\mathfrak{h}}_t(z) \rangle = \left(\mathrm{Re}\frac{2}{f_t(z)} \right)^2 dt.$$

Note that it follows from the form of the SDE for the centered reverse Loewner flow that $\mathrm{Im} f_t(z)$ is non-decreasing in t for any fixed $z \in \mathbf{H}$. Fix $K \subseteq \mathbf{H}$ compact and $T < \infty$. It consequently follows that there exists a constant $C > 0$ depending only on K and T such that

$$\sup_{z \in K} \langle \widehat{\mathfrak{h}}_t(z) - \widehat{\mathfrak{h}}_u(z) \rangle \leq C(t-u) \quad \text{for all} \quad 0 \leq u \leq t \leq T.$$

It therefore follows from the Burkholder-Davis-Gundy inequality that for each $p \geq 1$ there exists $C_p, C_p' > 0$ depending only on p, K, and T such that

$$\begin{aligned} \sup_{z \in K} \mathbf{E}\left[\sup_{u \leq s \leq t} |\widehat{\mathfrak{h}}_s(z) - \widehat{\mathfrak{h}}_u(z)|^p \right] &\leq C_p \sup_{z \in K} \mathbf{E}\left[\langle \widehat{\mathfrak{h}}_t(z) - \widehat{\mathfrak{h}}_u(z) \rangle^{p/2} \right] \\ &\leq C_p'(t-u)^{p/2} \quad \text{for all} \quad 0 \leq u \leq t \leq T. \end{aligned} \tag{6.4}$$

It is easy to see from (6.4) with $u = 0$ and Fubini's theorem that for each $K \subseteq \mathbf{H}$ compact we have that $\widehat{\mathfrak{h}}_t|_K$ is almost surely in $L^p(K)$. By combining (6.4) and the Kolmogorov-Centsov theorem, it is also easy to see that $t \mapsto (\mathfrak{h}_t, \phi)$ is almost surely continuous for any $\phi \in C_0^\infty(\mathbf{H})$ with $\int_{\mathbf{H}} \phi(z)dz = 0$. Lastly, it follows from (6.3) and (6.4) of Lemma 6.2 that $(\widehat{\mathfrak{h}}_t, \phi)$ is a square-integrable martingale. This completes the proof of both assertions of the lemma. □

For each $\phi \in C_0^\infty(\mathbf{H})$ with $\int_{\mathbf{H}} \phi(z)dz = 0$ and $t \geq 0$ we let

$$E_t(\phi) = \iint_{\mathbf{H}^2} \phi(y)G_t(y, z)\phi(z)dydz$$

be the conditional variance of $(h \circ f_t, \phi)$ given f_t.

Lemma 6.4. *For each $\phi \in C_0^\infty(\mathbf{H})$ with $\int_{\mathbf{H}} \phi(z)dz = 0$ we have that*

$$d\langle(\widehat{\mathfrak{h}}_t, \phi)\rangle = -dE_t(\phi).$$

Proof. Since $(\widehat{\mathfrak{h}}_t, \phi)$ is a continuous L^2 martingale, the process $\langle(\widehat{\mathfrak{h}}_t, \phi)\rangle$ is characterized by the property that

$$(\widehat{\mathfrak{h}}_t, \phi)^2 - \langle(\widehat{\mathfrak{h}}_t, \phi)\rangle$$

is a continuous local martingale in $t \geq 0$. Thus to complete the proof of the lemma, it suffices to show that

$$(\widehat{\mathfrak{h}}_t, \phi)^2 + E_t(\phi)$$

is a continuous local martingale. It follows from (6.2) and (6.3) of Lemma 6.2 that

$$\widehat{\mathfrak{h}}_t(y)\widehat{\mathfrak{h}}_t(z) + G_t(y, z)$$

evolves as the sum of a continuous martingale in $t \geq 0$ plus a drift term which can be expressed as a sum of terms, one of which depends only on y and the other only on z. These drift terms cancel upon integrating against $\phi(y)\phi(z)dydz$ which in turn implies the desired result. □

Proof of Theorem 6.1. Fix $\phi \in C_0^\infty(\mathbf{H})$ with $\int_{\mathbf{H}} \phi(z)dz = 0$. Let $\mathcal{F}_t$ be the filtration generated by f_t. Note that $\widehat{\mathfrak{h}}_t$ is $\mathcal{F}_t$-measurable and that, given $\mathcal{F}_t$, $(h \circ f_t, \phi)$ is a Gaussian random variable with mean zero and variance $E_t(\phi)$. Let $I_t(\phi) = (h \circ f_t + \widehat{\mathfrak{h}}_t, \phi)$. For $\theta \in \mathbf{R}$ we have that

$$\begin{aligned}
&\mathbf{E}[\exp(i\theta I_t(\phi))] = \mathbf{E}[\mathbf{E}[\exp(i\theta I_t(\phi))|\mathcal{F}_t]] \\
=&\mathbf{E}[\mathbf{E}[\exp(i\theta(h \circ f_t, \phi))|\mathcal{F}_t] \exp(i\theta(\widehat{\mathfrak{h}}_t, \phi))] \\
=&\mathbf{E}[\exp(i\theta(\widehat{\mathfrak{h}}_t, \phi) - \tfrac{\theta^2}{2}E_t(\phi))]
\end{aligned}$$

$$= \exp(i\theta(\widehat{\mathfrak{h}}_0, \phi) - \tfrac{\theta^2}{2} E_0(\phi)).$$

Therefore $I_t(\phi) \overset{d}{=} I_0(\phi)$ for each $\phi \in C_0^\infty(\mathbf{H})$ with $\int_{\mathbf{H}} \phi(z) dz = 0$. The result follows since this holds for all such test functions ϕ and $\phi \mapsto I_0(\phi)$ has a Gaussian distribution. □

In analogy with [MS13b, Theorem 5.1] and Theorem 6.1, it is also possible to couple reverse radial $\mathrm{SLE}_\kappa(\rho)$ with the GFF. This is proved in [MS13b, Theorem 5.5]; we restate the result here for the convenience of the reader since we will make use of it later in the article.

Theorem 6.5. *Fix $\kappa > 0$. Suppose that h is a free boundary GFF on $\mathbf{D}$ and let (f_t) be the centered reverse radial $\mathrm{SLE}_\kappa(\rho)$ Loewner flow which is driven by the solution U as in (3.25) with $V_0 = v_0 \in \partial\mathbf{D}$ taken to be independent of h. For each $t \geq 0$ and $z \in \mathbf{D}$ we let*

$$\begin{aligned} \mathfrak{h}_t(z) = &\frac{2}{\sqrt{\kappa}} \log|f_t(z) - 1| - \frac{\kappa + 6 - \rho}{2\sqrt{\kappa}} \log|f_t(z)| - \\ &\frac{\rho}{\sqrt{\kappa}} \log|f_t(z) - V_t| + Q \log|f_t'(z)|. \end{aligned} \tag{6.5}$$

Let τ be an almost surely finite stopping time for the filtration generated by the Brownian motion B which drives U which occurs at or before when the continuation threshold is reached. Then

$$\mathfrak{h}_0 + h \overset{d}{=} \mathfrak{h}_\tau + h \circ f_\tau \tag{6.6}$$

where we view the left and right sides as distributions defined modulo additive constant.

6.2 Forward coupling

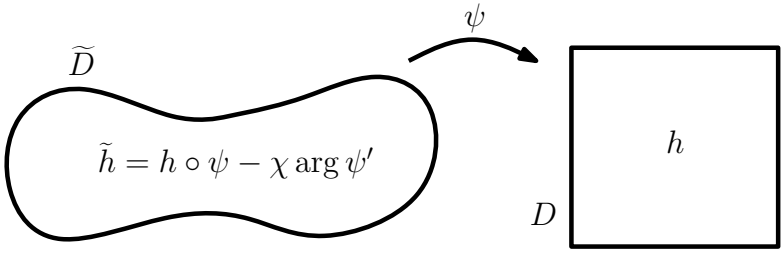

Figure 6.1: An imaginary surface coordinate change.

We will now give a brief overview of the theory of GFF flow lines developed in [MS12a, MS12b, MS12c, MS13a]. We assume throughout that $\kappa \in (0, 4)$ so that

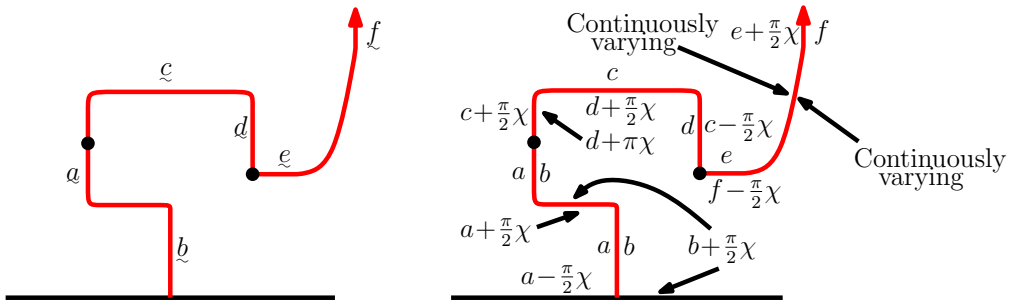

Figure 6.2: The notation on the left is a shorthand for the boundary data indicated on the right. We often use this shorthand to indicate GFF boundary data. In the figure, we have placed some black dots on the boundary ∂D of a domain D. On each arc L of ∂D that lies between a pair of black dots, we will draw either a horizontal or vertical segment L_0 and label it with $\underset{\sim}{x}$. This means that the boundary data on L_0 is given by x, and that whenever L makes a quarter turn to the right, the height goes down by $\frac{\pi}{2}\chi$ and whenever L makes a quarter turn to the left, the height goes up by $\frac{\pi}{2}\chi$. More generally, if L makes a turn which is not necessarily at a right angle, the boundary data is given by χ times the winding of L relative to L_0. If we just write x next to a horizontal or vertical segment, we mean to indicate the boundary data at that segment and nowhere else. The right side above has exactly the same meaning as the left side, but the boundary data is spelled out explicitly everywhere. Even when the curve has a fractal, non-smooth structure, the *harmonic extension* of the boundary values still makes sense, since one can transform the figure via the rule in Figure 6.1 to a half plane with piecewise constant boundary conditions.

$\kappa' := 16/\kappa \in (4, \infty)$. We will often make use of the following definitions and identities:

$$\lambda := \frac{\pi}{\sqrt{\kappa}}, \qquad \lambda' := \frac{\pi}{\sqrt{16/\kappa}} = \frac{\pi\sqrt{\kappa}}{4} = \frac{\kappa}{4}\lambda < \lambda, \qquad \chi := \frac{2}{\sqrt{\kappa}} - \frac{\sqrt{\kappa}}{2} \tag{6.7}$$

$$2\pi\chi = 4(\lambda - \lambda'), \qquad \lambda' = \lambda - \frac{\pi}{2}\chi \tag{6.8}$$

$$2\pi\chi = (4-\kappa)\lambda = (\kappa' - 4)\lambda'. \tag{6.9}$$

The boundary data one associates with the GFF on $\mathbf{H}$ so that its flow line η from 0 to ∞ is an $\mathrm{SLE}_\kappa(\underline{\rho}^L; \underline{\rho}^R)$ process with force points located at $\underline{x} = (\underline{x}^L; \underline{x}^R)$ for $\underline{x}^L = (x^{k,L} < \cdots < x^{1,L} \leq 0^-)$ and $\underline{x}^R = (0^+ \leq x^{1,R} < \cdots < x^{\ell,R})$ and with weights $(\underline{\rho}^L; \underline{\rho}^R)$ for $\underline{\rho}^L = (\rho^{1,L}, \ldots, \rho^{k,L})$ and $\underline{\rho}^R = (\rho^{1,R}, \ldots, \rho^{\ell,R})$ is

$$-\lambda\left(1 + \sum_{i=1}^{j} \rho^{i,L}\right) \quad \text{for} \quad x \in [x^{j+1,L}, x^{j,L}) \quad \text{and} \tag{6.10}$$

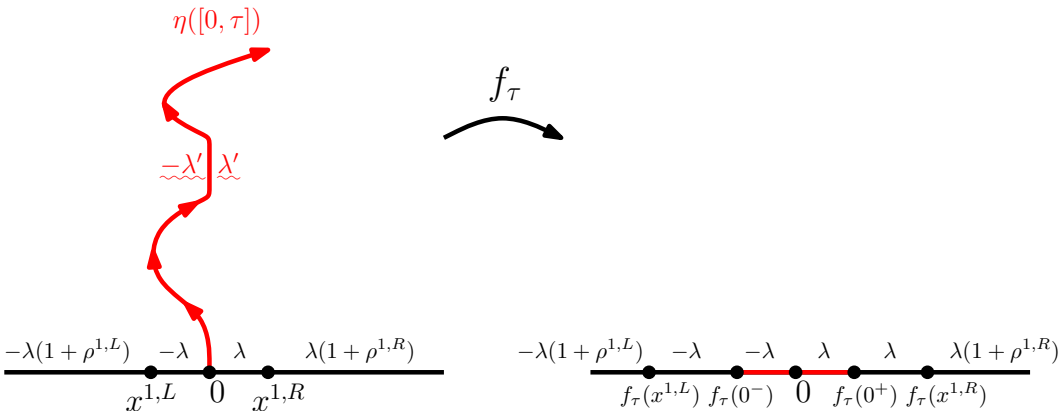

Figure 6.3: Suppose that h is a GFF on $\mathbf{H}$ with the boundary data depicted above. Then the flow line η of h starting from 0 is an $\mathrm{SLE}_\kappa(\underline{\rho}^L;\underline{\rho}^R)$ curve in $\mathbf{H}$ where $|\underline{\rho}^L| = |\underline{\rho}^R| = 1$. For any η stopping time τ, the law of h given $\eta([0,\tau])$ is equal in distribution to a GFF on $\mathbf{H}\setminus\eta([0,\tau])$ with the boundary data depicted above (the notation $\underset{\sim}{a}$ is explained in Figure 6.2). It is also possible to couple $\eta' \sim \mathrm{SLE}_{\kappa'}(\underline{\rho}^L;\underline{\rho}^R)$ for $\kappa' > 4$ with h and the boundary data takes on the same form (with $-\lambda' := \frac{\pi}{\sqrt{\kappa'}}$ in place of $\lambda := \frac{\pi}{\sqrt{\kappa}}$). The difference is in the interpretation. The (almost surely self-intersecting) path η' is not a flow line of h, but for each η' stopping time τ' the left and right *boundaries* of $\eta'([0,\tau'])$ are SLE_κ flow lines, where $\kappa = 16/\kappa'$, angled in opposite directions. The union of the left boundaries — over a collection of τ' values — is a tree of merging flow lines, while the union of the right boundaries is a corresponding dual tree whose branches do not cross those of the tree.

$$\lambda\left(1+\sum_{i=1}^{j}\rho^{i,R}\right) \quad \text{for} \quad x \in [x^{j,R}, x^{j+1,R}). \tag{6.11}$$

This is depicted in Figure 6.3 in the special case that $|\underline{\rho}^L| = |\underline{\rho}^R| = 1$. For any η stopping time τ, the conditional law of h given $\eta([0,\tau])$ is that of a GFF on $\mathbf{H}\setminus\eta([0,\tau])$. The boundary data of the conditional field agrees with that of h on $\partial\mathbf{H}$. On the right side of $\eta([0,\tau])$, it is $\lambda' + \chi\cdot\text{winding}$, where the terminology "winding" is explained in Figure 6.2, and to the left it is $-\lambda' + \chi\cdot\text{winding}$. This is also depicted in Figure 6.3.

A complete description of the manner in which GFF flow lines interact with each other is given in [MS12a, Theorem 1.5] and [MS13a, Theorem 1.7]. See, in particular, [MS13a, Figure 1.13]. For more on flow lines started from boundary points, see [MS12a] as well as [MS13a, Section 2.3]. The introduction to [MS13a] contains a detailed overview of the behavior of flow lines started from interior points. See also [MW13, Section 2] for an overview of the SLE/GFF coupling.

6.3 Law of an $\mathrm{SLE}_\kappa(\rho)$ excursion

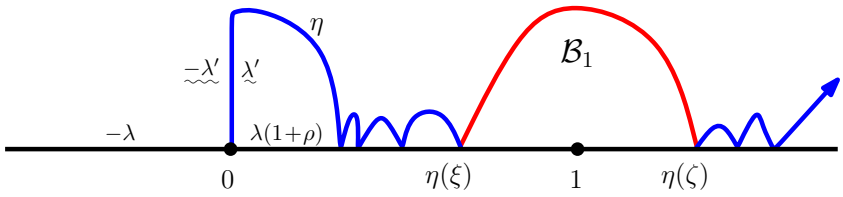

Figure 6.4: Shown is an $\mathrm{SLE}_\kappa(\rho)$ process η in $\mathbf{H}$ from 0 to ∞ with $\kappa \in (0,4)$ and $\rho \in (-2, \frac{\kappa}{2}-2)$ where the force point is located at 0^+ viewed as the flow line starting from 0 of a GFF on $\mathbf{H}$ with the indicated boundary data. The red segment represents the excursion of η from $\partial\mathbf{H}$ which traces the boundary of the component $\mathcal{B}_1$ of $\mathbf{H}\setminus\eta$ with 1 on its boundary. The time ξ (resp. ζ) is the start (resp. end) time of this excursion. In Theorem 6.6, we show that the conditional law of $\eta|_{[\xi,\zeta]}$ given $\eta|_{[0,\xi]}$ and $\eta|_{[\zeta,\infty)}$ is an $\mathrm{SLE}_\kappa(\widehat{\rho})$ process where $\widehat{\rho} = \kappa - 4 - \rho$.

In this section, we will determine the law of the excursion of a boundary intersecting $\mathrm{SLE}_\kappa(\rho)$ process in $\mathbf{H}$ with $\kappa \in (0,4)$ which disconnects a given boundary point from ∞ (see Figure 6.4). We will then use this result to determine the local behavior of the path at the starting and ending points of the excursion.

Theorem 6.6. *Fix $\kappa \in (0,4)$, $\rho \in (-2, \frac{\kappa}{2}-2)$, and let $\widehat{\rho} = \kappa - 4 - \rho > \frac{\kappa}{2} - 2$. Let η be an $\mathrm{SLE}_\kappa(\rho)$ process in $\mathbf{H}$ from 0 to ∞ with a single boundary force point of weight ρ located at 0^+. Let $\mathcal{B}_1$ be the component of $\mathbf{H}\setminus\eta$ which has 1 on its boundary and let ξ (resp. ζ) be the first (resp. last) time that η visits a point on $\partial\mathcal{B}_1$. Then the conditional law of $\eta|_{[\xi,\zeta]}$ given $\eta|_{[0,\xi]}$ and $\eta|_{[\zeta,\infty)}$ is that of an $\mathrm{SLE}_\kappa(\widehat{\rho})$ process in the component of $\mathbf{H}\setminus\big(\eta([0,\xi])\cup\eta([\zeta,\infty))\big)$ with 1 on its boundary with a single boundary force point of weight $\widehat{\rho}$ located at $(\eta(\xi))^+$.*

Theorem 6.6 gives the conditional law of $\eta|_{[\xi,\zeta]}$ given $\eta|_{[0,\xi]}$ and $\eta|_{[\zeta,\infty)}$. We also know the conditional law of $\eta|_{[\zeta,\infty)}$ given $\eta|_{[0,\zeta]}$: it is an $\mathrm{SLE}_\kappa(\rho)$ process in the unbounded component of $\mathbf{H}\setminus\eta([0,\zeta])$ from $\eta(\zeta)$ to ∞ with a single boundary force point located at $\eta(\zeta)$. This just follows from the conformal Markov property for $\mathrm{SLE}_\kappa(\rho)$. By the reversibility of $\mathrm{SLE}_\kappa(\rho)$ [MS12b, Theorem 1.1], we also know the conditional law of $\eta|_{[0,\xi]}$ given $\eta|_{[\xi,\infty)}$: it is an $\mathrm{SLE}_\kappa(\rho)$ in the component of $\mathbf{H}\setminus\eta([\xi,\infty))$ with 0 on its boundary from 0 to $\eta(\xi)$ with a single boundary force point of weight ρ located at 0^+. These facts will be important for us when we establish Proposition 6.7 below.

Proof of Theorem 6.6. The proof is based on resampling arguments which are the similar to those used to prove [MS12b, Theorem 1.1]. See Figure 6.5 for an illustration of the setup.

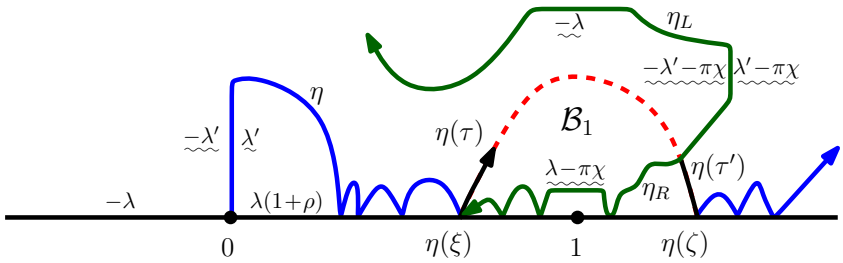

Figure 6.5: Setup for the proof of Theorem 6.6. We know the conditional law of $\eta|_{[\tau,\tau']}$ given $\eta|_{[0,\tau]}$, $\eta|_{[\tau',\infty)}$, and the dual flow lines η_L and η_R (i.e., with angles π and $-\pi$). We similarly know the conditional law of the dual flow lines η_L and η_R given all of η. As explained in the proof of [MS12b, Theorem 6.1], these resampling properties determine the conditional law of $\eta|_{[\tau,\tau']}$ given $\eta|_{[0,\tau]}$ and $\eta|_{[\tau',\infty)}$. The corresponding triple associated with an $\mathrm{SLE}_\kappa(\kappa-4-\rho)$ process satisfies the same resampling properties which gives the desired result.

As illustrated in Figure 6.4, we view η as the flow line starting from 0 of a GFF h on $\mathbf{H}$ with boundary conditions given by $-\lambda$ on $\mathbf{R}_-$ and $\lambda(1+\rho)$ on $\mathbf{R}_+$. Let τ be a forward stopping time for η with $\eta(\tau) \in \mathbf{H}$ almost surely, let σ be the first time after τ that $\eta(t) \in \partial\mathbf{H}$, and let τ' be a reverse stopping time for η given $\eta|_{[0,\tau]}$ and $\eta|_{[\sigma,\infty)}$ such that $\eta(\tau') \in \mathbf{H}$ almost surely. Assume that we are working on the positive probability event that $\eta|_{[\tau,\tau']}$ does not intersect $\partial\mathbf{H}$. We also assume that are working on the event that $\xi = \sup\{t < \tau : \eta(t) \in \partial\mathbf{H}\}$ and $\zeta = \inf\{t \geq \tau : \eta(t) \in \partial\mathbf{H}\}$. Let η_L (resp. η_R) be the flow line of h given η starting from $\eta(\tau')$ with angle π (resp. $-\pi$). Note that η_R almost surely terminates at $\eta(\xi)$. In particular, $\eta_R \cup \eta([0,\tau]) \cup \eta([\tau',\infty))$ separates $\eta|_{[\tau,\tau']}$ from $\partial\mathbf{H}$. From the boundary data for the conditional law of h given η, we can read off the conditional laws of η_L and η_R given η. Moreover, [MS12b, Lemma 5.13] gives us the conditional law of $\eta|_{[\tau,\tau']}$ given $\eta|_{[0,\tau]}$, $\eta|_{[\tau',\infty)}$, η_L, and η_R: it is given by an $\mathrm{SLE}_\kappa(\frac{\kappa}{2}-2;\frac{\kappa}{2}-2)$ process in the component of $\mathbf{H} \setminus (\eta_L \cup \eta_R \cup \eta([0,\tau]))$ with $\eta(\tau)$ on its boundary from $\eta(\tau)$ to $\eta(\tau')$.

Let $\widetilde{\eta}$ be an $\mathrm{SLE}_\kappa(\widehat{\rho})$ process in the component of $\mathbf{H} \setminus \big(\eta([0,\xi]) \cup \eta([\zeta,\infty))\big)$ with 1 on its boundary from $\eta(\xi)$ to $\eta(\zeta)$ with a single boundary force point located at $(\eta(\xi))^+$. Let $\widetilde{\tau}$ be a stopping time for $\widetilde{\eta}$ and let $\widetilde{\tau}'$ be a reverse stopping time for $\widetilde{\eta}$ given $\widetilde{\eta}|_{[0,\widetilde{\tau}]}$ and assume that we are working on the event that $\widetilde{\eta}|_{[0,\widetilde{\tau}]}$ and $\widetilde{\eta}|_{[\widetilde{\tau}',\infty)}$ are disjoint. Let $A = \eta([0,\xi]) \cup \eta([\zeta,\infty)) \cup \widetilde{\eta}$ and let $\widetilde{h}$ be a GFF on $\mathbf{H} \setminus A$ with the same boundary conditions as h on $\partial\mathbf{H}$ and with boundary conditions along A as if it were the flow line of h from 0 to ∞ (with angle 0). Let $\widetilde{\eta}_L$ (resp. $\widetilde{\eta}_R$) be the flow line of $\widetilde{h}$ starting from $\widetilde{\eta}(\widetilde{\tau}')$ with angle π (resp. $-\pi$). Then the conditional law of $\widetilde{\eta}_L$ and $\widetilde{\eta}_R$ given A is the same as the conditional law of η_L and η_R given η (in the setup described in the previous paragraph). Moreover, [MS12b, Proposition 5.12] gives us

the conditional law of $\widetilde{\eta}$ given $\widetilde{\eta}_L$, $\widetilde{\eta}_R$, $\eta|_{[0,\xi]}$, $\eta|_{[\zeta,\infty)}$, $\widetilde{\eta}|_{[0,\widetilde{\tau}]}$, and $\widetilde{\eta}|_{[\widetilde{\tau}',\infty)}$: it is given by an $\mathrm{SLE}_\kappa(\frac{\kappa}{2}-2;\frac{\kappa}{2}-2)$ process in the component of $\mathbf{H}\setminus(\widetilde{\eta}_L\cup\widetilde{\eta}_R\cup\eta([0,\xi])\cup\widetilde{\eta}([0,\widetilde{\tau}]))$ with $\widetilde{\eta}(\widetilde{\tau})$ on its boundary from $\widetilde{\eta}(\widetilde{\tau})$ to $\widetilde{\eta}(\widetilde{\tau}')$.

As explained in the proof of [MS12b, Theorem 6.1], this resampling invariance implies that the conditional law of η given $\eta|_{[0,\tau]}$ and $\eta|_{[\tau',\infty)}$ (conditioned on the event described in the first paragraph) is the same as the conditional law of $\widetilde{\eta}$ given $\eta|_{[0,\xi]}$, $\eta|_{[\zeta,\infty)}$, $\widetilde{\eta}|_{[0,\widetilde{\tau}]}$, and $\widetilde{\eta}|_{[\widetilde{\tau}',\infty)}$. This completes the proof since it holds for all τ, τ', $\widetilde{\tau}$, and $\widetilde{\tau}'$. □

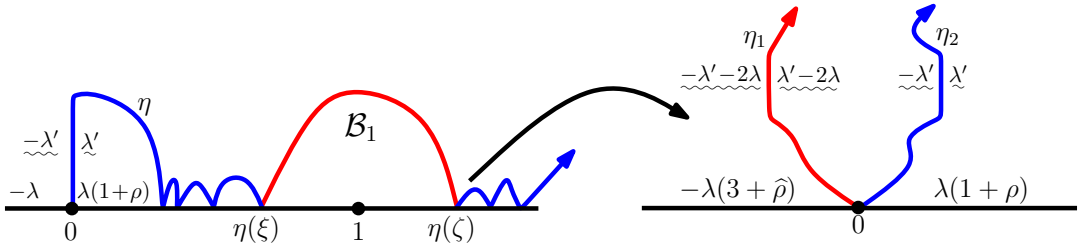

Figure 6.6: Illustration of the statement of Proposition 6.7. Shown on the left is an $\mathrm{SLE}_\kappa(\rho)$ process η with $\rho\in(-2,\frac{\kappa}{2}-2)$ and ζ is the first time that η separates 1 from ∞. In Proposition 6.7, we show that the local picture of the pair of paths $t\mapsto\eta(\zeta-t)$ and $t\mapsto\eta(\zeta+t)$ near $\eta(\zeta)$ is given by a pair of flow lines of a GFF with the boundary data on the right with angles $2\lambda/\chi$ (η_1) and 0 (η_2).

Proposition 6.7. *Suppose that $\kappa\in(0,4)$ and $\rho\in(-2,\frac{\kappa}{2}-2)$. Let η be an $\mathrm{SLE}_\kappa(\rho)$ process in $\mathbf{H}$ with a single boundary force point of weight ρ located at 0^+. Let ζ be the first time t that η separates 1 from ∞. For each $\delta>0$, we let $\eta_1^\delta=\delta^{-1}(\eta(\zeta-\cdot)-\eta(\zeta))$ and $\eta_2^\delta=\delta^{-1}(\eta(\zeta+\cdot)-\eta(\zeta))$. The joint law of $(\eta_1^\delta,\eta_2^\delta)$ converges weakly as $\delta\to0$ with respect to the topology of local uniform convergence modulo reparameterization to the law of a pair of paths (η_1,η_2) which are constructed as follows. Let $\widehat{\rho}=\kappa-4-\rho$ and let h be a GFF on $\mathbf{H}$ with boundary data given by $-\lambda(3+\widehat{\rho})$ on $\mathbf{R}_-$ and $\lambda(1+\rho)$ on $\mathbf{R}_+$. Then η_1 (resp. η_2) is the flow line of h starting from 0 with angle $2\lambda/\chi$ (resp. 0).*

See Figure 6.6 for an illustration of the setup. Let ξ be as in the statement of Theorem 6.6. Note that ξ corresponds to the first time that the time-reversal of η separates 1 from ∞. Consequently, by the reversibility of $\mathrm{SLE}_\kappa(\rho_1;\rho_2)$ [MS12b, Theorem 1.1], Proposition 6.7 can also be used to describe the local behavior of η near $\eta(\xi)$.

Proof of Proposition 6.7. We define the times ξ,ζ as in the statement of Theorem 6.6. By Theorem 6.6, we know the conditional law of $\eta|_{[\xi,\zeta]}$ given $\eta|_{[0,\xi]}$ and $\eta|_{[\tau,\infty)}$: it an

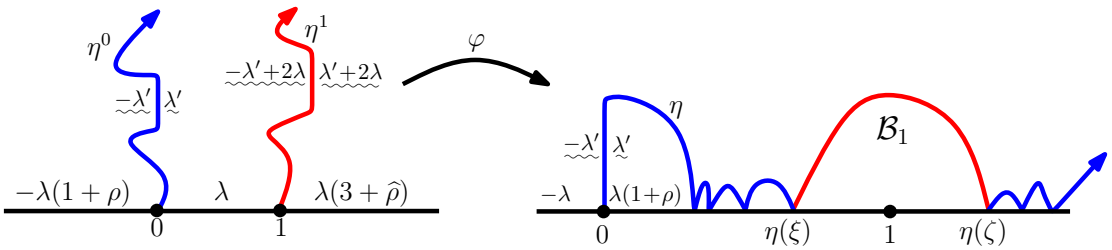

Figure 6.7: Setup for the proof of Proposition 6.7. On the left, we suppose that we have a GFF h on $\mathbf{H}$ with the indicated boundary data where η^0 (resp. η^1) is the flow line of h starting from 0 (resp. 1) with angle 0 (resp. $-2\lambda/\chi$). Then $\eta^0 \sim \mathrm{SLE}_\kappa(\rho; 2+\widehat{\rho})$ and $\eta^1 \sim \mathrm{SLE}_\kappa(\rho+2; \widehat{\rho})$. Moreover, the conditional law of η^0 given η^1 is that of an $\mathrm{SLE}_\kappa(\rho)$ process and the conditional law of η^1 given η^0 is that of an $\mathrm{SLE}_\kappa(\widehat{\rho})$ process. In particular, the conditional law of η^1 given η^0 is the same as $\eta|_{[\xi,\zeta]}$ given $\eta|_{[0,\xi]}$ and $\eta|_{[\zeta,\infty)}$ and the conditional law of η^0 given η^1 is the same as the time-reversal of $\eta|_{[\zeta,\infty)}$ given $\eta|_{[0,\xi]}$ and $\eta|_{[\xi,\zeta]}$. Consequently, [MS12b, Theorem 4.1] implies that with φ the unique conformal transformation from $\mathbf{H}$ to the unbounded component of $\mathbf{H} \setminus \eta([0,\xi])$ with $\varphi(0) = \infty$, $\varphi(1) = \eta(\xi)$, and $\varphi(\infty) = \eta(\zeta)$ we have that $\varphi(\eta^0, \eta^1) \overset{d}{=} (\eta|_{[\zeta,\infty)}, \eta|_{[\xi,\zeta]})$ given $\eta|_{[0,\xi]}$ (up to time-reversal).

$\mathrm{SLE}_\kappa(\widehat{\rho})$ process from $\eta(\xi)$ to $\eta(\zeta)$ in the component of $\mathbf{H} \setminus (\eta([0,\xi]) \cup \eta([\zeta,\infty)))$ with 1 on its boundary. Similarly, we know the conditional law of $\eta|_{[\zeta,\infty)}$ given $\eta|_{[0,\xi]}$ and $\eta|_{[\xi,\zeta]}$: it is an $\mathrm{SLE}_\kappa(\rho)$ process from $\eta(\zeta)$ to ∞ in the unbounded component of $\mathbf{H} \setminus \eta([0,\zeta])$. By the reversibility of $\mathrm{SLE}_\kappa(\rho)$ [MS12b, Theorem 1.1], we also know that the time-reversal of $\eta|_{[\zeta,\infty)}$ given $\eta|_{[0,\xi]}$ and $\eta|_{[\xi,\zeta]}$ is an $\mathrm{SLE}_\kappa(\rho)$ process. By [MS12b, Theorem 4.1], we have that these conditional laws determine the joint law of the pair $\eta|_{[\xi,\zeta]}$ and the time-reversal of $\eta|_{[\zeta,\infty)}$ conditional on $\eta|_{[0,\xi]}$.

The joint law can in particular be sampled from as follows (see Figure 6.7 for an illustration). Let h be a GFF on $\mathbf{H}$ with boundary data $-\lambda(1+\rho)$ on $(-\infty, 0]$, λ on $(0,1]$, and $\lambda(3+\widehat{\rho})$ on $(1,\infty)$. Let η^0 (resp. η^1) be the flow line of h starting from 0 (resp. 1) with angle 0 (resp. $-2\lambda/\chi$). Finally, let φ be the unique conformal transformation from $\mathbf{H}$ to the unbounded component of $\mathbf{H} \setminus \eta([0,\xi])$ taking 0 to ∞, 1 to $\eta(\xi)$, and ∞ to $\eta(\zeta)$. Then $(\varphi(\eta^0), \varphi(\eta^1), \eta|_{[0,\xi]})$ has the same law as $(\eta|_{[\zeta,\infty)}, \eta|_{[\xi,\zeta]}, \eta|_{[0,\xi]})$ (up to time-reversal). The behavior of η^0 and η^1 near ∞ is asymptotically the same as that of the flow lines $(\widetilde{\eta}_1, \widetilde{\eta}_2)$ of a GFF on $\mathbf{H}$ with boundary conditions given by $-\lambda(1+\rho)$ (resp. $\lambda(3+\widehat{\rho})$) on $\mathbf{R}_-$ (resp. $\mathbf{R}_+$) starting from 0 with angles 0 and $-2\lambda/\chi$. (See the discussion after the statement of [MS12b, Lemma 5.13] which explains how a flow line of a GFF from 0 to ∞ can be realized as the common boundary of a pair of counterflow lines starting from ∞.) This implies the result since the reversibility of $\mathrm{SLE}_\kappa(\rho_1; \rho_2)$ for $\kappa \in (0,4)$ and $\rho_1, \rho_2 > -2$ [MS12b, Theorem 1.1] implies that the joint law of $(\widetilde{\eta}_1, \widetilde{\eta}_2)$ is invariant under applying the map $z \mapsto -1/z$ and then

reversing time. □

Proposition 6.8. *Suppose that $\kappa \in (0,4)$. Fix weights $\rho_1 > -2$ and $\rho_2 \in (-2, \frac{\kappa}{2}-2)$. Let η be an $\mathrm{SLE}_\kappa(\rho_1;\rho_2)$ process with boundary force points located $x \le 0 \le y < 1$. Let ζ be the first time that η separates 1 from ∞. We define paths $\eta_1^\delta, \eta_2^\delta$ as in Proposition 6.7. Then the joint law of $(\eta_1^\delta, \eta_2^\delta)$ converges weakly as $\delta \to 0$ with respect to the topology of local uniform convergence modulo reparameterization to the law of a pair of paths (η_1, η_2) which are constructed as in Proposition 6.7 where $\rho = \rho_2$.*

Proof. This follows from absolute continuity and Proposition 6.7. □

Remark 6.9. Using the version of SLE duality established in [MS12a] and Proposition 6.8, we can also describe the local behavior of an $\mathrm{SLE}_{\kappa'}(\rho_1';\rho_2')$ process near the point where it first separates 1 from ∞. Indeed, fix $\kappa' > 4$, $\rho_1' > -2$, and $\rho_2' \in (\frac{\kappa'}{2}-4, \frac{\kappa'}{2}-2)$. Suppose that η' is an $\mathrm{SLE}_{\kappa'}(\rho_1';\rho_2')$ process in $\mathbf{H}$ from 0 to ∞ with boundary force points located at 0^- and 0^+. (Note that ρ_2' is in the range so that η' hits but does not fill $\mathbf{R}_+$.) Let η denote the right boundary of η'. Then η is an $\mathrm{SLE}_\kappa(\rho_1;\rho_2)$ process in $\mathbf{H}$ from ∞ to 0 with

$$\rho_1 = \frac{\kappa}{2} - 2 + \frac{\kappa\rho_1'}{4} \quad \text{and} \quad \rho_2 = \frac{\kappa}{2} - 4 + \frac{\kappa\rho_2'}{4}$$

where the force points are located immediately to the left and right of ∞. Let ζ' be the first time that η' separates 1 from ∞. Since the right boundary of η' is given by η and $\eta \sim \mathrm{SLE}_\kappa(\rho_1;\rho_2)$, we can consequently apply Proposition 6.8 to η to get that the law of the right boundary of η' near $\eta'(\zeta')$ is described by a certain pair of GFF flow lines (same law as would correspond to $\mathrm{SLE}_\kappa(\rho_2)$).

We finish this section by giving the radial version of Proposition 6.7.

Proposition 6.10. *Suppose that $\kappa \in (0,4)$ and $\rho \in (-2, \frac{\kappa}{2}-2)$. Let η be a radial $\mathrm{SLE}_\kappa(\rho)$ process in $\mathbf{D}$ starting from 1 and targeted at 0 with a single boundary force point of weight ρ located at 1^+. Fix $\theta \in (0, 2\pi)$ and let ζ be the first time that η separates $e^{i\theta}$ from 0. On the positive probability event that $\eta(\zeta) \in \partial\mathbf{D}$, we let $\varphi\colon \mathbf{D} \to \mathbf{H}$ be the unique conformal transformation which takes $\eta(\zeta)$ to 0 and 0 to i. Let $\eta_\delta^1 = \delta^{-1}\varphi(\eta(\zeta - \cdot))$ and $\eta_\delta^2 = \delta^{-1}\varphi(\eta(\zeta + \cdot))$. Then the joint law of $(\eta_1^\delta, \eta_2^\delta)$ converges weakly as $\delta \to 0$ with respect to the topology of local uniform convergence modulo reparameterization to the law of a pair of paths (η_1, η_2) which are constructed as in Proposition 6.7.*

Proof. This follows from absolute continuity and Proposition 6.7 using the same argument used to prove Proposition 6.8. □

7 Structure theorems and quantum natural time

The purpose of this section is to describe the Poissonian structure of the surfaces which are cut out of a γ-LQG surface by an independent SLE process. Sections 7.1, 7.2, and 7.3 respectively focus on the cases of boundary-intersecting $\mathrm{SLE}_\kappa(\rho)$ processes, radial and whole-plane $\mathrm{SLE}_\kappa(\rho)$ processes, and $\mathrm{SLE}_{\kappa'}$ processes. The strategy to derive each of these results is very similar. We have included all of the details in the case of boundary intersecting $\mathrm{SLE}_\kappa(\rho)$ processes (Theorem 7.1) and in the other cases we explain the necessary modifications to transfer the argument.

Associated with each of the aforementioned structure theorems is a local time which should be thought of as counting the number of small bubbles which have been cut off by the SLE. (As ϵ tends to zero, the number of excised bubbles of quantum mass between ϵ and 2ϵ — times an appropriate power of ϵ — converges to this local time.) The right-continuous inverse of this local time leads to an alternative time-parameterization for SLE which is intrinsic to these bubbles (viewed as quantum surfaces). We will refer to this notion of time as "quantum natural time." For $\kappa' \in (4,8)$, it is the LQG analog of the natural parameterization for SLE [LS11, LZ13, LR12] (for $\kappa \in (0,4)$ the LQG analog of the natural parameterization is γ-LQG length and for $\kappa' \geq 8$ it is γ-LQG area). In Section 7.4, we will show that the law of the free boundary GFF with an appropriately chosen log singularity is invariant under zipping/unzipping according to quantum natural time and that the same is true for certain types of quantum wedges. This is analogous to one of the main results of [She10] (where the notion of time is given by γ-LQG length).

Throughout, we let $\mathcal{S} = \mathbf{R} \times [0,\pi]$, $\mathcal{S}_+ = \mathbf{R}_+ \times [0,\pi]$, $\mathcal{S}_- = \mathbf{R}_- \times [0,\pi]$, and $\mathcal{H}_1(\cdot), \mathcal{H}_2(\cdot)$ be as in Section 4.

7.1 Boundary-intersecting $\mathrm{SLE}_\kappa(\rho)$ processes

The purpose of this section is to determine the law of the beaded surface which is to the right of a boundary intersecting $\mathrm{SLE}_\kappa(\rho)$ process for $\kappa \in (0,4)$ and $\rho \in (-2, \frac{\kappa}{2}-2)$. (Recall the correspondence between forward $\mathrm{SLE}_\kappa(\rho)$ and reverse $\mathrm{SLE}_\kappa(\widetilde{\rho})$ for $\widetilde{\rho} = \rho+4$ from Proposition 3.11.)

Theorem 7.1. *Fix $\kappa \in (0,4)$, $\rho \in (-2, \frac{\kappa}{2}-2)$, $\widetilde{\rho} = \rho + 4$, and let $\gamma = \sqrt{\kappa}$. Let $\widetilde{h}$ be a free boundary GFF on $\mathbf{H}$ and let*

$$h = \widetilde{h} + \frac{2-\widetilde{\rho}}{\gamma} \log|\cdot| = \widetilde{h} - \frac{2+\rho}{\gamma} \log|\cdot|.$$

Let η be an $\mathrm{SLE}_\kappa(\rho)$ process starting from 0 with a single boundary force point of weight ρ located at 0^+ and assume that η is independent of h. Then the law of the

beaded surface which consists of the components of $\mathbf{H} \setminus \eta$ *which are to the right of* η *is equal to that of a quantum wedge of weight* $2 + \rho$ *(as in Definition 4.4).*

Recalling (1.4) (as well as Table 1.1), we note that the dimension of the Bessel process associated with a wedge of weight $\rho + 2$ is given by:

$$\delta = \delta(\kappa, \rho) = 1 + \frac{2\rho + 4}{\kappa} = 1 + \frac{2\rho + 4}{\gamma^2}. \tag{7.1}$$

Note that the value of $\delta(\kappa, \rho)$ in (7.1) varies in $(1, 2)$ as ρ varies in $(-2, \frac{\kappa}{2} - 2)$.

Definition 7.2. Let η be as in the statement of Theorem 7.1 with the capacity time parameterization. Let ℓ be the local time at 0 of the Bessel process Y which encodes the quantum wedge in the statement of Theorem 7.1. For each $u \geq 0$, we let $\mathfrak{q}_u$ be the infimum of times t such that the local time as measured by ℓ of the bubbles cut off by $\eta|_{[0,t]}$ is at least u. We refer to the time-parameterization of η given by $u \mapsto \eta(\mathfrak{q}_u)$ as the **quantum natural time** parameterization of its bubbles.

Remark 7.3. As explained in Remark 4.14, the length of an excursion e from 0 of the Bessel process Y from Definition 7.2 has the interpretation of giving a constant times the conditional expectation (given e) of the γ-LQG mass of the corresponding bubble cut off by η.

Suppose that h, ρ, and $\widetilde{\rho}$ are as in the statement of Theorem 7.1. Let (f_t) denote the centered reverse Loewner flow associated with a reverse $\mathrm{SLE}_\kappa(\widetilde{\rho})$ process. Let (W, V) be the associated driving process and let $U = V - W$. Note $U \geq 0$ since we have taken the force point to start at 0^+. For each $s \leq t$, we also let $f_{s,t} = f_t \circ f_s^{-1}$.

In the coupling of reverse $\mathrm{SLE}_\kappa(\widetilde{\rho})$ with the GFF described in Theorem 6.1, the collision times of W and V correspond to the instances of time when new quantum surfaces are added to the big surface. Roughly speaking, the reason that the surfaces in $\mathbf{H} \setminus \eta$ which are to the right of η have a Poissonian law is that the structure of a newly zipped in surface (in an infinitesimal amount of time after it is added to the big surface) is determined by the values of the GFF in an infinitesimal region and the conditional law of the GFF given its values in a very small region will be very close to the law of the unconditioned field (see e.g., Lemma 8.2). This idea is sketched in Figure 7.1. The idea of how to obtain the form of the Poissonian law is illustrated in Figure 7.2.

In the proof, it will be useful to be able to keep track of the fields which arise when zipping and unzipping using a common probability space. This is the purpose of the following lemma.

Lemma 7.4. *There exists a family* (h^t) *such that for each* $t \geq 0$, h^t *can be expressed as the sum of a free boundary GFF on* $\mathbf{H}$ *plus* $\frac{2}{\gamma} \log |\cdot| - \frac{\widetilde{\rho}}{\gamma} \log |\cdot - U_t|$ *which satisfy*

$$h^s = h^t \circ f_{s,t} + Q \log |f'_{s,t}| \quad \text{for each} \quad 0 \leq s \leq t < \infty.$$

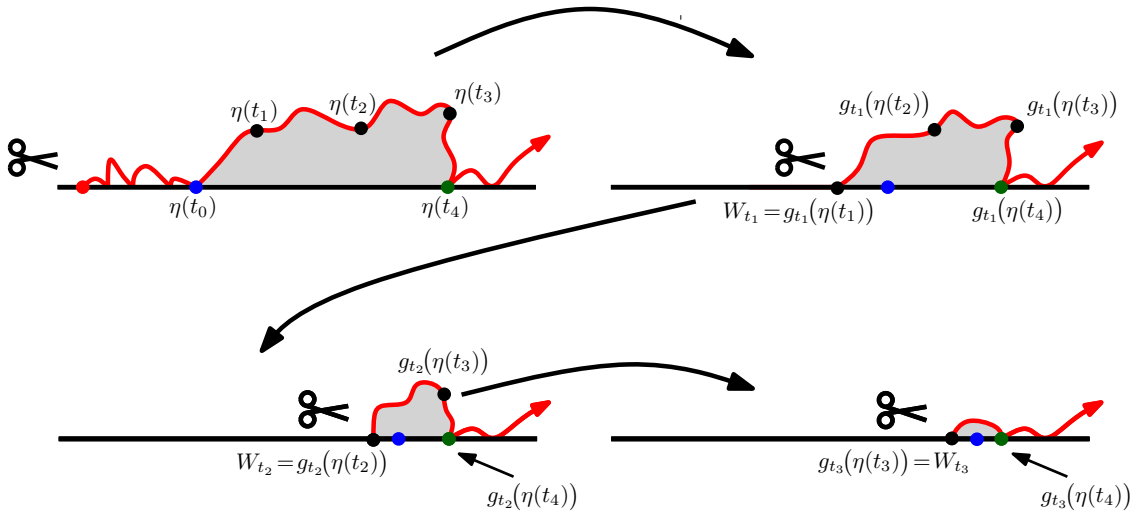

Figure 7.1: Imagine cutting (or "unzipping") along a boundary-intersecting $\mathrm{SLE}_\kappa(\rho)$ path η with a pair of scissors, and at each time t conformally mapping the (infinite) remaining region back to the upper half plane via the forward Loewner map g_t. In the figure, one particular excursion of η away from $\mathbf{R}$ is colored grey. Times $t_0 < t_1 < t_2 < t_3 < t_4$ are chosen so that η begins to trace this excursion at time t_0 and finishes at time t_4. In the second, third, and fourth figures, the blue dot represents the image of $\eta(t_0)$ (or a point infinitesimally close to the right of $\eta(t_0)$) under g_{t_1}, g_{t_2} and g_{t_3}, respectively, which in turn corresponds to the $\mathrm{SLE}_\kappa(\rho)$ force point location at the given time. At the time t_4, the entire grey region is "cut off" of the half plane by the scissors; in other words, the grey region is a subset of K_t, for any $t \geq t_4$. An important thing to see from this figure is that if one runs time in the reverse direction ("zipping up" instead of "unzipping") then the entire grey region, viewed as a quantum surface, is added to the big surface (the one parameterized by the entire upper half plane) at time t_4. If ϵ is tiny, then at time $t_3 = t_4 - \epsilon$ the figure should look like the one on the bottom right, with a very tiny (in the Euclidean sense) grey region and a blue dot (representing the force point) somewhere in the middle of that region. On the other hand, the quantum boundary length between the blue dot and the green dot to its left is the same (and of macroscopic order) in each of the four figures. In the bottom right figure, the quantum length of the upper boundary of the grey region is equal to the quantum length of the path between $\eta(t_3)$ and $\eta(t_4)$ in the upper left region; this quantity tends to zero as $\epsilon \to 0$.

There also exists a family of curves (η^s) where $\eta = \eta^0$ is an $\mathrm{SLE}_\kappa(\rho)$ process in $\mathbf{H}$ from 0 to ∞ with a single boundary force point of weight ρ located at 0^+ which is independent of h^0 and, for each $t > 0$, the hull of η^t is equal to the hull of $f_t(\partial\mathbf{H} \cup \eta^0)$.

The transformation from (h^s, η^s) to (h^t, η^t) for $t > s$ corresponds to zipping up for

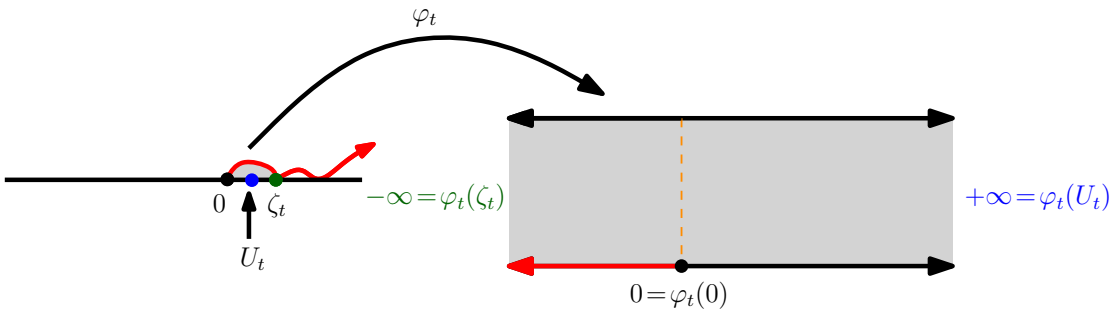

Figure 7.2: A conformal map from the bottom right part of Figure 7.1 (translated by $-W_{t_3}$) to the infinite strip $\mathcal{S}$. The $\mathrm{SLE}_\kappa(\rho)$ excursion that forms the upper boundary of the grey region on the left (the red curve) is mapped to $(-\infty, 0]$. The blue vertex on the left is mapped to the endpoint of the strip at $+\infty$, while the green vertex is mapped to the endpoint of the strip at $-\infty$. Note the field h on the right obtained from the quantum coordinate change does not change as more of the grey region is zipped up (modulo horizontal translation). Given $\mathcal{F}_t$ (defined just after the proof of Lemma 7.5), the conditional law of the field on $\mathcal{S}_+$ (right of the dotted orange line) is that of a GFF on $\mathcal{S}_+$ (with the field values to the left of the dotted orange line having been already determined), with free boundary conditions on the upper and lower boundaries, and an asymptotic linear growth rate at $+\infty$ depending on the weight of the force point.

$t - s$ units of capacity time and the transformation from (h^s, η^s) to (h^t, η^t) for $t < s$ corresponds to unzipping for $s - t$ units of capacity time.

Proof of Lemma 7.4. Theorem 6.1 implies that for each $T > 0$ we can define a collection of fields (h^t) and paths (η^t) which have this property for $0 \le t \le T$. The lemma follows by applying the Kolmogorov extension theorem. □

We will assume throughout that (h^t) and (η^t) are as in the statement of Lemma 7.4. By definition, η has the law of a (forward) $\mathrm{SLE}_\kappa(\rho)$ process. For general times $t \ge 0$, however, η^t does not have the law of a (forward) $\mathrm{SLE}_\kappa(\rho)$ process. Using the forward/reverse symmetry for $\mathrm{SLE}_\kappa(\rho)$ established in Proposition 3.11, we do have that η^t has the law of a (forward) $\mathrm{SLE}_\kappa(\rho)$ when we zip up to a given local time for U at 0. We record this fact in the following lemma.

Lemma 7.5. *Suppose that we have the setup as described above. Let L_t denote the local time of U_t at 0 and, for each $u > 0$, we let $T_u = \inf\{t > 0 : L_t > u\}$ be the right-continuous inverse of L_t. For each $u > 0$, we have that η^{T_u} has the law of a (forward) $\mathrm{SLE}_\kappa(\rho)$ process. In particular,*

$$(h^{T_u}, \eta^{T_u}) \stackrel{d}{=} (h^0, \eta^0) \quad \text{for each} \quad u \ge 0.$$

Proof. The first assertion of the lemma follows from Proposition 3.11. The second assertion follows by combining this with Theorem 6.1. □

Figure 7.1 illustrates what happens when one "unzips" along η. There are certain special times at which η completes an entire excursion away from $\partial\mathbf{H}$, and at each such time a positive-but-finite-quantum-area region is "cut off" from $\mathbf{H}$. If we parameterize time in the reverse direction, then at such a time, a positive area region is added all at once.

We are now going to define the objects which are used in the proof of Theorem 7.1; see Figure 7.2 for an illustration of the definitions. For each $t \geq 0$ such that $U_t \neq 0$, we let $\mathcal{B}_t$ denote the component of $\mathbf{H} \setminus \eta^t$ with U_t on its boundary. If $U_t = 0$, we take $\mathcal{B}_t = \emptyset$. Note that $\mathcal{B}_t$ gives the bubble which is being "zipped in" by the reverse Loewner flow at time t. For $t \geq 0$ such that $\mathcal{B}_t \neq \emptyset$, we let

- ζ_t be the closing point of $\mathcal{B}_t$ (the opening point is 0). In other words, 0 (resp. ζ_t) is the first (resp. last) point on $\partial\mathcal{B}_t$ which is visited by η^t.
- $\varphi_t \colon \mathcal{B}_t \to \mathcal{S}$ be the unique conformal transformation which takes U_t to $+\infty$, 0 to 0, and ζ_t to $-\infty$. Note that the choice of the images of U_t and ζ_t determines φ_t up to horizontal translation. Taking φ_t so that $\varphi_t(0) = 0$ fixes the horizontal translation.
- $\widetilde{h}^t = h^t \circ \varphi_t^{-1} + Q \log |(\varphi_t^{-1})'|$.
- $\widetilde{X}^t$ be the projection of $\widetilde{h}^t$ onto $\mathcal{H}_1(\mathcal{S})$.

There are different σ-algebras one can use with the zipping up process. One option is to keep track only of the path (and not make any additional observations about the field). Alternatively, one could imagine that one observes the entire field in $\mathbf{H}$; hence one gets discrete amounts of new information at the times when new regions are absorbed, but otherwise the evolution is deterministic. We will propose an intermediate approach. For each $t \geq 0$, we let $\mathcal{F}_t$ be the σ-algebra in which the following are measurable:

- Both $\eta = \eta^0$ and the driving pair (W_s, V_s) of the reverse Loewner flow for $s \leq t$.
- The field h^t restricted to $\mathbf{H} \setminus \mathcal{B}_t$ (i.e., h^t restricted to any component of $\mathbf{H} \setminus \eta^t$ *other* than the one currently being generated).
- The restriction of $\widetilde{h}^t$ to $\mathcal{S}_-$ (i.e., the restriction of h^t to the portion of the current bubble whose image under φ_t lies to the left of the dotted orange line of Figure 7.2).

Note that ζ_t, φ_t, and the restriction of $\widetilde{X}^t$ to $\mathcal{S}_-$ are all $\mathcal{F}_t$-measurable.

Fix $\epsilon, \overline{\epsilon} > 0$ and $r \in \mathbf{R}$. We now define stopping times inductively as follows. We let $\tau_1^{\epsilon,\overline{\epsilon},r}$ be the first time $t \geq 0$ that:

- The quantum length of $\partial\mathcal{B}_t \setminus \partial\mathbf{H}$ is at least $\epsilon > 0$ with respect to the γ-LQG length measure induced by h^t,
- $\widetilde{X}_u^t$ first hits r at time $u = 0$, and
- The γ-LQG mass of $\mathcal{S}_-$ associated with the field $\widetilde{h}^t$ is at least $\overline{\epsilon}$.

We then let $\sigma_1^{\epsilon,\overline{\epsilon},r}$ be the first time t after time $\tau_1^{\epsilon,\overline{\epsilon},r}$ that $U_t = 0$. Given that $\tau_j^{\epsilon,\overline{\epsilon},r}, \sigma_j^{\epsilon,\overline{\epsilon},r}$ for $1 \leq j \leq k$ have been defined for some $k \in \mathbf{N}$, we let $\tau_{k+1}^{\epsilon,\overline{\epsilon},r}$ be defined in exactly the same was as $\tau_1^{\epsilon,\overline{\epsilon},r}$ except with $t \geq \sigma_k^{\epsilon,\overline{\epsilon},r}$. We then let $\sigma_{k+1}^{\epsilon,\overline{\epsilon},r}$ be the first time t after time $\tau_{k+1}^{\epsilon,\overline{\epsilon},r}$ that $U_t = 0$.

For each j, we let $\widetilde{X}^{j,\epsilon,\overline{\epsilon},r}$ be given by $\widetilde{X}^{\tau_j^{\epsilon,\overline{\epsilon},r}}$ and $\widetilde{h}_j^{\epsilon,\overline{\epsilon},r}$ be given by $\widetilde{h}^{\tau_j^{\epsilon,\overline{\epsilon},r}}$. We emphasize that the horizontal translation is taken so that $\widetilde{X}^{j,\epsilon,\overline{\epsilon},r}$ first hits r at time 0.

The reason for this particular choice of stopping times is that in the proof of Theorem 7.1 we will analyze the structure of a given bubble when it has only been partially zipped into the big surface and γ-LQG boundary length is a useful way to restrict our attention to "large bubbles" since it is an intrinsic quantity. (For technical reasons, we will define our stopping times in a different way when we prove the analog of Theorem 7.1 for $\mathrm{SLE}_{\kappa'}$ processes which will complicate the proof somewhat in that case.) The condition that $\widetilde{X}_0^{j,\epsilon,\overline{\epsilon},r} = r$ will be useful when we construct a coupling between the bubbles and the excursions from 0 of a BES^δ process with δ as in (7.1). In particular, we will couple the excursions from 0 of the latter whose maximum is at least $\exp(\frac{\gamma}{2}r)$ with the processes $\exp(\frac{\gamma}{2}\widetilde{X}_u^{j,\epsilon,\overline{\epsilon},r})$ for $u \geq 0$ and reparameterized to have quadratic variation du to be the same. Finally, the condition that the γ-LQG mass of the bubbles which, when parameterizing by $\mathcal{S}$ as above, is contained in $\mathcal{S}_-$ is at least $\overline{\epsilon} > 0$ will be a useful technical tool to ensure that the bubbles that we consider are locally finite when we take a limit as $\epsilon \to 0$. By this, we mean that the number of bubbles with this property which have been zipped in before a given capacity time is almost surely finite. (Later in the proof of Theorem 7.1, we will see that in fact the condition that the supremum of $\widetilde{X}^{j,\epsilon,\overline{\epsilon},r}$ is at least r is enough to ensure this.)

Lemma 7.6. *For each $\overline{\epsilon} > 0$ and $r \in \mathbf{R}$, the limit and $(\widetilde{h}_j^{\overline{\epsilon},r})$ of the sequence $(\widetilde{h}_j^{\epsilon,\overline{\epsilon},r})$ as $\epsilon \to 0$ exists almost surely in the following sense: for each fixed $j \in \mathbf{N}$ and $r \in \mathbf{R}$ there almost surely exists $\epsilon_0 > 0$ (random) such that $\epsilon \in (0, \epsilon_0)$ implies that $\widetilde{h}_j^{\overline{\epsilon},r} = \widetilde{h}_j^{\epsilon,\overline{\epsilon},r}$.*

Note that Lemma 7.6 implies that the sequence $(\widetilde{X}^{j,\epsilon,\bar{\epsilon},r})$ has a limit $(\widetilde{X}^{j,\bar{\epsilon},r})$ which exists in the same sense.

Proof of Lemma 7.6. Suppose for contradiction that this is not the case for some fixed choice of $\bar{\epsilon} > 0$ and $r \in \mathbf{R}$. (We are going to get a contradiction to the fact that, in the present setup, the γ-LQG mass of every bounded neighborhood of the origin is almost surely finite.) Then there exists an event E with $\mathbf{P}[E] > 0$ such that the following is true. There exists $j \in \mathbf{N}$ and $r \in \mathbf{R}$ such that on E for every $\epsilon > 0$ there exists $\epsilon' \in (0, \epsilon)$ such that $\widetilde{h}_j^{\epsilon,\bar{\epsilon},r}$ is not the same as $\widetilde{h}_j^{\epsilon',\bar{\epsilon},r}$. Note that if $\epsilon' \in (0, \epsilon)$ then we necessarily have that the bubble which corresponds to $\widetilde{h}_j^{\epsilon',\bar{\epsilon},r}$ comes before (in the zipping up procedure) the bubble which corresponds to $\widetilde{h}_j^{\epsilon,\bar{\epsilon},r}$. That is, $\sigma_j^{\epsilon',\bar{\epsilon},r} \leq \sigma_j^{\epsilon,\bar{\epsilon},r}$. Thus if $\widetilde{h}_j^{\epsilon,\bar{\epsilon},r} \neq \widetilde{h}_j^{\epsilon',\bar{\epsilon},r}$ then $\sigma_j^{\epsilon',\bar{\epsilon},r} < \tau_j^{\epsilon,\bar{\epsilon},r} < \sigma_j^{\epsilon,\bar{\epsilon},r}$.

It is then easy to see that there exists a sequence (ϵ_k) of positive numbers decreasing to 0 such that, for each $k \in \mathbf{N}$, the bubble corresponding to $\widetilde{h}_j^{\epsilon_{k+1},\bar{\epsilon},r}$ is distinct from and necessarily comes before the bubble which corresponds to $\widetilde{h}_j^{\epsilon_k,\bar{\epsilon},r}$. Therefore we have an infinite number of bubbles which are zipped in before time $\tau_j^{\epsilon_1,\bar{\epsilon},r}$ each of which has γ-LQG mass which is at least $\bar{\epsilon}$. In particular, the total γ-LQG mass of these bubbles is infinite. Since $\mathbf{P}[\tau_j^{\epsilon_1,\bar{\epsilon},r} < \infty] = 1$, we get our desired contradiction because then we have an infinite amount of γ-LQG mass in a bounded subset of the origin on a positive probability event. □

One of the main inputs into the proof of Theorem 7.1 is the following observation regarding the law of the sequences $(\widetilde{X}^{j,\epsilon,\bar{\epsilon},r})$ and $(\widetilde{X}^{j,\bar{\epsilon},r}) = (\widetilde{X}^{j,0,\bar{\epsilon},r})$.

Proposition 7.7. *For each $\epsilon \geq 0$, $\bar{\epsilon} > 0$, and $r \in \mathbf{R}$ there exists a collection of i.i.d. standard Brownian motions $B^{j,\epsilon,\bar{\epsilon},r}$ with $B_0^{j,\epsilon,\bar{\epsilon},r} = r$ such that*

$$\widetilde{X}_t^{j,\epsilon,\bar{\epsilon},r} = B_{2t}^{j,\epsilon,\bar{\epsilon},r} + at \quad \text{where} \quad a = \frac{\rho+4}{\gamma} - Q = \frac{\rho+2}{\gamma} - \frac{\gamma}{2}.$$

We will write $\widetilde{B}^{j,\bar{\epsilon},r}$ for $\widetilde{B}^{j,0,\bar{\epsilon},r}$. Before we give the proof of Proposition 7.7, we will describe the behavior of the maps $\varphi_t^{-1} \colon \mathcal{S} \to \mathcal{B}_t$ near $+\infty$.

Lemma 7.8. *Fix $t \geq 0$ such that $U_t \neq 0$. Let $\psi_t \colon \mathbf{H} \to \mathcal{B}_t$ be the unique conformal transformation with $\psi_t(0) = U_t$, $\psi_t(-1) = 0$, and $\psi_t(\infty) = \zeta_t$. Then we have that*

$$\lim_{R \to \infty} \sup_{\substack{z \in \mathcal{S} \\ \mathrm{Re}(z) \geq R}} \left| e^z (\varphi_t^{-1})'(z) - \psi_t'(0) \right| = 0.$$

Proof. We first note that the map $-e^{-z}$ takes $\mathcal{S}$ to $\mathbf{H}$ with $+\infty$ sent to 0, $-\infty$ sent to ∞, and 0 sent to -1. The result then follows by since $\varphi_t^{-1}(z) = \psi_t(-e^{-z})$. □

In the proof of Proposition 7.7 and the subsequent lemmas, we will make use of the following notation. We let $w_j^{\epsilon,\bar{\epsilon},r} \in \mathbf{R}$ be such that the γ-LQG length associated with the field $\widetilde{h}_j^{\epsilon,\bar{\epsilon},r}$ of $(-\infty, w_j^{\epsilon,\bar{\epsilon},r}]$ is equal to ϵ. We then let $\widetilde{\psi}_j^{\epsilon,\bar{\epsilon},r}$ be the function which is harmonic in $[w_j^{\epsilon,\bar{\epsilon},r}, \infty) \times [0,\pi]$ with Neumann boundary conditions on the horizontal parts of the strip boundary (and at $+\infty$) and Dirichlet boundary conditions on $w_j^{\epsilon,\bar{\epsilon},r} + [0, i\pi]$ with boundary values given by those of $\widetilde{h}_j^{\epsilon,\bar{\epsilon},r}$. We emphasize that the function $\widetilde{\psi}_j^{\epsilon,\bar{\epsilon},r}$ has Neumann boundary conditions at $+\infty$; this rules out the possibility of a limit of the form $c_1 \mathrm{Re}(z) + c_2$ with $c_1 \neq 0$.

Proof of Proposition 7.7. We let $\widetilde{\Phi}_j^{\epsilon,\bar{\epsilon},r}$ be given by the restriction to $\mathcal{S}_+$ of the conditional expectation of $\widetilde{h}_j^{\epsilon,\bar{\epsilon},r}$ given its values on $w_j^{\epsilon,\bar{\epsilon},r} + [0, i\pi]$. Lemma 7.8 (and the coordinate change formula for quantum surfaces) implies that we can write $\widetilde{\Phi}_j^{\epsilon,\bar{\epsilon},r}$ as the sum of $\widetilde{\psi}_j^{\epsilon,\bar{\epsilon},r}$, a constant, and

$$\left(\frac{\widetilde{\rho}}{\gamma} - Q\right) \mathrm{Re}(z) = a \mathrm{Re}(z)$$

where a is as in the statement of Proposition 7.7. Conditionally on $\widetilde{\psi}_j^{\epsilon,\bar{\epsilon},r}$, we thus have that $\widetilde{X}_u^{j,\epsilon,\bar{\epsilon},r}$ evolves as the sum of $B_{2u} + au$, B a standard Brownian motion, and the average of $\widetilde{\psi}_j^{\epsilon,\bar{\epsilon},r}$ on $u + [0, i\pi]$. Since $\widetilde{\psi}_j^{\epsilon,\bar{\epsilon},r}$ is harmonic in $\mathcal{S}_+$ with Neumann boundary conditions on $\partial\mathcal{S}_+ \setminus [0, i\pi]$ (and, in particular, at $+\infty$), it from Lemma 5.2 that its average on $u + [0, i\pi]$ does not depend on u. This gives the desired result because, for each $j \geq 2$, we have that $\widetilde{X}^{j,\epsilon,\bar{\epsilon},r}$ is independent of $\widetilde{X}^{1,\epsilon,\bar{\epsilon},r}, \ldots, \widetilde{X}^{j-1,\epsilon,\bar{\epsilon},r}$ given $\widetilde{\psi}_j^{\epsilon,\bar{\epsilon},r}$. □

Lemma 7.9. *Fix $j \in \mathbf{N}$, $\bar{\epsilon} > 0$, and $r \in \mathbf{R}$. There exists a sequence (ϵ_k) of positive numbers decreasing to 0 such that $\widetilde{\psi}_j^{\epsilon_k,\bar{\epsilon},r}$ almost surely converges to the 0 function on $\mathcal{S}_+$ as $k \to \infty$ with respect to the topology of local uniform convergence modulo a global additive constant.*

Proof. Fix $u > 0$ rational and let $\mathcal{V}_u$ be the connected component of $\mathbf{H} \setminus \eta$ with u on its boundary. (Note that a unique such component exists almost surely for all $u > 0$ rational simultaneously since the probability that η hits any given point in $(0, \infty)$ is zero.) We also fix $\epsilon > 0$ and assume that we are working on the event that the quantum length of $\partial\mathcal{V}_u \setminus \partial\mathbf{H}$ is at least $\epsilon > 0$. Note that the probability of this event tends to 1 as $\epsilon \to 0$ (for u fixed). We let ξ (resp. ζ) be the first (resp. last) time that η hits a point on $\partial\mathcal{V}_u$ and let $\varphi^\epsilon \colon \mathcal{V}_u \to \mathcal{S}$ be the unique conformal transformation which takes $\eta(\xi)$ to $+\infty$ and $\eta(\zeta)$ to $-\infty$ where the horizontal translation has been fixed so that the quantum length of $(-\infty, 0]$ under the γ-LQG boundary measure associated with $h \circ (\varphi^\epsilon)^{-1} + Q \log |((\varphi^\epsilon)^{-1})'|$ is equal to ϵ. Let ψ^ϵ be the function

which is harmonic in $\mathcal{S}_+$ with Neumann boundary conditions on $\partial\mathcal{S}_+ \setminus [0, i\pi]$ and Dirichlet boundary conditions on $[0, i\pi]$ with boundary values given by the values of $h \circ (\varphi^\epsilon)^{-1} + Q \log |((\varphi^\epsilon)^{-1})'|$ on $[0, i\pi]$.

By Lemma 5.2, it suffices to show that, as $\epsilon \to 0$, the law of ψ^ϵ converges weakly with respect to the topology of local uniform convergence in $\mathcal{S}_+$ modulo a global additive constant to a function which is harmonic in $\mathcal{S}_+$. Indeed, here we are using that for each fixed $j \in \mathbf{N}$, $\epsilon > 0$, and $r \in \mathbf{R}$, if we "zip up" to a large enough local time as in Lemma 7.5 then with high probability the bubble associated with $\widetilde{\psi}_j^{\epsilon,\bar{\epsilon},r}$ will be a bubble of the zipped up process and the zipped up process has the law of a forward $\mathrm{SLE}_\kappa(\rho)$.

We are going to deduce this from Proposition 6.7 and the independence of η and h. For each $\delta > 0$ we let $\eta_1^\delta = \delta^{-1}(\eta(\zeta - \cdot) - \eta(\zeta))$ and $\eta_2^\delta = \delta^{-1}(\eta(\zeta + \cdot) - \eta(\zeta))$. Then Proposition 6.7 gives us that the law of $(\eta_1^\delta, \eta_2^\delta)$ converges as $\delta \to 0$ to the law of a certain pair of GFF flow lines (η_1, η_2) starting from 0. Let h^δ be the field which arises by precomposing h with $z \mapsto \delta(z + \eta(\zeta))$. Then h^δ converges as $\delta \to 0$ to a free boundary GFF on $\mathbf{H}$ by the scale and translation invariance of free boundary GFFs and the independence of h and η. By the independence of h and η, we get that the triple $(\eta_1^\delta, \eta_2^\delta, h^\delta)$ converges in law as $\delta \to 0$ to the law of a triple consisting of a pair of GFF flow lines and an independent free boundary GFF on $\mathbf{H}$.

For each $t \in (0, \zeta - \xi)$, we let $\widetilde{\varphi}_t^\epsilon$ be the conformal transformation which takes $\mathbf{H} \setminus \eta([\zeta - t, \zeta])$ to $\mathcal{S}$ with $\eta(\zeta)$ taken to $-\infty$, $\eta(\zeta - t)$ taken to $+\infty$, and the horizontal shift normalized so that the γ-LQG boundary measure of $(-\infty, 0]$ with respect to $h \circ (\widetilde{\varphi}_t^\epsilon)^{-1} + Q \log |((\widetilde{\varphi}_t^\epsilon)^{-1})'|$ is equal to ϵ. Then the law of the field $h \circ (\widetilde{\varphi}_t^\epsilon)^{-1} + Q \log |((\widetilde{\varphi}_t^\epsilon)^{-1})'|$ (viewed as a modulo additive constant distribution on $\mathcal{S}$) has a scaling limit as $t, \epsilon \to 0$ where $\epsilon \to 0$ at a sufficiently fast rate relative to the rate at which $t \to 0$. This follows from what we explained in the previous paragraph. Therefore the law of the function which is harmonic in $\mathcal{S}_+$ with Neumann boundary conditions on $\partial\mathcal{S}_+ \setminus [0, i\pi]$ and with Dirichlet boundary conditions on $[0, i\pi]$ given by the values of $h \circ (\widetilde{\varphi}_t^\epsilon)^{-1} + Q \log |((\widetilde{\varphi}_t^\epsilon)^{-1})'|$ on $[0, i\pi]$ converges weakly as $t, \epsilon \to 0$ as before with respect to the topology of local uniform convergence modulo a global additive constant.

The claimed result will follow by showing that $h \circ (\widetilde{\varphi}_t^\epsilon)^{-1} + Q \log |((\widetilde{\varphi}_t^\epsilon)^{-1})'|$ is close to $h \circ (\varphi^\epsilon)^{-1} + Q \log |(\varphi^\epsilon)^{-1})'|$ for small enough ϵ relative to t. That this is the case can be seen as follows. Let $t_\epsilon \in [\xi, \zeta]$ be such that the quantum length of $\eta([t_\epsilon, \zeta])$ is ϵ and assume that we are working on the event that $t_\epsilon \in (\zeta - t, \zeta)$. Note that the probability of this event tends to 1 as $\epsilon \to 0$ with t fixed. The image of a point $z \in \mathbf{H} \setminus \eta([t_\epsilon, \zeta])$ under $\widetilde{\varphi}_t^\epsilon$ is determined by the harmonic measure as seen from z of the boundary segments (counterclockwise) from $\eta(\zeta)$ to $\eta(t_\epsilon)$, from $\eta(t_\epsilon)$ to $\eta(\zeta - t)$, and from $\eta(\zeta - t)$ to $\eta(\zeta)$. Similarly, the image of $z \in \mathcal{V}_u$ under φ^ϵ is determined by the harmonic measure as seen from z of the boundary segments (counterclockwise)

of $\partial\mathcal{V}_u$ from $\eta(\zeta)$ to $\eta(t_\epsilon)$, $\eta(t_\epsilon)$ to $\eta(\xi)$, and from $\eta(\xi)$ to $\eta(\zeta)$. From this, it is easy to see that if $K \subseteq \mathcal{S}$ is any fixed compact set, then $\widetilde{\varphi}_t^\epsilon \circ (\varphi^\epsilon)^{-1}$ converges uniformly to the identity on K as $\epsilon \to 0$. □

Proof of Theorem 7.1. First of all, suppose that $X_t = B_{2t} + at$ where B is a standard Brownian motion and a is as in Proposition 7.7. By the discussion in the beginning of Section 4.4 (see also Proposition 3.4), we know that $Z_t = \exp(\frac{\gamma}{2}X_t)$ (reparameterized to have quadratic variation dt) evolves as a BES^δ with $\delta = \delta(\kappa, \rho)$ where $\delta(\kappa, \rho)$ is as in (7.1). Suppose that Y is a BES^δ. Fix $u > 0$ large and let T_u be as in the statement of Lemma 7.5. Proposition 7.7 then allows us to construct a coupling between Y and the ordered sequence of components of $\mathbf{H} \setminus \eta^{T_u}$ (viewed as quantum surfaces) as follows. For any given r, we can couple the excursions that Y makes above $\exp(\frac{\gamma}{2}r)$ with the sequence $\exp(\frac{\gamma}{2}\widetilde{X}^{j,\bar{\epsilon},r})$, where we view both processes as starting from the first time that they hit $\exp(\frac{\gamma}{2}r)$, to be the same (after reparameterizing the latter according to quadratic variation) for those j which correspond to bubbles zipped in before time T_u. Note that, for each r, given $(\widetilde{X}^{j,\bar{\epsilon},r})$ the bubbles are otherwise independent as quantum surfaces since Lemma 7.9 implies that the projection of $\widetilde{\psi}_j^{\epsilon_k,\bar{\epsilon},r}$ onto $\mathcal{H}_2(\mathcal{S})$ tends to 0 almost surely as $k \to \infty$ for a sequence (ϵ_k) of positive numbers that decreases to 0 sufficiently quickly.

The same argument as in the proof of Lemma 7.6 implies that for each fixed $j \in \mathbf{N}$ and $r \in \mathbf{R}$ there exists $\bar{\epsilon}_0 > 0$ (random) such that $\bar{\epsilon} \in (0, \bar{\epsilon}_0)$ implies that $\widetilde{X}^{j,r} = \widetilde{X}^{j,\bar{\epsilon},r}$. Indeed, recall that at this point in the proof we know that the bubbles which correspond to the $(\widetilde{X}^{j,\bar{\epsilon},r})$ are conditionally independent given the $(\widetilde{X}^{j,\bar{\epsilon},r})$. Moreover, note that the probability that the bubble which corresponds to $\widetilde{X}^{j,\bar{\epsilon},r}$ has γ-LQG mass at least $e^{\gamma r}$ is uniformly positive as $\bar{\epsilon} \to 0$. Thus if the claim were not true, we would easily be led to the contradiction that the amount of γ-LQG mass in compact subsets of the origin is almost surely finite.

Sending $\bar{\epsilon} \to 0$, we get an asymptotic coupling where the excursions of Y from 0 which reach level at least $\exp(\frac{\gamma}{2}r)$ up until some time S_u each correspond to a component of $\mathbf{H} \setminus \eta^{T_u}$ which is to the right of η^{T_u}. Sending $r \to -\infty$, we get an asymptotic coupling where the excursions of Y from 0 up until some time S_u each correspond to a component of $\mathbf{H} \setminus \eta^{T_u}$ which is to the right of η^{T_u} and this correspondence is bijective. Note that Y encodes these bubbles in the reverse order in which they are cut off by η^{T_u}. By the symmetry of the setup, however, we can reverse time so that Y encodes the bubbles in the same order in which they are cut off by η^{T_u}. Sending u to ∞ and using Lemma 7.5 gives a coupling where the excursions of Y from 0 encode all of the components of $\mathbf{H} \setminus \eta$. □

Remark 7.10. In the setting of Theorem 7.1, it is possible to encode the beaded quantum surface which consists of the components of $\mathbf{H} \setminus \eta$ which are to the right of η using a BES^δ for any $\delta \in (0, 2)$. Indeed, if $X_t = B_{2t} + at$ where B is a standard

Brownian motion and a is as in Proposition 7.7, then by Proposition 3.4 we have that $\exp(\frac{\widetilde{\gamma}}{2}X_t)$ (parameterized by its quadratic variation) evolves as a Bessel process of dimension

$$2 + \frac{2\rho + 4 - \gamma^2}{\gamma\widetilde{\gamma}}.$$

Since $\rho \in (-2, \frac{\kappa}{2} - 2)$, the second summand above is negative so varying $\widetilde{\gamma}$ gives any value of $\delta \in (0, 2)$, as claimed, and the proof of Theorem 7.1 goes through verbatim using $\exp(\frac{\widetilde{\gamma}}{2}X_t)$ in place of $\exp(\frac{\gamma}{2}X_t)$.

Note that changing from γ to $\widetilde{\gamma}$ changes the interpretation of the information encoded by the Bessel process. For example, if we choose $\widetilde{\gamma} = \frac{\gamma}{2}$, then the length of an excursion e from 0 of the corresponding Bessel process gives a constant times the conditional expectation (given e) of the γ-LQG boundary length of the bubble associated with e.

7.2 Radial and whole-plane $\mathrm{SLE}_\kappa(\rho)$ processes

We are now going to determine the law of the bubbles (viewed as quantum surfaces) which are cut off by radial and whole-plane $\mathrm{SLE}_\kappa(\rho)$ processes.

Theorem 7.11. *Fix $\kappa \in (0, 4)$, $\rho \in (-2, \frac{\kappa}{2} - 2)$, $\widetilde{\rho} = \rho + 4$, and let $\gamma = \sqrt{\kappa}$. Suppose that*

$$h = \widetilde{h} - \frac{\gamma^2 + 6 - \widetilde{\rho}}{2\gamma} \log|\cdot| + \frac{2 - \widetilde{\rho}}{\gamma} \log|\cdot - 1| = \widetilde{h} - \frac{\gamma^2 + 2 - \rho}{2\gamma} \log|\cdot| - \frac{\rho + 2}{\gamma} \log|\cdot - 1|$$

where $\widetilde{h}$ is a free boundary GFF on $\mathbf{D}$. Let η be a radial $\mathrm{SLE}_\kappa(\rho)$ process in $\mathbf{D}$ starting from 1 and targeted at 0 with a single boundary force point of weight ρ located at 1^+. Assume that η is independent of h. Then the ordered sequence of components of $\mathbf{D} \setminus \eta$, each viewed as a quantum surface, has the same law as in Theorem 7.1 (with ρ and κ values matched).

Before we explain how to modify the proof of Theorem 7.1 to give Theorem 7.11, we first state and prove the following corollary.

Corollary 7.12. *Fix $\kappa \in (0, 4)$, $\rho \in (-2, \frac{\kappa}{2} - 2)$, $\widetilde{\rho} = \rho + 4$, and let $\gamma = \sqrt{\kappa}$. Suppose that*

$$h = \widetilde{h} - \frac{\gamma^2 + 6 - \widetilde{\rho}}{2\gamma} \log|\cdot| = \widetilde{h} - \frac{\gamma^2 + 2 - \rho}{2\gamma} \log|\cdot|$$

where $\widetilde{h}$ is a whole-plane GFF. Let η be a whole-plane $\mathrm{SLE}_\kappa(\rho)$ process starting from 0 which is independent of h. Then the ordered sequence of components of $\mathbf{C} \setminus \eta$, each viewed as a quantum surface, has the same law as in Theorem 7.1 (with ρ and κ values matched).

Proof. This result follows from Theorem 7.11 by rescaling by ϵ^{-1} and then taking a limit as $\epsilon \to 0$. Indeed, under a such a rescaling the field converges to a whole-plane GFF with the log singularity at the origin indicated in the statement of the lemma and the path converges to a whole-plane $\mathrm{SLE}_\kappa(\rho)$ process from ∞ to 0. The result then follows from the reversibility of whole-plane $\mathrm{SLE}_\kappa(\rho)$ [MS13a, Theorem 1.20]. □

In the setting of Theorem 7.11 and Corollary 7.12 we define the quantum natural time parameterization of the bubbles cut off by η in the same manner as given in Definition 7.2.

Proof of Theorem 7.11. This follows from the same argument used to prove Theorem 7.1. The only difference that we need to explain is why the analogs of the functions $\widetilde{\psi}_j^{\epsilon_k,\bar{\epsilon},r}$ converge to 0 as $k \to \infty$ (modulo a global additive constant) where (ϵ_k) is a sequence of positive numbers which decrease to 0 sufficiently quickly. We can apply the same argument as in Theorem 7.1 (using Proposition 6.10 in place of Proposition 6.7) to get the result for the bubbles whose terminal boundary segment of γ-LQG length ϵ terminates in $\partial\mathbf{D}$ but we cannot apply this argument directly in the case of a bubble where the terminal boundary segment of length ϵ terminates in $\mathbf{D}$. (The latter correspond to self-intersection points of the path.) To get that all of the $\widetilde{\psi}_j^{\epsilon_k,\bar{\epsilon},r}$ converge to 0 as $k \to \infty$ (modulo a global additive constant), we can apply the above argument to the setting in which we have unzipped the path to a given rational time and use that, almost surely, for each bubble there exists a rational time such that if we unzip to that time then the terminal segment of γ-LQG length ϵ of the boundary of the bubble will end in $\partial\mathbf{D}$. □

7.3 $\mathrm{SLE}_{\kappa'}$ processes with $\kappa' \in (4,8)$

We will now determine the structure of the bubbles (viewed as quantum surfaces) which arise when cutting along an $\mathrm{SLE}_{\kappa'}$ process. The following theorem gives the analogs of Theorem 7.1, Theorem 7.11, and Corollary 7.12 in this case.

Theorem 7.13. *Fix $\kappa' \in (4,8)$, let $\gamma = 4/\sqrt{\kappa'}$, and suppose that*

$$h = \widetilde{h} + \frac{2}{\sqrt{\kappa'}} \log|\cdot| = \widetilde{h} + \frac{\gamma}{2} \log|\cdot|$$

where $\widetilde{h}$ is a free boundary GFF on $\mathbf{H}$. Let η' be an $\mathrm{SLE}_{\kappa'}$ process in $\mathbf{H}$ starting from 0 and targeted at ∞ which is independent of h. Then the ordered sequence of connected components of $\mathbf{H} \setminus \eta'$ (where a component $\mathcal{B}$ comes before another component $\mathcal{B}'$ if η' finishes drawing all of $\partial\mathcal{B}$ before it finishes drawing all of $\partial\mathcal{B}'$)

whose boundary is completely contained in η', each viewed as a quantum surface, can be sampled using a p.p.p. Λ with intensity measure

$$du \otimes \frac{1}{\nu_h(\partial \mathcal{S})} d\mathcal{M}_\delta^{4\gamma^{-1}}(h)$$

where du denotes Lebesgue measure on $\mathbf{R}_+$ and $\mathcal{M}_\delta^{4\gamma^{-1}}$ is as in Definition 4.19 with $\delta = 4 - \frac{8}{\gamma^2}$. The same also holds if we:

- *Take η' to be a radial $\mathrm{SLE}_{\kappa'}$ process in $\mathbf{D}$ from 1 to 0 and*

$$h = \widetilde{h} + \frac{2}{\sqrt{\kappa'}} \log|\cdot - 1| - \frac{\kappa' + 6}{2\sqrt{\kappa'}} \log|\cdot| = \widetilde{h} + \frac{\gamma}{2} \log|\cdot - 1| - \frac{3\gamma^2 + 8}{4\gamma} \log|\cdot|$$

  where $\widetilde{h}$ is a free boundary GFF on $\mathbf{D}$ independent of η'.

- *Take η' to be a whole-plane $\mathrm{SLE}_{\kappa'}$ process from 0 to ∞ and*

$$h = \widetilde{h} - \frac{\kappa' + 2}{2\sqrt{\kappa'}} \log|\cdot| = \widetilde{h} - \frac{\gamma^2 + 8}{4\gamma} \log|\cdot|$$

  where $\widetilde{h}$ is a whole-plane GFF independent of η'.

Definition 7.14. Let η' and Λ be as in the statement of Theorem 7.13 with the capacity time parameterization. For each $u \geq 0$, we let $\mathfrak{q}_u$ be the infimum of times t such that $\eta'|_{[0,t]}$ has finished drawing a bubble whose corresponding element $(v, e) \in \Lambda$ satisfies $v > u$. We refer to the time-parameterization of η' given by $u \mapsto \eta'(\mathfrak{q}_u)$ as **quantum natural time** for η'.

Note that the boundary of a component $\mathcal{B}$ of $\mathbf{H} \setminus \eta'$ naturally has a marked point which is given by the first point on $\partial\mathcal{B}$ which is drawn by η' (this is also the same as the last point on $\partial\mathcal{B}$ drawn by η'). It will be helpful in what follows to consider a modified setting in which $\partial\mathcal{B}$ has two marked points. To do so, we will take the intermediate step of considering the law of the surfaces corresponding to the components of $\mathbf{H} \setminus \eta'$ weighted by their γ-LQG boundary length. As shown in Lemma 5.6, this is equivalent to adding a certain log singularity to the boundary of each component of $\mathbf{H} \setminus \eta'$.

The setup for the proof of Theorem 7.13 is similar to that for Theorem 7.1. Let (f_t) denote the centered reverse Loewner flow associated with a reverse $\mathrm{SLE}_{\kappa'}$ process. For each $s \leq t$, we also let $f_{s,t} = f_t \circ f_s^{-1}$. As in the proof of Lemma 7.5, it is not hard to see that we can construct a family of fields (h^t) such that, for each t, h^t can be expressed as the sum of a free boundary GFF on $\mathbf{H}$ plus $\frac{\gamma}{2} \log|\cdot|$ which satisfy

$$h^s = h^t \circ f_{s,t} + Q \log|f'_{s,t}| \quad \text{for each} \quad 0 \leq s \leq t < \infty.$$

Let η' be an $\mathrm{SLE}_{\kappa'}$ process independent of h and (f_t) and, for each $t > 0$, we let $(\eta')^t$ be the curve associated with $f_t(\partial\mathbf{H} \cup \eta')$. Note that $(\eta')^t$ has the law of an $\mathrm{SLE}_{\kappa'}$ process for each $t \geq 0$.

Fix $\epsilon > 0$. We define stopping times inductively as follows. We let τ_1^ϵ be the first time t that the diameter of a partially zipped in bubble by the reverse Loewner flow at time t is at least ϵ (i.e., the connected components of $\mathbf{H} \setminus \eta'$ are not counted). Let $\mathcal{B}_1^\epsilon$ be the corresponding bubble. We let σ_1^ϵ be the time that $\mathcal{B}_1^\epsilon$ is finished being zipped in. Assuming that τ_j^ϵ and σ_j^ϵ have been defined for $1 \leq j \leq k$, some $k \in \mathbf{N}$, we let τ_{k+1}^ϵ be the first time t after time σ_k^ϵ that the diameter of a partially zipped in bubble is at least ϵ. Let $\mathcal{B}_{k+1}^\epsilon$ be the corresponding bubble and let σ_{k+1}^ϵ be the time at which $\mathcal{B}_{k+1}^\epsilon$ is finished being zipped in.

For each $\mathcal{B}$ which is not fully zipped in, we take $x_{\mathcal{B}}$ to be the endpoint of the interval corresponding to the interior of $\partial\mathcal{B} \cap \partial\mathbf{H}$ which is closest to 0. We let $y_{\mathcal{B}_j^\epsilon}$ be a point independently picked in the interior of $\partial\mathcal{B}_j^\epsilon \cap \partial\mathbf{H}$ according to Lebesgue measure. Let $G_j^\epsilon(u, v)$ be the Green's function on $\mathcal{B}_j^\epsilon$ with Neumann boundary conditions on $\partial\mathcal{B}_j^\epsilon \cap \partial\mathbf{H}$ and Dirichlet boundary conditions on $\partial\mathcal{B}_j^\epsilon \setminus \partial\mathbf{H}$. By Lemma 5.6, the law of $(\mathcal{B}_j^\epsilon, h^{\tau_j^\epsilon} + \frac{\gamma}{2} G_j^\epsilon(y_{\mathcal{B}_j^\epsilon}, \cdot))$ (viewed as a quantum surface) is equal to the law of $(\mathcal{B}_j^\epsilon, h^{\tau_j^\epsilon})$ weighted by the γ-LQG boundary length of the interior of $\partial\mathcal{B}_j^\epsilon \cap \partial\mathbf{H}$.

Let $G(u, v)$ be the Green's function on $\mathcal{S}$ with Neumann boundary conditions on $\partial\mathcal{S} \setminus (-\infty, 0]$ and Dirichlet boundary conditions on $(-\infty, 0]$ and let $G(u) = \lim_{v \to \infty} G(u, v)$; this limit exists by Lemma 5.2. For each $j \in \mathbf{N}$ and $\epsilon > 0$, we let

- $\varphi_j^\epsilon \colon \mathcal{B}_j^\epsilon \to \mathcal{S}$ be the unique conformal transformation which takes $x_{\mathcal{B}_j^\epsilon}$ to $-\infty$ and $y_{\mathcal{B}_j^\epsilon}$ to $+\infty$ with the horizontal translation fixed so that $\partial\mathcal{B}_j^\epsilon \cap \mathbf{H}$ is mapped to $(-\infty, 0]$.
- $\widetilde{h}_j^\epsilon = h^{\tau_j^\epsilon} \circ (\varphi_j^\epsilon)^{-1} + \frac{\gamma}{2} G(u) + Q \log |((\varphi_j^\epsilon)^{-1})'|$.
- $\widetilde{X}^{j,\epsilon}$ be the projection of $\widetilde{h}_j^\epsilon$ onto $\mathcal{H}_1(\mathcal{S})$.

By Lemma 5.6, $(\mathcal{S}, \widetilde{h}_j^\epsilon)$ viewed as a quantum surface has the law of $(\mathcal{B}_j^\epsilon, h^{\tau_j^\epsilon})$ weighted by the γ-LQG boundary length of the interior of $\partial\mathcal{B}_j^\epsilon \cap \partial\mathbf{H}$.

For each j and $\widetilde{\epsilon} > 0$, let $u_j^{\epsilon,\widetilde{\epsilon}} \in \mathbf{R}$ be such that the γ-LQG length measure associated with $\widetilde{h}_j^\epsilon$ assigns mass $\widetilde{\epsilon}$ to $(-\infty, u_j^{\epsilon,\widetilde{\epsilon}}]$; we take $u_j^{\epsilon,\widetilde{\epsilon}} = +\infty$ if the γ-LQG length of $\mathbf{R}$ is smaller than $\widetilde{\epsilon}$. We let $\widetilde{\psi}_j^{\epsilon,\widetilde{\epsilon}}$ be the function which is harmonic on $[u_j^{\epsilon,\widetilde{\epsilon}}, \infty) \times [0, \pi]$ with Neumann boundary conditions on the horizontal part of the strip boundary (and at $+\infty$) and Dirichlet boundary conditions on $u_j^{\epsilon,\widetilde{\epsilon}} + [0, i\pi]$ given by the values of $\widetilde{h}_j^\epsilon$.

We similarly let $\widetilde{\psi}_j^\epsilon$ be the function which is harmonic on $\mathcal{S}_+$ with Neumann boundary conditions on $\partial\mathcal{S}_+ \setminus [0, i\pi]$ (in particular, also at $+\infty$) and Dirichlet boundary conditions on $[0, i\pi]$ equal to those of $\widetilde{h}_j^\epsilon$ on $[0, i\pi]$.

We next record the following analog of Lemma 7.9 for the present setting.

Lemma 7.15. *Fix $j \in \mathbf{N}$ and $\epsilon > 0$. There exists a sequence $(\widetilde{\epsilon}_k)$ of positive numbers with $\widetilde{\epsilon}_k \to 0$ as $k \to \infty$ such that $\widetilde{\psi}_j^{\epsilon,\widetilde{\epsilon}_k}$ almost surely converges to the 0 function on $\mathcal{S}_+$ as $k \to \infty$ with respect to the topology of local uniform convergence modulo a global additive constant.*

Proof. This follows from an argument which is very similar to that given in Lemma 7.9 (using Remark 6.9 in place of Proposition 6.7), so we will omit the details. □

Fix $\overline{\epsilon} > 0$ and $r \in \mathbf{R}$. Let $\varsigma_j^{\epsilon,r} = \inf\{u : \widetilde{X}_u^{j,\epsilon} \geq r\}$. For each k, let j_k be the kth index j such that both

- $\varsigma_j^{\epsilon,r} \in [0, \infty)$ and
- the total variation distance between the conditional law of the projection of $\widetilde{h}_j^\epsilon(\cdot + \varsigma_j^{\epsilon,r})$ onto $\mathcal{H}_2(\mathcal{S})$ restricted to $\mathcal{S}_+$ given $\widetilde{\psi}_j^\epsilon(\cdot + \varsigma_j^{\epsilon,r})$ and the corresponding projection of a free boundary GFF on $\mathcal{S}$ is at most $\overline{\epsilon}$.

We then let $\mathcal{B}_k^{\epsilon,\overline{\epsilon},r} = \mathcal{B}_{j_k}^\epsilon$. We also let $\widetilde{X}^{k,\epsilon,\overline{\epsilon},r}$, $\widetilde{h}_k^{\epsilon,\overline{\epsilon},r}$, and $\widetilde{\psi}_k^{\epsilon,\overline{\epsilon},r}$ be respectively given by $\widetilde{X}^{j_k,\epsilon}$, $\widetilde{h}_{j_k}^\epsilon$, and $\widetilde{\psi}_{j_k}^\epsilon$ with the horizontal translation for each chosen so that $\widetilde{X}^{k,\epsilon,\overline{\epsilon},r}$ first reaches r at $u = 0$. We also let $w_k^{\epsilon,r} = -\varsigma_{j_k}^{\epsilon,r}$. Then $\partial_k^{\epsilon,r}\mathcal{S} = \partial\mathcal{S} \setminus (-\infty, w_k^{\epsilon,r}]$ gives the of image of the part of the boundary of the corresponding bubble which lies in $\partial\mathbf{H}$.

Note that Lemma 7.15 implies that for every given bubble generated by the reverse Loewner flow and $\overline{\epsilon} > 0$ there exists $\epsilon_0 > 0$ and $r_0 \in \mathbf{R}$ such that for all $\epsilon \in (0, \epsilon_0)$ and $r \leq r_0$ we have that the bubble will be part of the sequence $(\widetilde{h}_k^{\epsilon,\overline{\epsilon},r})$ (of course, the index j associated with any fixed bubble is changing as $\epsilon \to 0$).

We are now going to identify the law of the sequence $(\widetilde{X}^{k,\epsilon,\overline{\epsilon},r})$.

Proposition 7.16. *For each $\epsilon \geq 0$, $\overline{\epsilon} > 0$, and $r \in \mathbf{R}$ there exists a collection of i.i.d. standard Brownian motions $(B^{k,\epsilon,\overline{\epsilon},r})$ with $B_0^{k,\epsilon,\overline{\epsilon},r} = r$ such that*

$$\widetilde{X}_u^{k,\epsilon,\overline{\epsilon},r} = B_{2u}^{k,\epsilon,\overline{\epsilon},r} + au \quad \text{where} \quad a = \gamma - Q = \frac{\gamma}{2} - \frac{2}{\gamma}.$$

Proof. The proof is analogous to that of Proposition 7.7. □

Throughout the rest of this subsection, we let $\delta = 4 - \frac{8}{\gamma^2} = 4 - \frac{\kappa'}{2}$ (as in the statement of Theorem 7.13). For each $C > 1$ and $r \in \mathbf{R}$, we let E^r be the set of distributions on $\mathcal{S}$ whose projection onto $\mathcal{H}_1(\mathcal{S})$ has supremum which is at least r. Note that $\mathcal{M}_\delta^{4\gamma^{-1}}(E^r) \in (0, \infty)$ (recall Remark 3.7).

Lemma 7.17. *For each $k \in \mathbf{N}$, the total variation distance between the conditional law of $\widetilde{h}_k^{\epsilon,\bar{\epsilon},r}$ given $\widetilde{\psi}_k^{\epsilon,\bar{\epsilon},r}$ and $\mathcal{M}_\delta^{4\gamma^{-1}}$ conditional on E^r (where we take the horizontal translation for samples from the latter law so that the projection onto $\mathcal{H}_1(\mathcal{S})$ first hits r at $u = 0$) and restricted to $\mathcal{S}_+$ is at most $\bar{\epsilon}$.*

Proof. By Proposition 7.16, we know that the conditional law given $\widetilde{\psi}_k^{\epsilon,\bar{\epsilon},r}$ of the projection of $\widetilde{h}_k^{\epsilon,\bar{\epsilon},r}$ onto $\mathcal{H}_1(\mathcal{S})$ is the same as the corresponding projection for a sample chosen from $\mathcal{M}_\delta^{4\gamma^{-1}}$ given E^r (with the horizontal translation chosen as in the statement). Therefore it is just a matter of showing that the conditional law given $\widetilde{\psi}_k^{\epsilon,\bar{\epsilon},r}$ of the projection of $\widetilde{h}_k^{\epsilon,\bar{\epsilon},r}$ onto $\mathcal{H}_2(\mathcal{S})$ and restricted to $\mathcal{S}_+$ has total variation distance at most $\bar{\epsilon}$ from the law of the corresponding projection of sample chosen from $\mathcal{M}_\delta^{4\gamma^{-1}}$ conditional E^r. This, in turn, follows from the definition of $\widetilde{h}_k^{\epsilon,\bar{\epsilon},r}$ since the latter is given by the law of the projection of a free boundary GFF on $\mathcal{S}$ onto $\mathcal{H}_2(\mathcal{S})$ and then restricted to $\mathcal{S}_+$. □

For each $C > 0$, we let E_C^r be the set of elements in E^r whose associated γ-LQG boundary measure assigns mass at least C to $\partial\mathcal{S} \cap \partial\mathcal{S}_+$, mass at most $C^{-1}e^r$ to $\partial\mathcal{S} \setminus \partial\mathcal{S}_+$, and whose associated γ-LQG area measure assigns mass at least C to $\mathcal{S}_+$. In what follows, when we refer to the γ-LQG boundary length of $\partial\mathcal{S}_+$ (either in words or using the notation $\nu_h(\partial\mathcal{S}_+)$) we mean the γ-LQG boundary length of $\partial\mathcal{S} \cap \partial\mathcal{S}_+$. In particular, we do not want to count the length of $[0, i\pi]$. Let $\mu_k^{\epsilon,\bar{\epsilon},r}$ denote the conditional law of $\widetilde{h}_k^{\epsilon,\bar{\epsilon},r}$ given $\widetilde{\psi}_k^{\epsilon,\bar{\epsilon},r}$.

Lemma 7.18. *The total variation distance between $(\nu_h(\partial\mathcal{S}_+))^{-1} d\mathcal{M}_\delta^{4\gamma^{-1}}(h)$ conditional on E_C^r (with the horizontal translation chosen as in Lemma 7.17 and restricted to $\mathcal{S}_+$) and $(\nu_h(\partial\mathcal{S}_+))^{-1} d\mu_k^{\epsilon,\bar{\epsilon},r}(h)$ conditional on E_C^r and given $\widetilde{\psi}_k^{\epsilon,\bar{\epsilon},r}$ (and restricted to $\mathcal{S}_+$) is $O(\bar{\epsilon})$ where the implicit constants depend on r and C but not $\bar{\epsilon}$ or ϵ.*

Proof. We begin with three observations. First, suppose that μ_1, μ_2 are measures on some space $\mathcal{X}$ with μ_2 absolutely continuous with respect to μ_1. Suppose that f is a positive function on $\mathcal{X}$ and, for $i = 1, 2$, let ν_i be the measure whose Radon-Nikodym derivative with respect to μ_i is f. Using that $d\nu_2/d\nu_1 = d\mu_2/d\mu_1$, we have that

$$\begin{aligned} \|\nu_1 - \nu_2\|_{TV} &= \int \left| 1 - \frac{d\nu_2}{d\nu_1} \right| d\nu_1 \leq \left(\sup_{x \in \mathcal{X}} f(x) \right) \int \left| 1 - \frac{d\mu_2}{d\mu_1} \right| d\mu_1 \\ &= \left(\sup_{x \in \mathcal{X}} f(x) \right) \|\mu_1 - \mu_2\|_{TV}. \end{aligned}$$

For $i = 1, 2$, let $N_i = \nu_i(\mathcal{X})$ be the total amount of ν_i mass, assume that $N_i \in (0, \infty)$, and let $\overline{\nu}_i = \nu_i / N_i$. Second, we have that:

$$\|\overline{\nu}_1 - \overline{\nu}_2\|_{TV} \leq \frac{1}{N_2} |N_1 - N_2| + \frac{1}{N_2} \|\nu_1 - \nu_2\|_{TV}.$$

Third, we have that

$$|N_1 - N_2| = \left| \int f(x) d\mu_1(x) - \int f(x) d\mu_2(x) \right| \leq \left(\sup_{x \in \mathcal{X}} f(x) \right) \|\mu_1 - \mu_2\|_{TV}.$$

Combining all three observations, we have

$$\|\overline{\nu}_1 - \overline{\nu}_2\|_{TV} \leq \frac{2}{N_2} \left(\sup_{x \in \mathcal{X}} f(x) \right) \|\mu_1 - \mu_2\|_{TV}.$$

Combining this with Lemma 7.17 implies the result because the probability that each assigns to E_C^r is uniformly bounded from below as $\overline{\epsilon} \to 0$ (in this context, $\sup_{x \in \mathcal{X}} f(x) \leq C^{-1}$). □

Lemma 7.19. *The total variation distance between $(\nu_h(\partial \mathcal{S}))^{-1} d\mathcal{M}_\delta^{4\gamma^{-1}}(h)$ conditional on E_C^r (with the horizontal translation chosen as in Lemma 7.18 and restricted to $\mathcal{S}_+$) and $(\nu_h(\partial_k^{\epsilon,r} \mathcal{S}))^{-1} d\mu_k^{\epsilon,\overline{\epsilon},r}(h)$ conditional on E_C^r and given $\widetilde{\psi}_k^{\epsilon,\overline{\epsilon},r}$ (and restricted to $\mathcal{S}_+$) is $O(\overline{\epsilon}) + O(C^{-2} e^r)$ where the implicit constants in the first summand depend on r and C but not $\overline{\epsilon}$ or ϵ and the implicit constants in the second summand are uniform.*

Proof. Lemma 7.18 gives us that the total variation distance between $(\nu_h(\partial \mathcal{S}_+))^{-1} d\mathcal{M}_\delta^{4\gamma^{-1}}(h)$ conditional on E_C^r and $(\nu_h(\partial \mathcal{S}_+))^{-1} d\mu_k^{\epsilon,\overline{\epsilon},r}(h)$ conditional on E_c^r and given $\widetilde{\psi}_k^{\epsilon,\overline{\epsilon},r}$ is $O(\overline{\epsilon})$. Thus to prove the result we just have to bound the total variation distance between

- $(\nu_h(\partial \mathcal{S}))^{-1} d\mathcal{M}_\delta^{4\gamma^{-1}}(h)$ and $(\nu_h(\partial \mathcal{S}_+))^{-1} d\mathcal{M}_\delta^{4\gamma^{-1}}(h)$ conditional on E_C^r and
- $(\nu_h(\partial_\epsilon^{k,r} \mathcal{S}))^{-1} d\mu_k^{\epsilon,\overline{\epsilon},r}(h)$ and $(\nu_h(\partial \mathcal{S}_+))^{-1} d\mu_k^{\epsilon,\overline{\epsilon},r}(h)$ conditional on E_C^r and given $\widetilde{\psi}_k^{\epsilon,\overline{\epsilon},r}$.

We have for $h \in E_C^r$ that

$$1 \leq \frac{\nu_h(\partial \mathcal{S})}{\nu_h(\partial \mathcal{S}_+)} = 1 + \frac{\nu_h(\partial \mathcal{S} \setminus \partial \mathcal{S}_+)}{\nu_h(\partial \mathcal{S}_+)} = 1 + O(C^{-2} e^r).$$

Therefore it is easy to see in the first case that the Radon-Nikodym derivative between the two measures is equal to $1 + O(C^{-2} e^r)$ with uniform constants. It is similarly easy to see that this holds in the second case, which proves the result. □

Proof of Theorem 7.13. Fix $r \in \mathbf{R}$, $C > 0$, and let $(H_k^{r,C})$ be an i.i.d. sequence chosen from $(\nu_h(\partial\mathcal{S}))^{-1} d\mathcal{M}_\delta^{4\gamma^{-1}}(h)$ conditional on E_C^r with the horizontal translation chosen so that the projection of $H_k^{r,C}$ onto $\mathcal{H}_1(\mathcal{S})$ first hits r at $u = 0$. Fix $\bar{\epsilon} > 0$. We also let $(\widetilde{h}_k^{\epsilon,\bar{\epsilon},r})$ be a sequence chosen from $\prod_{k=1}^\infty (\nu_{h_k}(\partial_k^{\epsilon,r}\mathcal{S}))^{-1} d\mu_k^{\epsilon,\bar{\epsilon},r}(h_k)$. Note that the $(\widetilde{h}_k^{\epsilon,\bar{\epsilon},r})$ have the same law as the subsequence of bubbles which are zipped in (viewed as quantum surfaces) by the reverse Loewner flow such that a certain event occurs. Let $(\acute{h}_k^{\epsilon,\bar{\epsilon},r,C})$ be the subsequence of $(\widetilde{h}_k^{\epsilon,\bar{\epsilon},r})$ for which E_C^r occurs. Fix $n \in \mathbf{N}$. Lemma 7.19 implies that the total variation distance between the law of the first n of the $H_k^{r,C}$ and the law of the first n of the $\acute{h}_k^{\epsilon,\bar{\epsilon},r,C}$ (both restricted to $\mathcal{S}_+$) is $O(\bar{\epsilon}) \cdot n + O(C^{-2}e^r) \cdot n$ where the $O(\bar{\epsilon})$ term tends to 0 as $\bar{\epsilon} \to 0$ with r and C fixed and the constants in the $O(C^{-2}e^r)$ term are uniform.

It is easy to see that the quantum surfaces $(\mathcal{S}, \acute{h}_k^{\epsilon,\bar{\epsilon},r,C})$ converge to a limiting family of quantum surfaces $(\mathcal{S}, \acute{h}_k^C)$ when we take a limit first as $\epsilon \to 0$, then $r \to -\infty$, and then as $\bar{\epsilon} \to 0$. (One can take the horizontal translation so that the mass assigned to $\mathcal{S}_+$ is exactly equal to $C/2$.) Indeed, this follows from the same argument used to prove Lemma 7.6 (for otherwise we would get a contradiction to the statement that the amount of γ-LQG mass in each bounded neighborhood of zero is almost surely finite — recall that the γ-LQG mass of each bubble is at least C). Moreover, we have that the $(\acute{h}_k^C)$ are i.i.d. sampled from $(\nu_h(\partial\mathcal{S}))^{-1} d\mathcal{M}_\delta^{4\gamma^{-1}}(h)$ conditioned on having both γ-LQG boundary length and γ-LQG area at least C. Sending $C \to 0$ proves the result. □

Remark 7.20. In the setting of Theorem 7.13 (analogous to Remark 7.10), it is possible to encode the ordered sequence of bubbles $\mathbf{H} \setminus \eta'$ using a Bessel excursion measure of a different dimension. Indeed, by replacing $\frac{\gamma}{4}$ with $\frac{\widetilde{\gamma}}{4}$ when taking the exponential of the $\widetilde{X}^{j,r}$ gives a Bessel dimension of

$$\delta = 2 + \frac{2\gamma}{\widetilde{\gamma}} - \frac{8}{\gamma\widetilde{\gamma}}.$$

Then a p.p.p.with intensity measure $du \otimes \mathcal{M}_\delta^{4\widetilde{\gamma}^{-1}}$ encodes the bubbles of $\mathbf{H} \setminus \eta'$ weighted by their γ-LQG boundary length. The claim then follows by unweighting by the γ-LQG boundary length measure (as in the statement of Theorem 7.13).

We are now going to give an alternative formulation of the Poisson law described in Theorem 7.13 in terms of the unit area and unit boundary length quantum disks of Definition 4.21.

Proposition 7.21. *There exists constants $c_1, c_2 > 0$ such that the law on quantum surfaces described in the statement of Theorem 7.13 admits the following equivalent method of sampling. Sample a p.p.p. Λ on $\mathbf{R}_+ \times \mathbf{R}_+$ with intensity measure $c_2 du \otimes t^{-\kappa'/4-1} dt$ where du and dt denote Lebesgue measure on $\mathbf{R}_+$. Then sample an i.i.d.*

collection of unit boundary length quantum disks $(D_{u,t} : (u,t) \in \Lambda)$ *indexed by the elements of* Λ. *Finally, take the process* $((u, \widetilde{D}_{u,t}) : (u,t) \in \Lambda)$ *where* $\widetilde{D}_{u,t}$ *for* $(u,t) \in \Lambda$ *is given by taking* $D_{u,t}$ *and then scaling so that its boundary length is equal to* t.

Proof. Let $\delta = 4 - \frac{8}{\gamma^2} = 4 - \frac{\kappa'}{2} \in (0,2)$ as in the statement of Theorem 7.13. For each $t > 0$, let $\mathcal{V}^t_{\delta,1}$ denote the law on functions on $\mathcal{S}$ which is obtained by sampling a BES^δ excursion e from 0 given that its supremum is equal to t (a sample can be produced from this law by joining back to back two $\mathrm{BES}^{4-\delta}$ processes starting from 0 and stopped upon hitting t as explained in Remark 3.7), then taking $4\gamma^{-1}\log(e)$, and then finally reparameterizing so that it has constant quadratic variation $2ds$. We can fix the horizontal translation so that the supremum is reached at $s = 0$. We also let $\mathcal{V}_2$ be the law of the projection of a free boundary GFF on $\mathcal{S}$ onto $\mathcal{H}_2(\mathcal{S})$. Note that the infinite measure $(\nu_h(\partial\mathcal{S}))^{-1} d\mathcal{M}_\delta^{4\gamma^{-1}}(h)$ used to describe the Poisson law in the statement of Theorem 7.13 is equivalent to:

$$\frac{1}{\nu_h(\partial\mathcal{S})} d\mathcal{V}^t_{\delta,1}(h_1) d\mathcal{V}_2(h_2) d\nu^*_\delta(t) = \frac{t^2}{\nu_h(\partial\mathcal{S})} d\mathcal{V}^t_{\delta,1}(h_1) d\mathcal{V}_2(h_2) d\nu^*_{\delta-2}(t)$$

where $h = h_1 + h_2$ and ν^*_δ is as in Remark 3.7. Let

$$d\mathcal{V}^t(h) = \frac{t^2}{\nu_h(\partial\mathcal{S})} d\mathcal{V}^t_{\delta,1}(h_1) d\mathcal{V}_2(h_2).$$

Observe that a sample from $\mathcal{V}^t$ can be produced by picking h from $\mathcal{V}^1$ and then adding $4\gamma^{-1}\log(t)$ to h.

We can describe $\mathcal{V}^1$ explicitly as follows. We let $\widetilde{\mathcal{V}}^1$ be the law on distributions on $\mathcal{S}$ which can be sampled from by:

1. Taking its projection X onto $\mathcal{H}_1(\mathcal{S})$ to be given by $X_u = B_{2u} + (\gamma - Q)u$ for $u \geq 0$ where B is a standard Brownian motion and to be given by $X_u = \widehat{B}_{-2u} - (\gamma - Q)u$ for $u < 0$ where $\widehat{B}$ is a standard Brownian motion with $B_0 = \widehat{B}_0 = 0$ conditioned so that $X_u \leq 0$ for all u.
2. Independently sampling its projection onto $\mathcal{H}_2(\mathcal{S})$ using the corresponding projection of a free boundary GFF on $\mathcal{S}$.

Then $d\mathcal{V}^1(h) = (\nu_h(\partial\mathcal{S}))^{-1} d\widetilde{\mathcal{V}}^1(h)$.

It thus follows from the discussion so far that if we let $\widetilde{\Lambda}$ be a p.p.p. with intensity measure $du \otimes d\mathcal{V}^1(h) \otimes \nu^*_{\delta-2}$ then $\Lambda = \{(u, h + 4\gamma^{-1}\log(t)) : (u,h,t) \in \widetilde{\Lambda}\}$ is a p.p.p. with the same intensity measure as in Theorem 7.13.

We want to argue now that $\nu_h(\partial\mathcal{S})$ with h sampled from $\mathcal{V}^1$ has a finite $\frac{\kappa'}{4}$-moment. Note that this moment is equal to $\int(\nu_h(\partial\mathcal{S}))^{\kappa'/4-1}d\widetilde{\mathcal{V}}^1(h)$. Since $\kappa'/4-1\in(0,1)$ as $\kappa'\in(4,8)$, it suffices to show that $\int\nu_h(\partial\mathcal{S})d\widetilde{\mathcal{V}}^1(h)<\infty$. This, in turn, follows from Lemma 4.18.

It thus follows from Lemma 4.17 (as in the proof of Proposition 4.16), that there exists a constant $c_2>0$ such that $\{(u,h+4\gamma^{-1}\log(t),t^2\nu_h(\partial\mathcal{S})):(u,h,t)\in\widetilde{\Lambda}\}$ is a p.p.p. with intensity measure given by $c_2du\otimes\left(t^{-\kappa'/4-1}d\mathcal{U}^tdt\right)$ where $\mathcal{U}^t$ is the law of the unit boundary length quantum disk scaled to have boundary length equal to t. The result thus follows because the γ-LQG boundary length of $\partial\mathcal{S}$ associated with the field $h+4\gamma^{-1}\log(t)$ is equal to $t^2\nu_h(\partial\mathcal{S})$. □

7.4 Zipping according to quantum natural time

Suppose that (h,η) is as in the statement of Theorem 7.1, let (W,V) be the driving pair for η, let (f_t) be the centered (forward) Loewner flow associated with η, let L_t be the local time at 0 of the Bessel process $\kappa^{-1/2}(V-W)$, and let T_u be the right continuous inverse of L_t. In this setting, in Theorem 7.1 we showed that the beaded surface which consists of the components of $\mathbf{H}\setminus\eta$ which are to the right of η can be described in terms of a certain Bessel process Y (i.e., as in Definition 4.13). Let ℓ_t denote the local time of Y at 0 and let t_u denote the right-continuous inverse of ℓ_t.

We have two notions of time for η: capacity time and quantum natural time. Throughout this section, we will need to go back and forth between these two notions. To do so, we let:

- s_u be the first time t that the capacity of the bubbles cut off by η encoded by the excursions of $Y|_{[0,t]}$ from 0 is equal to T_u. That is, s_u serves to convert from local time as measured with respect to L_t to time as measured by Y.
- $\mathfrak{q}_u$ be the quantum natural time associated with η as in Definition 7.2. That is, $\mathfrak{q}_u$ gives the capacity of the bubbles cut off by η which are encoded by $Y|_{[0,t_u]}$.

Thus far, we have established two different types of invariance for the present setup:

(i) Theorem 6.1 implies that the law of $(h\circ f_{T_u}^{-1}+Q\log|(f_{T_u}^{-1})'|,f_{T_u}(\eta))$ is the same as the law of (h,η). That is, the law of (h,η) is invariant under the operation of cutting along η until time T_u and then conformally mapping back to $\mathbf{H}$. (Lemma 7.5 is the reverse version of this statement.)

(ii) Theorem 7.1 implies that the law of the ordered sequence of bubbles encoded by Y is invariant under the operation of cutting along η until time $\mathfrak{q}_u$ and then

conformally mapping back to $\mathbf{H}$. That is, the law of the beaded surface which consists of the components of $\mathbf{H} \setminus \eta$ which are to the right of $\eta|_{[\mathfrak{q}_u,\infty)}$ has the same law as the beaded surface which consists of the components which are to the right of η. This follows since $Y_{\cdot+t_u} \overset{d}{=} Y$.

Since the stopping time $\mathfrak{q}_u$ is field-dependent, Theorem 6.1 does not apply to give that the law of (h, η) is invariant under the operation described in (ii). The purpose of this section is to show that we can make the law of (h, η) invariant under this operation by modifying the multiple of the log singularity for h at 0. The result will be important in Section 8 when we describe the weldings of quantum wedges.

The following theorem and Theorem 7.27 stated below are the main results of this section.

Theorem 7.22. *Fix $\kappa \in (0,4)$, $\rho \in (-2, \frac{\kappa}{2} - 2)$, and suppose that*

$$h = \widetilde{h} + \frac{\rho + 2 - \gamma^2}{\gamma} \log|\cdot|$$

where $\widetilde{h}$ is a free boundary GFF on $\mathbf{H}$. Let η be an $\mathrm{SLE}_\kappa(\rho)$ process in $\mathbf{H}$ from 0 to ∞ with a single boundary force point of weight ρ located at 0^+ and assume that η is independent of h. Then the following hold:

(i) The law of the beaded surface consisting of the components of $\mathbf{H} \setminus \eta$ which are to the right of η is that of a quantum wedge of weight $\rho + 2$ (as in Theorem 7.1).

(ii) Let $\mathfrak{q}_u$ and (f_t) be as described above. For each $u > 0$, we have that

$$(h, \eta) \overset{d}{=} \left(h \circ f_{\mathfrak{q}_u}^{-1} + Q \log|(f_{\mathfrak{q}_u}^{-1})'|, f_{\mathfrak{q}_u}(\eta)\right) \tag{7.2}$$

where we view h as a distribution modulo a global additive constant.

The same also holds if

- *h is replaced with a quantum wedge $(\mathbf{H}, h)$ of weight $\rho + 4$.*
- *We take η to be a radial $\mathrm{SLE}_\kappa(\rho)$ process in $\mathbf{D}$ from 1 to 0 with a single boundary force point of weight ρ located at 1^+ and*

$$h = \widetilde{h} + \frac{\rho + 2 - \gamma^2}{\gamma} \log|\cdot - 1| - \frac{\gamma^2 + 2 - \rho}{2\gamma} \log|\cdot|$$

where $\widetilde{h}$ is a free boundary GFF on $\mathbf{D}$ independent of η.

The proof of Theorem 7.22 will follow the strategy used in [She10] to deduce [She10, Theorem 1.8] from [She10, Theorem 1.2].

Fix $\delta \in (0,2)$ and recall the description of the Itô excursion measure $\nu_\delta^{\mathrm{BES}}$ for the excursions made by a BES^δ process from 0 given in Remark 3.7. As in Section 3, for each $\epsilon > 0$, we let $\mathcal{E}(\epsilon)$ be the set of excursions with length at least ϵ. Then (3.10) leads to the value of $\nu_\delta^{\mathrm{BES}}(\mathcal{E}(\epsilon))$. We record this in the following lemma.

Lemma 7.23. *Fix $\delta \in (0,2)$ and let $\nu_\delta^{\mathrm{BES}}$ be the Itô excursion measure associated with a BES^δ process. There exists a constant $C_\delta > 0$ depending only on δ such that $\nu_\delta^{\mathrm{BES}}(\mathcal{E}(\epsilon)) = C_\delta \epsilon^{\delta/2-1}$.*

Using Lemma 7.23, we can now describe how ℓ changes when we perturb the field by adding a smooth function.

Lemma 7.24. *Fix a smooth function ϕ with $\|\phi\|_\nabla < \infty$. Assume that we have the same setup as in Theorem 7.1 and recall that ℓ is the local time at 0 of Y. We let Y^ϕ be the corresponding process with h replaced by $h + \phi$ (which we assume to be parameterized according to its quadratic variation) and let ℓ^ϕ be the local time at 0 of Y^ϕ. For each $u > 0$, we let s_u (resp. s_u^ϕ) be as described before the statement of Theorem 7.22 with respect to Y (resp. Y^ϕ). Let m (resp. m^ϕ) be the measure on $\mathbf{R}_+$ induced by the non-decreasing function ℓ_{s_u} (resp. $\ell^\phi_{s_u^\phi}$). For each $u \geq 0$, we have that*

$$m^\phi([0,u]) = \int_0^u \exp\left(\frac{\gamma(2-d)}{2}\phi(\eta(T_v))\right) dm(v) \tag{7.3}$$

where d is the Bessel dimension of Y as given in (7.1).

Before we give the proof of Lemma 7.24, we first make the following remark.

Remark 7.25. (i) Since the law of $h + \phi$ is mutually absolutely continuous with respect to the law of h, it follows that the law of Y^ϕ is mutually absolutely continuous with respect to the law of Y. In particular, the local time ℓ^ϕ exists (and can be defined, for example, as in [Kal02, Corollary 19.6]).

(ii) It is natural in (7.3) to see $\frac{1}{2}\gamma(2-d)$ rather than $\gamma(2-d)$ in the exponential because $u \mapsto \ell_{s_u}$ induces a *boundary* (rather than bulk) measure supported on $\eta \cap \partial\mathbf{H}$.

Proof of Lemma 7.24. Let $\overline{\nu}$ (resp. $\overline{\nu}^\phi$) denote the empirical measure of the excursions made by Y (resp. Y^ϕ) from 0 in the time interval $[0, s_u]$ (resp. $[0, s_u^\phi]$). If ϕ is a constant function, then Y^ϕ is given by transforming Y by scaling spatially by $\exp(\frac{\gamma}{2}\phi)$ and then speeding up time by the factor $\exp(\gamma\phi)$ (recall that Y^ϕ is parameterized by quadratic variation so that $d\langle Y^\phi\rangle_t = dt$). This means that an excursion of length r

made by Y will correspond to an excursion of length $e^{-\gamma\phi}r$ made by Y^ϕ. Fix $\epsilon > 0$. We then have that

$$\overline{\nu}^\phi(\mathcal{E}(\epsilon)) = \overline{\nu}(\mathcal{E}(e^{-\gamma\phi}\epsilon)). \tag{7.4}$$

We also let ν_d^{BES} denote the Itô excursion measure associated with a BES^d. Using Lemma 7.23 in the final equality, we then have that

$$\begin{aligned}\frac{\overline{\nu}^\phi(\mathcal{E}(\epsilon))}{\nu_d^{\mathrm{BES}}(\mathcal{E}(\epsilon))} &= \frac{\overline{\nu}(\mathcal{E}(e^{-\gamma\phi}\epsilon))}{\nu_d^{\mathrm{BES}}(\mathcal{E}(\epsilon))} = \frac{\nu_d^{\mathrm{BES}}(\mathcal{E}(e^{-\gamma\phi}\epsilon))}{\nu_d^{\mathrm{BES}}(\mathcal{E}(\epsilon))} \times \frac{\overline{\nu}(\mathcal{E}(e^{-\gamma\phi}\epsilon))}{\nu_d^{\mathrm{BES}}(\mathcal{E}(e^{-\gamma\phi}\epsilon))} \\ &= \exp\left(\frac{\gamma(2-d)}{2}\phi\right)\frac{\overline{\nu}(\mathcal{E}(e^{-\gamma\phi}\epsilon))}{\nu_d^{\mathrm{BES}}(\mathcal{E}(e^{-\gamma\phi}\epsilon))}.\end{aligned}$$

By [Kal02, Proposition 19.12], as $\epsilon \to 0$, the left side converges to $\ell^\phi_{s_u^\phi} = m^\phi([0,u])$ and the right side converges to $\exp(\frac{\gamma(2-d)}{2}\phi)\ell_{s_u} = \exp(\frac{\gamma(2-d)}{2}\phi)m([0,u])$. This proves (7.3) if ϕ is a constant function.

We are now going to generalize to the case that ϕ is a smooth function. For each $u < v$, we let $\overline{\nu}_{u,v}$ (resp. $\overline{\nu}^\phi_{u,v}$) be the empirical measure for the excursions from 0 made by Y (resp. Y^ϕ) in the time interval $(s_u, s_v]$ (resp. $(s_u^\phi, s_v^\phi]$). We let $b_{u,v}$ (resp. $B_{u,v}$) be the infimum (resp. supremum) of the values that ϕ takes on in the interval $[\eta(T_u), \eta(T_v)]$. Arguing as in (7.4), we have that

$$\overline{\nu}_{u,v}(\mathcal{E}(e^{-\gamma b_{u,v}}\epsilon)) \le \overline{\nu}^\phi_{u,v}(\mathcal{E}(\epsilon)) \le \overline{\nu}_{u,v}(\mathcal{E}(e^{-\gamma B_{u,v}}\epsilon)). \tag{7.5}$$

Pick a partition $0 \le u_1 < \cdots < u_k \le u$. Applying (7.5) in the inequality, we have that

$$\begin{aligned}\frac{\overline{\nu}^\phi(\mathcal{E}(\epsilon))}{\nu_d^{\mathrm{BES}}(\mathcal{E}(\epsilon))} &= \sum_{j=1}^k \frac{\overline{\nu}^\phi_{u_{j-1},u_j}(\mathcal{E}(\epsilon))}{\nu_d^{\mathrm{BES}}(\mathcal{E}(\epsilon))} \\ &\le \sum_{j=1}^k \frac{\nu_d^{\mathrm{BES}}(\mathcal{E}(e^{-\gamma B_{u_{j-1},u_j}}\epsilon))}{\nu_d^{\mathrm{BES}}(\mathcal{E}(\epsilon))} \times \frac{\overline{\nu}_{u_{j-1},u_j}(\mathcal{E}(e^{-\gamma B_{u_{j-1},u_j}}\epsilon))}{\nu_d^{\mathrm{BES}}(\mathcal{E}(e^{-\gamma B_{u_{j-1},u_j}}\epsilon))} \\ &= \sum_{j=1}^k \exp\left(\frac{\gamma(2-d)}{2}B_{u_{j-1},u_j}\right)\frac{\overline{\nu}_{u_{j-1},u_j}(\mathcal{E}(e^{-\gamma B_{u_{j-1},u_j}}\epsilon))}{\nu_d^{\mathrm{BES}}(\mathcal{E}(e^{-\gamma B_{u_{j-1},u_j}}\epsilon))}.\end{aligned} \tag{7.6}$$

Recall that the law of Y^ϕ is mutually absolutely continuous with respect to the law of Y. It thus follows from [Kal02, Proposition 19.12] that $\overline{\nu}^\phi(\mathcal{E}(\epsilon))/\nu(\mathcal{E}(\epsilon)) \to m^\phi([0,u])$ as $\epsilon \to 0$. The existence of the limit as $\epsilon \to 0$ of the expression in (7.6) also follows from [Kal02, Proposition 19.12]. Combining, we have that

$$m^\phi([0,u]) \le \sum_{j=1}^k \exp\left(\frac{\gamma(2-d)}{2}B_{u_{j-1},u_j}\right)\left(\ell_{s_{u_j}} - \ell_{s_{u_{j-1}}}\right).$$

Since T_u is right continuous and ϕ is smooth, we note that $u \mapsto \phi(\eta(T_u))$ is also right continuous. Note also that $\ell_{s_{u_j}} - \ell_{s_{u_{j-1}}} = m((u_{j-1}, u_j])$. Thus taking a limit as the mesh size of the partition tends to zero, we get that

$$m^\phi([0,u]) \leq \int_0^u \exp\left(\frac{\gamma(2-d)}{2}\phi(\eta(T_v))\right) dm(v).$$

This gives the upper bound in (7.3). The lower bound is proved in exactly the same manner (using $b_{u,v}$ in place of $B_{u,v}$), which gives (7.3). □

Lemma 7.26. *Assume that we have the same setup as in Theorem 7.1 and recall that*

$$h = \widetilde{h} - \frac{2+\rho}{\gamma}\log|\cdot| \tag{7.7}$$

where $\widetilde{h}$ is a free boundary GFF on $\mathbf{H}$. For each $0 \leq u < v$, we let $m_{u,v}$ be the restriction of m as in Lemma 7.24 to subsets of $[u,v]$. Consider the law on (w,h,η) triples given by $dm_{u,v}dhd\eta$ where dh denotes the law of h as in (7.7). (Note that $m_{u,v}$ depends on h and η while h and η are independent). Under $dm_{u,v}dhd\eta$, given both w and $\eta|_{[0,T_v]}$ we have that:

(i) The conditional law of h is equal to the law of

$$\widetilde{h} - \frac{2+\rho}{\gamma}\log|\cdot| - \gamma(2-d)\log|\cdot - \eta(T_w)|$$

where $\widetilde{h}$ is a free boundary GFF on $\mathbf{H}$ and d is the dimension of the Bessel process Y as given in (7.1).

(ii) The conditional law of $\eta|_{[T_v,\infty)}$ is that of an $\mathrm{SLE}_\kappa(\rho)$ process in the unbounded component of $\mathbf{H}\setminus\eta([0,T_v])$ from $\eta(T_v)$ to ∞ with a single boundary force point of weight ρ located at $(\eta(T_v))^+$.

(iii) $\eta|_{[T_v,\infty)}$ and h are conditionally independent.

(iv) The law of the beaded surface which consists of the components of $\mathbf{H}\setminus\eta$ which are to the right of $\eta|_{[T_v,\infty)}$ has the same law as described in Theorem 7.1 (i.e., a quantum wedge of weight $\rho+2$).

Proof. Let (ϕ_n) be an orthonormal basis for $H(\mathbf{H})$ consisting of smooth functions and write $\widetilde{h} = \sum_n \widetilde{\alpha}_n\phi_n$ where $(\widetilde{\alpha}_n)$ are i.i.d. $N(0,1)$ random variables. For each $N \in \mathbf{N}$, let $\widetilde{h}_N = \sum_{n=1}^N \widetilde{\alpha}_n\phi_n$, $h^N = h - \widetilde{h}_N$, $m^N_{u,v}$ be the restriction of m^ϕ to $[u,v]$ where $\phi = -\widetilde{h}_N$, and $\ell^N_t = \ell^\phi_t$. By Lemma 7.24, we have that

$$dm_{u,v}(w)dhd\eta = \exp\left(\frac{\gamma(2-d)}{2}\widetilde{h}_N(\eta(T_w))\right) dm^N_{u,v}(w)dhd\eta. \tag{7.8}$$

Since $\widetilde{h}_N$ is independent of (ℓ_t^N, h^N, η), we can rewrite (7.8) as

$$dm_{u,v}(w)dhd\eta = \exp\left(\frac{\gamma(2-d)}{2}\widetilde{h}_N(\eta(T_w))\right) d\widetilde{h}_N dm_{u,v}^N(w)dh^N d\eta.$$

Let $G(y,z) = -\log|y-z| - \log|y-\overline{z}|$ be the Neumann Green's function on $\mathbf{H}$. Since $\Delta G(\cdot, \eta(T_w))$ is given by -2π times the Dirac mass located at $\eta(T_w)$, by performing an integration by parts we can write

$$\widetilde{h}_N(\eta(T_w)) = \left(\widetilde{h}_N, G(\cdot, \eta(T_w))\right)_\nabla.$$

Consequently, under $dm_{u,v}dhd\eta$ the conditional law of $\widetilde{h}_N$ given w and $\eta|_{[0,T_v]}$ is equal to the law of

$$\widehat{h}_N - \gamma(2-d)g_N$$

where $\widehat{h}_N = \sum_{n=1}^N \widehat{\alpha}_n \phi_n$ for i.i.d. $N(0,1)$ random variables $\widehat{\alpha}_1, \ldots, \widehat{\alpha}_N$ and g_N is the orthogonal projection of $\log|\cdot - \eta(T_w)|$ onto the subspace of $H(\mathbf{H})$ spanned by $\phi_1, \ldots, \phi_N$. Taking a limit as $N \to \infty$ implies part (i).

It is also easy to from what we have done so far that part (ii) and part (iii) both hold.

It is left to justify part (iv). Under the (unweighted) law $dhd\eta$, it follows from Theorem 7.1 that the beaded surface which consists of those bubbles in $\mathbf{H} \setminus \eta$ which are to the right of $\eta|_{[T_v,\infty)}$ is independent of the σ-algebra $\mathcal{G}$ generated by $\eta|_{[0,T_v]}$ and the bubbles which are to the right of $\eta|_{[0,T_v]}$. (Recall Lemma 7.5.) Since $m_{u,v}$ is determined by $\mathcal{G}$, it thus follows that the bubbles which are to the right of $\eta|_{[T_v,\infty]}$ has the same law under both $dm_{u,v}dhd\eta$ and under $dhd\eta$. □

Proof of Theorem 7.22. For $0 \leq u < v$, we let $m_{u,v}$ be as in the statement of Lemma 7.26 and let $m_v = m_{0,v}$. Let (f_t) be the centered, forward Loewner flow associated with η. We first recall that by Lemma 7.5 we know that $dhd\eta$ is invariant under applying f_{T_u}. That is, if (h,η) are sampled from $dhd\eta$ then $(h \circ f_{T_u}^{-1} + Q\log|(f_{T_u}^{-1})'|, f_{T_u}(\eta)) \overset{d}{=} (h,\eta)$. For given $0 < u < v$, this implies that if (h,η) are sampled from $dm_{u,v}dhd\eta$ then the law of $(h \circ f_{T_u}^{-1} + Q\log|(f_{T_u}^{-1})'|, f_{T_u}(\eta))$ is given by $dm_{v-u}dhd\eta$. By applying this for a given value of $u > 0$ and then taking a limit as $v \downarrow u$, this implies that if we sample (h,η) from $dhd\eta$, then we can write

$$h \circ f_{T_u}^{-1} - \gamma(2-d)\log|f_{T_u}^{-1}(\cdot) - \eta(T_u)| + Q\log|(f_{T_u}^{-1})'| = \widetilde{h} + \frac{\rho + 2 - \gamma^2}{\gamma}\log|\cdot|$$

where $\widetilde{h}$ is a free boundary GFF on $\mathbf{H}$ independent of $f_{T_u}(\eta)$. (Note that $f_{T_u}(\eta) \overset{d}{=} \eta$.) Part (iv) of Lemma 7.26 also implies that the bubbles which are to the right of $f_{T_u}(\eta)$

are as described in the statement of Theorem 7.1 (i.e., a quantum wedge of weight $\rho + 2$). This proves part (i).

To see part (ii), we let $u, v > 0$ and consider the law $dm_v dh d\eta$. We will eventually take a limit as $v \to \infty$ but we will leave u fixed. Suppose that w has been picked from m_v, $t = s_w$, and let $t' = t_{\ell_t + u}$. That is, t' is the first time after t that the local time of Y at 0 has increased by u. Note that we can sample t as follows: we first pick U uniformly in $[0, m([0,v])]$ and then take $t = t_U$. We can similarly sample from t' as follows: we pick U' uniformly in $[0, m([0,v])]$ and then take $t' = t_{U'+u}$. Since $m([0,v]) \to \infty$ as $v \to \infty$ almost surely, it follows that the total variation distance between the law of U and the law of $U' + u$ almost surely tends to 0 as $v \to \infty$, which implies that the same is true for the laws of t and t'. Therefore it follows that, as $v \to \infty$, the total variation distance between the laws of $(h \circ f^{-1}_{\mathfrak{q}_{\ell_t}} + Q \log |(f^{-1}_{\mathfrak{q}_{\ell_t}})'|, f_{\mathfrak{q}_{\ell_t}}(\eta))$ and $(h \circ f^{-1}_{\mathfrak{q}_{\ell_{t'}}} + Q \log |(f^{-1}_{\mathfrak{q}_{\ell_{t'}}})'|, f_{\mathfrak{q}_{\ell_{t'}}}(\eta))$ tends 0. By the proof of part (i) given above, we have that the law of $(h \circ f^{-1}_{\mathfrak{q}_{\ell_t}} + Q \log |(f^{-1}_{\mathfrak{q}_{\ell_t}})'|, f_{\mathfrak{q}_{\ell_t}}(\eta))$ is equal to the law of the pair on the left side of (7.2). Note that the right side of (7.2) is obtained by shifting time in the left side by u units of quantum local time. Part (ii) follows because $(h \circ f^{-1}_{\mathfrak{q}_{\ell_{t'}}} + Q \log |(f^{-1}_{\mathfrak{q}_{\ell_{t'}}})'|, f_{\mathfrak{q}_{\ell_{t'}}}(\eta))$ is obtained from $(h \circ f^{-1}_{\mathfrak{q}_{\ell_t}} + Q \log |(f^{-1}_{\mathfrak{q}_{\ell_t}})'|, f_{\mathfrak{q}_{\ell_t}}(\eta))$ in the same manner.

The result in the case of a wedge follows by combining the above with part (ii) of Proposition 4.6. The proof in the radial setting is the same as above. □

We now give the analog of Theorem 7.22 for $\mathrm{SLE}_{\kappa'}$ processes. We will not provide a separate proof since it follows from the same argument used to prove Theorem 7.22 (using the representation of the Poissonian structure from Proposition 7.21).

Theorem 7.27. *Fix $\kappa' \in (4,8)$, let $\gamma = 4/\sqrt{\kappa'}$, and suppose that*

$$h = \widetilde{h} + \frac{\gamma^2 - 8}{2\gamma} \log |\cdot|$$

where $\widetilde{h}$ is a free boundary GFF on $\mathbf{H}$. Let η' be an $\mathrm{SLE}_{\kappa'}$ process in $\mathbf{H}$ from 0 to ∞ which is independent of η'. Then the following hold:

(i) The law of the beaded surface consisting of the components of $\mathbf{H} \setminus \eta'$ whose boundary is contained in η' can be sampled from as in Theorem 7.13 (with the κ' value matched).

(ii) Let (f_t) be the centered (forward) Loewner flow for η' and let $\mathfrak{q}_u$ be the quantum natural time associated with η' as in Definition 7.14. For each $u \geq 0$, we have that

$$(h, \eta') \stackrel{d}{=} (h \circ f^{-1}_{\mathfrak{q}_u} + Q \log |(f^{-1}_{\mathfrak{q}_u})'|, f_{\mathfrak{q}_u}(\eta')) \tag{7.9}$$

where we view h as a distribution modulo a global additive constant.

The same also holds if we

- *Replace h with a quantum wedge $(\mathbf{H}, h)$ of weight $\frac{3\gamma^2}{2} - 2$.*
- *Take η' to be a radial $\mathrm{SLE}_{\kappa'}$ process in $\mathbf{D}$ from 1 to 0 and*

$$h = \widetilde{h} + \frac{\gamma^2 - 8}{2\gamma} \log|\cdot - 1| - \frac{3\gamma^2 + 8}{4\gamma} \log|\cdot|$$

where $\widetilde{h}$ is a free boundary GFF on $\mathbf{D}$ independent of η'.

Remark 7.28. (i) It is also possible to apply the argument of Theorem 7.22 in the setting of Remark 7.10. In this case, the analogous statement holds with Y replaced by the Bessel process described in Remark 7.10. The resulting multiple of the log at the origin does not depend on the choice of $\widetilde{\gamma}$. The same holds in the setting of Remark 7.20 and Theorem 7.27.

(ii) In the setting of Theorem 7.27, the multiple of log singularity at the starting point of η' is given by $-\sqrt{8/3}$ in the case that $\kappa' = 6$. This is natural to expect in the context of [MS13b] because $\mathrm{QLE}(8/3, 0)$ has the interpretation of corresponding to first passage percolation on a $\sqrt{8/3}$-LQG surface. In particular, this implies that in the quantum natural time version of $\mathrm{QLE}(8/3, 0)$ (as opposed to the capacity time version constructed in [MS13b]) we can pick the points from which we draw independent segments of SLE_6 from the $\sqrt{8/3}$-LQG boundary measure.

8 Welding quantum wedges

The purpose of this section is to describe the conformal welding of wedges with general weights, thus generalizing the results of [She10]. The first step is Section 8.1, in which we will explain how to weld together a weight $W \geq \frac{\gamma^2}{2}$ wedge with a wedge of weight 2 and that the resulting object is a wedge of weight $W + 2$. This will follow the strategy of [She10], though we will provide most of the details of the proof. We will then show in Section 8.2 that conformally welding the left and right boundaries of a wedge of weight $W \geq \frac{\gamma^2}{2}$ yields a quantum cone of weight W with an independent non-self-intersecting whole-plane $\mathrm{SLE}_\kappa(\rho)$ process ($\kappa = \gamma^2$) with $\rho = W - 2$ drawn on top of it. Combining the results of Section 8.1 and Section 8.2, we will complete the proof of Theorem 1.9 by showing in Section 8.3 that the conformal welding of two wedges of weights $W_1, W_2 > 0$ yields a wedge of weight $W_1 + W_2$. We will then show in Section 8.4 that welding the left and right sides of a wedge of weight $W \in (0, \frac{\gamma^2}{2})$ yields a quantum cone of weight W with an independent self-intersecting whole-plane

$\mathrm{SLE}_\kappa(\rho)$ with $\rho = W - 2$ drawn on top of it. Though it will not be used in the later sections of this article, in Section 8.5 we show that the fan of GFF flow lines with continuously varying angles [MS12a, MS13a] describes the set of interfaces which arise when gluing together infinitesimally thin wedges.

8.1 Welding a thick wedge and a weight 2 wedge

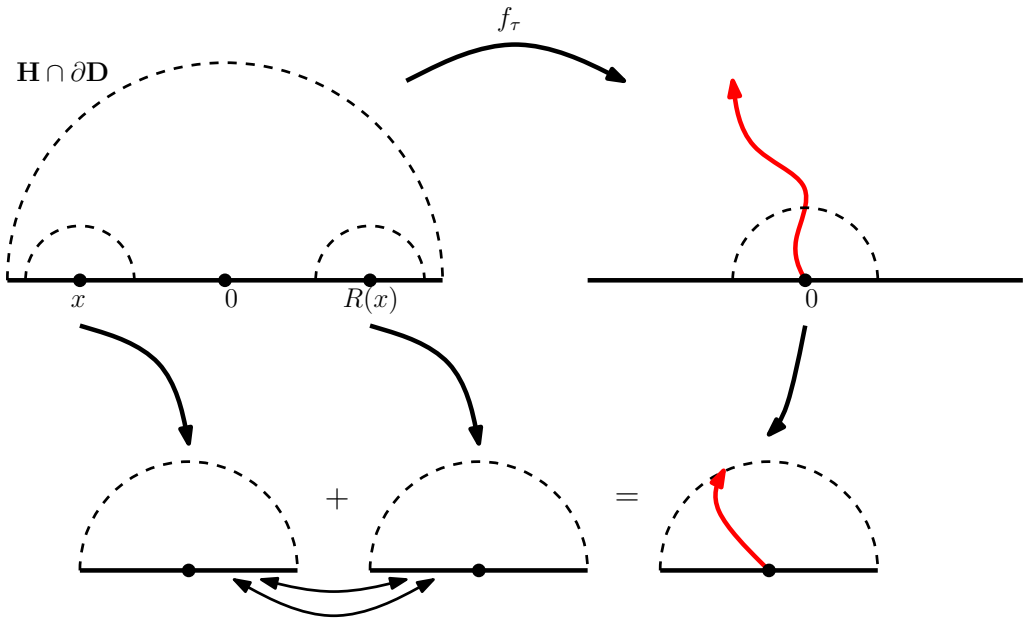

Figure 8.1: Illustration of the proof of Proposition 8.1. For some fixed $x \in (-1, 0)$, write $h = \widetilde{h} + \frac{2}{\gamma} \log|\cdot| - \alpha \log|x - \cdot|$, where $\widetilde{h}$ is a free boundary GFF on $\mathbf{H}$ normalized so that the mean of h on $\mathbf{H} \cap \partial\mathbf{D}$ is equal to 0. Suppose that (f_t) is the centered reverse Loewner flow associated with a reverse $\mathrm{SLE}_\kappa(\rho)$ process with a single boundary force point of weight $\rho = \alpha\gamma$ located at x. Let $\tau = \inf\{t \geq 0 : f_t(x) = 0\}$ so that f_τ is zips $[x, 0]$ up with $[0, R(x)]$. Consider the three random surfaces obtained by choosing a semi-disk of quantum mass ε centered at each of x and $R(x)$ (on the left side) and 0 (on the right side), and multiplying areas by $1/\varepsilon$ (zooming in) so that three balls each have unit quantum mass. In the $\varepsilon \to 0$ limit, part (ii) of Proposition 4.6 implies that the left two quantum surfaces respectively converge to an independent α-quantum wedge and γ-quantum wedge, and the right surface converges to the conformal welding of these two.

Suppose that $h = \widetilde{h} - \alpha \log|\cdot|$ where $\widetilde{h}$ is a free boundary GFF on $\mathbf{H}$. Recall from (1.4) that the formula for the weight W of the wedge $\mathcal{W}$ which arises by rescaling h near

0 as in part (ii) of Proposition 4.6 is given by

$$W = \gamma\left(\gamma + \frac{2}{\gamma} - \alpha\right).$$

The purpose of this section is to show that the conformal welding of a wedge with weight $W_1 \geq \frac{\gamma^2}{2}$ with a wedge of weight $W_2 = 2$ yields a wedge of weight $W_1 + W_2$. The main result is the following proposition.

Proposition 8.1. *Suppose that $\mathcal{W}$ is a wedge of weight $W \geq \frac{\gamma^2}{2} + 2$ represented by some $(D, h, (z_1, z_2))$ with $z_1, z_2 \in \partial D$ distinct. Let η be an $\mathrm{SLE}_\kappa(W-4; 0)$ process in D independent of $\mathcal{W}$ from z_1 to z_2 with a single boundary force point located at z_1^-. (Note that η almost surely does not hit ∂D except at its starting and terminal points since $W - 4 \geq \frac{\kappa}{2} - 2$.) Let D_1 and D_2 denote the left and right components of $D \setminus \eta$. Then the quantum surfaces $\mathcal{W}_1 = (D_1, h, (z_1, z_2))$ and $\mathcal{W}_2 = (D_2, h, (z_1, z_2))$ are independent and $\mathcal{W}_1$ (resp. $\mathcal{W}_2$) has the law of a quantum wedge with weight $W_1 = W - 2$ (resp. $W_2 = 2$).*

We are going to prove Proposition 8.1 in the case that $W > \frac{\gamma^2}{2} + 2$; the case that $W = \frac{\gamma^2}{2} + 2$ then follows by taking a limit as $W \downarrow \frac{\gamma^2}{2} + 2$. The proof of Proposition 8.1 will follow from Lemmas 8.3–8.5, stated and proved below, and the argument sketched in Figure 8.1. In particular, Lemma 8.3 gives the rightmost downward arrow in Figure 8.1 and Lemma 8.4 and Lemma 8.5 respectively give the leftmost and middle downward arrows in Figure 8.1. We begin with the following elementary lemma for the free boundary GFF.

Lemma 8.2. *Suppose that h is a free boundary GFF on $\mathbf{H}$ and $x \in \partial\mathbf{H}$. For each $\delta > 0$, let $\mathcal{F}_{x,\delta}$ be the σ-algebra generated by the restriction of h to $\mathbf{H} \cap B(x, \delta)$. Then $\cap_{\delta>0}\mathcal{F}_{x,\delta}$ is trivial. The same holds if we replace h with the sum of a free boundary GFF and a function $\mathfrak{h}$ which is harmonic in $\mathbf{H}$.*

Proof. For simplicity, we will give the proof in the case that $\mathfrak{h} = 0$.

Let $\phi \in C_0^\infty(\mathbf{H})$ with $\int \phi(z)dz = 0$. It suffices to show that the conditional law of (h, ϕ) given $\mathcal{F}_{x,\delta}$ converges as $\delta \to 0$ to the unconditioned law of (h, ϕ). Note that the latter is explicitly given by that of a Gaussian random variable with mean zero and variance $\iint \phi(y)G(y, z)\phi(z)dydz$ where G is the Neumann Green's function on $\mathbf{H}$. For each $\delta > 0$, we let $\mathfrak{h}_{x,\delta}$ be the harmonic extension of the boundary values of h from $\mathbf{H} \cap \partial B(x, \delta)$ to $\mathbf{H} \setminus B(x, \delta)$. We also let $G_{x,\delta}$ be the Green's function on $\mathbf{H} \setminus B(x, \delta)$ with Dirichlet (resp. Neumann) boundary conditions on $\mathbf{H} \cap \partial B(x, \delta)$ (resp. $\partial\mathbf{H} \setminus B(x, \delta)$). By the Markov property for the GFF, the conditional law of (h, ϕ) given $\mathcal{F}_{x,\delta}$ is given by that of a Gaussian random variable with mean $(\mathfrak{h}_{x,\delta}, \phi)$ and variance $\int \phi(y)G_{x,\delta}(y, z)\phi(z)dydz$. It is clear that

$$\iint \phi(y)G_{x,\delta}(y, z)\phi(z)dydz \to \iint \phi(y)G(y, z)\phi(z)dydz \quad \text{as} \quad \delta \to 0$$

since $G_{x,\delta} - G \to 0$ locally uniformly as $\delta \to 0$.

To complete the proof, it suffices to show that $(\mathfrak{h}_{x,\delta}, \phi) \to 0$ in probability as $\delta \to 0$. To see this, we note that $(\mathfrak{h}_{x,\delta}, \phi)$ is a Gaussian random variable with mean zero and variance given by $\iint \phi(y)\mathrm{cov}(\mathfrak{h}_{x,\delta}(y), \mathfrak{h}_{x,\delta}(z))\phi(z)dydz$ (see e.g., [MS13b, Section 4.2.4]). Letting $\mathcal{P}_{x,\delta}$ be the Poisson kernel on $\mathbf{H} \setminus B(x,\delta)$, we have that

$$\mathrm{cov}(\mathfrak{h}_{x,\delta}(y), \mathfrak{h}_{x,\delta}(z)) = \iint \mathcal{P}_{x,\delta}(y,u)\mathcal{P}_{x,\delta}(z,v)G(u,v)dudv$$

where the integral is over $(\mathbf{H} \cap \partial B(x,\delta))^2$. This quantity is easily seen to tend to 0 as $\delta \to 0$ since $\mathcal{P}_{x,\delta}(y,u) = O(1)$ uniformly over y in the support of ϕ and $u \in \mathbf{H} \cap \partial B(x,\delta)$ as $\delta \to 0$. □

Lemma 8.3. *Fix $\kappa \in (0,4)$, $\alpha < Q$, and let $\rho = \alpha\gamma$. Suppose that $\widetilde{h}$ is a free boundary GFF on $\mathbf{H}$, $x < 0$, and let $h = \widetilde{h} + \frac{2}{\gamma}\log|\cdot| - \alpha\log|\cdot - x|$. Let (f_t) be the centered reverse Loewner flow associated with a reverse $\mathrm{SLE}_\kappa(\rho)$ process with a single boundary force point of weight ρ located at x. For each $t \geq 0$, let*

$$h^t = h \circ f_t^{-1} + Q\log|(f_t^{-1})'(\cdot)|. \tag{8.1}$$

Let $\tau = \inf\{t \geq 0 : f_t(x) = 0\}$ and let $\eta_\tau = \mathbf{H} \setminus f_\tau(\mathbf{H})$. Then the pair (h^τ, η_τ) rescaled as in part (ii) *of Proposition 4.6 converges in law to $(\mathcal{W}, \eta)$ where $\mathcal{W}$ is a wedge of weight $\gamma^2 + 4 - \alpha\gamma$ and η is a forward $\mathrm{SLE}_\kappa(\widetilde{\rho})$ process with $\widetilde{\rho} = \kappa - \gamma\alpha$ with a single boundary force point located at 0^-. Moreover, $\mathcal{W}$ and η are independent.*

Proof. The assumption that $\alpha < Q$ implies that $\rho = \alpha\gamma < \frac{\kappa}{2} + 2$. This, in turn, implies that the dimension δ of the Bessel process $f_t(x)/\gamma$ (recall (3.18) and (3.19)) satisfies $\delta < 2$. This implies that $\mathbf{P}[\tau < \infty] = 1$ (recall Section 3.2).

By Proposition 3.9, we also know that η_τ is given by the initial segment of a forward $\mathrm{SLE}_\kappa(\widetilde{\rho})$ process with a single boundary force point located at 0^- of weight $\widetilde{\rho} = \kappa - \rho$ stopped at an almost surely positive time. Moreover, by Theorem 6.1, we know that f_τ and h^τ are independent hence η_τ and h^τ are also independent. Since h^τ can be written as the sum of a free boundary GFF on $\mathbf{H}$ plus $(\frac{2}{\gamma} - \alpha)\log|\cdot|$, it follows that the quantum surface described by h^τ rescaled as in part (ii) of Proposition 4.6 converges to the type of wedge indicated in the statement. Likewise, it is clear that η_τ converges to an independent $\mathrm{SLE}_\kappa(\widetilde{\rho})$ process drawn from 0 to ∞ upon applying the same scaling. Combining gives the result. □

Lemma 8.4. *Suppose that $\widetilde{h}$ is a free boundary GFF on $\mathbf{H}$, $x < 0$, and $\alpha < Q$. Let ν_h be the γ-LQG boundary length measure associated with $h = \widetilde{h} + \frac{2}{\gamma}\log|\cdot| - \alpha\log|x - \cdot|$. Fix $r > 0$. Conditional on both the values of h restricted to $\mathbf{H} \setminus B(x,r)$ and $\nu_h([x, x+r])$, the law of the field near x rescaled as in part* (ii) *of Proposition 4.6 converges to a wedge of weight $\gamma^2 + 2 - \alpha\gamma$.*

Proof. For each $\delta > 0$, we let $\mathcal{F}_{x,\delta}$ be the σ-algebra generated by the values of h restricted to $\mathbf{H} \cap B(x,\delta)$. By Lemma 8.2, $\cap_{\delta>0}\mathcal{F}_{x,\delta}$ is trivial. In particular, by the reverse martingale convergence theorem, the conditional law of the pair $(h|_{\mathbf{H}\setminus B(x,r)}, \nu_h([x,x+r]))$ given $\mathcal{F}_{x,\delta}$ converges to the unconditioned law as $\delta \to 0$. The result then follows by applying Bayes' rule to reverse the order of the conditioning (i.e., to consider the conditional law of the restriction of h to $\mathbf{H}\cap B(x,\delta)$ given the pair $(h|_{\mathbf{H}\setminus B(x,r)}, \nu_h([x,x+r]))$) and then combining with part (ii) of Proposition 4.6. □

Lemma 8.5. *Suppose that $\widetilde{h}$ is a free boundary GFF on $\mathbf{H}$, $x < 0$, and $\alpha < Q$. Let $\rho = \alpha\gamma$ and let (f_t) be the centered reverse Loewner flow associated with a reverse $\mathrm{SLE}_\kappa(\rho)$ process with a single boundary force point of weight ρ located at x. Assume that (f_t) and h are independent. Let $R(x) > 0$ be the unique point which is identified with x under (f_t). Then the joint law on quantum surfaces which arises by rescaling as in part* (ii) *of Proposition 4.6 near both x and $R(x)$ is that of independent wedges respectively of weight $\gamma^2 + 2 - \alpha\gamma$ and of weight 2.*

Before we prove Lemma 8.5, we first recall [She10, Proposition 5.5].

Proposition 8.6. *Fix $\gamma \in [0,2)$ and let D be a bounded subdomain of $\mathbf{H}$ for which $\partial D \cap \mathbf{R}$ is a segment of positive length. Let $\widetilde{h}$ be a GFF with zero boundary conditions on $\partial D \setminus \mathbf{R}$ and free boundary conditions on $\partial D \cap \mathbf{R}$. Let $[a,b]$ be any sub-interval of $\partial D \cap \mathbf{R}$ and let $\mathfrak{h}_0$ be a continuous function on D that extends continuously to the interval (a,b). Let dh be the law of $\mathfrak{h}_0 + \widetilde{h}$, and let $\nu_h([a,b])dh$ denote the measure whose Radon-Nikodym derivative with respect to dh is $\nu_h([a,b])$. Now suppose we:*

1. *Sample h from $\nu_h([a,b])dh$ (normalized to be a probability measure).*
2. *Sample x uniformly from ν_h restricted to $[a,b]$ (normalized to be a probability measure).*
3. *Let h^* be h translated by $-x$ units horizontally.*

Then as $C \to \infty$ the random surfaces $(\mathbf{H}, h^* + \frac{C}{\gamma})$ converge in law (with respect to the topology of convergence of doubly-marked quantum surfaces) to a γ-quantum wedge. Moreover, the same remains true even if, when we choose h and x, we condition on a particular pair of values $L_1 = \nu_h([a,x])$ and $L_2 = \nu_h([x,b])$.

We note that the first part of Proposition 8.6 is a consequence of part (ii) of Proposition 4.6.

Proof of Lemma 8.5. We first note that it follows from [She10, Theorems 1.2 and 1.3] and the absolute continuity properties of the GFF that $\nu_h([x,0]) = \nu_h([0,R(x)])$.

Fix $r > 0$ so that $B(x,r) \cap \partial\mathbf{H} \subseteq \mathbf{R}_-$. Let $L_1 = \nu_h([x, x+r])$, $L_2 = \nu_h([x+r, 0])$, and let $L = L_1 + L_2$. Fix $y > 0$ large. Proposition 8.6 implies that the following is true. Suppose that we pick $u \in [0, y]$ according to ν_h and condition on $\nu_h([0,u]) = L$. Then the conditional law of h translated by $-u$ given L_1, L_2, and the restriction of h to $\mathbf{H} \cap \partial B(x,r)$ rescaled as in part (ii) of Proposition 4.6 is described by that of a γ-quantum wedge (i.e., of weight 2). We also know from Lemma 8.4 that the conditional law of h translated by $-x$ given L_1 and h restricted to $\mathbf{H} \cap \partial B(x,r)$ rescaled as in part (ii) of Proposition 4.6 converges to that of a wedge of weight $\gamma^2 + 2 - \alpha\gamma$. The lemma thus follows because the restriction of h to $\mathbf{H} \cap B(x,r)$ is conditionally independent of the pair consisting of the restriction of h to $\mathbf{H} \setminus B(x,r)$ and L given the restriction of h to $\mathbf{H} \cap \partial B(x,r)$ and L_1. □

Proof of Proposition 8.1. Combine Lemmas 8.3–8.5 with the argument described in the caption of Figure 8.1. □

8.2 Zipping up a thick wedge

Fix $\alpha < Q$. Recall from Section 4.3 that an α-quantum cone is the surface which arises by starting with an instance of the whole-plane GFF, adding to it $-\alpha \log|\cdot|$, and then rescaling as part (ii) of Proposition 4.11 so that the resulting surface is invariant under the operation of multiplying its area by a constant. Recall that the weight of an α-quantum cone is given by

$$W = 2\gamma(Q - \alpha).$$

The purpose of this section is to explain how zipping up the left and right sides of a quantum wedge with weight $W \geq \frac{\gamma^2}{2}$ (so that the wedge is homeomorphic to $\mathbf{H}$) according to quantum length yields a quantum cone of weight W where the image of the welding of $\mathbf{R}_-$ with $\mathbf{R}_+$ is given by an independent whole-plane $\mathrm{SLE}_\kappa(\rho)$ process with $\rho = W - 2$. This is equivalent to stating that cutting a quantum cone of weight W along an independent whole-plane $\mathrm{SLE}_\kappa(\rho)$ process with $\rho = W - 2$ yields a quantum wedge of weight W and, moreover, that the quantum length of the image of the left side of a segment of the path is the same as that of the image of its right side. This result is contained in the following theorem. (See Figure 1.12 for an illustration; in Section 8.4 we will explain how to generalize this procedure to wedges which are not homeomorphic to $\mathbf{H}$.)

Proposition 8.7. *Fix $W \geq \frac{\gamma^2}{2}$ and suppose that $\mathcal{C} = (\mathbf{C}, h, 0, \infty)$ is a quantum cone of weight W. Suppose that η is a whole-plane $\mathrm{SLE}_\kappa(W-2)$ process independent of $\mathcal{C}$ starting from 0. Then $(\mathbf{C} \setminus \eta, 0, \infty)$ is a quantum wedge of weight W. Moreover, if $f : \mathbf{H} \to \mathbf{C} \setminus \eta$ is a conformal transformation fixing 0 and ∞, $\widehat{h} = h \circ f + Q \log|f'|$, and $x \in \eta$, then the lengths of the intervals connecting 0 and the two images of x under f^{-1} are the same with respect to the γ-LQG boundary measure $\nu_{\widehat{h}}$ on $\mathbf{R}$.*

Note that the assumption that $W \geq \frac{\gamma^2}{2}$ implies that $\rho = W - 2 \geq \frac{\kappa}{2} - 2$. This is the critical threshold at or above which the whole-plane $\mathrm{SLE}_\kappa(\rho)$ processes are simple and below which they are self-intersecting (see [MS13a, Section 2.1]).

Proof of Proposition 8.7. In the proof, we are going to describe our cones in terms of α values rather than weights. We are going to prove the result in the case that $\alpha < \frac{2}{\gamma} + \frac{\gamma}{4}$; the case in which $\alpha = \frac{2}{\gamma} + \frac{\gamma}{4}$ then follows by taking a limit as $\alpha \uparrow \frac{2}{\gamma} + \frac{\gamma}{4}$. Suppose that $\widetilde{h}$ is a free boundary GFF on $\mathbf{H}$. Let $\rho' = 2\alpha\gamma$ and let (f_t) be the centered reverse Loewner flow associated with a centered reverse $\mathrm{SLE}_\kappa(\rho')$ process with a single interior force point which starts infinitesimally above 0. Note that $\alpha < \frac{2}{\gamma} + \frac{\gamma}{4}$ implies that $\rho' < \frac{\kappa}{2} + 4$ so that the existence of this process is given by Proposition 3.8. We assume that $\widetilde{h}$ and (f_t) are independent. Let Z_t denote the evolution of the force point under f_t. Let G be the Neumann Green's function on $\mathbf{H}$ (recall (6.1)). For each $t \geq 0$, we let

$$h^t = \widetilde{h} \circ f_t + \frac{2}{\gamma} \log |f_t(\cdot)| + \frac{\rho'}{2\gamma} G(f_t(\cdot), Z_t) + Q \log |f_t'(\cdot)|. \tag{8.2}$$

By Theorem 6.1, we have that $h^t \overset{d}{=} h^0$ for all $t \geq 0$.

For each $r > 0$, let $\tau_r = \inf\{t > 0 : \mathrm{Im}(Z_t) = r\}$. By Proposition 3.10, we know that we can also sample from the law of f_{τ_r} by first sampling Z_{τ_r}, then drawing an independent (forward) $\mathrm{SLE}_\kappa(\widetilde{\rho})$ process η_{τ_r} from 0 to ∞ in $\mathbf{H}$ with a single interior force point located at Z_{τ_r} of weight

$$\widetilde{\rho} = \rho' - 8 = 2\alpha\gamma - 8$$

and then take f_{τ_r} to be the unique conformal map $\mathbf{H} \to \mathbf{H} \setminus \eta_{\tau_r}$ with $f_{\tau_r}(z) = z(1 + o(1))$ as $z \to \infty$. Note that

$$\rho = 2 + \kappa - 2\alpha\gamma = \kappa - 6 - \widetilde{\rho}.$$

The above is thus in turn the same as drawing an independent radial $\mathrm{SLE}_\kappa(\rho)$ process η_{τ_r} with a single boundary force point of weight ρ and targeted at Z_{τ_r} (see [SW05, Theorem 3]).

Let

$$\overline{h}^{\tau_r} = \widetilde{h}(\cdot + Z_{\tau_r}) + \frac{2}{\gamma} \log |\cdot + Z_{\tau_r}| + \frac{\rho'}{2\gamma} G(\cdot + Z_{\tau_r}, Z_{\tau_r}),$$

$\overline{\eta}_{\tau_r} = \eta_{\tau_r} - Z_{\tau_r}$, and $\overline{f}_{\tau_r} = f_{\tau_r} - Z_{\tau_r}$. Then the law of the triple $(\overline{h}^{\tau_r}, \overline{\eta}_{\tau_r}, \overline{f}_{\tau_r})$ converges as $r \to \infty$ to the law of the triple (h, η, f) where: h is a whole-plane GFF plus $-\alpha \log |\cdot|$, η (after reversing time and applying [MS13a, Theorem 1.20]) is a whole-plane $\mathrm{SLE}_\kappa(\rho)$ process from 0 to ∞ independent of h, and $f \colon \mathbf{H} \to \mathbf{C} \setminus \eta$ is a conformal transformation fixing 0 and ∞.

Let $\widehat{h} = h \circ f + Q \log |f'(\cdot)|$. Then we know that $\widehat{h} \overset{d}{=} h^0$ where h^0 is as in (8.2). For each $x < 0$, we let $R(x) > 0$ be the unique point identified with x under f. Let $\nu_{\widehat{h}}$ be the γ-LQG boundary measure associated with $\widehat{h}$. By applying absolute continuity for $\mathrm{SLE}_\kappa(\rho)$ processes and the GFF and combining with [She10, Theorem 1.3], we know that the quantum lengths of $[x, 0]$ and $[0, R(x)]$ under $\nu_{\widehat{h}}$ almost surely agree.

Rescaling $(\mathbf{H}, \widehat{h})$ as in part (ii) of Proposition 4.6 yields a $(2\alpha - \frac{2}{\gamma})$-quantum wedge, say $\mathcal{W}$. We claim that the image of the rescaled surface is an α-quantum cone. Suppose that $\mathcal{W}$ is represented by $(\mathbf{H}, \acute{h})$ exactly as in Definition 4.4. Then the law of $\acute{h}$ restricted to $\mathbf{D} \cap \mathbf{H}$ is the same as what one gets by taking a free boundary GFF on $\mathbf{H}$ and adding to it $(\frac{2}{\gamma} - 2\alpha) \log |\cdot|$ and then restricting to $\mathbf{D} \cap \mathbf{H}$. From the discussion above, it is then clear that the law of the image surface in a sufficiently small neighborhood of 0 (of random size) is the same as what one gets by starting with a whole-plane GFF and adding $-\alpha \log |\cdot|$ and then restricting to the same small neighborhood. Moreover, the law of the image surface is invariant under the operation of multiplying its area by a constant because it is given as the image of a surface which has this property. Thus the claim follows by applying Proposition 4.12. □

8.3 Welding more general wedges: proof of Theorem 1.9

In this section, we are going to complete the proof of Theorem 1.9. The following are the main steps:

1. Show that dividing a weight $2 + W$ wedge by an independent $\mathrm{SLE}_\kappa(0; W - 2)$ process for $W > 0$ yields independent wedges of weight 2 and W. Proposition 8.1 is the case that $W \geq \frac{\gamma^2}{2}$ and Lemma 8.8 generalizes Proposition 8.1 to include the case that $W \in (0, \frac{\gamma^2}{2})$.
2. Show that dividing a weight 2 wedge by an independent $\mathrm{SLE}_\kappa(-W; W - 2)$ process with $W \in (0, 2)$ yields independent wedges of weight $2 - W$ and W (Lemma 8.9).
3. Show how to weld together wedges with weights $W_1, W_2 > 0$ with $W_1 + W_2 \in (0, 2]$ and that the result is a wedge with weight $W_1 + W_2$ (Lemma 8.11).
4. Generalize to the setting of welding together wedges with weights $W_1, W_2 > 0$ and that the result is a wedge with weight $W_1 + W_2$. Upon showing this, the proof of Theorem 1.9 will be complete.

Lemma 8.8. *Fix $W > 0$ and suppose that $\mathcal{W} = (\mathbf{H}, h, 0, \infty)$ is a wedge of weight $2 + W$. Let η be an $\mathrm{SLE}_\kappa(0; W - 2)$ process in $\mathbf{H}$ from 0 to ∞ with a single boundary*

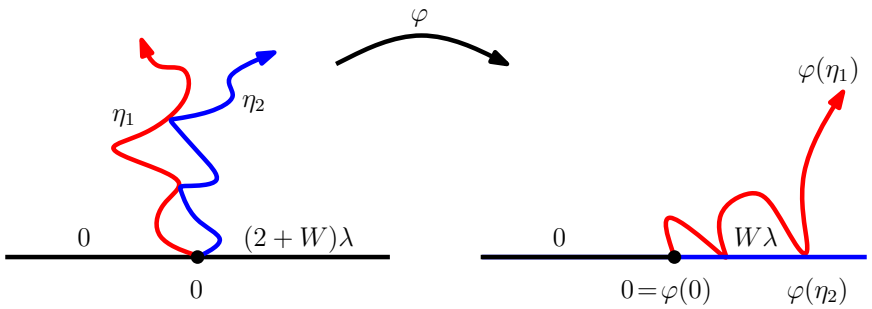

Figure 8.2: Illustration of the setup of the proof of Lemma 8.8. On the left, we have a wedge $\mathcal{W}$ of weight $4+W$ and drawn on top of $\mathcal{W}$ are flow lines of a common GFF on $\mathbf{H}$ which is independent of $\mathcal{W}$ with the boundary data shown. The angle of η_1 (resp. η_2) is $-\lambda/\chi$ (resp. $-(1+W)\lambda/\chi$). The conformal map φ takes the component of $\mathbf{H}\setminus\eta_2$ which is to the left of η_2 to $\mathbf{H}$ with 0 and ∞ fixed. The resulting surface is, by Proposition 8.1, a weight $2+W$ wedge which is sliced by $\varphi(\eta_1)$, an independent $\mathrm{SLE}_\kappa(0;W-2)$ process.

force point of weight $W-2$ located at 0^+ independent of $\mathcal{W}$. Then the regions which are to the left and right of η (viewed as quantum surfaces) are independent of each other and are respectively given by wedges of weight 2 and W.

In the statement of Lemma 8.8, the quantum surface to the right of η is not connected in the case that $W \in (0, \frac{\gamma^2}{2})$ so that the ρ value associated with the force point of η located at 0^+ is in $(0, \frac{\kappa}{2}-2)$: it is a countable collection of open sets that comes with a natural ordering (the order in which the boundaries are drawn by η), and a marked pair of boundary points for each set (corresponding to the first and last points on the boundary hit by η). For the moment, we will take this as our definition of a wedge of weight $W \in (0, \frac{\gamma^2}{2})$ and show momentarily that this definition is equivalent to the one given in Definition 4.4.

Proof of Lemma 8.8. See Figure 8.2 for an illustration of the setup. Proposition 8.1 gives the result in the case that $W \geq \frac{\gamma^2}{2}$, so we will assume that $W \in (0, \frac{\gamma^2}{2})$. We will prove the result by considering the following modified setup. Let $\mathcal{W} = (\mathbf{H}, h, 0, \infty)$ be a wedge of weight $4+W$. Let η_1 and η_2 be flow lines of a common GFF on $\mathbf{H}$ with boundary conditions given by 0 (resp. $(2+W)\lambda$) on $\mathbf{R}_-$ (resp. $\mathbf{R}_+$) with respective angles given by $-\lambda/\chi$ and $-(1+W)\lambda/\chi$ starting from 0 and targeted at ∞. Let $\mathcal{W}_1$ (resp. $\mathcal{W}_3$) be the region which is to the left (resp. right) of η_1 (resp. η_2) and let $\mathcal{W}_2$ be the region in between η_1 and η_2, where we view $\mathcal{W}_1, \mathcal{W}_2, \mathcal{W}_3$ as quantum surfaces. Note that η_1 (resp. η_2) is marginally an $\mathrm{SLE}_\kappa(0;W)$ (resp. $\mathrm{SLE}_\kappa(W;0)$) process independent of $\mathcal{W}$. Moreover, the conditional law of η_1 given η_2 is that of an $\mathrm{SLE}_\kappa(0;W-2)$ and the conditional law of η_2 given η_1 is an $\mathrm{SLE}_\kappa(W-2;0)$ process.

Proposition 8.1 implies that $(\mathcal{W}_1, \mathcal{W}_2)$ is independent of $\mathcal{W}_3$ and $\mathcal{W}_1$ is independent of $(\mathcal{W}_2, \mathcal{W}_3)$. This implies that $\mathcal{W}_1$, $\mathcal{W}_2$, and $\mathcal{W}_3$ are all independent of each other. Moreover, the region which is to the left of η_2 is a wedge of weight $2 + W$ sliced by an $\mathrm{SLE}_\kappa(0; W-2)$ process, which proves the result. □

Lemma 8.9. *Suppose that $\mathcal{W} = (\mathbf{H}, h, 0, \infty)$ is a wedge of weight 2, fix $W \in (0,2)$, and suppose that η is an $\mathrm{SLE}_\kappa(-W; W-2)$ process in $\mathbf{H}$ from 0 to ∞ with force points located at $0^-, 0^+$ and independent of $\mathcal{W}$. Then the regions which are to the left and right of η (viewed as quantum surfaces) are independent of each other and are respectively given by wedges of weight $2 - W$ and W.*

Proof. We consider the following modified setup. We suppose that $\mathcal{W} = (\mathbf{H}, h, 0, \infty)$ is a wedge of weight $2 + W$. We let η_1 and η_2 be flow lines of a common GFF on $\mathbf{H}$ independent of $\mathcal{W}$ with boundary conditions given by 0 on $\mathbf{R}_-$ and $W\lambda$ on $\mathbf{R}_+$ with respective angles given by $(1-W)\lambda/\chi$ and $-\lambda/\chi$. Then η_1 is marginally an $\mathrm{SLE}_\kappa(W-2; 0)$ process and η_2 is marginally an $\mathrm{SLE}_\kappa(0; W-2)$ process. Moreover, the conditional law of η_2 given η_1 is that of an $\mathrm{SLE}_\kappa(-W; W-2)$ process and the conditional law of η_1 given η_2 is that of an $\mathrm{SLE}_\kappa(W-2; -W)$ process. Let $\mathcal{W}_1$ (resp. $\mathcal{W}_3$) be the region which is to the left (resp. right) of η_1 (resp. η_2) and $\mathcal{W}_2$ be the region which is in between η_1 and η_2. We view $\mathcal{W}_1, \mathcal{W}_2, \mathcal{W}_3$ each as quantum surfaces. Lemma 8.8 implies that $(\mathcal{W}_1, \mathcal{W}_2)$ is independent of $\mathcal{W}_3$ and that $\mathcal{W}_1$ is independent of $(\mathcal{W}_2, \mathcal{W}_3)$. This implies that $\mathcal{W}_1$, $\mathcal{W}_2$, and $\mathcal{W}_3$ are all independent of each other. Moreover, the region which is to the right of η_1 (viewed as a quantum surface) is a wedge of weight 2 sliced by an independent $\mathrm{SLE}_\kappa(-W; W-2)$ process. This proves the result since the region to the right of η_2 (viewed as a quantum surface) is a wedge of weight W. □

The following shows that there is a family of equivalent ways to construct a wedge of weight $W \in (0, \frac{\gamma^2}{2})$ as a slice of a weight 2 wedge.

Lemma 8.10. *Fix $W_1, W_2 > 0$ with $W_1 + W_2 \in (2 - \frac{\gamma^2}{2}, 2)$. Suppose that η_1 and η_2 are given by the flow lines starting from 0 and targeted at ∞ of a GFF on $\mathbf{H}$ with zero boundary values and with angles respectively given by $(1-W_1)\lambda/\chi$ and $-(1-W_2)\lambda/\chi$. (Note that the marginal law of η_1 (resp. η_2) is given by that of an $\mathrm{SLE}_\kappa(W_1 - 2; -W_1)$ (resp. $\mathrm{SLE}_\kappa(-W_2; W_2 - 2)$ process in $\mathbf{H}$ from 0 to ∞ with force points located at $0^-, 0^+$). Let $\mathcal{W} = (\mathbf{H}, h, 0, \infty)$ be a wedge of weight 2 which is independent of (η_1, η_2). Then the beaded quantum surface bounded between η_1 and η_2 has the law of a wedge of weight $W = 2 - (W_1 + W_2)$.*

Proof. See Figure 8.3 for an illustration of the proof. We are first going to apply Proposition 8.7 to zip up $\mathcal{W}$ to yield a cone of weight 2 cone and an independent path whole-plane SLE_κ path $\widetilde{\eta}$.

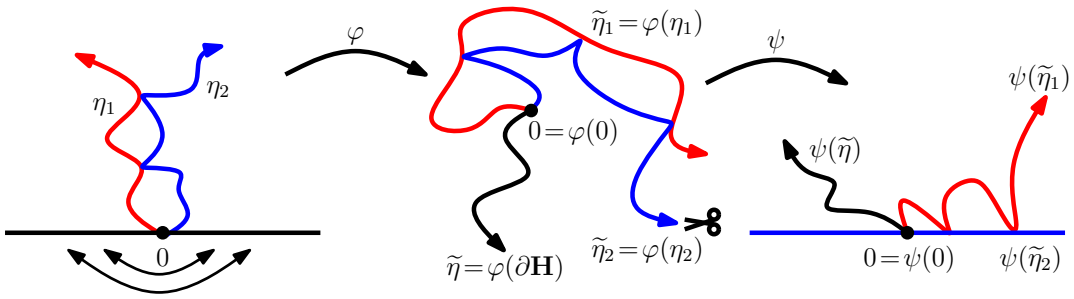

Figure 8.3: Illustration of the proof of Lemma 8.10. On the left, we have a weight 2 wedge $\mathcal{W} = (\mathbf{H}, h, 0, \infty)$ with two paths η_1, η_2 (GFF flow lines) drawn on top of it which are independent of $\mathcal{W}$. To go from the picture on the left to the picture on the right, we zip up the left and right sides of $\mathcal{W}$. The zipping up map is φ and the resulting object is, by Proposition 8.7, a quantum cone decorated with three independent paths whose joint law can be described in terms of whole-plane GFF flow lines. We then unzip along $\widetilde{\eta}_2 = \varphi(\eta_2)$ to yield, again by Proposition 8.7, a weight 2 wedge $\widetilde{\mathcal{W}}$ decorated with two independent paths whose joint law can be described in terms of GFF flow lines. In particular, $(\psi(\widetilde{\eta}_1), \widetilde{\mathcal{W}})$ is as in the statement of Lemma 8.9.

Let $\varphi\colon \mathbf{H} \to \mathbf{C} \setminus \widetilde{\eta}$ be the conformal transformation associated with the zipping up process. By [MS13a, Theorem 1.4], we can view $\widetilde{\eta}$ as the flow line starting from 0 of a whole-plane GFF plus $-(\frac{\gamma}{2} - \frac{1}{\gamma})\arg(\cdot)$. Moreover, we can realize $\widetilde{\eta}_1 = \varphi(\eta_1)$ and $\widetilde{\eta}_2 = \varphi(\eta_2)$ as flow lines of the same GFF starting from 0 with angles respectively given by $(1-W_1)\lambda/\chi$ and $-(1-W_2)\lambda/\chi$. This, in turn, gives us the marginal law of $\widetilde{\eta}_2$ along with the conditional laws of each of $\widetilde{\eta}$ and $\widetilde{\eta}_1$ given the other two paths; see [MS13a, Theorem 1.11]. In particular, $\widetilde{\eta}_2$ is a whole-plane SLE_κ process. Thus we can apply Proposition 8.7 a second time to unzip along $\widetilde{\eta}_2$ to yield a weight 2 wedge $\widetilde{\mathcal{W}}$ decorated with two independent paths. Let $\psi\colon \mathbf{C} \setminus \widetilde{\eta}_2 \to \mathbf{H}$ be the corresponding unzipping map. Then we know the joint law of $(\psi(\widetilde{\eta}), \psi(\widetilde{\eta}_1))$ can be sampled from by taking the paths to be flow lines starting from 0 and targeted at ∞ of a GFF on $\mathbf{H}$ with zero boundary values and with respective angles $-(W_2-1)\lambda/\chi$ and $(W-1)\lambda/\chi$. In particular, $\psi(\widetilde{\eta}_1)$ is an $\mathrm{SLE}_\kappa(-W; W-2)$ process and the pair $(\psi(\widetilde{\eta}_1), \widetilde{\mathcal{W}})$ is as in the setting of Lemma 8.9. We therefore know that the beaded surface to the right of $\psi(\widetilde{\eta}_1)$ is a weight W wedge. This completes the proof since this is the same (as quantum surfaces) as the region of $\mathcal{W}$ between η_1 and η_2. □

In Lemma 8.9, we showed that slicing a wedge of weight 2 with an $\mathrm{SLE}_\kappa(-W; W-2)$ process yields a wedge of weight W. We now generalize this to the case of wedges with weight in $(0, 2]$.

Lemma 8.11. *Fix $W \in (0,2]$ and let $\mathcal{W} = (\mathbf{H}, h, 0, \infty)$ be a wedge of weight W. Fix $W_1, W_2 > 0$ with $W_1 + W_2 = W$ and let η be an $\mathrm{SLE}_\kappa(W_1 - 2; W_2 - 2)$ process in $\mathbf{H}$ from 0 to ∞ with force points located at $0^-, 0^+$ which is independent of $\mathcal{W}$. (In the case that $W \in (0, \frac{\gamma^2}{2})$, we have an independent $\mathrm{SLE}_\kappa(W_1 - 2; W_2 - 2)$ process in each of the beads of $\mathcal{W}$.) Then the region $\mathcal{W}_1$ (resp. $\mathcal{W}_2$) which is to the left (resp. right) of η, viewed as a quantum surface, is a weight W_1 (resp. W_2) wedge and $\mathcal{W}_1, \mathcal{W}_2$ are independent.*

Proof. We consider the following modified setup. We suppose that $\mathcal{W}$ is a wedge of weight 2. We let η_1 and η_2 be flow lines of a GFF on $\mathbf{H}$ with zero boundary conditions with respective angles $(W-1)\lambda/\chi$ and $(W_2 - 1)\lambda/\chi$. Then the marginal law of η_1 is that of an $\mathrm{SLE}_\kappa(-W; W-2)$ process and the marginal law of η_2 is that of an $\mathrm{SLE}_\kappa(-W_2; W_2 - 2)$ process, both in $\mathbf{H}$ from 0 to ∞ with force points located at $0^-, 0^+$. Moreover, the conditional law of η_2 given η_1 is that of an $\mathrm{SLE}_\kappa(W_1 - 2; W_2 - 2)$ process in each of the components of $\mathbf{H} \setminus \eta_1$ which are to the right of η_1. Let $\mathcal{W}_1$ be the region which is to the left of η_1, $\mathcal{W}_2$ be the region between η_1 and η_2, and $\mathcal{W}_3$ be the region to the right of η_2. We also let $\widetilde{\mathcal{W}}$ be the region which is to the right of η_1. We view $\mathcal{W}_1, \mathcal{W}_2, \mathcal{W}_3, \widetilde{\mathcal{W}}$ as quantum surfaces. Lemma 8.9 implies that $\mathcal{W}_1$ is a wedge of weight $2 - W$, $\widetilde{\mathcal{W}}$ is a wedge of weight W, and $\mathcal{W}_3$ is a wedge of weight W_2. Lemma 8.10 implies that $\mathcal{W}_2$ is a wedge of weight W_1. The same argument as in the end of the proofs of Lemma 8.8 and Lemma 8.9 (with Lemma 8.9 and Lemma 8.10 in place of Proposition 8.1) implies that $\mathcal{W}_2$ and $\mathcal{W}_3$ are independent, which implies the result. □

Lemma 8.12. *Fix $W > 0$, $j \in \mathbf{N}$, and let $\mathcal{W} = (\mathbf{H}, h, 0, \infty)$ be a wedge of weight $2j + W$. Let η be an $\mathrm{SLE}_\kappa(2j - 2; W - 2)$ process in $\mathbf{H}$ from 0 to ∞ with force points located at $0^-, 0^+$ independent of $\mathcal{W}$. Let $\mathcal{W}_1$ (resp. $\mathcal{W}_2$) be the region which is to the left (resp. right) of η, viewed as a quantum surface. Then $\mathcal{W}_1$ (resp. $\mathcal{W}_2$) is a wedge of weight $2j$ (resp. W) and $\mathcal{W}_1$ and $\mathcal{W}_2$ are independent.*

Proof. We will prove the result by induction on j. The case that $j = 1$ is given in Lemma 8.8. Suppose that the result holds for some $k \geq 1$; we will now show that the result holds for $j = k + 1$. Note that we can sample η as a flow line starting from 0 and targeted at ∞ of a GFF on $\mathbf{H}$ independent of $\mathcal{W}$ with boundary values given by 0 on $\mathbf{R}_-$ and $(W + 2k)\lambda$ on $\mathbf{R}_+$ where the angle of η is given by $-(2j-1)\lambda/\chi$. Let $\widetilde{\eta}$ be the flow line of the same GFF starting from 0 and targeted at ∞ with angle $-\lambda/\chi$. Then $\widetilde{\eta}$ is marginally an $\mathrm{SLE}_\kappa(0; W + 2k - 2)$ process. It thus follows from Lemma 8.8 that the region $\widetilde{\mathcal{W}}_1$ (resp. $\widetilde{\mathcal{W}}_2$) which is to the left (resp. right) of $\widetilde{\eta}$, viewed as a quantum surface, is a wedge of weight 2 (resp. $W + 2k$) and $\widetilde{\mathcal{W}}_1$, $\widetilde{\mathcal{W}}_2$ are independent. Note that the conditional law of η given $\widetilde{\eta}$ is that of an $\mathrm{SLE}_\kappa(2k - 2; W - 2)$ process. Therefore it follows from the induction hypothesis that η splits $\widetilde{\mathcal{W}}_2$ into independent

wedges of weight $2k$ and W. Applying Lemma 8.8, gluing the former to $\widetilde{\mathcal{W}}_1$ yields a wedge of weight $2j$ which proves the result. □

Proof of Theorem 1.9. Suppose that we have a wedge $\mathcal{W} = (\mathbf{H}, h, 0, \infty)$ of weight $W \geq \frac{\gamma^2}{2}$ and that $W_1, W_2 > 0$ with $W_1 + W_2 = W$. If $W \in (0, 2]$, then we know from Lemma 8.11 that drawing an independent $\mathrm{SLE}_\kappa(W_1 - 2; W_2 - 2)$ process in $\mathbf{H}$ from 0 to ∞ with force points located at $0^-, 0^+$ on top of $\mathcal{W}$ divides it into independent wedges of weight W_1 and W_2. Lemma 8.12 implies that the result holds if $W_1 = 2j$ for $j \in \mathbf{N}$.

To complete the proof, we thus assume that $W_1 > 0$ is not an even integer with $W_1 + W_2 > 2$. Let $j = \lfloor W_1/2 \rfloor$ and $k = \lfloor W_2/2 \rfloor$ and let η_1, η, and η_2 be flow lines of a common GFF on $\mathbf{H}$ independent of $\mathcal{W}$ with boundary values given by 0 on $\mathbf{R}_-$ and $(W-2)\lambda$ on $\mathbf{R}_+$ with respective angles $-(2j-1)\lambda/\chi$, $(1-W_1)\lambda/\chi$, and $(1-(W-2k))\lambda/\chi$. Note that η_1, η, and η_2 are respectively given by $\mathrm{SLE}_\kappa(2j-2; W-2j-2)$, $\mathrm{SLE}_\kappa(W_1-2; W_2-2)$, and $\mathrm{SLE}_\kappa(W-2k-2; 2k-2)$ processes in $\mathbf{H}$ from 0 to ∞ with force points located at $0^-, 0^+$. Lemma 8.12 implies that the region $\widehat{\mathcal{W}}_1$ (resp. $\widehat{\mathcal{W}}_2$) which is to the left (resp. right) of $\widehat{\eta}_1$ (resp. $\widehat{\eta}_2$), viewed as a quantum surface, is a wedge of weight $2j$ (resp. $2k$) and the region $\widehat{\mathcal{W}}$ which is between $\widehat{\eta}_1$ and $\widehat{\eta}_2$ is a wedge of weight $W - 2j - 2k$. Moreover, $\widehat{\mathcal{W}}_1$, $\widehat{\mathcal{W}}_2$, and $\widehat{\mathcal{W}}$ are independent. It suffices to show that η divides $\widehat{\mathcal{W}}$ into independent wedges of weight $W_1 - 2j$ and $W_2 - 2k$ because then we can apply Lemma 8.12 to glue the former to $\widehat{\mathcal{W}}_1$ and the latter to $\widehat{\mathcal{W}}_2$ to yield independent wedges of weight W_1 and W_2, respectively. If $W - 2j - 2k \leq 2$, then the claim follows from Lemma 8.11. If $W - 2j - 2k > 2$, then note that $W - 2j - 2k < 4$ by the definition of j, k. In this case, the claim follows by slicing $\widehat{\mathcal{W}}$ with a flow line of angle $-(2j+1)\lambda/\chi$ to yield independent wedges of weight 2 and $W - 2j - 2k - 2$ using Lemma 8.8 and then slicing the resulting wedge containing η with η and applying Lemma 8.11.

To complete the proof, it is left to show that the notion of a wedge with weight in $(0, \frac{\gamma^2}{2})$ is the same as that given in Definition 4.13. We state and prove this result in the next lemma. □

Lemma 8.13. *The definition of a wedge of weight $W \in (0, \frac{\gamma^2}{2})$ given in Lemma 8.8 is equivalent to the definition given in Definition 4.13.*

Proof. Note that if we apply the rescaling procedure from part (ii) of Proposition 4.6 to the setting of Theorem 7.22 then the result consists of a wedge of weight $\rho + 4$ sliced by an independent $\mathrm{SLE}_\kappa(0; \rho)$ process. The result above implies that the ordered sequence of surfaces which are to the right of the path together form a wedge of weight $\rho + 2$ as defined earlier in this section. On the other hand, Theorem 7.22 implies that this sequence of surfaces has the law of a wedge of weight $\rho + 2$ as defined in Definition 4.13. □

Proposition 8.14. *Fix $W \geq \frac{\gamma^2}{2}$ and let $\mathcal{W} = (\mathbf{H}, h, 0, \infty)$ be a wedge of weight W. Consider a GFF on $\mathbf{H}$ independent of $\mathcal{W}$ with boundary conditions given by 0 on $\mathbf{R}_-$ and $(W-2)\lambda$ on $\mathbf{R}_+$. Fix angles $(1-W)\lambda/\chi < \theta_1 < \cdots < \theta_n < \lambda/\chi$ and, for each i, let η_i be the flow line starting from 0 and targeted at ∞ with angle θ_i. (Each η_i is marginally an $\mathrm{SLE}_\kappa(r_i - 2; W - 2 - r_i)$ process in $\mathbf{H}$ from 0 to ∞ with force points at $0^-, 0^+$ where $r_i = 1 - \theta_i\chi/\lambda$. We take the convention that $\eta_0 = \mathbf{R}_+$, $\theta_0 = (1-W)\lambda/\chi$, $r_0 = W$, $\eta_{n+1} = \mathbf{R}_-$, $\theta_{n+1} = \lambda/\chi$, and $r_{n+1} = 0$.) Then for each $i \in \{1, 2, \ldots, n+1\}$, the (possibly beaded) quantum surface bounded between η_{i-1} and η_i (which we denote by $\mathcal{W}_i$) is a quantum wedge of weight $r_{i-1} - r_i = (\theta_i - \theta_{i-1})\chi/\lambda$ and $\mathcal{W}_1, \ldots, \mathcal{W}_{n+1}$ are independent.*

The result similarly holds if $W \in (0, \frac{\gamma^2}{2})$ except for each bubble $\mathcal{B}$ of $\mathcal{W}$ we sample an independent GFF (with boundary data as above) and then view η_j as the concatenation of paths from the GFFs according to the natural ordering of the bubbles $\mathcal{B}$.

Proof. Note that if $n = 1$, we have that η_1 is an $\mathrm{SLE}_\kappa(r_1 - 2; W - 2 - r_1)$ process independent of $\mathcal{W}$. Since the region which is between η_1 and $\eta_2 = \mathbf{R}_-$ is the same as the region which is to the left of η_1 and the region which is between η_1 and $\eta_0 = \mathbf{R}_+$ is the same as the region which is to the right of η_1, the result thus follows in this case from Theorem 1.9. Then general case follows by iterating. □

8.4 Zipping up a thin wedge

We are now going to generalize Proposition 8.7 to show that slicing a quantum cone with an independent self-intersecting whole-plane $\mathrm{SLE}_\kappa(\rho)$ process yields a thin wedge. Equivalently, conformally welding the left and right sides of a thin wedge yields a certain quantum cone decorated with an independent self-intersecting whole-plane $\mathrm{SLE}_\kappa(\rho)$ process.

Proposition 8.15. *Fix $W \in (0, \frac{\gamma^2}{2})$, suppose that $\mathcal{C} = (\mathbf{C}, h, 0, \infty)$ is a quantum cone of weight W. Suppose that η is a whole-plane $\mathrm{SLE}_\kappa(W-2)$ process independent of $\mathcal{C}$ starting from 0. (Note that $\rho \in (-2, \frac{\kappa}{2} - 2)$ so that η is self-intersecting.) Then the beaded surface $(\mathbf{C} \setminus \eta, h, 0, \infty)$ is a quantum wedge of weight W.*

Proof. Proposition 4.11 combined with Corollary 7.12 implies that the structure of the bubbles which arise when cutting a quantum cone of weight W with an independent whole-plane $\mathrm{SLE}_\kappa(W-2)$ process is the same as the structure of the bubbles which constitute a quantum wedge of weight W. This, in turn, implies the result. □

We can also slice a quantum cone with a collection of paths coupled together as flow lines of a GFF to yield a collection of independent quantum wedges. This is the quantum cone version of Proposition 8.14.

Proposition 8.16. *Fix $W \geq \frac{\gamma^2}{2}$, suppose that $\mathcal{C} = (\mathbf{C}, h, 0, \infty)$ is a quantum cone of weight W. Let $\widehat{h}$ be given by a whole-plane GFF minus $\frac{1}{2\gamma}(W + \gamma^2 - 4)\arg(\cdot)$ and assume that $\widehat{h}$ is independent of h. Fix angles $0 \leq \theta_1 < \cdots < \theta_n < \frac{2\pi}{4-\gamma^2}W = \frac{\pi}{\gamma\chi}W$ and, for each j, let η_j be the flow line of $\widehat{h}$ starting from 0 with angle θ_j. For each $1 \leq j \leq n$, let $\mathcal{W}_j$ be the region between η_{j-1} and η_j (in the counterclockwise direction) where we take $\eta_0 = \eta_n$. Then $\mathcal{W}_1, \ldots, \mathcal{W}_n$ are independent and $\mathcal{W}_j$ is a wedge of weight $(\theta_j - \theta_{j-1})\frac{\chi}{\lambda}$ where we take $\theta_0 = \theta_n - \frac{2\pi}{4-\gamma^2}W$.*

If we describe our cone in terms of α rather than weight, then argument singularity for the whole-plane GFF is given by minus $(\gamma - \alpha)\arg(\cdot)$ and the range of angles is given by $2\pi(\chi + \gamma - \alpha)/\chi$.

Proof of Proposition 8.16. The case that $n = 1$ is given in Proposition 8.7 for $W \geq \frac{\gamma^2}{2}$ and Proposition 8.15 gives the case that $W \in (0, \frac{\gamma^2}{2})$. Now suppose that $n \geq 2$. Then we can describe the conditional law of $\eta_2, \ldots, \eta_n$ given η_1 as follows. First suppose that $W \geq \frac{\gamma^2}{2}$ so that η is a whole-plane $\mathrm{SLE}_\kappa(\rho)$ process with $\rho = W - 2 \geq \frac{\kappa}{2} - 2$. That is, η_1 is non-self-intersecting. Then $\eta_2, \ldots, \eta_n$ are given by the conformal image of flow lines $\widetilde{\eta}_2, \ldots, \widetilde{\eta}_n$ of a GFF on $\mathbf{H}$ with boundary conditions

$$\lambda(5 - \gamma^2 - W) - (\theta_1 + 2\pi)\chi \quad \text{on} \quad \mathbf{R}_- \quad \text{and} \quad -\lambda - \theta_1\chi \quad \text{on} \quad \mathbf{R}_+.$$

starting from 0 and targeted at ∞ with respective angles given by $\theta_2, \ldots, \theta_n$. (See [MS13a, Theorem 1.11] and [MS13a, Figure 3.25].) By adding a constant to shift the boundary data of the field and adjusting the angles appropriately, we can take our GFF to have boundary conditions given by

$$0 \quad \text{on} \quad \mathbf{R}_- \quad \text{and} \quad (W-2)\lambda \quad \text{on} \quad \mathbf{R}_+.$$

This puts us into the setting of Proposition 8.14 in the case of slicing a wedge of weight W which, by Proposition 8.7, is exactly the weight of the wedge corresponding to $\mathbf{C} \setminus \eta_1$. This completes the proof in this case. The proof is analogous for $W \in (0, \frac{\gamma^2}{2})$ except the above describes the conditional law of $\eta_2, \ldots, \eta_n$ in each of the components of $\mathbf{C} \setminus \eta_1$. Proposition 8.14 still applies in this case, which gives the result. □

8.5 Gluing infinitesimally thin wedges: the Poissonian formulation

We are now going to give a Poissonian description of the bubbles which arise when cutting a quantum wedge or cone along GFF flow lines starting from a given point with a continuum of angles. This is the so-called **fan F** introduced in [MS12a, MS13a]. Recall from [MS12a, Proposition 7.33] that the Lebesgue measure of **F** is almost surely equal to zero.

Theorem 8.17. *Suppose that $\mathcal{W} = (\mathbf{H}, h, 0, \infty)$ is a wedge of weight $W \geq \frac{\gamma^2}{2}$. Let $\widehat{h}$ be a GFF on $\mathbf{H}$ independent of $\mathcal{W}$ with boundary values given by 0 on $\mathbf{R}_-$ and $(W-2)\lambda$ on $\mathbf{R}_+$. Fix a countable, dense set $\mathcal{D}$ of $[(1-W)\lambda/\chi, \lambda/\chi]$ and let $\mathbf{F}$ be the closure of the set of points accessible by flow lines of $\widehat{h}$ from 0 to ∞ with angles in $\mathcal{D}$. Then the collection of surfaces corresponding to $\mathbf{H} \setminus \mathbf{F}$ can be sampled from as follows:*

1. *Sample a p.p.p. Λ on $\mathbf{R}_+ \times [(1-W)\lambda/\chi, \lambda/\chi] \times \mathcal{E}$ with intensity measure given by $du \times d\theta \times \nu_1^{\mathrm{BES}}$ where du denotes Lebesgue measure on $\mathbf{R}_+$, $d\theta$ denotes the uniform measure on $[(1-W)\lambda/\chi, \lambda/\chi]$, and ν_1^{BES} is the Itô excursion measure associated with a BES^1 process.*
2. *Associate with each $(u, \theta, e) \in \Lambda$ a quantum surface on $\mathcal{S}$ as in Definition 4.4.*

If $\mathcal{C}$ is a quantum cone of weight W and $\mathbf{F}$ is defined in the analogous manner except in terms of flow lines from 0 to ∞ with angles in a countable dense subset of $[0, \frac{\pi}{\gamma\chi}W]$ of a whole-plane GFF minus $(W+\gamma^2-4)/(2\gamma)\arg(\cdot)$ then the surfaces corresponding to $\mathbf{C} \setminus \mathbf{F}$ admit the same description except we replace the interval $[(1-W)\lambda/\chi, \lambda/\chi]$ of angles with $[0, \frac{\pi}{\gamma\chi}W]$.

Proof. By Proposition 8.7 and Proposition 8.15, the case of a quantum cone will follow once we establish the version for a quantum wedge. Suppose that $\mathcal{W}$, W, and $\widehat{h}$ are as in the statement of the theorem. Fix $n \in \mathbf{N}$ and equally spaced angles $(1-W)\lambda/\chi < \theta_1 < \cdots < \theta_{n-1} < \theta_n = \lambda/\chi$. For each $1 \leq j \leq n$, we let η_j be the flow line of $\widehat{h}$ starting from 0 and targeted at ∞ with angle θ_j. For each $1 \leq j \leq n-1$, we let $\mathcal{W}_j$ be the (possibly beaded) quantum surface which is between η_{j-1} and η_j where we take $\eta_0 = \mathbf{R}_-$ and $\eta_n = \mathbf{R}_+$. Proposition 8.14 implies that $\mathcal{W}_1, \ldots, \mathcal{W}_n$ are independent and each $\mathcal{W}_j$ is a quantum wedge of weight $\frac{W}{n}$.

Assume that n is sufficiently large so that $\frac{W}{n} < \frac{\gamma^2}{2}$. It follows (by Definition 4.4) that the ordered sequence of bubbles of each $\mathcal{W}_j$ can be encoded using an independent $\mathrm{BES}^{\delta_\delta}$ with $\delta_n = 1 + \frac{2W}{n\gamma^2}$. This implies that we can encode all of the bubbles of $\mathbf{H} \setminus \cup_{j=1}^n \eta_j$ using a p.p.p. on $\mathbf{R}_+ \times [(1-W)\lambda/\chi, \lambda/\chi] \times \mathcal{E}$ with intensity measure given by the product of Lebesgue measure on $\mathbf{R}_+$, the measure which gives mass $\frac{1}{n}$ to each of n equal length and disjoint intervals $I_1, \ldots, I_n$ with union $[(1-W)\lambda/\chi, \lambda/\chi]$, and the Itô excursion measure associated with a BES^{δ_n}. The points (u, θ, e) in this process with $\theta \in I_j$ (ordered by u) correspond to the ordered bubbles of $\mathcal{W}_j$. Taking a limit as $n \to \infty$ gives the desired result. □

9 Space-filling SLE and Brownian motion

Throughout, we let $\kappa \in [2,4)$ and $\kappa' = 16/\kappa \in (4,8]$. Consider a γ-quantum cone $\mathcal{C} = (\mathbf{C}, h, 0, \infty)$ (i.e., $W = 4-\gamma^2$ and $\theta = 2\pi$) , together with a space-filling $\mathrm{SLE}_{\kappa'}$ process η' from ∞ to ∞ within $\mathbf{C}$, parameterized so that $\eta'(0) = 0$. We assume that η' is first sampled independently of $\mathcal{C}$ and then reparameterized according to γ-LQG area so that for $s,t \in \mathbf{R}$ with $s < t$ we have that $\mu_h(\eta'([s,t])) = t - s$. That is, η' traces t units of quantum area in t units of time. Let L_t (resp. R_t) denote the change in the left (resp. right) γ-LQG boundary length between times 0 and t. Note that $L_0 = R_0 = 0$. The main result of this section is that (L,R) evolves as a certain 2-dimensional Brownian motion.

Theorem 9.1. *Fix $\kappa \in [2,4)$ and let*

$$\theta_\kappa = \frac{\pi\kappa}{4}. \tag{9.1}$$

There exists (non-random) $a > 0$ such that (L,R) evolves as a 2-dimensional Brownian motion with $\mathrm{var}(L_1) = \mathrm{var}(R_1) = a^2$ and $\mathrm{cov}(L_1, R_1) = -a^2\cos(\theta_\kappa)$.

Note that $\cos(\theta_\kappa) < 0$ for $\kappa \in (2,4)$ so that $\mathrm{cov}(L_1, R_1) > 0$. In the case that $\kappa = 2$, $\cos(\theta_\kappa) = 0$ so that L and R are independent.

Before we give the proof of Theorem 9.1, we will relate (L,R) to the scaling limits of the discrete random planar map models considered in [She11]. We first note that it follows from Theorem 9.1 that $L+R$ and $L-R$ are independent Brownian motions. Moreover, Theorem 9.1 implies that

$$\mathrm{var}(L_1 + R_1) = 2a^2(1-\cos(\theta_\kappa)) \quad \text{and} \quad \mathrm{var}(L_1 - R_1) = 2a^2(1+\cos(\theta_\kappa)).$$

By a (non-random) linear reparameterization of time, we can take $a = (2(1-\cos(\theta_\kappa)))^{-1/2}$ so that $\mathrm{var}(L_1 + R_1) = 1$. Then,

$$\mathrm{var}(L_1 - R_1) = \frac{1+\cos(\theta_\kappa)}{1-\cos(\theta_\kappa)}. \tag{9.2}$$

Let

$$p = -\frac{\cos(\theta_\kappa)}{1-\cos(\theta_\kappa)} \tag{9.3}$$

and note from (9.2) that with this choice we have

$$\mathrm{var}(L_1 - R_1) = 1 - 2p. \tag{9.4}$$

The first co-author [Dup03], following work by den Nijs [dN83], Nienhuis [Nie84, Nie87], his and Saleur [DS88] (see also Kager and Nienhuis [KN04]), has conjectured

that the relationship between the parameter $q \in (0,4)$ of the FK representation of the q-state Potts model and κ' is given by

$$q = 2 + 2\cos\left(\frac{8\pi}{\kappa'}\right) = 2 + 2\cos\left(\frac{\pi\kappa}{2}\right). \tag{9.5}$$

Rewriting (9.5) in terms of θ_κ as in (9.1) yields

$$q = 2 + 2\cos(2\theta_\kappa) = 4\cos^2(\theta_\kappa). \tag{9.6}$$

Combining this with (9.3) yields

$$p = \frac{\sqrt{q}}{2+\sqrt{q}}, \tag{9.7}$$

as desired. Summarizing, we have that $(L+R, L-R)$ is a pair of independent Brownian motions with

$$\mathrm{var}(L_1 + R_1) = 1 \quad \text{and} \quad \mathrm{var}(L_1 - R_1) = 1 - 2p$$

which matches the scaling limit determined in [She11, Theorem 2.5] and the value of p matches the value in the bijection described in [She11, Section 4].

We now turn to the proof of Theorem 9.1. The first step (Lemma 9.2) is to show that (L, R) evolves as *some* 2-dimensional Brownian motion. This result will hold for all $\kappa' > 4$. We will then identify the diffusion matrix in the case that $\kappa \in (2,4)$ so that $\kappa' \in (4,8)$ Lemma 9.5 as a consequence of Lemma 9.4 which gives the almost sure Hausdorff dimension of the local cut times for η'. We will then identify the diffusion matrix in the case that $\kappa = 2$ so that $\kappa' = 8$ in Lemma 9.6 using a different method.

Lemma 9.2. *Fix $\kappa > 0$ (so that $\kappa' \in (4,\infty)$). There exists a pair of independent standard Brownian motions (X^1, X^2) defined for $t \in \mathbf{R}$ with $X^1_0 = X^2_0 = 0$ and a linear transformation Λ such that $(L,R) = \Lambda(X^1, X^2)$.*

Before we prove Lemma 9.2, we first need the following.

Lemma 9.3. *For each $t \in \mathbf{R}$, the joint law of $(\mathcal{C}, \eta')$ is invariant under the operation of translating by t units of (quantum area) time and then recentering so that $\eta'(t)$ is translated to the origin. That is, for each $t \in \mathbf{R}$ we have that*

$$(h, \eta) \overset{d}{=} (h(\cdot - \eta'(t)), \eta'(\cdot - t) - \eta'(t)).$$

Proof. Let η' be a space-filling $\mathrm{SLE}_{\kappa'}$ process normalized so that $\eta'(0) = 0$. We assume here (in contrast to the above) that η' is parameterized according to Lebesgue measure so that for $s, t \in \mathbf{R}$ with $s < t$ we have that the Lebesgue measure of $\eta'([s,t])$

is equal to $t-s$. Let dh denote the law of a whole-plane GFF and, for each $t>0$, let $A_t = \mu_h(\eta'([0,t]))$. Fix $S>0$ large. Note that A_s is a continuous, increasing function of s so that dA_s induces a measure on $[0,S]$. Consider the law $dA_s dh d\eta'$. Under this law, the marginal of h can be sampled from by first picking s in $[0,S]$ according to Lebesgue measure, η' independently as a space-filling $\mathrm{SLE}_{\kappa'}$ normalized so that $\eta'(0)=0$, and then taking $h = \widetilde{h} - \gamma \log|\cdot - \eta'(s)|$ where $\widetilde{h}$ has the law of a whole-plane GFF independent of η'. Indeed, this follows from the same argument used to prove Lemma 5.9. The conditional law of s given h and η' is given by dA_s. Equivalently, we first pick a uniformly in $[0, A_S]$ and then take $s = \inf\{u \geq 0 : A_u = a\}$.

Now suppose that s is picked in $[0,S]$ from dA_s. Fix $t>0$ and let $\sigma = \inf\{u \geq s : A_u = A_s + t\}$. Equivalently, we first pick a uniformly in $[0, A_S]$, and then let σ be the first time u that $A_u = a+t$. Note that $A_S \to \infty$ almost surely as $S \to \infty$. Consequently, it follows that the total variation distance between the laws of a and $a+t$ tends to zero as $S \to \infty$, hence the same is also true for the laws of s and σ. Note that this in particular holds even if we condition on h and η' and that h and η' together determine A. Therefore, the total variation distance between the laws of $(h(\cdot - \eta'(s)), \eta'(\cdot - s) - \eta'(s))$ and $(h(\cdot - \eta'(\sigma)), \eta'(\cdot - \sigma) - \eta'(\sigma))$ tends to 0 as $S \to \infty$.

Consider the pair (h, η') where $h = \widetilde{h} - \gamma \log|\cdot|$ with $\widetilde{h}$ a whole-plane GFF and η' a space-filling $\mathrm{SLE}_{\kappa'}$ first sampled independently of h and then reparameterized by a μ_h-time (which we emphasize is in contrast to the above where we parameterized time according to Lebesgue measure). Our argument above implies that $(h, \eta') \overset{d}{=} (h(\cdot - \eta'(t)), \eta'(\cdot - t) - \eta'(t))$ for each fixed $t \in \mathbf{R}$. It then follows from part (ii) of Proposition 4.11 that this invariance also holds for quantum cones. □

Proof of Lemma 9.2. By the definition of whole-plane $\mathrm{SLE}_{\kappa'}$ and [MS13a, Theorem 1.1] we have that the left side η_L of the outer boundary of $\eta'([-\infty, 0])$ is a whole-plane $\mathrm{SLE}_\kappa(2-\kappa)$ process. Consequently, it follows from Theorem 1.12 that the surface described by cutting $\mathcal{C}$ along η_L is a quantum wedge of weight $4-\gamma^2$. Since the relative angle between η_L and η_R is given by π, Proposition 8.16 implies that the (beaded if $\gamma^2 > 2$) quantum surfaces corresponding to $\eta'([0,\infty])$ and $\eta'([-\infty, 0])$ are independent quantum wedges, both of weight $2 - \frac{\gamma^2}{2}$. Lemma 9.3 states that the joint law of $(\mathcal{C}, \eta')$ is invariant under the operation of translating time by one unit and recentering at $\eta'(1)$, hence we also find that $\eta'([1,\infty])$ and $\eta'((-\infty, 1])$ parameterize independent quantum wedges of weight $2 - \frac{\gamma^2}{2}$.

Let $\mathcal{S}_{a,b}$ denote the (possibly beaded) quantum surface parameterized by $\eta'([a,b])$. Suppose that $A = \mathcal{S}_{-\infty,0}$, $B = \mathcal{S}_{0,1}$ and $C = \mathcal{S}_{1,\infty}$. Since the pair (A,B) is independent of C and the pair (B,C) is independent of A, it follows that A, B, and C are all independent of each other. Repeating this argument, we find that the

increments $\mathcal{S}_{n,n+1}$, for integer n, are i.i.d. A similar argument shows that for any $\epsilon > 0$, the increments $\mathcal{S}_{n\epsilon,(n+1)\epsilon}$ are i.i.d.

The discussion above implies that both L_t and R_t are infinitely divisible random variables. Moreover,

1. by the scale invariance of $\mathcal{C}$ and the fact that quantum area scales as the square of quantum length, it follows that L_t is equal in law to $\sqrt{t}L_1$, and
2. by the symmetry of the construction, we also have that L_t is equal in law to L_{-t}.

It is well known in the literature on stable processes, that these properties imply that L_1 is a Gaussian with mean zero [Nol03].[12]

The same follows for any linear combination of L_1 and R_1, hence the pair is jointly Gaussian, and by symmetry the joint law is the same if the laws of L_1 and R_1 are reversed. □

We say that a time $t \in \mathbf{R}$ is a local cut time for η' if there exists $\epsilon > 0$ such that $\eta'([t-\epsilon, t))$ is disjoint from $\eta'((t, t+\epsilon])$. If t is a local cut time for η', then we call $\eta'(t)$ a local cut point for η'. The following lemma, which gives the almost sure Hausdorff dimension of the local cut times of η', will be used to identify the diffusion matrix of (L, R).

Lemma 9.4. *Suppose that $\kappa \in (2, 4)$ so that $\kappa' \in (4, 8)$. Then the Hausdorff dimension of the set of local cut times for η' (parameterized by quantum area) is almost surely $1 - \frac{2}{\gamma^2}$.*

Proof. Let η_L (resp. η_R) denote the left (resp. right) side of the outer boundary of $\eta'([-\infty, 0])$. Then the points in $\left(\eta_L \cap \eta_R\right) \setminus \{0\}$ are all local cut points for η'. More generally, we let η_L^t (resp. η_R^t) denote the left (resp. right) side of the outer boundary of $\eta'([-\infty, t])$. Then

$$\bigcup_{t \in \mathbf{Q}} \left(\eta_L^t \cap \eta_R^t\right) \setminus \{\eta'(t)\}$$

gives all of the local cut points of η'. By the invariance of the setup, the law of the dimension of the amount of time that η' spends in $\left(\eta_L^t \cap \eta_R^t\right) \setminus \{\eta'(t)\}$ does not depend on t. Thus to prove the result, it suffices to show that the dimension of the amount of time that η' spends in $\left(\eta_L \cap \eta_R\right) \setminus \{0\}$ is almost surely $1 - \frac{2}{\gamma^2}$.

[12] This can be seen directly by observing that equivalence in law of L_1 and $-L_1$ imply that the characteristic function $\phi(t) = \mathbf{E}e^{iL_1}$ is real; the divisibility and scaling rules imply that $\log \phi(a) = \log \phi(1) a^2$ for rational a, and hence $\log \phi$ is a centered parabola, which implies that L_1 is Gaussian.

Recall from the proof of Lemma 9.2 that $\eta'([-\infty, 0])$ parameterizes a wedge of weight $2 - \frac{\gamma^2}{2}$. Consequently, the γ-LQG area of the surface beads in $\eta'([-\infty, 0])$ between η_L and η_R can be sampled from by first sampling a Bessel process $\widehat{Y}$ of dimension $\frac{4}{\gamma^2}$ (recall Proposition 4.16). Note that $\{t < 0 : \eta'(t) \in (\eta_L \cap \eta_R) \setminus \{0\}\} = \{t < 0 : \widehat{Y}_{-t} = 0\}$. Let $\widehat{\ell}$ be the local time at 0 of $\widehat{Y}$ and let $\widehat{T}$ be the right-continuous inverse of $\widehat{\ell}$. Note that the latter set is equal to the range of $\widehat{T}$. Recall that the inverse local time of a Bessel process of dimension δ is a $1 - \frac{\delta}{2}$ stable subordinator. By [Ber96, Chapter III, Theorem 15], the almost sure Hausdorff dimension of the range of a $1 - \frac{\delta}{2}$ stable subordinator is given by $1 - \frac{\delta}{2}$. Plugging in the value $\delta = \frac{4}{\gamma^2}$ gives $1 - \frac{2}{\gamma^2}$, as desired. □

We are now going to determine the matrix Λ from Lemma 9.2. Before we do so, we first need to recall the definition of a cone time. For each $\theta \in [0, 2\pi)$, we let $\mathbf{W}_\theta = \{z \in \mathbf{C} : \arg(z) \in [0, \theta]\}$ be the Euclidean wedge of opening angle θ. Suppose that Z is a continuous process taking values in $\mathbf{R}^2$. A time $t_0 \geq 0$ is said to be a **θ-cone time**, $\theta \in (0, 2\pi)$, if there exists $\epsilon > 0$ such that $Z([t_0, t_0 + \epsilon]) \subseteq \mathbf{W}_\theta + Z_{t_0}$. We will make use of a result due to Evans [Eva85] which gives that the almost sure Hausdorff dimension of the set of θ-cone times for a 2-dimensional standard Brownian motion (i.e., with covariance matrix given by the identity) is equal to 0 if $\theta \in [0, \frac{\pi}{2}]$ and given by $1 - \frac{\pi}{2\theta}$ for $\theta \in (\frac{\pi}{2}, 2\pi)$. This result will allow us to determine Λ from Lemma 9.2.

Lemma 9.5. *For each $\kappa \in (2, 4)$ (hence $\kappa' \in (4, 8)$) there exists a constant $a > 0$ such that the linear transformation Λ of Lemma 9.2 is represented by the matrix*

$$\Lambda = a \begin{pmatrix} \sin(\theta_\kappa) & -\cos(\theta_\kappa) \\ 0 & 1 \end{pmatrix}. \tag{9.8}$$

In particular, $\operatorname{cov}(L_1, R_1) = -a^2 \cos(\theta_\kappa)$.

Proof. As in the statement of Lemma 9.2, we write $(L, R) = \Lambda(X^1, X^2)$. We note that a local cut time as in Lemma 9.4 corresponds to a $\frac{\pi}{2}$-cone time for the process (L, R). This, in turn, corresponds to a θ-cone time for (X^1, X^2) for some value of θ. Applying the main result of [Eva85], the value of θ is determined by $1 - \frac{2}{\kappa} = 1 - \frac{\pi}{2\theta}$. That is, $\theta = \theta_\kappa = \frac{\pi\kappa}{4}$. This implies that Λ maps the line with angle θ (relative to the first coordinate axis) to the second coordinate axis, fixes the first coordinate axis, and applies the same scaling to both of these lines. Therefore, up to a constant rescaling, Λ is given by

$$\begin{pmatrix} 1 & \cos(\theta_\kappa) \\ 0 & \sin(\theta_\kappa) \end{pmatrix}^{-1} = \begin{pmatrix} 1 & -\cot(\theta_\kappa) \\ 0 & \csc(\theta_\kappa) \end{pmatrix}.$$

Scaling this matrix by $\sin(\theta_\kappa)$ gives the matrix in the right hand side of (9.8). □

Lemma 9.6. *For $\kappa = 2$ (hence $\kappa' = 8$) there exists a constant $a > 0$ such that the linear transformation Λ of Lemma 9.2 is represented by a times the identity matrix. In particular,* $\mathrm{cov}(L_1, R_1) = 0$.

Proof. First, since SLE_8 does not have cut points, it must be that $\mathrm{cov}(L_1, R_1) \leq 0$, so it is just a matter of showing that $\mathrm{cov}(L_1, R_1) = 0$. One can see this because if we take the quantum wedge of weight $2 - \frac{\gamma^2}{2} = 1$ corresponding to $\mathbf{C} \setminus \eta'((-\infty, 0])$ and then conformally map it to $\mathcal{S}$, then the projection of the corresponding field onto $\mathcal{H}_1(\mathcal{S})$ has zero drift. In other words, $a = 0$ using the notation of Table 1.1. From this perspective, it is clear that (L, R) gets arbitrarily close to reaching simultaneous running global minimum infinitely often (but never reaches an actual simultaneous global running minimum, since this would correspond to a cut point in the path). From this, it follows that $\mathrm{cov}(L_1, R_1) = 0$ as a pair of standard Brownian motions with negative covariance will not get arbitrarily close to reaching simultaneous running global minima infinitely often. Indeed, to see this final claim suppose that (Y^1, Y^2) is such a pair of Brownian motions. Then we can write $Y^2 = \alpha Y^1 + \widetilde{Y}^2$ where $\alpha \in (-1, 0)$ and $\widetilde{Y}^2$ is a Brownian motion independent of Y^1 with $\mathrm{var}(\widetilde{Y}_1^2) = 1 - \alpha^2$. By the law of the iterated logarithm, we know that if Y_t^1, Y_t^2 are close to being at a global simultaneous minimum then they are both with high probability given by $-\sqrt{2t \log\log t^{-1}}(1 + o(1))$ for t large (since each of the Y_t^j is marginally a standard Brownian motion). At such a time, this implies that $\widetilde{Y}_t^2 = Y_t^2 - \alpha Y_t^1$ is close to $-(1 - \alpha)\sqrt{2t \log\log t^{-1}}(1 + o(1))$. This, in turn, cannot happen with positive probability for arbitrarily large t since another application of the law of the iterated logarithm implies that the global running minimum of $\widetilde{Y}_t^2$ is with high probability given by $-\sqrt{2(1 - \alpha^2)t \log\log t^{-1}}(1 + o(1))$ and $1 - \alpha > \sqrt{1 - \alpha^2}$ for $\alpha \in (-1, 0)$. □

Proof of Theorem 9.1. The result follows by combining Lemma 9.2 with Lemma 9.5 if $\kappa \in (2, 4)$ and with Lemma 9.6 if $\kappa = 2$. □

10 Trees determine embedding

10.1 Theorem statement and proof using three lemmas

Let $(\mathbf{C}, h, 0, \infty)$ be a γ-quantum cone, and let η' be an independent space-filling $\mathrm{SLE}_{\kappa'}$ in $\mathbf{C}$ from ∞ to ∞ with $\kappa' = 16/\gamma^2 \in (4, \infty)$. We assume that η' is parameterized according to γ-LQG area so that for each $s < t$ we have $\mu_h(\eta'([s, t])) = t - s$. It will be convenient for this section to fix the embedding of the quantum cone in $\mathbf{C}$ in a particular way (different from the "canonical description" discussed in Section 4.3):

namely, by redefining h and η' via a quantum coordinate change by a translation and dilation as necessary so that there exists a conformal map

$$F\colon \mathbf{C} \setminus \overline{\mathbf{D}} \to \mathbf{C} \setminus \eta'([-1,1]),$$

whose range is the entire unbounded component of $\mathbf{C} \setminus \eta'([-1,1])$, that has the Laurent expansion

$$F(z) = z + \sum_{n=1}^{\infty} \alpha_n z^{-n}. \tag{10.1}$$

Using terms that we will define in Section 10.3, this amounts to scaling the embedding so that $\eta'([-1,1])$ (together with the set of points disconnected from ∞ by $\eta'([-1,1])$) has "harmonic center" zero and "outer conformal radius" one. In a certain conformal sense (see Section 10.3) this means that $\eta'([-1,1])$ has the same size and center as the unit disk. Given this embedding in $\mathbf{C}$, we will not expect that the quantum cone marked point $\eta'(0)$ is exactly equal to 0. However, the "infinite" endpoint of the cone will be ∞ as usual.

We have already shown in Section 9 that $(\mathbf{C}, h, \eta')$ determines the Brownian motion pair (L_t, R_t) indexed by $t \in \mathbf{R}$. The aim of this section is to show that (L_t, R_t) a.s. uniquely determines the triple $(\mathbf{C}, \mu_h, \eta')$ up to a rotation of $\mathbf{C}$.[13] (The scaling and translation are otherwise determined by the requirement that F can be written as in (10.1).)

Now, note that F^{-1} maps the unbounded component of $\mathbf{C} \setminus \eta'([-1,1])$ back to $\mathbf{C} \setminus \overline{\mathbf{D}}$, and applying this map as a coordinate change, we obtain a quantum surface $(\mathbf{C} \setminus \overline{\mathbf{D}}, \widetilde{h})$ that corresponds to what we get by "cutting out" the piece $\eta'([-1,1])$. Let $\mathcal{F}$ be the σ-algebra generated by measurable functions of this $\widetilde{h}$. Informally, $\mathcal{F}$ contains the events that only depend on the overall quantum surface obtained by deleting $\eta'([-1,1])$ (though it also encodes the way the rotation is fixed at ∞). Now let $\mathcal{B}$ be the σ-algebra generated by the restriction of (L_t, R_t) to $[-1,1]$.

The main result of this section is the following:

Theorem 10.1. *The conditional law of F given the σ-algebra generated by* both $\mathcal{F}$ *and $\mathcal{B}$ is a.s. deterministic.*

Before going on, let us point out that Theorem 10.1 immediately implies a seemingly stronger statement, Corollary 10.2 below, which states that the parameterized path

[13]The question of whether μ_h determines h will not be addressed in this paper; however, the third author has a work in progress with Nathanael Berestycki and Xin Sun that will show that μ_h indeed a.s. determines h. We remark that it is not difficult to imagine that μ_h might determine h. One could mollify μ_h by smooth bump function supported on an ϵ radius ball, and thus obtain a measure with a smooth density function — the logarithm of which might be a good approximation for γh, and might perhaps a.s. converge to γh (modulo additive constant) as $\epsilon \to 0$.

η' and the measure μ_h are both determined by the Brownian motion (L_t, R_t), up to a rotation of $\mathbf{C}$ about 0. In other words, the infinite volume peanosphere described by L_t and R_t a.s. has a uniquely defined conformal structure, which determines its embedding in $\mathbf{C}$. Establishing this has been one of the main goals of this paper.

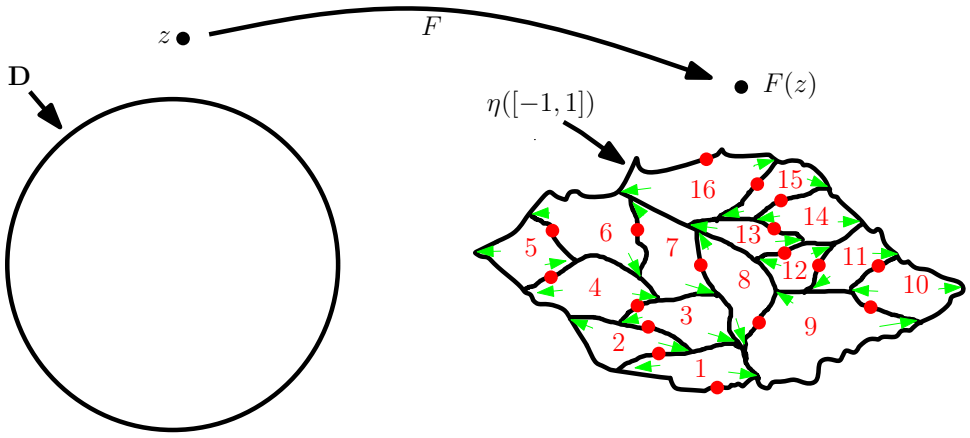

Figure 10.1: The conformal map $F\colon \mathbf{C}\backslash\overline{\mathbf{D}} \to \mathbf{C}\backslash\eta'([-1,1])$ is normalized to look like the identity near infinity. Taking $k = 3$, we divide $[-1, 1]$ into $2^{k+1} = 16$ equal-sized subintervals and illustrate their images, numbered according to the order in which they are traversed by η'. The red dots indicate the η' images of the endpoints of these intervals. The green arrow heads point to η' images of the times at which L_t and R_t were minimal within each given interval. This figure should correspond to $\kappa' \geq 8$, because the interval images shown do not have cut points. A $\kappa' \in (4, 8)$ image would be similar but somewhat more complicated to illustrate.

Corollary 10.2. *In the setting described just above, the pair (L_t, R_t) a.s. uniquely determines the measure μ_h and the path η' up to a coordinate change by a rotation of $\mathbf{C}$ about the origin.*

Proof. Suppose first that $\kappa' \geq 8$ so that the interior of $\eta'([-1, 1])$ is a.s. a connected open set, homeomorphic to the disk. In this case, there is a unique way to conformally map this set to a unit disk so that $\eta'(\pm 1)$ map to ± 1 and a third special point (say the $\eta'(t)$ where t the value in $[-1, 1]$ for which L_t is minimal) maps to i. The quantum measure on the boundary of $\eta'([-1, 1])$ then maps to a measure on the unit circle. Theorem 10.1 implies that the restriction of (L_t, R_t) to $[-1, 1]$ determines this measure. Thus, the restriction of (L_t, R_t) to $[-1, 1]$ tells us at least *some* information about the quantum surface parameterized by $[-1, 1]$, namely, what the boundary measure looks like when the surface is parameterized by the unit disk. This is the information we need to know the shape the surface takes when it is welded onto

another surface. In the case that $\kappa' < 8$, one obtains similar information about each of the beads comprising the surface.

By scaling, and the fact that recentering a quantum cone at a deterministic time yields another quantum cone, Theorem 10.1 implies the analog of Theorem 10.1 in which $[-1, 1]$ is replaced by $[a, b]$ for any a and b. If we partition $[-1, 1]$ into finitely many intervals, then we obtain this information about each of these intervals; from this, we see that the η' image of each of these intervals is determined by the restriction of (L_t, R_t) to $[-1, 1]$, together with the quantum surface parameterized by the complement of $[-1, 1]$. If $[a, b]$ is such an interval, then $\eta'([a, b])$ is determined. The measure μ_h is the one for which $\mu_h(\eta'([a, b])) = b - a$. Exhausting over pairs a and b in $[-1, 1]$ we find that the quantum surface parameterized by $[-1, 1]$ is determined (together with its conformal structure) by the restriction of (L_t, R_t) to $[-1, 1]$. The same holds for $[-C, C]$ for any C, and taking the $C \to \infty$ limit, we find that the entire conformal structure, together with the measure and path, is determined by (L_t, R_t). □

We will actually establish a stronger quantitative version of Theorem 10.1 that implies Theorem 10.1. To make this stronger statement, let us define $\mathcal{B}_k$ to be the σ-algebra generated by the following random variables:

1. The values L_t and R_t for each $t \in [-1, 1]$ that is an integer multiple of $\delta = 2^{-k}$.
2. The infimum of L_t and the infimum of R_t when restricted to each interval of the form $[a2^{-k}, (a + 1)2^{-k}] \subseteq [-1, 1]$, for $a \in \mathbf{Z}$.

Also, let $\mathcal{N}_1, \mathcal{N}_2, \ldots, \mathcal{N}_{2^{k+1}}$ denote the quantum surfaces parameterized by these intervals. As illustrated in Figure 10.1, each $\mathcal{N}_j$ comes with four marked points, and the information encoded by the $\mathcal{B}_k$ determines the lengths of the four boundary segments bounded by the red dots and green arrowheads in Figure 10.1. We have already established that, given these boundary lengths, the $\mathcal{N}_j$ are conditionally independent of each other (recall the proof of Lemma 9.2), and that together the $\mathcal{N}_j$ determine the conformal structure of the combined quantum surface obtained by gluing them all together (this follows from Theorem 1.11 and Theorem 1.12). Intuitively, we might expect that once we know $\mathcal{B}_k$ for a large k value, the extra information we obtain by sampling the $\mathcal{N}_j$ would typically "average out" and not have a big effect on the function F. This is indeed the case:

Theorem 10.3. *Write $\delta = 2^{-k}$ and let Δ be the positive solution to the KPZ equation*

$$x = \frac{\gamma^2}{4}\Delta^2 + \left(1 - \frac{\gamma^2}{4}\right)\Delta, \tag{10.2}$$

with $x = 2$. (Note that when $\gamma \in (0, 2)$ (10.2) says that $x = 2$ is a convex combination of Δ and Δ^2, which implies $\Delta \in (\sqrt{2}, 2)$, so in particular $\Delta - 1 > 0$.) Then almost surely

$$\liminf_{k \to \infty} \frac{\log \mathbf{E}\Big[\mathrm{Var}\big(F(z) \,|\, \mathcal{B}_k, \mathcal{F}\big)\Big|\mathcal{F}\Big]}{\log \delta} \geq \Delta - 1.$$

Informally, Theorem 10.3 states that once the outer surface (the unbounded component of the complement of $\eta'([-1, 1])$) is fixed, the conditional variance of $F(z)$ given $\mathcal{B}_k$ a.s. decays at least as fast as $\delta^{\Delta - 1}$ (up to a factor whose log is $o(|\log \delta|)$) where $\delta = 2^{-k}$. Note that Theorem 10.3 implies that for each fixed $z \in \mathbf{C} \setminus \overline{\mathbf{D}}$, the quantity

$$F_k(z) := \mathbf{E}[F(z) \,|\, \mathcal{B}_k, \mathcal{F}]$$

converges a.s. to $F(z)$ exponentially fast as a function of k, which in particular implies that $F(z)$ is $(\mathcal{B}, \mathcal{F})$ measurable (up to redefinition on a set of measure zero) and hence implies Theorem 10.1. Note that these maps F_k are approximations to F, and that for each fixed z, $F_k(z)$ is a martingale in k. We remark that it is not hard to see that for each z, there are uniform bounds on what the value of $F(z)$ can be (see Section 10.3) — and thus, since each $F_k(z)$ is an average of analytic, uniformly bounded functions, the maps F_k are themselves a.s. analytic on $\mathbf{C} \setminus \overline{\mathbf{D}}$. However, one would not necessarily expect the maps F_k be one-to-one.

The proof of Theorem 10.3 will be a consequence of three lemmas, which we state here and then prove in the coming subsections. The first of these is a simple and very general variance bound known as the Efron-Stein bound, established by Efron and Stein in 1981 [ES81]:

Lemma 10.4. *Let $A = A(X_1, X_2, \ldots, X_n)$ be a function of n independent random variables defined on a common measure space such that $\mathbf{E}[A^2] < \infty$. Then*

$$\mathrm{Var}(A) \leq \sum_{i=1}^{n} \mathbf{E}[\mathrm{Var}(A \,|\, X_j : j \neq i)].$$

As stated above, given $\mathcal{B}_k$ the quantum surfaces $\mathcal{N}_j$ are conditionally independent of each other, and $F(z)$ is a function of these objects. That is the context in which Lemma 10.4 will be used. To bound the overall variance of $F(z)$ it is enough to bound the expected amount of variance involved in resampling the quantum surface corresponding to a randomly chosen *one* of the pockets from Figure 10.1 conditioned on $\mathcal{F}$ and on all of the other pockets. One way to bound this variance would be to give an absolute bound on how much z can move when a pocket is replaced; the variance would then be at most the square of that bound. Indeed, the second lemma we introduce is a simple complex analysis observation that is relevant to the

following question: when one cuts out a small piece of a quantum surface, such as one of the $\mathcal{N}_j$, and glues another piece in its place, how much can the embedding of the remainder of the quantum surface be distorted?

Lemma 10.5. *There exist constants $C_1, C_2 > 0$ such that the following is true. Let K_1 be a hull of diameter at most r and K_2 another hull such that there exists a conformal map $F\colon \mathbf{C} \setminus K_1 \to \mathbf{C} \setminus K_2$ of the form*

$$F(z) = z + \sum_{n=1}^{\infty} \alpha_n z^{-n}.$$

Then whenever $\operatorname{dist}(z, K_1) \geq C_1 r$ *we have that*

$$|F(z) - (z + b_2 - b_1)| \leq C_2 r^2 |z - b_1|^{-1} \tag{10.3}$$

where b_i for $i = 1, 2$ is the harmonic center of K_i as defined in Section 10.3 below.

Note that if the diameter of a pocket is r, and resampling it affects $F(z)$ by at most $O(r^2)$, then the variance involved in this resampling is $O(r^4)$. The third lemma we need is a fact, closely related to a special case of the KPZ theorem, that will help us control the diameters of the pockets.

Lemma 10.6. *For a given k, suppose that j is chosen uniformly at random from the set $\{1, 2, \ldots, 2^{k+1}\}$. Then it is almost surely the case that the conditional expected size of* $\operatorname{diam}(\mathcal{N}_j)^4$ *given $\mathcal{F}$ decays almost as fast as δ^{Δ} (see the precise statement below) where Δ solves the KPZ equation* (10.2) *with $x = 2$. The precise statement is that a.s.*

$$\liminf_{k \to \infty} \frac{\log \mathbf{E}[\operatorname{diam}(\mathcal{N}_j)^4 \mid \mathcal{F}]}{\log \delta} \geq \Delta, \tag{10.4}$$

where here $\operatorname{diam}(\mathcal{N}_j)$ *is the diameter of the embedding of $\mathcal{N}_j$ into* $\mathbf{C}$.

We next observe that Theorem 10.3 is a simple consequence of these three lemmas (which we have yet to prove).

Proof of Theorem 10.3. Lemma 10.5 implies that the conditional variance of $F(z)$ involved when one resamples one of the $\mathcal{N}_j$ is at most of order $\operatorname{diam}(\mathcal{N}_j)^4$. (Note that if z is fixed, then it follows from basic complex analysis — see the discussion in Section 10.3 — that the distance from $F(z)$ to $\eta'([-1, 1])$ is at least some constant that depends only on z.) Together with Lemma 10.4, this implies that the conditional variance of $F(z)$ given $\mathcal{F}$ and $\mathcal{B}_k$ is at most (a constant times) the expected sum of the $\operatorname{diam}(\mathcal{N}_j)^4$ over all j values, which is just δ^{-1} times the expectation of $\operatorname{diam}(\mathcal{N}_j)^4$ when j is chosen uniformly from $\{1, 2, \ldots, 2^{k+1}\}$. This latter expectation is bounded in Lemma 10.6, which shows that it decays at least as fast as δ^{Δ} (in the sense that the lim inf of the ratio of the logarithms is at most one), and this implies Theorem 10.3. □

The proofs of Lemma 10.4 and Lemma 10.5 are both fairly straightforward, but the proof of Lemma 10.6 is a bit more interesting. Essentially, it will be a variant of the KPZ theorem, but we will have to use some tricks to account for the fact that the parameterization of the random quantum surface in question is not fixed as it is in the KPZ formulation of [DS11a] and also the fact that the statement involves random chunks of the surface traced by η' over δ increments of time, instead of the random Euclidean balls of quantum mass δ that appear in the KPZ formulation of [DS11a].

10.2 Proof of variance bound

We next include a short proof of Lemma 10.4 (originally proved by Efron and Stein in [ES81]). We include this for completeness, and to emphasize that this is an easy fact to derive, but the reader who is already familiar with this inequality may skip this subsection.[14]

Proposition 10.7. *Let I be an arbitrary index set. Let (X_i) for $i \in I$ be a collection of real-valued random variables on a common measure space. Let ν be a probability measure on I and assume that $\int \mathbf{E}[X_i^2] d\nu(i) < \infty$. Write $X = \int X_i d\nu(i)$. In words, X is an average of the X_i, where the average is taken with respect to ν. Then*

$$\operatorname{Var} X \leq \int_I \operatorname{Var}(X_i) d\nu(i). \tag{10.5}$$

Proof. The map $X \to \operatorname{Var}(X)$ is a quadratic, non-negative map from L^2 of the measure space to $\mathbf{R}$. In particular it is convex. Applying Jensen's inequality to this map yields (10.5). □

Proposition 10.8. *Let Y and Z be independent random variables and let $A = A(Y, Z)$ be a random variable that is a function of the pair (Y, Z) with $\mathbf{E}[A^2] < \infty$. The variance of the upper left increment in Figure 10.2 is less than or equal to the expected conditional variance of the lower right increment. That is,*

$$\operatorname{Var}(\mathbf{E}[A \,|\, Y]) \leq \mathbf{E} \operatorname{Var}\big[A \,|\, Z\big]. \tag{10.6}$$

Informally, Proposition 10.8 states that the expected amount of fluctuation of our expectation of A when we observe Y if we *have not* already observed Z is less than the expected amount of fluctuation when we observe Y if we *have* already observed Z. For example, suppose Y and Z are both uniformly chosen from $\{-1, 1\}$ and $A(Y, Z) = YZ$. If we do not know Z, then observing Y does not change our

[14] We thank Asaf Nachmias for bringing [ES81] to our attention.

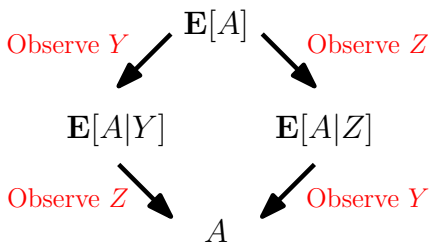

Figure 10.2: Two martingale pathways describing updated conditional expectations of A as we observe Y and Z, in either of the two orders. The variance of the upper left arrow is at most that of the lower right arrow on average.

conditional expectation of A. But if we do know Z, then observing Y changes our conditional expectation for A from 0 to an element of $\{\pm 1\}$. Thus, in this particular case, the left hand side of (10.6) evaluates to 0 while the right hand side evaluates to 1.

Proof of Proposition 10.8. The quantity $B = \mathbf{E}[A \,|\, Y]$ is a random variable that can be written as a function of Y. If z is fixed, then $B_z = \mathbf{E}[A \,|\, Y, Z = z] = \mathbf{E}[A(Y, z) \,|\, Y]$ is also a random variable that can be written as a function of Y. Note that $B = \int B_z dz$ where dz is the law of Z. Thus it follows from (10.5) that $\operatorname{Var} B \leq \mathbf{E} \operatorname{Var} B_z$, where the expectation on the right is taken w.r.t. z values chosen from the law of Z. This is another way of writing (10.6). □

Proof of Lemma 10.4. Consider the martingale $Y_j = \mathbf{E}[A \,|\, X_1, X_2, \ldots, X_j]$, indexed by $j = 0, \ldots, n$. By the orthogonality of martingale increments, we have

$$\operatorname{Var}(A) = \sum_{i=1}^{n} \mathbf{E} \operatorname{Var}[Y_j \,|\, X_1, X_2, \ldots, X_{j-1}]. \tag{10.7}$$

We will now apply Proposition 10.8 to argue that the variance (of the change in our conditional expectation for A) that comes from observing X_i, given that we know only $X_1, X_2, \ldots, X_{i-1}$, is less than the variance that comes from observing X_i when we know *all* of X_j with $j \neq i$. By treating $X_1, X_2, \ldots, X_{i-1}$ as given and applying Proposition 10.8 with X_i playing the role of Y and the variables $X_{i+1}, X_{i+2}, \ldots, X_n$ together playing the role of Z, we obtain

$$\begin{aligned} \mathbf{E} \operatorname{Var}[Y_i \,|\, X_1, X_2, \ldots, X_{i-1}] &= \mathbf{E} \operatorname{Var}\Big[\mathbf{E}[A|X_1, X_2, \ldots, X_i] \,|\, X_1, X_2, \ldots, X_{i-1}\Big] \\ &\leq \mathbf{E} \operatorname{Var}[A \,|\, X_j : j \neq i] \end{aligned}$$

Applying this bound to each term of (10.7) yields the proposition. □

10.3 Proof of basic distortion lemma

This subsection recalls a few standard complex analysis facts (see, e.g., the text [Rud87]). We will work in the whole plane setting and use the term *hull* to refer to a closed, bounded, connected subset K of $\mathbf{C}$ for which $\mathbf{C} \setminus K$ is also connected. By the Riemann mapping theorem, and using the standard Laurent expansion, there exists a unique conformal map $F\colon \mathbf{C} \setminus \overline{\mathbf{D}} \to \mathbf{C} \setminus K$ that has the form

$$F(z) = a_{-1}z + a_0 + \sum_{n=1}^{\infty} \alpha_n z^{-n}, \tag{10.8}$$

where a_{-1} is positive and real. (This map fixes ∞.) We refer to the a_0 of (10.8) as the *harmonic center* of K. Computing term by term, we see that the mean value of F on $\partial B(0, r)$, for any $r > 1$, is given by a_0. If F extends continuously to $\partial\mathbf{D}$, then taking $r \to 1$ shows that the mean value of the extension of F to $\partial\mathbf{D}$ is also a_0. Another way to say this (which makes sense regardless of whether F extends continuously to the boundary) is that a_0 is the average value of the points in ∂K sampled according to harmonic measure viewed from infinity. We say that K is *centered* if its harmonic center is 0.

We refer to the value a_{-1} of (10.8) as the *outer conformal radius* of K. (It can also be called "whole plane capacity"; recall that whole plane Loewner evolution, directed toward ∞, describes an increasing sequence of hulls parameterized by the log of this quantity.) Observe that $r\overline{\mathbf{D}}$ has outer conformal radius r. The following is known as the area theorem [Rud87, Theorem 14.13].

Proposition 10.9. *Let K be a centered hull of outer conformal radius 1, so that there exists a conformal map $F\colon \mathbf{C} \setminus \overline{\mathbf{D}} \to \mathbf{C} \setminus K$ of the form*

$$F(z) = z + \sum_{n=1}^{\infty} \alpha_n z^{-n}. \tag{10.9}$$

Then $\sum_{n=1}^{\infty} n|\alpha_n|^2 \leq 1$.

In particular, Proposition 10.9 implies that $|\alpha_n| \leq n^{-1/2}$ for each n, so

$$|F(z) - z| \leq \sum_{n=1}^{\infty} n^{-1/2}|z|^{-n}.$$

When $|z| > 2$, the right hand side is dominated by the first term, which implies

$$|F(z) - z| \leq 2|z|^{-1}. \tag{10.10}$$

Similarly $|F'(z) - 1| \leq \sum_{n=1}^{\infty} n^{1/2}|z|^{-n-1}$, which is dominated by the first term when $|z| > 4$, so that in this case

$$|F'(z) - 1| \leq 2|z|^{-2}. \tag{10.11}$$

Proposition 10.10. *If a hull K has outer conformal radius r, then K has diameter at most $4r$. Also, the smallest closed ball containing K has radius at least r (and diameter at least $2r$).*

Proof. By scaling and translating, we may reduce to the case that K has outer conformal radius 1 and $0 \in K$. We now let F be as in (10.8) and apply the Koebe 1/4 theorem to the function $\Phi(z) = 1/F(1/z)$ (we take $\Phi(0) = 0$). Observe that Φ is a conformal map from $\mathbf{D}$ to a subset of the complex plane; since $\Phi(0) = 0$ and $\Phi'(0) = 1$, Koebe 1/4 states that its image contains $B(0, \frac{1}{4})$. This in turn implies that the image of $\mathbf{C} \setminus \overline{\mathbf{D}}$ under F contains the set $\mathbf{C} \setminus \overline{B(0,4)}$, so that $K \subseteq \overline{B(0,4)}$. Since this is true for any translation of K (as long as $0 \in K$), we conclude that K has diameter at most 4. The second sentence follows from the Schwarz lemma, which states that if the map $1/F(1/z)$ has derivative $1/z$ at the origin, then it cannot map $\mathbf{D}$ into a strict subset of a radius 1 disk. □

We remark that both of the bounds mentioned in Proposition 10.10 are tight. For the tightness of the first, one can check explicitly that $K = [0,4] \subseteq \mathbf{R} \subseteq \mathbf{C}$ has outer conformal radius 1. This is related to the fact that the inverted set $\{z : 1/z \in K\} = [1/4, \infty]$, is the complement of a domain $\mathbf{C} \setminus [1/4, \infty)$ whose conformal radius (viewed from zero) is one. (This is the standard example that shows the tightness of the Koebe 1/4 theorem.) For the tightness of the second bound in Proposition 10.10, it suffices to consider the trivial case $K = \overline{\mathbf{D}}$.

Proof of Lemma 10.5. If $r = 1$ and $a = 0$, then (10.3) can be seen by applying (10.10) and (10.11) to the pair of maps $F_i \colon \mathbf{C} \setminus \mathbf{D} \to \mathbf{C} \setminus K_i$ and noting that $F = F_2 \circ F_1^{-1}$. The general case follows by scaling and translation. □

10.4 Proof of KPZ lemma on diameter fourth powers

10.4.1 A "fixed parameterization" variant of the fourth power estimate

As part of the proof of a form of the KPZ scaling dimension relation, as presented in [DS11a, Section 4], one lets h denote an instance of the zero-boundary GFF on a bounded domain D. One then fixes a $\delta > 0$ and then seeks to compute the expectation of ϵ^{2x} where ϵ is a random number chosen through the following steps:

1. Sample μ_h from its law weighted by $\mu_h(S)$, where S is a bounded, open set with $\overline{S} \subseteq D$.
2. Sample a point z from μ_h restricted to S.

3. Let ϵ be the radius of the ball centered at z with quantum mass exactly δ.

The version of the KPZ theorem[15] established in [DS11a] states that

$$\lim_{\delta \to 0} \frac{\log \mathbf{E}[\epsilon^{2x}]}{\log \delta^{\Delta}} = 1, \tag{10.12}$$

where Δ and x are related by (10.2).

We would like to do something similar but with a slightly modified third step. Namely, we will take ϵ to be the radius of the smallest ball centered at z that contains $\eta'([b-\delta, b+\delta])$ where $\eta'(b) = z$. (Note that there is a.s. a unique b for which $\eta'(b) = z$.) The ϵ we define this way can only be larger than the one defined above. We are only concerned with bounding $\mathbf{E}[\epsilon^4]$ from above which amounts to considering the case $x = 2$.

Proposition 10.11. *Let S be open with $\overline{S} \subseteq \mathbf{D}$. Let h be an instance of the GFF on $\mathbf{C}$ with the additive constant fixed so that $h_1(0) = 0$ (i.e., the average of h on $\partial\mathbf{D}$ is equal to 0) and define μ_h as usual using a fixed $\gamma \in (0,2)$. Let η' be an independent full plane space-filling $\mathrm{SLE}_{\kappa'}$ from ∞ to ∞, parameterized so that $\mu_h(\eta'([s,t])) = t - s$ for all $s < t$ and $\eta'(0) = 0$. Now suppose that we*

1. *Sample μ_h from its law weighted by $\mu_h(S)$.*
2. *Sample a point z from μ_h restricted to S.*
3. *Let ϵ be the radius of the smallest closed ball centered at z that contains $\eta'([b-\delta, b+\delta])$ where b is taken so that $\eta'(b) = z$.*

Then using this definition of ϵ, we still have that $\mathbf{E}[\epsilon^4]$ is approximately δ^{Δ} in the sense that

$$\liminf_{\delta \to 0} \frac{\log \mathbf{E}[\epsilon^4]}{\log \delta^{\Delta}} = 1 \tag{10.13}$$

where Δ is the positive solution to (10.2) with $x = 2$.

The proof of (10.12) given in [DS11a, Section 4] implies that (10.13) would hold if we instead took ϵ to be the radius of the Euclidean ball centered at z containing δ

[15] The presentation in [DS11a] assumes that there is a random fractal set $\mathcal{X}$, independent of h, and that the x is a scaling exponent associated to $\mathcal{X}$, so that the probability that any given ϵ ball intersects $\mathcal{X}$ is approximately ϵ^{2x}. The quantity Δ is then interpreted as a quantum scaling exponent associated the fractal $\mathcal{X}$, which gives the probability that a δ quantum area ball centered at a quantum typical point intersects $\mathcal{X}$. However, we stress that (10.12) also makes sense without reference to any particular $\mathcal{X}$.

units of μ_h area.[16] It turns out that with a couple of supplemental arguments, the same proof also implies Proposition 10.11. We will not repeat the entire proof of [DS11a, Section 4] here, but we will give a short overview and explain the necessary supplemental arguments during the remainder of this subsection.

The proof in [DS11a, Section 4] actually begins with yet another analog of (10.12) which is stated as [DS11a, Theorem 4.2]. For this analog, one notes that if one has h and z, one can construct $h_r(z)$, which evolves as a Brownian motion in $-\log r$. One then establishes (10.12) with ϵ replaced by the smallest r for which

$$\gamma h_r(z) + \gamma Q \log r = \log \delta. \tag{10.14}$$

Roughly speaking, this is interpreted as the smallest r such that the "typical value" of $\log \mu_h\big(B(z,r)\big)$, conditioned on $h_r(z)$, is equal to $\log \delta$.

The next step in [DS11a, Section 4] is to derive (10.12) from [DS11a, Theorem 4.2]. This is done by deriving bounds ([DS11a, Lemmas 4.6–4.7]) on the probability that the actual value of $\log \mu_h\big(B(z,r)\big)$ differs from the LHS of (10.14) by a large amount. In order to establish Proposition 10.11 using the argument of [DS11a, Section 4], it suffices to establish variants of these lemmas using the definition of ϵ from Proposition 10.11.

The proofs of these variants are exactly the same as the proofs in [DS11a, Lemmas 4.6–4.7] except that one requires an analog, appropriate for our setting, of [DS11a, Lemma 4.5]. The statement and proof of this analog comprise the remainder of this subsection. We begin by giving a restatement of [DS11a, Lemma 4.5].

Proposition 10.12. *(Restatement of [DS11a, Lemma 4.5]) Fix $\gamma \in [0,2)$, let h be an instance of the GFF on $\mathbf{C}$ with $h_1(0) = 0$, and let μ_h be the γ-LQG area measure associated with h. Then the random variable $A = \log \mu_h(B(0,1/2))$ satisfies $p_A(t) := \mathbf{P}[A \leq t] \leq e^{-Ct^2}$ for some fixed constant $C > 0$ and all sufficiently negative values of t.*

The KPZ argument in [DS11a, Section 4] actually only requires the fact that $p_A(t)$ decays superexponentially (i.e., faster than e^{-Ct} for any C). Thus, the fact that $p_A(t)$ decays quadratic exponentially, as stated in Proposition 10.12, is somewhat more than is necessary for the purposes of [DS11a, Section 4]. Proposition 10.12 can be interpreted as bounding, within the particular setting of the proposition, the probability that $\epsilon > 1/2$ when $\delta = e^{-t}$ is extremely small and ϵ is defined to make $\log \mu_h\big(B(0,\epsilon)\big) = 0$. To bound the probability that the ϵ defined as in Proposition 10.11 exceeds $1/2$, we will need the following analog of Proposition 10.12.

[16] The setup in [DS11a, Section 4] assumes fixed boundary conditions on a bounded domain, which is somewhat different from our setup here. However, this distinction is not relevant to the argument in [DS11a, Section 4].

Proposition 10.13. *Fix $\gamma \in [0,2)$, let h be an instance of the GFF on $\mathbf{C}$ with $h_1(0) = 0$, and let μ_h be the γ-LQG area measure associated with h. Let η' be an independent space-filling $\mathrm{SLE}_{\kappa'}$ from ∞ to ∞ in $\mathbf{C}$ parameterized so that $\eta'(0) = 0$ and $\mu_h(\eta'([s,t])) = t - s$ for $s < t$. Let $a = \sup\{s < 0 : |\eta'(s)| = 1/2\}$ and $b = \inf\{s > 0 : |\eta'(s)| = 1/2\}$, and write $A' = \log\min(-a, b)$. Then*

$$p_{A'}(t) := \mathbf{P}[A' \leq t] \leq e^{-Ct^2/\log|t|} \tag{10.15}$$

for some fixed constant $C > 0$ and all sufficiently negative values of t.

Proof. It is enough to prove that (10.15) holds if we replace A' with either $\log(-a)$ or $\log b$ (which are equivalent by symmetry) since combining the two affects the RHS of (10.15) by at most a factor of 2. For the proof below, we redefine A' to be $\log b$.

The difficulty in proving Proposition 10.13 is that there are essentially two things that can make η' get to $\partial B(0, 1/2)$ in a small amount of time (which would make b small), only the first of which is dealt with in Proposition 10.12:

1. The total mass of $B(0, 1/2)$ being small.
2. The path η' filling only very small amounts of Euclidean area before reaching $\partial\mathbf{D}$ and/or somehow managing to avoid the parts of $B(0, 1/2)$ containing the most mass during its trajectory from 0 to $\partial B(0, 1/2)$.

To proceed with the analysis, let us imagine that we do the sampling in two steps. First we choose η', which determines the set $\eta'([0, b])$, although the value of b is not known yet. Then we let r denote the radius of the largest ball contained in $\eta'([0, b])$. Then we single out the value z such that $B(z, r) \subseteq \eta'([0, b])$. Then we sample h and check whether $\mu_h\big(B(z, r)\big) \leq e^t$. The latter condition is *necessary* in order for us to have to have $b < e^t$, so to establish (10.15) it suffices to show that

$$\mathbf{P}\Big[\log \mu_h\big(B(z, r)\big) \leq t\Big] \leq e^{-Ct^2/\log|t|}.$$

First, we observe that the random variable $T = 1/r$ decays exponentially, in that $\mathbf{P}[T \geq s] \leq e^{-Cs}$ for some C and all sufficiently large s. This can be seen by considering $\lfloor 1/2r \rfloor$ disks centered at 0 with radii $2r, 4r, 6r, \ldots$ and noting that conditioned on η' up to the first time it exits one of these disks, there is always a uniformly positive chance that it fills a disk of radius r before it exits the next disk outward. (See analogous bounds in [MS13a, Section 4.3.1].)

Second, observe that given η' and z, the law of $h_r(z)$ is given by a Gaussian with variance $\log T$ (plus or minus a constant); if we redefine T to be exactly this variance, then we can write $h_r(z) = W_{\log(T)}$ where W is a standard Brownian motion.

Third, observe that once $h_r(z)$ is known, there is a constant c such that the conditional law of the random variable $Z = \log \mu_h(B(z,r)) - \gamma h_r(z) + c \log r$ has quadratic exponential decay independently of r and $h_r(z)$. (This is included in [DS11a, Lemma 4.6].) The result now follows immediately from Proposition 10.14 as stated below. □

Proposition 10.14. *Let T be a random variable with the property that*

$$\mathbf{P}[T \geq s] \leq e^{-Cs} \tag{10.16}$$

for some $C > 0$ and all sufficiently large s. Independently of T, sample a standard Brownian motion W. Then define the random variable $X = W_{\log(T)} + c \log T + Y$ where c is a fixed constant and Y is an independent random variable such that

$$\mathbf{P}[Y \geq s] \leq e^{-Cs^2} \tag{10.17}$$

for sufficiently large s. Then for all sufficiently large a and some C' we have

$$\mathbf{P}[X \geq a] \leq e^{-C'a^2/\log(a)} \tag{10.18}$$

Proof. On can break the probability considered in (10.18) into two cases: $T > a^2$ and $T \leq a^2$. In the former case, we get a bound of e^{-Ca^2} from (10.16). In the latter case, $W_{\log(T)}$ is a Brownian motion stopped at time at most $2 \log a$. Thus, for an appropriate C', the probability that $W_{\log(T)}$ exceeds $a/2$ decays as fast as the RHS of (10.18), and the probability that $Y > a/2$ decays faster than the RHS of (10.18) by (10.17). □

10.4.2 Quantum cones: smooth centering and resampling

We would now like to use Proposition 10.11 to establish Lemma 10.6. The statements of these two results are quite similar in a sense. Both involve expected fourth powers of ϵ values, which are defined from h, η', and δ in a similar way. However, the statements are set up rather differently. The former involves a GFF h on $\mathbf{C}$ and the quantum surface parameterized by a fixed domain S. Although S is fixed, its quantum measure $\mu_h(S)$ is random (and one weights by this quantum measure before sampling the quantum typical point z). The latter involves the random piece of a quantum cone traced by η' during the time interval $[-1, 1]$. Although the quantum size of the glued-in quantum surface is fixed, the set $\eta'([-1, 1])$ that parameterizes it is random.

Despite these differences between the setups, one might expect that the way that $\mathbf{E}[\epsilon^4]$ scales as $\delta \to 0$ in the two settings should depend somehow on the bulk behavior of the quantum surfaces, and that we could use this intuition to somehow derive Lemma 10.6 from Proposition 10.11. That is the purpose of the current section.

To begin with, let $(\mathbf{C}, h, 0, \infty)$ be a γ-quantum cone with the projection of h onto $\mathcal{H}_1(\mathbf{C})$ normalized as in Definition 4.9. For $t \geq 0$, let R_t be such that $e^{\gamma R_t}$ is the expected γ-LQG mass in $B(0, e^{-t})$ given the mean value of h on $\partial B(0, e^{-t})$. Then $R_t = B_t + (\gamma - Q)t$ where B_t for $t > 0$ is a standard Brownian motion; note that $\gamma - Q < 0$.

Fix $\epsilon > 0$ very small. Now we will consider the quantity $\int_{-\epsilon}^{0} R_t \phi(t) dt$ where ϕ is a non-negative C^∞ bump function supported on $(-\epsilon, 0]$ with total integral one. This is an integral of h against a smooth rotationally invariant bump function. We apply a coordinate change rescaling to h so that this function achieves the value 0 for the first time at 0. We refer to the h with this type of scaling as the *smooth canonical description* for the quantum cone. Now let S be a closed, simply-connected subset of $\mathbf{D} \setminus \{0\}$ with non-empty interior. We also fix values $t_2 > t_1 > 0$ and $r > 0$. Given a smooth canonical description h of a γ-quantum cone as above, and an independently chosen η', we say that the configuration (h, η') is (S, t_1, t_2, r)**-stable** if the following are true:

1. $\eta'([t_1, t_2]) \subseteq S$ and $\operatorname{diam}(\eta'([t_1, t_2])) > r$
2. The previous item continues to hold if we cut out the surface parameterized by $\eta'([t_1, t_2])$ and weld in any surface at all of the same γ-LQG area and γ-LQG boundary length in its place. In other words, if we consider any conformal map ψ from the unbounded connected component of $\mathbf{C} \setminus \eta'([t_1, t_2])$ to $\mathbf{C} \setminus K$, for some K, that is normalized so that
   (i) ψ fixes ∞ and 0,
   (ii) ψ has a positive real derivative at ∞,
   (iii) ψ is scaled in such a way that the pushforward of h via the quantum coordinate change described by ψ corresponds to a smooth canonical description (note that on the event $K \subseteq S$ this statement does not depend on how the pushforward is defined on K itself),

   then $K \subseteq S$ and $\operatorname{diam}(K) \geq r$.

Remark 10.15. Let $F \colon \mathbf{C} \setminus \overline{\mathbf{D}} \to \mathbf{C} \setminus \eta'([t_1, t_2])$ be the unique conformal transformation which looks like the identity at ∞. The convenient property that this definition possesses is that it is measurable with respect to the σ-algebra generated by $h \circ F^{-1} + Q \log |(F^{-1})'|$ (this is the σ-algebra $\mathcal{F}$ introduced earlier with $[t_1, t_2]$ in place of $[-1, 1]$). That is, it is completely independent of the quantum surface parameterized by $\eta'([t_1, t_2])$ — i.e., one can cut out this piece and replace it with any quantum surface (with the same boundary lengths and area) without affecting whether the overall configuration is (S, t_1, t_2, r)-stable or not. If we had omitted Condition 2 from the definition of (S, t_1, t_2, r)-stability (and only included Condition 1), then whether

a configuration is (S, t_1, t_2, r)-stable would not be $\mathcal{F}$-measurable. This point will be very important when we complete the proof of Lemma 10.6 below. In particular, we will:

1. Argue (Proposition 10.20) that we have the desired fourth moment control on the event that a configuration is (S, t_1, t_2, r)-stable.
2. We will then argue that there almost surely exists some (S, t_1, t_2, r) such that the configuration is (S, t_1, t_2, r)-stable after applying a linear a change of coordinates. Due to our definition of stability, the values of t_1, t_2, r, and S are determined by $\mathcal{F}$ hence we get the desired fourth moment control conditional on $\mathcal{F}$.

We first observe that stable configurations occur with positive probability:

Proposition 10.16. *Let h be a smooth canonical description of a γ-quantum cone, and let η' be an independent space-filling* $\mathrm{SLE}_{\kappa'}$ *in $\mathbf{C}$ from ∞ to ∞, so that $\mu_h(\eta'([s,t])) = t - s$ for all $s < t$. Fix $t_2 > t_1 > 0$ and let $\mathcal{A}(S, t_1, t_2, r)$ denote the event that (h, η') is (S, t_1, t_2, r)-stable. Then there exists a closed, simply-connected set $S \subseteq \mathbf{D} \setminus \{0\}$ with non-empty interior and $r > 0$ for which $\mathcal{A}(S, t_1, t_2, r)$ has positive probability.*

This proposition may seem obvious — of course there is *some* probability that $\eta'([t_1, t_2])$ has very small diameter and lies in the middle of S, and then one would expect that cutting out the quantum surface traced by $\eta'([t_1, t_2])$ and gluing in a new should roughly preserve the location of $\eta'([t_1, t_2])$ in the center of S while changing its diameter by at most a constant factor. The trouble is that after replacing $\eta'([t_1, t_2])$ with a new surface, the field h undergoes a quantum coordinate change that changes its values everywhere, and after this modification, the degree of rescaling that is required in order to produce a smooth canonical description could be drastically different (enough so that the point no longer lies in S). To understand how the degree of rescaling required might change after a coordinate change, we will have to consider how much (h, ϕ) can change under small perturbations of ϕ. Before we prove Proposition 10.16 we will need some preliminary results along these lines. We begin by recalling some general facts about families of Gaussian random variables. The following proposition is stated in the introduction of [Cha08], which contains a short account of its history.

Proposition 10.17. *If $X_1, X_2, \ldots, X_k$ are centered jointly Gaussian random variables (not necessarily independent) each with variance at most σ^2, then*

$$\mathrm{Var}\big(\min X_i\big) = \mathrm{Var}\big(\max X_i\big) \leq \sigma^2.$$

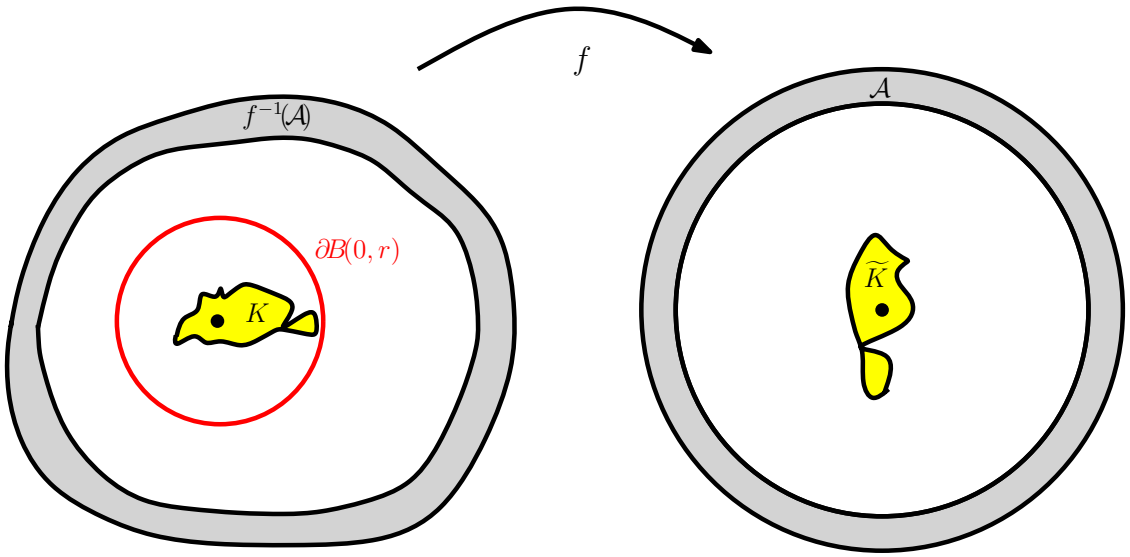

Figure 10.3: The set K is a subset of $B(0,r)$ (whose boundary is shown as a red circle the left) and f is a continuous homeomorphism from $\mathbf{C}$ to $\mathbf{C}$ that maps $\mathbf{C} \setminus K$ conformally to $\mathbf{C} \setminus \widetilde{K}$, has derivative 1 at ∞, and fixes the origin. On the right, a fixed annulus $\mathcal{A}$ is shown in grey, and on the left we have the f preimage of that set. Suppose that h is the field on the left and $\widetilde{h} = h \circ f^{-1} + Q \log |f'|$ is the field defined on the right. Let $\rho \colon \mathcal{A} \to \mathbf{R}$ be a radially symmetric bump function supported in $\mathcal{A}$. Then there is a constant b and $\widetilde{\rho}$ such that $(\widetilde{h}, \rho) = (h, \widetilde{\rho}) + b$. As K and $\widetilde{K}$ vary, the supremum and infimum of $(\widetilde{h}, \rho)$ are random finite quantities.

The following is an easy extension:

Proposition 10.18. *If $X_1, X_2, \ldots$ is a countable sequence of jointly Gaussian variables, each with variance at most σ^2, such that $\min X_i$ and $\max X_i$ are a.s. finite, then*

$$\operatorname{Var}\bigl(\min X_i\bigr) = \operatorname{Var}\bigl(\max X_i\bigr) \leq \sigma^2.$$

Proof. Proposition 10.18 can be obtained from Proposition 10.17 by considering the monotone sequence of random variables $\min\{X_1, X_2, \ldots, X_k\}$, for $k = 1, 2, 3, \ldots$, and observing that if the variance of the limit exceeds σ^2, then for all k sufficiently large, the variance of $\min\{X_1, X_2, \ldots, X_k\}$ must exceed σ^2, which would contradict Proposition 10.17. □

Now let Φ be the set of "distorted bump functions" of the form $|g'|^2 \phi \circ g$ for which g^{-1} is conformal outside of K for some $K \subseteq B_{1/10}(0)$, and is normalized to look like the identity near infinity, and fixes the origin. Then Φ is a sequentially compact

subset of the space of test functions w.r.t. the topology of uniform convergence of all derivatives on compact sets. Since this space is a Fréchet space (thus metrizable) Φ is also compact. In particular, for any distribution h, both of the quantities

$$M_1(h) = \inf_{\widetilde{\phi} \in \Phi} (h, \phi - \widetilde{\phi}) \quad \text{and} \quad M_2(h) = \sup_{\widetilde{\phi} \in \Phi} (h, \phi - \widetilde{\phi})$$

are finite. By continuity, they are equal to the infimum and supremum taken over a countable dense subset of $\phi \in \Phi$. Since the variance of $(h, \phi - \widetilde{\phi})$ is a continuous function of $\widetilde{\phi}$, it also has a maximum over Φ, and it follows from Proposition 10.18 that the variances of $M_1(h)$ and $M_2(h)$ are finite.

Now, for $j \in \{1, 2\}$ we can write $R_t^j = M_j(z \to h(e^t z) + Qt)$. Roughly speaking, R_t^1 and R_t^2 describe minimal and maximal averages on the distorted annular bump functions with inner radius about e^t (with the Qt term to account for the coordinate change). Now we observing the following:

Proposition 10.19. *It is a.s. the case that the processes R_t^1 and R_t^2 both tend to ∞ as $t \to \infty$ and to $-\infty$ as $t \to -\infty$.*

Proof. The continuity argument above also implies that the minimum and maximum values obtained by R_t^1 and R_t^2, as t varies over a compact range of values, are also a.s. finite and have bounded variance. The different between the minima (or maxima) over $[n, n+1]$ and over $[n, n+2]$ thus has finite variance and finite expectation, and the result is easily obtained by the ergodic theorem. □

Proof of Proposition 10.16. Proposition 10.19 implies that there almost surely exists $c \in (0, \infty)$ (random) such that we have $R_t^1, R_t^2 > 0$ for $t > c$ and $R_t^1, R_t^2 < 0$ for $t < -c$. Pick $c_1 \in (0, \infty)$ such that $\mathbf{P}[c \geq c_1] \leq \frac{1}{2}$. Fix a square $S \subseteq \mathbf{D} \setminus \{0\}$ with side length $\frac{1}{2}$ very close to 0. It is easy to see that we can find $K \subseteq S$ closed with non-empty interior such that $aK \subseteq S$ for any $a \in (\frac{1}{10} e^{-c_1}, 10 e^{c_1})$ and that $\eta'([t_1, t_2])$ lies in K with positive probability. On this event, it is not hard to check that if one swaps in a new quantum surface for the one traced by $\eta'([t_1, t_2])$, then resulting appropriately scaled surface will still belong to S, and also that its diameter is scaled by some factor which is contained in the interval $[\frac{1}{10} e^{-c}, 10 e^c]$. This, in turn, implies that for some $r > 0$, the diameter of $\eta'([t_1, t_2])$ is greater than r no matter what piece is swapped in. This implies the proposition statement. □

Proposition 10.20. *On the event $\mathcal{A}(S, t_1, t_2, r)$, we have the analog of* (10.4) *in which the $\mathcal{N}_j$ are obtained by dividing $[t_1, t_2]$, rather than $[-1, 1]$, into size δ increments.*

Proof. In this proof, will be considering two different laws:

1. The law on triples (h, η', z) where h is a GFF on $\mathbf{C}$ with the additive constant fixed so that $h_1(0) = 0$ (i.e., its average on $\partial\mathbf{D}$ is equal to 0) weighted by $\mu_h(S)$ and z is picked from μ_h. We will denote the corresponding probability and expectation by $\mathbf{P}^*$ and $\mathbf{E}^*$. This is the setting of Proposition 10.11.

2. The law on triples (h, η', z) where we have *not* weighted the law of h by $\mu_h(S)$. We will denote the corresponding probability and expectation by $\mathbf{P}$ and $\mathbf{E}$.

Suppose that we have a triple (h, η', z) picked from $\mathbf{P}^*$ as in (1) above. The bound (10.13) in Proposition 10.11 bounds $\mathbf{E}^*[\epsilon^4]$. Let E be the event that both $\mathcal{A}(S, t_1, t_2, r)$ and $z \in \eta'([t_1, t_2])$ hold. Since ϵ^4 is a.s. positive, we also get an upper bound on $\mathbf{E}^*[\epsilon^4 \mathbf{1}_E]$.

On E, we have that $\mu_h(\eta'([t_1, t_2])) = t_2 - t_1 \leq \mu_h(S)$ since $\eta'([t_1, t_2]) \subseteq S$. Consequently, we have that

$$\frac{d\mathbf{P}^*}{d\mathbf{P}} \mathbf{1}_E = c_1 \mu_h(S) \mathbf{1}_E \geq c_1 (t_2 - t_1) \mathbf{1}_E$$

where $c_1 \in (0, \infty)$ is a normalizing constant. Rearranging, we have that

$$\mathbf{1}_E \leq \left(\frac{1}{c_1 (t_2 - t_1)} \right) \frac{d\mathbf{P}^*}{d\mathbf{P}} \mathbf{1}_E. \tag{10.19}$$

In particular, when we integrate a non-negative random variable on E we can replace $\mathbf{E}$ with $\mathbf{E}^*$ and only lose a constant factor.

On E, let j be such that $\mathcal{N}_j$ contains z. Note that $\mathcal{N}_j$ is then uniform among the surfaces parameterized by δ-length intervals of $[t_1, t_2]$. With b the hitting time of z by η', note also that $\mathcal{N}_j \subseteq \eta'([b - \delta, b + \delta])$. Combining everything, we see that there exists a constant $c_2 > 0$ depending only on t_1, t_2, and S such that

$$\mathbf{E}[\mathrm{diam}(\mathcal{N}_j)^4 \mathbf{1}_E] \leq \mathbf{E}[\mathrm{diam}(\eta'([b - \delta, b + \delta]))^4 \mathbf{1}_E] \leq c_2 \mathbf{E}^*[\epsilon^4] \quad \text{(by (10.19))}.$$

This does not quite complete the proof yet because in (10.4), we have normalized η' so that $\eta'([-1, 1])$ has outer conformal radius equal to 1. In the present context, we note that the scaling factor necessary to normalize $\eta'([t_1, t_2])$ to have outer conformal radius 1 on E is at most a constant times $1/r$ since $\mathrm{diam}(\eta'([t_1, t_2])) \geq r$ on E. Therefore the result follows from (10.13). □

Proof of Lemma 10.6. Fix $t_2 > t_1 > 0$. Since the pair which consists of the quantum cone and η' is invariant under scaling, we may consider the map ψ that sends the pair (h, η') to the rescaled and reparameterized configuration obtained by applying the affine map of time that sends the triple $(0, t_1, t_2)$ to $(t', -1, 1)$ for some t'. Thus, it follows from Proposition 10.20 that the bound (10.4) holds for the (h, η') configuration

on the event that its ψ preimage belongs to $\mathcal{A}(S, t_1, t_2, r)$. We emphasize that (as mentioned in Remark 10.15) this event is $\mathcal{F}$-measurable.

Fix $p_0 \in (0, 1)$. To finish the proof, it suffices to show that there exists t_1, t_2, r and S with $\mathbf{P}[\mathcal{A}(S, t_1, t_2, r)] \geq p_0$. One can see that there has to be such t_1, t_2, r, and S using the following variant of the argument used to prove Proposition 10.16. Using the continuity of η' and the argument used to prove Proposition 10.16 it follows that we can pick $t_1, t_2, r > 0$ and take $S = \{z \in \mathbf{C} : \epsilon \leq |z| \leq \frac{1}{2},\ \arg(z) \in [0, 2\pi - \epsilon]\}$ with $\epsilon > 0$ very small such that the following are true:

1. The probability that $\eta'(t_1) \in S$ and $\operatorname{dist}(\eta'(t_1), \partial S) \geq \epsilon$ is at least $\frac{1}{2} + \frac{p_0}{2}$.
2. Given that $\eta'(t_1) \in S$ and $\operatorname{dist}(\eta'(t_1), \partial S) \geq \epsilon$, we have that the conditional probability of $\mathcal{A}(S, t_1, t_2, r)$ is at least $\frac{1}{2} + \frac{p_0}{2}$.

Therefore $\mathbf{P}[\mathcal{A}(S, t_1, t_2, r)] \geq p_0$, which proves the claim. □

10.5 Discrete models and topology strengthening

As we promised in the introduction, we will offer a few ideas about how one might be able to use the techniques of this section to "strengthen the topology" of convergence w.r.t. which FK-decorated RPM converges to CLE-decorated LQG. Specifically, we would like to obtain convergence in a topology that encodes the conformal embedding of the discrete models. We stress that this remains a major open problem, and that implementing the ideas sketched in this subsection would be a major challenge. The reader who lacks patience for speculation is encouraged to skip this subsection.

As very briefly described in Section 1.2, the results in [She11] imply that FK-decorated random planar maps come endowed with a natural tree and dual tree pair, together with a "space-filling path" that forms the interface between them, and that as one moves along this space-filling path, "tree branch length" and "dual tree branch length" evolve as random processes that scale to Brownian motion.

Also, as explained in [She11], there is a well known way to put a conformal structure on these planar maps: namely, one replaces each edge by a quadrilateral, and then endows each such quadrilateral with the geometry of a unit square. (Each such square is further divided into a pair of triangles by an edge or dual edge, depending on whether the corresponding edge is in the FK set — see [She11] for details.) We will not explain the full details here. Fix a large number M and let $\mathcal{M}_j$ denote the surface (which is formally a collection of right triangles glued together along edges) parameterized by steps jM through $(j+1)M - 1$ of the space-filling path. Each such surface comes with four distinguished boundary points (like the surfaces $\mathcal{N}_j$, as parameterized by the regions in Figure 10.1) which correspond to the first and last

points of the space-filling path (red dots in Figure 10.1), and to the lowest location on the tree or dual tree (green arrows in Figure 10.1).

The results of [She11] imply that when M is sufficiently large, one can couple the (infinite volume) discrete model with the continuum model described in this paper in such a way that the boundary lengths of the $\mathcal{M}_j$ (appropriately rescaled) are very close in law to the lengths of the $\mathcal{N}_j$ surfaces parameterized by the regions shown in Figure 10.1.

What if we start with a continuum picture such as the one shown in Figure 10.1, and then we one-by-one (in some random order) cut out each $\mathcal{N}_j$ surface (i.e., each of the $2\delta^{-1}$ surfaces parameterized by length δ intervals of $[-1, 1]$) and replace it with an $\mathcal{M}_j$ surface? (See [AKSJ11] for a proof that welding quantum surfaces to flat surfaces makes sense; alternatively, one could smooth the boundaries of the $\mathcal{N}_j$ surfaces in some way so that welding them to the $\mathcal{M}_j$ becomes straightforward.) At each stage, we can normalize the embedding so that the map from the pre-replacement to the post-replacement embedding (which is conformal on the complement of the piece being replaced) looks like the identity near infinity. This gives us a way to gradually move from the continuum model to a discrete model.

One could then pick a point z of constant order distance from $\eta'([-1, 1])$ and try to argue that this point stays relatively fixed (when δ is small) throughout this replacement process.

If one could show that throughout this process, the diameters of the regions to be replaced remain small, then one could control the variance of the amount that the point that begins at z is shifted at each stage. If one could further show that the jumps at successive stages are approximately uncorrelated, one could bound the overall variance of the amount that z is shifted, which would ultimately allow us to deduce that the conformal structure of the discrete surface is in some sense close to that of the continuum surface.

The problem of showing that individual regions are small is related to the following problem. Consider a collection of a small number of $\mathcal{N}_j$ surfaces whose union is an annulus, so that a Brownian motion started somewhere in the middle of that annulus has some probability p (depending on the conformal modulus of the annulus) of having its trace "make a loop" separating the inside and outside of the annulus at a time before it exits the annulus. Show that this p remains of constant order (independently of δ, with at least some constant order probability that is also independent of δ) after some of the $\mathcal{N}_j$ are replaced by the corresponding $\mathcal{M}_j$. In other words one would like to show that if one considers an annulus built out of a constant-order number of $\mathcal{N}_j$ surfaces with some conformal modulus, the conformal modulus has at least some good chance of not changing by more than a constant factor when these surfaces are replaced with their discrete analogs. The hope would be that by applying this

argument on different scales, one could show that individual surfaces are indeed highly likely to remain non-macroscopic throughout the replacement process.

A toy problem (which may avoid some of the challenges discussed in the paragraph above) would be to show that the point z does not get shifted very much if one replaces each $\mathcal{N}_j$ with an ordinary Euclidean disk of the same boundary length (instead of replacing it with $\mathcal{M}_j$) which would then be welded to the surface outside of it and embedded in some way.

In fact, by replacing every δ-interval-parameterized surface in the whole plane with a corresponding Euclidean disk, we would obtain a welded collection of disks that is in some sense a discrete model (it is formed by welding together discrete and distinct positive radii disks) but that also has a very straightforward relationship to the continuum model. We also like the idea of letting the interval boundaries be a Poisson collection of times of intensity δ^{-1} (instead of integer multiples of δ) since with that approach, one can gradually decrease δ by gradually throwing in more Poissonian points — which in turn corresponds to randomly subdividing existing disks into pairs of disks, according to independent exponential clocks (one for each existing disk). We wonder whether it might be possible to bound the sizes of the embedded-disk diameters one obtains during this subdivision process, and thereby prove existence of the $\delta \to 0$ limit, perhaps even before identifying it with the continuuum surface described in this paper.

11 KPZ interpretation

Suppose that $D \subseteq \mathbf{C}$ is a domain with smooth boundary and that $X \subseteq \overline{D}$ is a random fractal which is independent of a γ-LQG surface described by h. Let $B_\epsilon(X)$ (resp. $B^\delta(X)$) be the ϵ-Euclidean neighborhood (resp. δ-quantum neighborhood) of X as defined in [DS11a, Section 1.3]. Recall that the quantum and Euclidean expectation scaling exponents Δ and x are respectively given by:

$$\Delta = \lim_{\delta \to 0} \frac{\log \mathbf{E}[\mu_h(B^\delta(X))]}{\log \delta} \quad \text{and} \quad x = \lim_{\epsilon \to 0} \frac{\log \mathbf{E}[\mu_0(B_\epsilon(X))]}{\log \epsilon^2}$$

where μ_0 denotes Lebesgue measure. The exponents are defined analogously if $X \subseteq \partial D$ except with ν_h in place of μ_h and ϵ in place of ϵ^2 (see [DS11a, Section 6.3]). If $X \subseteq D$ (resp. $X \subseteq \partial D$), then $2-2x$ (resp. $1-x$) gives the Euclidean expectation dimension of X. The KPZ formula, which relates Δ and x, is given by:

$$x = \frac{\gamma^2}{4}\Delta^2 + \left(1 - \frac{\gamma^2}{4}\right)\Delta. \tag{11.1}$$

(See [DS11a, Theorem 1.4] for the bulk version and [DS11a, Theorem 6.1] for the boundary version.)

Following the discussion begun in Section 2.3, we are now going to use (11.1) and the quantum wedge and cone theory developed earlier in this article to give a heuristic derivation of both the quantum and Euclidean dimensions of a number of random fractals which arise in SLE and related discrete models. As we mentioned in Section 2.3, we believe that with some additional work these arguments can be converted into rigorous proofs.

11.1 General principles

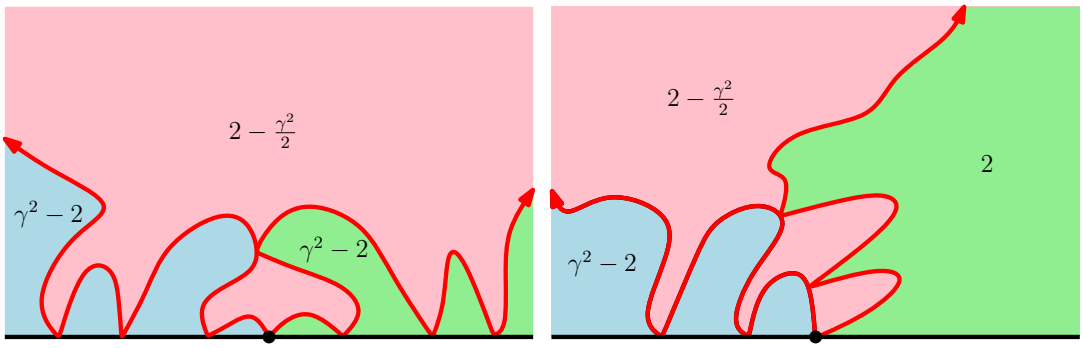

Figure 11.1: Fix $\kappa' \in (4,8)$. **Left:** an $\mathrm{SLE}_{\kappa'}$ process (red) divides a quantum wedge of weight $\frac{3\gamma^2}{2}-2$ into three independent wedges of respective weights γ^2-2 (blue), $2-\frac{\gamma^2}{2}$ (red), and γ^2-2 (green) corresponding to those regions which are to the left of the path, surrounded by the path, and to the right of the path. **Right:** an $\mathrm{SLE}_{\kappa'}$ process (red) *conditioned* not to hit $(0,\infty)$ divides a quantum wedge of weight $\frac{\gamma^2}{2}+2$ into three independent wedges of weight γ^2-2 (blue), $2-\frac{\gamma^2}{2}$ (red), and 2 (green) corresponding to those regions which are to the left of the path, surrounded by the path, and to the right of the path.

The general strategy is the following:

- We will (using certain heuristics) argue that the local behavior at a "quantum typical" point in X looks like a particular type of α-quantum cone (bulk case) or α-quantum wedge (boundary case). By quantum typical, we mean a point chosen from the measure on X constructed by restricting the γ-LQG measure to $B^\delta(X)$ and then taking a limit of these measures as $\delta \to 0$ with appropriate rescaling so that the limit is non-trivial. (We will not actually construct this measure in each case; see [DS11b] for SLE quantum measures, in particular the SLE quantum length or natural parameterization.)

- It is explained in [DS11a, Equation (63)] that a quantum typical point z_0 in X is $\gamma - \gamma\Delta$ thick for h; this means that the circle average process of h centered at z_0 has growth $(\gamma - \gamma\Delta)\log\epsilon^{-1}$ as $\epsilon \to 0$. The circle average process associated with an α-quantum cone or an α-quantum wedge centered at the origin grows like $\alpha \log \epsilon^{-1}$ as $\epsilon \to 0$ and this allows us to match α and Δ. That is, $\alpha = \gamma(1-\Delta)$, hence $\Delta = 1 - \frac{\alpha}{\gamma}$.

- We can determine x from Δ using (11.1). This, in turn, should give that the Euclidean dimension of X is $2-2x$ (resp. $1-x$) if $X \subseteq D$ (resp. $X \subseteq \partial D$).

We emphasize again that the presentation in this section will be heuristic, and not fully detailed. In this section, we are going to consider two different settings depending on whether $\kappa = \gamma^2 \in (0,4)$ or $\kappa' = \frac{16}{\gamma^2} \in (4,8)$.

In the former setting, there are a few wedge types which occur naturally:

- Wedge of weight 2, which is the weight of an γ-quantum wedge obtained by zooming in at a "typical boundary measure" point, as mentioned in Section 1.4. In the simplest setting of Theorem 1.9, gluing two weight 2 wedges yields a wedge of weight 4 decorated by an independent chordal SLE_κ process from 0 to ∞ [She10].

- Wedges of weight $W_i = 2 + \rho_i, i = 1, 2$, obtained by cutting out from a quantum wedge of weight $W = W_1 + W_2$, an independent $\mathrm{SLE}_\kappa(\rho_1, \rho_2)$ process from 0 to ∞ with force points located at 0^- and 0^+. (See Theorem 1.9.)

- Wedge of weight $W = 2 + \rho$, obtained by cutting out from a quantum cone $\mathcal{C} = (\mathbf{C}, h, 0, \infty)$ of same weight W, an independant whole-plane $\mathrm{SLE}_\kappa(\rho)$ process η starting from 0. (See Theorem 1.12.)

- Wedge of weight $W = 2 + \rho$, corresponding to the region cut off by a boundary-intersecting $\mathrm{SLE}_\kappa(\rho)$ process before or after hitting a typical boundary intersection point.

In the latter setting, we fix $\kappa' \in (4,8)$ and suppose that η' is an $\mathrm{SLE}_{\kappa'}$ process in $\mathbf{H}$ from 0 to ∞. Fix a quantum wedge $\mathcal{W}$ parameterized by $\mathbf{H}$ which is independent of η'. In the computations that follow, there will be three different types of wedges that will be important for us to consider. These correspond to:

- The region surrounded by η',

- The region which is to the left or to the right of η',

- The region which is to the right of η' when it is conditioned not to hit $(0, \infty)$.

In view of Theorem 1.17, it is natural in the first two cases to take $\mathcal{W}$ to have weight $\frac{3\gamma^2}{2} - 2$. Theorem 1.17 implies that the regions which are to the left and to the right of η' correspond to wedges of weight $\gamma^2 - 2$ and the set of points surrounded by η' corresponds to a wedge of weight $2 - \frac{\gamma^2}{2}$. Moreover, these three wedges are independent. (See left side of Figure 11.1.)

Recall that the law of η' conditioned not to hit $(0, \infty)$ is that of an $\mathrm{SLE}_{\kappa'}(\kappa' - 4)$ process [Dub05, MS12b]. By Theorem 1.17, it is natural to take $\mathcal{W}$ to be a wedge of weight $\frac{\gamma^2}{2} + 2$ and it follows that the region of $\mathbf{H}$ which is to the right of η' corresponds to a wedge of weight 2.[17] As in the unconditioned case, the region surrounded by η' itself is a wedge of weight $2 - \frac{\gamma^2}{2}$ and the region which is to the left of η' to a wedge of weight $\gamma^2 - 2$. Moreover, these three wedges are independent. (See right side of Figure 11.1.)

We can now glue together wedges of these three types in various ways to form other types of surfaces. In particular,

- A wedge of weight $2 - \frac{\gamma^2}{2}$ corresponds to an $\mathrm{SLE}_{\kappa'}$ process,
- Gluing a wedge of weight 2 between two wedges of weight $2 - \frac{\gamma^2}{2}$ corresponds to conditioning the two $\mathrm{SLE}_{\kappa'}$ processes not to intersect, and
- Gluing a wedge of weight $\gamma^2 - 2$ in between two wedges of weight $2 - \frac{\gamma^2}{2}$ corresponds to not performing any conditioning (i.e., interpreting the paths as though they were $\mathrm{SLE}_{\kappa'}$ interfaces arising from the same statistical physics model, which reflect off one another but do not overlap).

For example, consider the surface which results when gluing together independent wedges $\mathcal{W}_1, \ldots, \mathcal{W}_5$ with respective weights $\gamma^2 - 2$, $2 - \frac{\gamma^2}{2}$, 2, $2 - \frac{\gamma^2}{2}$, and $\gamma^2 - 2$. This corresponds to having two $\mathrm{SLE}_{\kappa'}$ paths η_1' and η_2' (represented respectively by $\mathcal{W}_2$ and $\mathcal{W}_4$) in $\mathbf{H}$ from 0 to ∞ with η_1' to the left of and conditioned not to hit η_2'.

Remark 11.1. Besides the quantum scaling exponents Δ, the Liouville quantum gravity literature discusses so-called *dual* quantum scaling exponents $\widetilde{\Delta}$ [Kle95, KH95, KH96, Dup04, Dup06, DS09, Dup10, BJRV13], defined via the duality relation

$$\alpha = \gamma(1 - \Delta) = \gamma'(1 - \widetilde{\Delta}), \tag{11.2}$$

where $\gamma' := \sqrt{\kappa'} = 4/\sqrt{\kappa} = 4/\gamma$ is the dual $\gamma' > 2$ of the usual LQG parameter $\gamma < 2$. (We then have $\widetilde{\Delta} = 1 - \frac{\gamma^2}{4} + \frac{\gamma^2}{4}\Delta$.) This remark will provide an extremely

[17] This is also natural because the dimension of the Bessel process which corresponds to a wedge of weight $\gamma^2 - 2$ is $3 - \frac{4}{\gamma^2}$ (recall Table 1.1). Conditioning this Bessel process not to hit 0 corresponds to conditioning the wedge to be homeomorphic to $\mathbf{H}$. The conditioned Bessel process has dimension $4 - (3 - \frac{4}{\gamma^2}) = 1 + \frac{4}{\gamma^2}$ and this is the Bessel dimension which corresponds to a weight 2 wedge.

rough sense of the meaning of these exponents, and related formulas that have been derived in the physics literature. As argued above, the local behavior at a "quantum typical" point in a random fractal X of exponent Δ, where the measure on X is constructed by using the γ-LQG measure, looks like a particular type of α-quantum cone (bulk case) or α-quantum wedge (boundary case). In a certain sense, the dual scaling exponents $\widetilde{\Delta}$ should correspond to the same value of α, but should arise when one chooses a typical point (conditioned to belong to X) using the atomic quantum measure $\mu_{\gamma'}$ introduced in Section 2.2, instead of the standard Liouville measure $\mu = \mu_\gamma$ (1.1) (or the boundary atomic measure corresponding to the quantum natural time, instead of the standard boundary LQG measure $\nu = \nu_\gamma$ (1.2)), as discussed in (12.3) in Section 12.2. The dual quantum exponents obey a dual version of the KPZ formula, which relates the triple γ', $\widetilde{\Delta}$ and x [Kle95, Dup04, DS09, Dup10], and was proved rigorously in the context of Gaussian multiplicative chaos [BJRV13],

$$x = \frac{\gamma'^2}{4}\widetilde{\Delta}^2 + \left(1 - \frac{\gamma'^2}{4}\right)\widetilde{\Delta}; \tag{11.3}$$

standard and dual quantum exponents are then such that the identity $x = \Delta\widetilde{\Delta}$ holds. In the wedge parametrization, Table 1.1, the relation $W = 2 + \gamma^2\Delta$ becomes in terms of the dual quantum exponent $\widetilde{\Delta}$,

$$W = \gamma^2 - 2 + 4\widetilde{\Delta}. \tag{11.4}$$

We can then generalize to $\mathrm{SLE}_{\kappa'}$ processes, the Remark 1.10, made in the case of SLE_κ, that the additivity of wedge weights under gluing should correspond to the additivity of certain non-intersection (boundary) quantum exponents. Indeed, we have seen above that gluing a wedge of weight $\gamma^2 - 2$ in between the boundary and a wedge (of weight $2 - \frac{\gamma^2}{2}$) corresponding to an $\mathrm{SLE}_{\kappa'}$ process (see Fig. 11.1), or between two wedges corresponding to two $\mathrm{SLE}_{\kappa'}$ processes, corresponds to not performing any conditioning between the boundary and the $\mathrm{SLE}_{\kappa'}$ path, or between the two paths. The addititivity of wedge weights in Theorem 1.17 therefore implies that $W - (\gamma^2 - 2)$ should be a linear function of the number of paths. The relation (11.4) then implies a similar additivity of dual quantum boundary exponents with respect to the set of paths [Dup04, Dup06]. An illustration of this fact will appear in Section 11.3 when computing the $\mathrm{SLE}_{\kappa'}$ double-point dimension and the generalization thereof.

11.2 Non-intersecting paths and cut point dimension

Consider first the simplest case of a quantum wedge $\mathcal{W}$ of weight $W = 2n$, made by gluing together n independent quantum wedges $\mathcal{W}_i$, $i = 1, \cdots, n$, each of weight 2. By the remarks above, and by Theorem 1.9 and Proposition 8.14 , the resulting $n - 1$

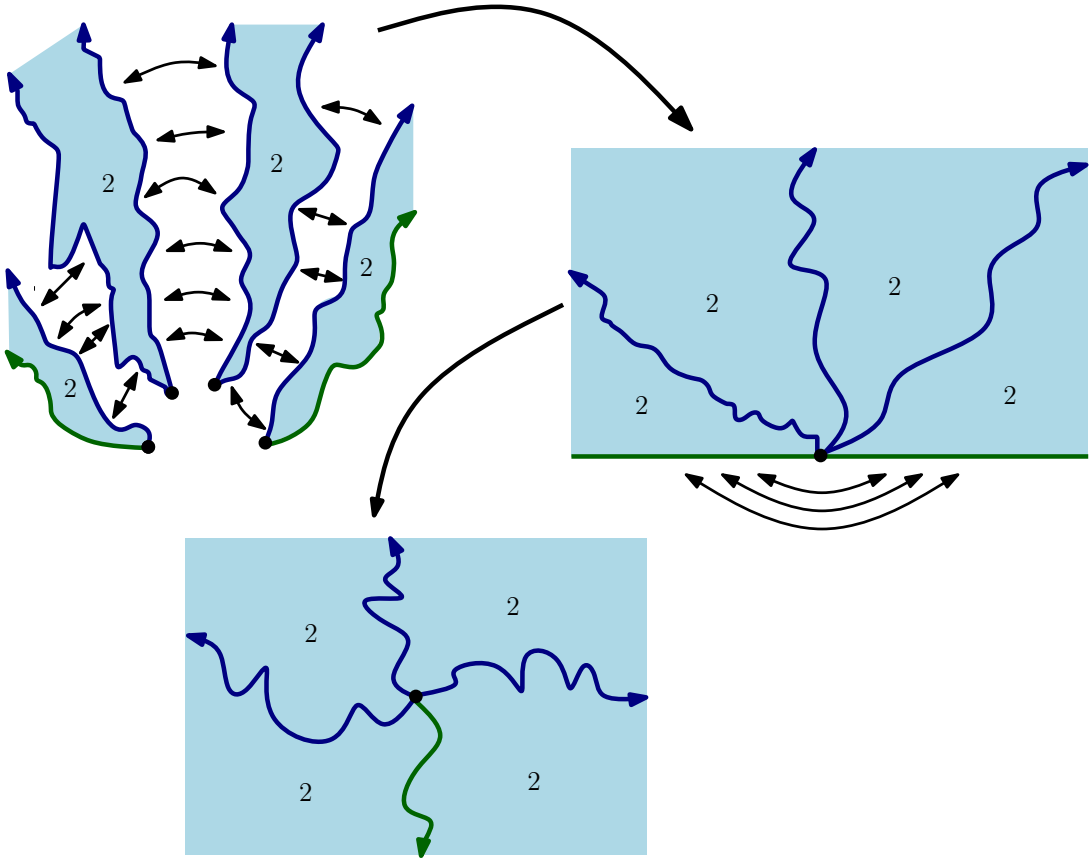

Figure 11.2: **Top:** Conformal welding according to their γ-LQG boundary length of $n(=4)$ independent identical quantum wedges of weight 2, followed by a conformal mapping to $\mathbf{H}$. The resulting $n-1$ interfaces, η_i, $i = 1, \cdots, n-1$, are coupled $\mathrm{SLE}_\kappa(\rho_i, \widetilde{\rho}_i)$ processes, with $\kappa = \gamma^2 \in (0,4)$, and $\rho_i = 2i-2, \widetilde{\rho}_i = 2(n-i)-2$. **Bottom:** Conformally welding the left and right boundaries ($\mathbf{R}_-$ and $\mathbf{R}_+$) of the resulting wedge $\mathcal{W}$ according to quantum length yields a quantum cone decorated with an independent whole-plane $\mathrm{SLE}_\kappa(\rho)$, with $\rho = 2(n-1)$. Its conditional law, given the other $n-1$ paths, is that of a chordal SLE_κ process in the sector between η_{n-1} and η_1. By symmetry, this also holds for any path given the others, resulting in a non-intersecting n-star configuration.

interfaces are represented by a collection of paths $\eta_1, \ldots, \eta_{n-1}$ where the marginal law of η_i for each $i = 1, \ldots, n-1$ is that of an $\mathrm{SLE}_\kappa(2i-2; 2(n-i)-2)$ process and the conditional law of η_i given η_j for $j \neq i$ is that of an SLE_κ process, $\kappa = \gamma^2 \in (0,4)$, in the component of $\mathbf{H} \setminus \cup_{j \neq i} \eta_j$ between η_{i-1} and η_{i+1} with the convention that $\eta_0 = \mathbf{R}_-$ and $\eta_n = \mathbf{R}_+$. See Figure 11.2 for an illustration. Then $\mathcal{W}$ is an α-quantum

wedge with $\alpha = \gamma - \frac{2}{\gamma}(n-1) \leq Q$, corresponding to a boundary quantum scaling exponent

$$\Delta = 1 - \frac{\alpha}{\gamma} = \frac{2}{\gamma^2}(n-1) = \frac{2}{\kappa}(n-1). \tag{11.5}$$

Observe here the additivity of boundary quantum exponents, as advocated in [Dup03, Dup04], with a contribution $2/\kappa$ for each of the $n-1$ mutually-avoiding paths.

By Theorem 1.12, zipping-up the left and right sides of the thick wedge $\mathcal{W}$ gives an α'-quantum cone decorated with an independent whole-plane $\mathrm{SLE}_\kappa(\rho)$, with from (1.7), $\alpha' = \frac{\alpha}{2} + \frac{1}{\gamma}$, and from (1.6) $\rho = 2 + \gamma^2 - 2\alpha'\gamma = \gamma^2 - \alpha\gamma = 2(n-1)$. The conditional law of the path which corresponds to the zipped up boundary given the other paths is that of a chordal SLE_κ process (see Proposition 8.16). In particular, this path does not intersect the other $n-1$ paths originally drawn on the quantum wedge $\mathcal{W}$ (see also [Dup06, Section 10.5]); this yields a collection of n non-intersecting whole-plane simple $\mathrm{SLE}_\kappa(\rho)$ processes, with $\kappa \in (0,4)$. The corresponding bulk quantum scaling exponent is

$$\Delta' = 1 - \frac{\alpha'}{\gamma} = \frac{1}{2\kappa}\left(2n + \kappa - 4\right). \tag{11.6}$$

Both Δ (11.5) and Δ' (11.6) coincide (see, e.g., [Dup04, Equation (11.36)]) with the quantum exponents obtained by random matrix techniques for multiple paths in the $O(N)$ critical model on a random lattice [DK88a, Kos89, DK90, Dup03, Dup04, Dup06], with the conjectural identification $N = -2\cos(4\pi/\kappa), N \in [-2,2], \kappa \in [2,4]$ [Dup03, KN04].

The corresponding Euclidean scaling exponents, i.e., conformal weights, are obtained by using the KPZ relation (11.1), to get

$$x = \frac{n}{2\kappa}(2n + 4 - \kappa) \quad \text{and} \quad x' = \frac{1}{16\kappa}\big(4n^2 - (4-\kappa)^2\big), \tag{11.7}$$

for, respectively, the boundary and bulk exponents of n non-intersecting SLE_κ paths with $\kappa < 4$. They agree with the corresponding exponents predicted for the critical $O(N)$ model or the tricritical Potts model; see [Car84, DS86, BS93] and [Nie82, Nie84, Nie87, Sal86, Dup87, BB88].

We are now going to explain how to derive the Brownian intersection exponents and the cut point dimension for $\mathrm{SLE}_{\kappa'}, \kappa' \in (4,8)$.

Consider a wedge of weight $\mathcal{W}$ which is given by gluing together independent wedges with weights $2 - \frac{\gamma^2}{2}$ and 2. Then the weight of $\mathcal{W}$ is $4 - \frac{\gamma^2}{2}$. That is, $\mathcal{W}$ is an α-quantum wedge with $\alpha = \frac{3\gamma}{2} - \frac{2}{\gamma}$. Let

$$\alpha' = \frac{\alpha}{2} + \frac{1}{\gamma} = \frac{3\gamma}{4}.$$

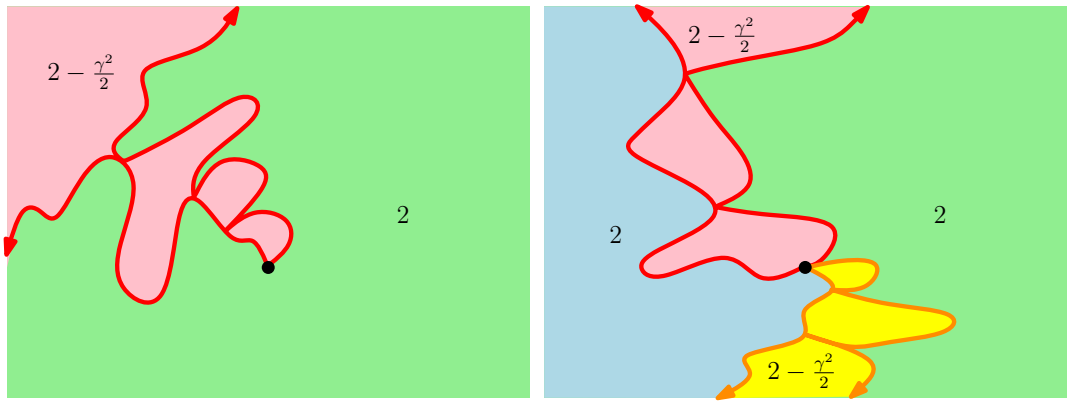

(a) (b)

Figure 11.3: **Left:** quantum cone formed by gluing a weight $2-\frac{\gamma^2}{2}$ wedge with a weight 2 wedge. The wedge of weight $2-\frac{\gamma^2}{2}$ corresponds to the range of a whole-plane $\mathrm{SLE}_{\kappa'}$ process η' conditioned on the event that it does not separate the origin from ∞. (The conditional law of η' is that of a whole-plane $\mathrm{SLE}_{\kappa'}(\kappa'-4)$ process.) **Right:** quantum cone formed by gluing two weight $2-\frac{\gamma^2}{2}$ wedges with two weight 2 wedges, alternating between the two types. The two wedges of weight $2-\frac{\gamma^2}{2}$ correspond to two whole-plane $\mathrm{SLE}_{\kappa'}$ processes starting from the origin conditioned not to intersect each other. This describes the local behavior of an $\mathrm{SLE}_{\kappa'}$ process near a quantum typical cut point.

Theorem 1.12 (recall also (1.6) and (1.7)) implies that if we zip up the left and right sides of $\mathcal{W}$, then we get an α'-quantum cone $\mathcal{C} = (\mathbf{C}, h, 0, \infty)$ decorated with an independent whole-plane $\mathrm{SLE}_{\kappa'}(\kappa'-4)$ process η' from 0 to ∞ (see also Theorem 1.18; equivalently, η' is a whole-plane $\mathrm{SLE}_{\kappa'}$ process conditioned not to intersect itself). See Figure 11.3a for an illustration.

Suppose that $\kappa' = 6$ and imagine that B is a standard 2-dimensional Brownian motion drawn on top of an independent $\sqrt{8/3}$-LQG surface described by some h. Then we can view $(\mathcal{C}, \eta')$ as describing the local picture of the set X consisting of those points z where B gets very close to and then travels macroscopically far away from without separating z from ∞. Let Δ denote the quantum scaling associated with this set. As explained earlier, a quantum typical point in X should be $\gamma - \gamma\Delta$ thick for h. That is, we should have that $\alpha' = \gamma - \gamma\Delta$. This gives that $\Delta = \frac{1}{4}$. Plugging this into (11.1) gives that the Euclidean scaling of X is $x = \frac{1}{8}$ so that the Euclidean dimension of X should be $\frac{7}{4}$, in agreement with that of pioneer points of Brownian motion [LSW01a].

We can generalize this further by considering additional paths. Suppose now that we

have n paths $\eta'_1, \ldots, \eta'_n$ in $\mathbf{H}$ from 0 to ∞ where each η'_j lies to the right of η'_{j-1} and to the left of η'_{j+1} and that the conditional law of η'_j given η'_{j-1} and η'_{j+1} is that of an $\mathrm{SLE}_{\kappa'}$ conditioned not to hit η'_{j-1} and η'_{j+1}. (Equivalently, the conditional law is that of an $\mathrm{SLE}_{\kappa'}(\kappa'-4;\kappa'-4)$ process [Dub05, MS12b].) If we draw these paths on top of an independent wedge $\mathcal{W}$ of weight $W = (4 - \frac{\gamma^2}{2})n$, then their left and right boundaries divide $\mathcal{W}$ into independent wedges $\mathcal{W}_1, \mathcal{V}_1, \ldots, \mathcal{W}_n, \mathcal{V}_n$ where each $\mathcal{W}_i$ has weight $2 - \frac{\gamma^2}{2}$ and each $\mathcal{V}_j$ has weight 2.

Welding together the left and right sides of $\mathcal{W}$ yields an α-quantum cone, where by (1.5)

$$\alpha = Q - \frac{W}{2\gamma} = Q - \left(\frac{2}{\gamma} - \frac{\gamma}{4}\right) n,$$

decorated by paths $\widetilde{\eta}'_1, \ldots, \widetilde{\eta}'_n$ which can be viewed as n whole-plane $\mathrm{SLE}_{\kappa'}$ processes starting from the origin conditioned not to intersect. See Figure 11.3b for an illustration. Let Δ be so that $\alpha = \gamma - \gamma\Delta$. That is,

$$\Delta = 1 - \frac{\alpha}{\gamma} = \frac{1}{2} - \frac{2}{\gamma^2} + \left(\frac{2}{\gamma^2} - \frac{1}{4}\right) n.$$

This exponent matches the multiple disconnection exponent of n $\mathrm{SLE}_{\kappa'}$ paths, obtained by using the quantum gravity methods of [Dup04, Section 12.3]. In the case that $\gamma = \sqrt{8/3}$, this gives that

$$\Delta = \frac{1}{2}\left(n - \frac{1}{2}\right)$$

so that by (11.1) we have that

$$x = \frac{1}{24}\left(4n^2 - 1\right).$$

This case has the interpretation of describing n whole-plane SLE_6 processes conditioned not to intersect (or n non-intersecting clusters or $2n$ path crossings in percolation [SD87, Dup99, ADA99]). By the relationship between SLE_6 and Brownian motion, it in turn has the interpretation as describing n Brownian motions starting near the origin conditioned not to intersect. In particular, the probability that n Brownian motions starting from distance ϵ from the origin make it macroscopically far from the origin without intersecting should be proportional to ϵ^{2x}. These are the Brownian intersection exponents derived in [DK88b] and later in [Dup98] using quantum gravity methods. The values of the Brownian intersection exponents were determined rigorously by Lawler, Schramm, and Werner in [LSW01b, LSW01c, LSW02].

These exponents for other values of $\gamma \in (\sqrt{2}, 2)$ also have an interesting interpretation. In particular, for $n = 2$ and $\gamma = \sqrt{16/\kappa'}$, Δ and x have the interpretation of giving

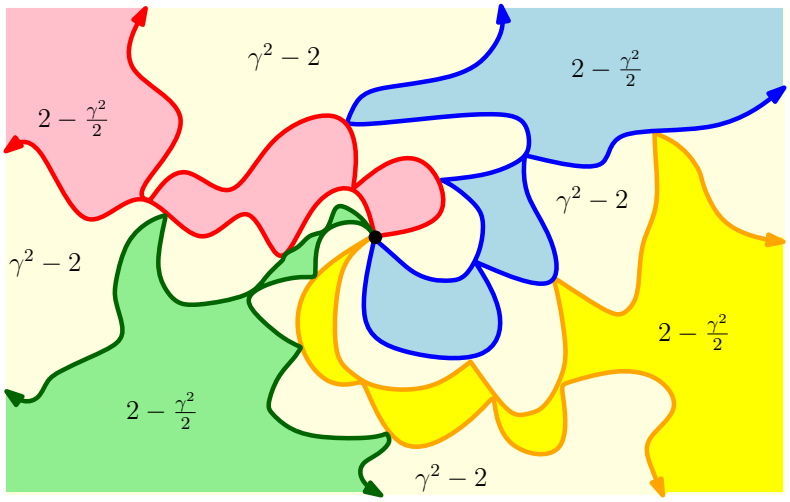

Figure 11.4: The configuration of paths which at a quantum typical double point z_0 for an $\mathrm{SLE}_{\kappa'}$ process η' with $\kappa' \in (4, 8)$ can be described by the quantum cone which arises by welding together four wedges of weight $2 - \frac{\gamma^2}{2}$ and four wedges of weight $\gamma^2 - 2$ where the wedges of different types alternate as shown. The boundaries of the $2 - \frac{\gamma^2}{2}$ wedges are drawn by η' either in counterclockwise or clockwise order depending on whether z_0 is on the left or right side of η', respectively.

the quantum and Euclidean scaling exponents for the cut points of an $\mathrm{SLE}_{\kappa'}$ process (Figure 11.3b). This translates into a prediction of the dimension of the cut points given by

$$3 - \frac{3\kappa'}{8}. \tag{11.8}$$

This matches the prediction for the $n = 2$ SLE disconnection exponent [Dup04, Equations (12.48), (12.50)] as well as the rigorous derivation of this dimension given in [MW13, Theorem 1.2].

11.3 $\mathrm{SLE}_{\kappa'}$ double point dimension

In order for a point z_0 to a be a double point for an $\mathrm{SLE}_{\kappa'}$ process η', it has to be that η' hits z_0 and then gets macroscopically far away from z_0 before returning. Therefore we can represent the local behavior of η' near a quantum typical double point by gluing together eight wedges of alternating weight $2 - \frac{\gamma^2}{2}$ and $\gamma^2 - 2$. The former correspond to the two segments of η' that approach z_0 and the two segments of η' that leave from z_0 (for a total of four). The latter correspond to the regions between these four segments. The reason that it is natural to expect these latter regions to be $\gamma^2 - 2$ wedges is that if one conditions on three of the four segments of

η', then the conditional law of the fourth should be an $\mathrm{SLE}_{\kappa'}$ (no extra ρ values). See Figure 11.4 for an illustration.

By Proposition 8.16, gluing together these eight wedges yields a $\left(\frac{2}{\gamma} - \frac{\gamma}{2}\right)$-quantum cone. This leads to the following predictions of the quantum and Euclidean scaling exponents

$$\Delta = \frac{3}{2} - \frac{\kappa'}{8} \quad \text{and} \quad x = \frac{1}{2} + \frac{3}{\kappa'} - \frac{\kappa'}{16}. \tag{11.9}$$

This, in turn, leads to the prediction that the Euclidean dimension of the double points should be

$$2 - \frac{(12-\kappa')(4+\kappa')}{8\kappa'}. \tag{11.10}$$

This matches the heuristic derivation given by in [SD87, Dup87] in the context of contours of the FK model and the rigorous derivation given in [MW13, Theorem 1.1].

This can be generalized to the local behavior of η' near a quantum typical multiple point of order n, by gluing together $2n$ wedges of alternating weight $2 - \frac{\gamma^2}{2}$ and $\gamma^2 - 2$, yielding a quantum wedge of total weight $W = \frac{n\gamma^2}{2}$. Zipping up its two sides, one gets by Proposition 8.16 an α-quantum cone with $\alpha = Q - \frac{W}{2\gamma}$, and a quantum scaling dimension

$$\Delta = 1 - \frac{\alpha}{\gamma} = \frac{1}{2} + \frac{n}{4} - \frac{\kappa'}{8}. \tag{11.11}$$

For describing the local behavior near a boundary quantum typical multiple point of order n, one glues together in an alternating way $n+1$ quantum wedges of weight $\gamma^2 - 2$ with the n quantum wedges of weight $2 - \frac{\gamma^2}{2}$ drawn by η', yielding an α'-quantum wedge of total weight $W' = (n+2)\frac{\gamma^2}{2} - 2$, with $\alpha' = \frac{4}{\gamma} - n\frac{\gamma}{2}$, and a boundary quantum exponent

$$\Delta' = 1 - \frac{\alpha'}{\gamma} = 1 + \frac{n}{2} - \frac{\kappa'}{4}. \tag{11.12}$$

Equations (11.11) and (11.12) match the exponents of multiple non-simple $\mathrm{SLE}_{\kappa'}$ paths obtained by quantum gravity methods in [Dup04, Equation (11.37)], together with the boundary-bulk quantum rule for non-simple paths, $\Delta' = 2\Delta$. Notice that the *dual* dimension associated with Δ' (11.12), is $\widetilde{\Delta}' = \frac{2}{\kappa'}n$, hence linear in n, in agreement with Remark 11.1 above, and is the analog of (11.5) with κ simply replaced by κ' [Dup04]. These results also match the multiple path exponents obtained by random matrix techniques for the so-called dense phase of the $O(N)$ model on a random lattice [DK88a, Kos89, DK90, KK92, Dup04].

The corresponding boundary and bulk Euclidean exponents of n non-intersecting $\mathrm{SLE}_{\kappa'}$ paths, with $\kappa' \geq 4$, are obtained by using the KPZ relation (11.1), which yields the same results as in (11.7), with κ there simply replaced by κ'. They agree with

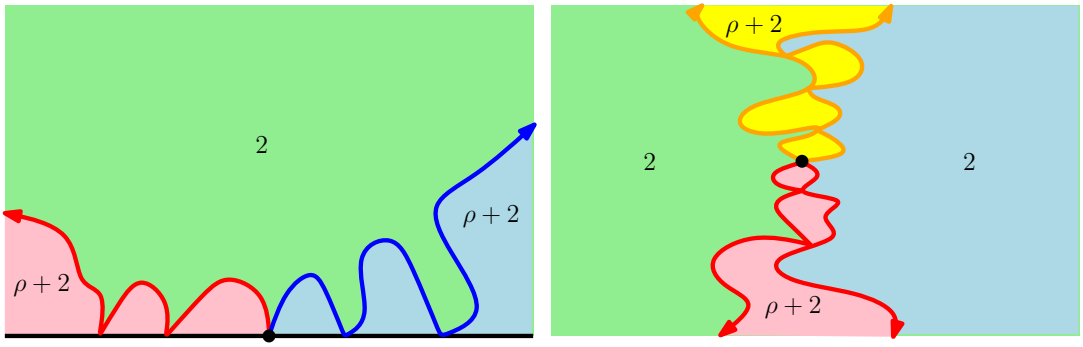

Figure 11.5: **Left:** a typical boundary intersection point z_0 for a boundary-intersecting $\mathrm{SLE}_\kappa(\rho)$ process looks like the welding of wedges of weight $\rho+2$, 2, and $\rho+2$. The first and third wedges correspond to the region cut off by the path before and after hitting z_0 and the weight 2 wedge corresponds to the region which is not cut off by the path. **Right:** a typical intersection point for two GFF flow lines with relative angle θ looks like the quantum cone which arises by welding together wedges of weights $\rho+2$, 2, $\rho+2$, and 2 where $\rho = \theta\chi/\lambda - 2$.

the corresponding exponents predicted for the dense phase critical $O(N)$ model or, equivalently, for the critical Potts model [dN83, Nie84, Nie87, Dup86, DS87, Dup87, BB88, Car92, BS93].

11.4 Boundary intersection dimension for $\mathrm{SLE}_\kappa(\rho)$

Suppose that η is a boundary intersecting $\mathrm{SLE}_\kappa(\rho)$ process with its force point immediately to the right of its seed. We know from Theorem 1.9 that if we draw η on top of an independent wedge $\mathcal{W}$ of weight $\rho+4$ then η divides $\mathcal{W}$ into independent wedges of weight 2 and $\rho+2$. From Section 7.4, we also know that the joint law of $(\mathcal{W},\eta)$ is invariant under the operation of cutting along η until reaching a "quantum typical" intersection point of η with $\partial\mathbf{H}$. Hence, the law of the part of $\mathcal{W}$ which is to the right of η at a quantum typical intersection point should be a wedge of weight $\rho+2$. By symmetry, such a wedge should also describe the local behavior of the surface to the left of η before a quantum typical intersection point. Therefore, gluing together three independent wedges with respective weights $\rho+2$, 2, and $\rho+2$ should describe the local behavior of $\mathcal{W}$ near a quantum typical intersection point of η with $\partial\mathbf{H}$. (See Figure 11.5a for an illustration.)

This leads to the prediction that the (boundary) quantum and Euclidean scaling

exponents for $\eta \cap \partial\mathbf{H}$ are respectively given by:

$$\Delta = \frac{2(2+\rho)}{\kappa} \quad \text{and} \quad x = \frac{(2+\rho)(2(4+\rho)-\kappa)}{2\kappa}. \tag{11.13}$$

Comparing this expression for Δ to (11.5) shows that ρ can be interpreted as a number of equivalent SLE_κ paths, in agreement with the quantum gravity equivalence predicted in [Dup06, Section 10.4]. This, in turn, leads to a prediction of the dimension of $\eta \cap \partial\mathbf{H}$ given by

$$\frac{(4+\rho)(\kappa - 2(2+\rho))}{2\kappa}. \tag{11.14}$$

This prediction matches the almost sure Hausdorff dimension for $\eta \cap \partial\mathbf{H}$ which was rigorously derived in [MW13, Theorem 1.6]. By SLE duality, for $\kappa \in (2,4)$ and $\rho = \kappa - 4$ this gives the dimension $2 - \frac{16}{\kappa'}$ of the intersection of an $\mathrm{SLE}_{\kappa'}$ process, $\kappa' = \frac{16}{\kappa}$, with $\partial\mathbf{H}$, predicted in [DS86, Dup89], and first derived in [AS08].

11.5 Intersection dimension of GFF flow lines

Suppose that we have SLE_κ flow lines η_1, η_2 of a GFF on $\mathbf{H}$ with angles $\theta_1 < \theta_2$ with angle difference $\theta = \theta_2 - \theta_1 \in (0, \pi\kappa/(4-\kappa))$; recall that this is the range of angle differences that allows two such paths to intersect and bounce off each other [MS12a, Theorem 1.5]. If we conformally map away the region which is to the right of η_1, then a quantum typical intersection point z_0 of η_1 and η_2 should be mapped to a quantum typical intersection point of the image of η_2 with the domain boundary. Let $\rho = \theta\chi/\lambda - 2$. By our heuristic for the intersection of $\mathrm{SLE}_\kappa(\rho)$ with $\partial\mathbf{H}$, this suggests that the local behavior of the surface near z_0 and to the left of η_1 should look like a gluing of three independent wedges with respective weights $\rho+2$, 2, and $\rho+2$. Moreover, these wedges should be independent of the local behavior of the surface to the right of η_1. By symmetry, this region should look like another independent wedge of weight 2. Therefore the whole picture should look like two weight $\rho+2$ wedges glued with two weight 2 wedges where the different types alternate. (See Figure 11.5b for an illustration.)

This leads to the prediction that the quantum and Euclidean scaling exponents are given by

$$\Delta = \frac{4+\kappa+2\rho}{2\kappa} \quad \text{and} \quad x = \frac{1}{4\kappa}\left(\rho + \frac{\kappa}{2} + 2\right)\left(\rho - \frac{\kappa}{2} + 6\right). \tag{11.15}$$

This leads to the prediction that the dimension of $\eta_1 \cap \eta_2 \cap \mathbf{H}$ is given by

$$2 - \frac{1}{2\kappa}\left(\rho + \frac{\kappa}{2} + 2\right)\left(\rho - \frac{\kappa}{2} + 6\right). \tag{11.16}$$

This matches the rigorous derivation of the almost sure Hausdorff dimension of $\eta_1 \cap \eta_2 \cap \mathbf{H}$ given in [MW13, Theorem 1.5].

12 Weldings of forested wedges and duality

Section 12.1 will add more detail to the explanation, provided in Section 1.7, of the fact that cutting an appropriate quantum wedge with a counterflow line produces a Lévy tree of quantum disks. We will see that this tree can be constructed from a totally asymmetric $\frac{\kappa'}{4}$-stable process. (The exponent $\frac{\kappa'}{4}$ was mentioned but not derived in Section 1.7.) This will imply that the lengths of the left and right boundaries of η' evolve as independent totally asymmetric $\frac{\kappa'}{4}$-stable processes. We will use this machinery to prove several of our main results about gluings of forested wedges: namely, Theorems 1.16–1.19.

As mentioned in Section 2.2, forested wedges (along with the closely related trees of quantum spheres constructed there) correspond to the "dual quantum gravity" surfaces that have been constructed non-rigorously in the physics literature. Section 12.2 will explain how these objects are related to certain random atomic measures that have been mathematically constructed elsewhere (see [BJRV13], as well related work in [DS09, Dup10]).

12.1 Brownian motion and SLE

We are now going to recall how to construct a Lévy tree to encode the genealogy structure of the quantum disks which are cut out by an $\mathrm{SLE}_{\kappa'}$ process for $\kappa' \in (4,8)$. In order to do so, we first need to derive the form of the process which describes the time-evolution of the left and right boundary lengths of such an object when drawn on top of a certain type of quantum wedge.

Theorem 12.1. *Fix $\kappa' \in (4,8)$. Suppose that η' is an $\mathrm{SLE}_{\kappa'}$ process drawn on top of an independent quantum wedge $\mathcal{W}$ of weight $\frac{3\gamma^2}{2} - 2$. Let $\mathfrak{q}_u$ (resp. (f_t)) be the quantum natural time (resp. centered Loewner flow) for η'. Let A_t (resp. B_t) be the leftmost (resp. rightmost) point on $\mathbf{R}$ hit by $\eta'|_{[0,t]}$ and let X_u (resp. Y_u) be the difference of the γ-LQG length of the segment of the outer boundary of $\eta'([0,\mathfrak{q}_u])$ which is to the left (resp. right) of $\eta'(\mathfrak{q}_u)$ minus the γ-LQG length of $(A_{\mathfrak{q}_u}, 0]$ (resp. $[0, B_{\mathfrak{q}_u})$). Then (X_u, Y_u) evolves as a pair of independent totally asymmetric $\frac{\kappa'}{4}$-stable processes. The same statement remains true if we instead draw η' on top of $h = \widetilde{h} + \frac{\gamma^2-8}{2\gamma}\log|\cdot|$ where $\widetilde{h}$ is a free boundary GFF on $\mathbf{H}$ independent of η'.*

Before we start to give the proof of Theorem 12.1, we first give the following corollary which gives the time-evolution of the boundary length of a radial $\mathrm{SLE}_{\kappa'}$ process drawn on top of an independent free boundary GFF on $\mathbf{D}$ parameterized by quantum natural time.

Corollary 12.2. *Fix $\kappa' \in (4,8)$. Suppose that*

$$h = \widetilde{h} + \frac{\gamma^2 - 8}{2\gamma} \log|\cdot - 1| - \frac{3\gamma^2 + 8}{4\gamma} \log|\cdot|$$

where $\widetilde{h}$ is a free boundary GFF on $\mathbf{D}$. Let η' be a radial $\mathrm{SLE}_{\kappa'}$ process on $\mathbf{D}$ from 1 to 0 which is independent of $\widetilde{h}$ and let $\mathfrak{q}_u$ be the quantum natural time for η'. Then the γ-LQG boundary length of the boundary of the component of $\mathbf{D} \setminus \eta'([0, \mathfrak{q}_u])$ containing 0 evolves as a totally asymmetric $\frac{\kappa'}{4}$-stable process conditioned to be non-negative. The same holds if η' is a whole-plane $\mathrm{SLE}_{\kappa'}$ process from 0 to ∞ and either

$$h = \widetilde{h} - \frac{\gamma^2 + 8}{4\gamma} \log|\cdot|$$

where $\widetilde{h}$ is a whole-plane GFF independent of η' or $\mathcal{C} = (\mathbf{C}, h, 0, \infty)$ is a quantum cone of weight $\frac{\gamma^2}{2}$ (i.e., $\alpha = \frac{\gamma^2+8}{4\gamma}$).

Proof. Theorem 12.1 implies that if we perform a chordal $\mathrm{SLE}_{\kappa'}$ exploration on top of a free boundary GFF on $\mathbf{H}$ plus $\frac{\gamma^2-8}{2\gamma} \log|\cdot|$ with the quantum natural time parameterization then the change in the left and right boundary lengths evolve as independent totally asymmetric $\frac{\kappa'}{4}$-stable processes. By taking the sum, this implies that the change in the total boundary length evolves as a totally asymmetric $\frac{\kappa'}{4}$-stable process. This, in turn, implies that if we perform reverse rather than forward $\mathrm{SLE}_{\kappa'}$ with the quantum natural time parameterization, then the change in the total boundary length evolves as a totally asymmetric $\frac{\kappa'}{4}$-stable process (but now with only positive rather than only negative jumps). Note that the evolution of the boundary length is determined by the bubbles cut out by the $\mathrm{SLE}_{\kappa'}$ (since the bubbles determine the jumps and the jumps determine the boundary length process since it is a Lévy process without a Gaussian part). By Theorem 7.27, the structure of the bubbles cut out by a radial $\mathrm{SLE}_{\kappa'}$ in the setting described in the statement of the corollary is the same as the structure of the bubbles cut out by a chordal $\mathrm{SLE}_{\kappa'}$. Therefore the length of $\partial\mathbf{D}$ evolves as a totally asymmetric $\frac{\kappa'}{4}$-stable process when one runs a reverse $\mathrm{SLE}_{\kappa'}$ radial Loewner flow parameterized by a quantum natural time. The result for radial $\mathrm{SLE}_{\kappa'}$ then follows by combining this with the time-reversal result from [Ber96, Theorem 18, Chapter 7]. The result for whole-plane $\mathrm{SLE}_{\kappa'}$ follows by applying the change of coordinates formula with the map $z \mapsto 1/z$ and rescaling. □

As mentioned in Section 1.7.3, Theorem 12.1 and Corollary 12.2 are consistent with other conjectures and results in the literature [Ang03, Kri05, Le 14] in the context of random planar maps and the Brownian plane.

We will derive Theorem 12.1 from the results of Section 9 and a general result about planar Brownian motion (Proposition 12.3 below).

Fix a value of $\theta \in [\frac{\pi}{2}, \pi)$ and let $p = -\cos(\theta)/(1-\cos(\theta)) \in [0, \frac{1}{2})$ (recall (9.3)). Suppose that $Z_t = (L_t, R_t)$ is a planar Brownian motion with $\text{var}(L_1) = \text{var}(R_1) = \frac{1}{2} - \frac{p}{2}$ and $\text{cov}(L_1, R_1) = \frac{p}{2}$. We say that a s is an ancestor of a time t if for all $r \in (s,t]$ we have that $L_r > L_s$ and $R_r > R_s$. If a time t has an ancestor s, then we will also refer to t as being **pinched**. Note that if a time t is pinched, then t is a $\frac{\pi}{2}$-cone time for (L,R) as defined in Section 9 just before Lemma 9.5. If t is not pinched, then we say that t is **ancestor free**. Note that the set of times which have an ancestor (resp. are ancestor free) is open (resp. closed) in $[0,\infty)$. In particular, we can express the times with an ancestor as a countable disjoint union of open intervals I_j; we will refer to such an interval as a pinched interval.

Proposition 12.3. *Suppose that Z_t is as described just above. There exists a non-decreasing RCLL process ℓ_t which is adapted to the filtration generated by Z_t and is almost surely constant on the pinched intervals such that the following is true. Let $T_u = \inf\{t \geq 0 : \ell_t > u\}$ be the right-continuous inverse of ℓ_t. Then L_{T_u} and R_{T_u} are independent, totally asymmetric $\frac{\pi}{\theta}$-stable processes.*

The process ℓ_t constructed in Proposition 12.3 should be thought of as the local time for Z in the ancestor free times. We note that Proposition 12.3 implies Proposition 1.15.

Proof of Proposition 12.3. For each $\alpha \in [0, 2\pi)$, we let $\mathbf{W}_\alpha = \{z \in \mathbf{C} : \arg(z) \in [0, \alpha]\}$ be the Euclidean wedge in $\mathbf{C}$ of opening angle α centered at 0. Note that a time t is pinched if and only if there exists $s \in (0,t]$ such that $Z_r \in \mathbf{W}_{\pi/2} + Z_s$ for all $r \in (s,t]$.

It will be useful for us now to perform a change of coordinates. Let

$$\widetilde{Z}_t = \frac{1}{\sin(\theta/2)} \begin{pmatrix} 1 & \cos(\theta) \\ 0 & \sin(\theta) \end{pmatrix} Z_t.$$

Then $\widetilde{Z}_t$ is a standard two-dimensional Brownian motion. Moreover, t is a pinched time for Z_t if and only if there exists $s \in (0,t]$ such that $\widetilde{Z}_r \in \mathbf{W}_\theta + \widetilde{Z}_s$ for all $r \in (s,t]$.

We are now going to identify the Poissonian structure of the pinched excursions. Fix $\epsilon > 0$ and then inductively define stopping times as follows. We let

$$\tau_{1,\epsilon} = \inf\left\{ s \geq 0 : \exists t \geq s : \widetilde{Z}_u \in \mathbf{W}_\theta + \widetilde{Z}_s \quad \forall u \in [s,t] \quad \text{and} \quad |\widetilde{Z}_t - \widetilde{Z}_s|^{\pi/\theta} \geq \epsilon \right\}$$

and

$$\sigma_{1,\epsilon} = \inf\left\{ t \geq \tau_{1,\epsilon} : \widetilde{Z}_t \notin \mathbf{W}_\theta + \widetilde{Z}_{\tau_{1,\epsilon}} \right\}.$$

Given that $\tau_{1,\epsilon}, \sigma_{1,\epsilon}, \ldots, \tau_{k,\epsilon}, \sigma_{k,\epsilon}$ have been defined for some $k \in \mathbf{N}$ we let

$$\tau_{k+1,\epsilon} = \inf\left\{ s \geq \sigma_{k,\epsilon} : \exists t \geq s : \widetilde{Z}_u \in \mathbf{W}_\theta + \widetilde{Z}_s \quad \forall u \in [s,t] \quad \text{and} \quad |\widetilde{Z}_t - \widetilde{Z}_s|^{\pi/\theta} \geq \epsilon \right\}$$

and

$$\sigma_{k+1,\epsilon} = \inf\left\{ t \geq \tau_{k+1,\epsilon} : \widetilde{Z}_t \notin \mathbf{W}_\theta + \widetilde{Z}_{\tau_{k+1,\epsilon}} \right\}.$$

Let

$$\Delta_{j,\epsilon} = |\widetilde{Z}_{\sigma_{j,\epsilon}} - \widetilde{Z}_{\tau_{j,\epsilon}}| = \frac{1}{\sin(\theta/2)} |Z_{\sigma_{j,\epsilon}} - Z_{\tau_{j,\epsilon}}|.$$

We also let $\xi_{j,\epsilon} = 1$ if $\widetilde{Z}_{\sigma_{j,\epsilon}}$ is contained in the horizontal component of $\partial \mathbf{W}_\theta \backslash \{0\} + \widetilde{Z}_{\tau_{j,\epsilon}}$, otherwise we let $\xi_{j,\epsilon} = -1$. Equivalently, $\xi_{j,\epsilon} = 1$ (resp. $\xi_{j,\epsilon} = -1$) if $Z_{\sigma_{j,\epsilon}} - Z_{\tau_{j,\epsilon}}$ has zero imaginary (resp. real) part. With $\Sigma_{j,\epsilon} = \xi_{j,\epsilon} \Delta_{j,\epsilon}$, the signed jump sizes $(\Sigma_{j,\epsilon})$ are i.i.d. by the strong Markov property for Z. (The law of the lengths of the excursions is described, for example, in [Spi58].)

We can describe the law of the $\Sigma_{j,\epsilon}$ as follows. For each $k \geq 1$ we let

$$\zeta_{k,\epsilon} = \inf\left\{ t \geq \tau_{k,\epsilon} : |\widetilde{Z}_t - \widetilde{Z}_{\tau_{k,\epsilon}}|^{\pi/\theta} \geq \epsilon \right\}.$$

Let μ denote the law of $\arg\left((\widetilde{Z}_{\zeta_{k,\epsilon}} - \widetilde{Z}_{\tau_{k,\epsilon}})^{\pi/\theta}\right)$. Then μ is supported on $(0,\pi)$. By the scale-invariance of Brownian motion, we have that μ does not depend on ϵ. Recall that the Poisson kernel on $\mathbf{H}$ is given by $P_y(x) = y/(\pi(x^2+y^2))$. Thus if $\theta = \pi$, the law of $\Sigma_{j,\epsilon}$ has density with respect to Lebesgue measure on $\mathbf{R}$ which is proportional to

$$\left(\int_0^\pi \frac{\mathrm{Im}(e^{i\psi})}{(u - \epsilon \mathrm{Re}(e^{i\psi}))^2 + \epsilon^2 \mathrm{Im}(e^{i\psi})^2} d\mu(\psi) \right) du.$$

For general values of θ, we can use the conformal invariance of Brownian motion and the map $z \mapsto z^{\pi/\theta}$ to determine the law of the $\Sigma_{j,\epsilon}$. In particular, the law of $\Sigma_{j,\epsilon}$ is proportional to

$$\varsigma_{\theta,\epsilon}(du) = \left(\int_0^\theta \frac{u^{\pi/\theta - 1} \mathrm{Im}(e^{i\psi})}{(u^{\pi/\theta} - \epsilon \mathrm{Re}(e^{i\psi}))^2 + \epsilon^2 \mathrm{Im}(e^{i\psi})^2} d\mu(\psi) \right) du. \tag{12.1}$$

Let

$$\varsigma_\theta(du) = u^{-1-\pi/\theta} du. \tag{12.2}$$

For each $u_0 > 0$ we note that both $\varsigma_{\theta,\epsilon}$ and ς_θ give finite mass to $A_{u_0} = \{u \in \mathbf{R} : |u| \geq u_0\}$. Since $\mu(\{0\}) = \mu(\{\pi\}) = 0$, it follows that for each $u_0 > 0$ the conditional law of $\varsigma_{\theta,\epsilon}$ given A_{u_0} (i.e., the restriction of $\varsigma_{\theta,\epsilon}$ to A_{u_0} normalized to be a probability measure) converges in total variation as $\epsilon \to 0$ to the conditional law of ς_θ given A_{u_0}.

Let Λ be a p.p.p. on $\mathbf{R}_+ \times \mathbf{R}$ with intensity measure $du \otimes \varsigma_\theta$ where du denotes Lebesgue measure on $\mathbf{R}_+$. It therefore follows that for each $u_0 > 0$, we can couple

together the pinched excursions of Z with displacement at least u_0 with the elements $(u, \Sigma) \in \Lambda$ with $|\Sigma| \geq u_0$ to be the same. Since this holds for each $u_0 > 0$, we can identify the pinched excursions of Z with the elements of Λ.

If $(u, \Sigma) \in \Lambda$, then u gives the value of ℓ_t in the pinched interval corresponding to Σ and it is clear that we can extend ℓ_t to be RCLL on $\mathbf{R}_+$. It follows from the law of large numbers argument used to prove [Kal02, Proposition 19.12] that ℓ_t is in fact adapted to the filtration generated by Z_t. In particular, ℓ_t is construct as an a.s. limit.

Recall that $(u, \Sigma) \in \Lambda$ corresponds to a jump of size $|\Sigma|$ in L_t (resp. R_t) if $\Sigma > 0$ (resp. $\Sigma < 0$). Let T_u be the right-continuous inverse of ℓ_t as in the statement of the proposition. Then L_{T_u} and R_{T_u} are Lévy processes with the same law. They are both totally asymmetric $\frac{\pi}{\theta}$-stable since they do not have a Gaussian part, only have negative jumps, and the Lévy measure for the jump part of each is given by restricting ς_θ to $\mathbf{R}_-$. Moreover, L_{T_u} and R_{T_u} are independent since their jump parts are independent. □

Recall from Section 9 that we can think of (L_t, R_t) as being the two-dimensional Brownian motion which encodes the change in the boundary lengths of the left and right sides of an independent space-filling $\mathrm{SLE}_{\kappa'}$ process η' drawn on top of a γ-quantum cone with $\gamma = 4/\sqrt{\kappa'}$. In this context, the pinched excursions come with a notion of "area" (namely, the length of the excursion) and "boundary length" (the displacement of whichever of L_t and R_t is not at the same place at the two interval endpoints). The "boundary length" is precisely the size of the jump of the stable process from Proposition 12.3. Using the notion of a Lévy tree, there is also a partial order on these jumps corresponding to the ancestor/descendant relationship. We want to use this to put a tree structure on the bubbles cut off by an $\mathrm{SLE}_{\kappa'}$ process. To do so, we first need to relate the range of an $\mathrm{SLE}_{\kappa'}$ process with the ancestor free times of Z.

Consider the thin quantum wedge which corresponds to $\eta'([0, \infty))$. By the definition of space-filling $\mathrm{SLE}_{\kappa'}$, this is the region between the flow lines of the whole-plane GFF used to generate η' with angles $-\frac{\pi}{2}$ and $\frac{\pi}{2}$. We then let $\widetilde{\eta}'$ be the counterflow line from ∞. By [MS13a, Theorem 1.14], the conditional law of $\widetilde{\eta}'$ given $\eta'([0, \infty))$ (i.e., the outer boundary of $\widetilde{\eta}'$) is independently that of an $\mathrm{SLE}_{\kappa'}(\frac{\kappa'}{2} - 4; \frac{\kappa'}{2} - 4)$ in each of the bubbles of $\eta'([0, \infty))$.

Lemma 12.4. *Let $\widetilde{\eta}'$ be the counterflow line from ∞ to 0 which travels through the thin wedge which corresponds to $\eta'([0, \infty))$ as described above. Then a point of $\eta'([0, \infty))$ is in the range of $\widetilde{\eta}'$ if and only if it is hit at an ancestor free time for Z.*

Proof. We will prove the lemma by showing that a point $z \in \eta'([0, \infty))$ is not in the range of $\widetilde{\eta}'$ if and only if t is a pinch time for Z. (See Figure 1.16 and Figure 1.17 for an illustration.)

Suppose that t is a time such that $\eta'(t)$ is not in the range of $\widetilde{\eta}'$. Then $\eta'(t)$ is contained in a bubble B which is pinched off by $\widetilde{\eta}'$. Let σ be the time that $\widetilde{\eta}'$ pinches off B (i.e., disconnects B from its target point) and let s be the time that η' first visits $\widetilde{\eta}'(\sigma)$. Then it is easy to see from the definition of space-filling $\mathrm{SLE}_{\kappa'}$ that $L_t > L_s$ and $R_t > R_s$. In fact, if $u \in (s,t)$ then $L_u > L_s$ and $R_u > R_s$. That is, t is a pinch time for (L,R).

Conversely, suppose that t is a pinch time for Z and let s be the left endpoint of the corresponding pinched interval. Then s is a local cut time for η'. Consequently, the time-reversal of η' will hit $\eta'(s)$ twice hence separate $\eta'(t)$ from ∞. Therefore $\widetilde{\eta}'$ will not visit $\eta'(t)$. □

Remark 12.5. Observe that if draw an independent $\mathrm{SLE}_{\kappa'}(\frac{\kappa'}{2}-4; \frac{\kappa'}{2}-4)$ process on top of a wedge of weight $2-\frac{\gamma^2}{2}$ (more precisely, one independent process for each bubble of the wedge), then we have two equivalent Poissonian descriptions for the bubbles cut out of the wedge by the path. The first is given in terms of the cone-excursions of a two-dimensional Brownian motion and the second is given in terms of the excursion measure of a Bessel process. Indeed, this first description follows from Proposition 12.3 above and the second follows by combining Proposition 8.14 and Theorem 7.27.

Combining Lemma 12.4 with Proposition 12.3 and Proposition 7.21 we get that gluing together two forested lines yields a $2-\frac{\gamma^2}{2}$ wedge. We record this result in the following proposition.

Proposition 12.6. *Suppose that $\mathcal{W}$ is a wedge of weight $2-\frac{\gamma^2}{2}$. If we cut $\mathcal{W}$ with a concatenation of independent $\mathrm{SLE}_{\kappa'}(\frac{\kappa'}{2}-4; \frac{\kappa'}{2}-4)$ processes (one for each bead of $\mathcal{W}$), then the bubbles which are to the left (resp. right) of the path have the structure of two independent forested lines.*

Proposition 12.6 gives the first part of Theorem 1.16. To finish proving Theorem 1.16, we need to show that the pair of forested lines almost surely determines the wedge of weight $2-\frac{\gamma^2}{2}$. We are going to deduce this result from the main result of Section 10, which implies that the entire wedge of weight $2-\frac{\gamma^2}{2}$ which corresponds to $\eta'([0,\infty))$ is almost surely determined by the pair (L,R) of Brownian motions for $t \geq 0$. In order to do so, we first need to collect the following observation.

Proposition 12.7. *Let A, B and C be random variables defined on a common probability space. Suppose that A and B together almost surely determine C. (That is, suppose there exists a function f such that $C = f(A,B)$ almost surely.) Suppose further that given A, the values B and C are conditionally independent. Then A almost surely determines C.*

We are now going to give the proofs of Theorems 1.16–1.19.

Proof of Theorem 1.16. As we mentioned earlier, the first part of Theorem 1.16 is given in Proposition 12.6. To finish the proof, we need to show that the pair of forested lines almost surely determine the zipping. Let A be the pair of forested lines, which we view as arising by cutting a $2-\frac{\gamma^2}{2}$ wedge with a concatenation of independent $\mathrm{SLE}_{\kappa'}(\frac{\kappa'}{2}-4;\frac{\kappa'}{2}-4)$ processes $\widetilde{\eta}'$. As described above, we can view $\widetilde{\eta}'$ as corresponding to the set of ancestor free times of a space-filling $\mathrm{SLE}_{\kappa'}$ process η'. Let B be the countable collection of paths obtained by restricting η' to each of the countably many disks of A. Let C be the entire quantum surface traced by $\eta'([0,t])$. It is not hard to see that A and B together determine the boundary length processes (i.e., the pair of Brownian motions) that determine C. By construction, we have that B and C are conditionally independent given A. The result then follows from Proposition 12.7. □

Proof of Theorem 1.17. The theorem in the case that $\kappa' \geq 8$ is a consequence of Proposition 8.14, so we will focus on the case that $\kappa' \in (4,8)$ (hence $\gamma \in (\sqrt{2},2)$).

Theorem 1.16 gives the result for forested lines, i.e. when $W_1 = W_2 = 0$. We are now going to generalize the result to the case that $W_1, W_2 \geq 0$. Fix $\rho_1, \rho_2 \geq \frac{\kappa'}{2}-4$ and let $W_i = \gamma^2 - 2 + \frac{\gamma^2}{4}\rho_i \geq 0$. Suppose that $\mathcal{W} = (\mathbf{H}, h, 0, \infty)$ is a wedge of weight $W = W_1 + W_2 + 2 - \frac{\gamma^2}{2}$. Further, suppose that η_1 (resp. η_2) is the flow line starting from 0 and targeted at ∞ of a GFF on $\mathbf{H}$ with boundary conditions given by 0 on $\mathbf{R}_-$ and $(W-2)\lambda$ on $\mathbf{R}_+$ with angle $\theta_1 = \frac{\lambda}{\chi}(1-W_1)$ (resp. $\theta_2 = -\frac{\lambda}{\chi}(1-\frac{\gamma^2}{2}+W_1)$). Proposition 8.14 implies that the region which is to the left (resp. right) of η_1 (resp. η_2), viewed as a quantum surface, is a wedge of weight W_1 (resp. W_2). Moreover, the region between η_1 and η_2, viewed as a quantum surface, is a wedge of weight $2-\frac{\gamma^2}{2}$ and these three wedges are independent. The counterflow line η' of this GFF plus $\pi(\frac{\gamma}{4}-\frac{W_1}{\gamma})$ from ∞ is marginally an $\mathrm{SLE}_{\kappa'}(\rho_1;\rho_2)$ process and, by [MS12a, Proposition 7.30], the conditional law of η' given η_1 and η_2 is independently that of an $\mathrm{SLE}_{\kappa'}(\frac{\kappa'}{2}-4;\frac{\kappa'}{2}-4)$ process in each of the bubbles between η_1 and η_2. (The reason that we have to add an angle to the field in the definition of η' is that we have normalized the boundary data to be consistent with Proposition 8.14.) Theorem 1.16 implies that these bubbles have the structure of independent forested lines and, moreover, these forested lines almost surely determine the middle wedge of weight $2-\frac{\gamma^2}{2}$. Combining everything proves the result. □

Proof of Theorem 1.18. This follows by applying Proposition 8.16 with a pair of GFF flow lines with an angle gap of π and then applying Theorem 1.16 to the resulting wedge of weight $2-\frac{\gamma^2}{2}$. □

Proof Theorem 1.19. The first part of the result is a consequence of Theorem 1.17. The second part of the theorem is given in Theorem 7.27. □

Proof of Theorem 12.1. The result in the case of a quantum wedge of weight $\frac{3\gamma^2}{2} - 2$ is given in Corollary 1.20. The result in the case of a free boundary GFF follows by rescaling. □

12.2 Surfaces with bottlenecks and atomic measures

The rigorous construction of the singular quantum measures $\mu_{\gamma'}$ with $\gamma' > 2$ uses the dual measure μ_γ, $\gamma := 4/\gamma' < 2$, and the additional randomness of a set of point masses $\{z_i : i \in \mathbf{N}\}$ such that $\{(\mu_{\gamma'}(z_i), z_i) : i \in \mathbf{N}\}$ is distributed as a p.p.p. $\mathcal{N}_{\gamma'}(du, dz)$ on $\mathbf{R}_+ \times D$ with intensity measure $\vartheta_\theta \otimes \mu_\gamma$, where $\vartheta_\theta(du) := u^{-1-\theta} du$ and du denotes Lebesgue measure on $\mathbf{R}_+$ and $\theta := 4/\gamma'^2 = \gamma^2/4 \in (0, 1)$ [DS09, Dup10]. Each point (u, z) represents an atom of size u located at z, and the quantum measure for $\gamma' > 2$ is then *purely atomic*,

$$\mu_{\gamma'}(dz) := \int_0^\infty u \, \mathcal{N}_{\gamma'}(du, dz), \quad \gamma' > 2. \tag{12.3}$$

In [BJRV13], a slightly different approach was proposed, the so-called "atomic Gaussian multiplicative chaos". After regularization, its limit coincides in the GFF case with the present construction.

For any subdomain $U \subseteq D$, the Laplace transforms of the atomic γ'-quantum measure (12.3) and the dual γ-quantum measure (1.1) then obey the *duality identity* [Dup10, Section 18.6.2],

$$\mathbf{E}\left[\exp(-\phi\, \mu_{\gamma'}(U))\right] = \mathbf{E}\left[\exp(\Gamma(-\theta)\phi^\theta \mu_\gamma(U))\right], \quad \gamma\gamma' = 4, \quad \forall \phi \geq 0. \tag{12.4}$$

This is a Lévy-Khintchine formula for an independently scattered stable process valid for all $\phi \in \mathbf{R}_+$, and where $\Gamma(-\theta) = -\Gamma(1-\theta)/\theta < 0$ is the usual Euler Γ-function. It can also be seen as the probabilistic formulation of the *Legendre transform* relating the free energies of dual Liouville theories, as first observed in [KH95].

The conjugate variable ϕ to the quantum area measure $\mu_{\gamma'}$ is often called "cosmological constant" in Liouville quantum gravity [Pol81, GM93, DFGZJ95, Nak04]. The duality identity (12.4) implies that the dual cosmological constant of μ_γ is $\phi' := -\Gamma(-\theta)\phi^\theta$; in other words, given μ_γ, the "typical size" (say, the median size) of $\mu_{\gamma'}(U)$ is of order $\mu_\gamma(U)^{\gamma'^2/4} = \mu_\gamma(U)^{4/\gamma^2}$. Consider indeed the conditional exponential expectation associated with (12.4),

$$\mathbf{E}\left[\exp(-\phi\mu_{\gamma'}(U)) \,|\, \mu_\gamma(U)\right] = \exp\big(\Gamma(-\theta)\phi^\theta \mu_\gamma(U)\big).$$

This yields the moment formula (see also [BJRV13]),

$$\mathbf{E}\left[\big(\mu_{\gamma'}(U)\big)^p \,|\, \mu_\gamma(U)\right] = \frac{\Gamma(1-\frac{p}{\theta})\big(-\Gamma(-\theta)\big)^{p/\theta}}{\Gamma(1-p)}\big(\mu_\gamma(U)\big)^{p/\theta}, \;\; 0 \leq p < \theta = \frac{4}{\gamma'^2} < 1,$$

which precisely illustrates the announced scaling relation existing between dual Liouville measures.

We are now going to explain how to view these measures for $\gamma'^2 \in (4,8)$ as corresponding to trees of surfaces using Lévy trees. We first need to recall a few facts about Lévy processes from [Ber96]. Fix $\alpha \in (1,2)$. Suppose that X is a totally asymmetric α-stable process with $\alpha \in (1,2)$ and let $I_t = \inf_{0 \le s \le t} X_s$ be the running infimum of X. Then $X_t - I_t$ is a Markov process [Ber96, Proposition 1, Chapter 6] with a local time ℓ_t at 0. In fact, $\ell_t = I_0 - I_t$. The right-continuous inverse $T_u = \inf\{t > 0 : \ell_t > u\}$ of ℓ_t is called the ladder time process. By [Ber96, Lemma 1, Chapter 8], we have that T_u is a stable subordinator of index $1/\alpha$. This implies that if $X_0 = v$ for $v > 0$, $u < v$, and $\tau = \inf\{t \ge 0 : X_t \le u\}$, then we can sample the lengths of the excursions of $X - I$ from 0 in $[0, \tau]$ as follows. Let Λ be a p.p.p. on $[u, v] \times \mathbf{R}_+$ with intensity measure given by $dt \otimes \vartheta_{\alpha^{-1}}$ where dt denotes Lebesgue measure on $[u, v]$. Then the elements of Λ are in correspondence with the excursions of $X - I$ from 0. In particular, $(w, \Sigma) \in \Lambda$ corresponds to an excursion of $X - I$ from 0 where the value of I at the start and end of the excursion is given by w and Σ gives its length.

To give the Lévy tree construction of the surfaces with $\gamma'^2 \in (4,8)$, we now suppose that X is a totally asymmetric $\frac{\gamma'^2}{4}$-stable process with $X_0 = u$ for some $u > 0$ and let I be the running infimum of X. Consider the tree of quantum surfaces which correspond to the Lévy tree generated by X (recall Figure 1.7). In this construction, we associate with each jump of X a conditionally independent γ-LQG sphere, $\gamma = 4/\gamma'$, as in Definition 4.21 with γ-LQG mass given by the size of the jump; we view the vertical segment from 0 to X_0 as the first jump of X. We think of the surface S associated with the first jump as being the principle bubble of the γ'-LQG surface. An excursion of $X - I$ from 0 is naturally associated with a root location on the vertical segment from 0 to X_0 given by the value that X takes on at the start of the excursion (which is also the same as the value taken on by I at this time). We then define the mass of such a point to be the length of time that it takes for $X - I$ to complete the corresponding excursion. This defines a purely atomic measure on the vertical segment from 0 to X_0.

We can use this purely atomic measure to define a purely atomic measure on S as follows. Pick a point $z_0 \in S$ from its γ-LQG area measure and then let η' be a space-filling $\mathrm{SLE}_{\kappa'}$ process on S starting from z_0 which is otherwise sampled conditionally independently of S. We then reparameterize η' according to γ-LQG area. Then the map which takes $t \in [0, X_0]$ to η' given by $t \mapsto \eta'(t)$ induces a measure preserving transformation from the vertical segment from 0 to X_0 onto S. It follows from the discussion in the previous paragraph that the induced point measure on S is equal in law to the γ'-LQG measure, $\gamma'^2 \in (4,8)$, described at the beginning of this subsection. We also note that the Lévy tree structure is the same as the Lévy tree structure we deduced for the surfaces cut out by an $\mathrm{SLE}_{\kappa'}$ process as described in Section 12.1.

13 Open Questions

First let us recall a few problems that have already been posed in this paper. In the beginning of Section 1, we asked the following.

Question 13.1. *Can one define a metric space structure on the peanosphere directly?*

Question 13.2. *Fix $\kappa' \in (4, 8)$. Consider the random graph whose vertices are the components of the complement of an $\mathrm{SLE}_{\kappa'}$ curve, where two components are considered adjacent if their boundaries intersect. Is this graph a.s. connected? In other words, is it a.s. the case that for any two such components U and V there exists a finite sequence of adjacent components $U_0, U_1, \ldots, U_n$ such that $U_0 = U$ and $U_n = V$?*

Section 10.5 discussed the problem of strengthening the topology of convergence to the peanosphere for certain discrete models, in order to understand the conformal structure of the discrete embedding. We remark that the number of ways to frame this problem is at least kmn if one has

1. k random planar map models (triangulations, quadrangulations, planar maps with unrestricted face sizes, etc.)
2. m ways to put a statistical physics structure on the planar map (uniform spanning tree, Ising model, three state Potts model, critical percolation, double dimer model, etc.)
3. n ways to embed a discrete graph "conformally" in the plane (circle packing, square tiling, discrete analytic mapping, Riemann conformal mapping of surface obtained by gluing unit polygons, etc.)

Solving even one of these formulations would be a significant breakthrough, and given the flexibility, one can reasonably argue that the variant that is easiest to solve is the most natural one to consider. Section 10.5 also discussed a toy problem (involving gluing of spheres) that was somewhere in between the discrete and continuum settings. A variant of that problem would be to show that a simple random walk on the graph of δ-area regions of Figure 10.1 (with two regions adjacent when the boundaries intersect) scales to two dimensional Brownian motion, up to a time change.

Additional problems include the following:

Question 13.3. *Use the hamburger cheeseburger machinery to strengthen the topology of convergence in a more modest (but still interesting) way: namely, show that in FK-decorated RPM, the lengths of the k largest loops (together with the adjacency graph on those loops, and the areas surrounded by the loops) scale to the corresponding continuum quantities defined for CLE-decorated LQG.*

Update: This question has been solved in [GM16], building on the works [GMS15, GS15a, GS15b].

Question 13.4. *In the peanosphere construction, compute the relationship between κ' and the Brownian correlation coefficient for $\kappa' > 8$.*

Update: This question has been solved in [GHMS15].

Question 13.5. *Understand near critical FK-decorated RPM models and their scaling limits from the peanosphere perspective.*

We also direct the reader to the open questions sections of [She10, MS13b] for additional questions.

References

[AC13] O. Angel and N. Curien. Percolations on random maps I: half-plane models. *ArXiv e-prints*, January 2013, 1301.5311.

[ADA99] M. Aizenman, B. Duplantier, and A. Aharony. Path-crossing exponents and the external perimeter in 2d percolation. *Phys. Rev. Lett.*, 83:1359–1362, 1999. cond-mat/9901018.

[ADJ94] J. Ambjørn, B. Durhuus, and T. Jónsson. A solvable 2D gravity model with $\gamma > 0$. *Modern Phys. Lett. A*, 9(13):1221–1228, 1994. hep-th/9401137. MR1279108

[AGBC93] L. Alvarez-Gaumé, J. L. F. Barbón, and Č. Crnković. A proposal for strings at $D > 1$. *Nuclear Phys. B*, 394(2):383–422, 1993. hep-th/9208026. MR1214333 (94e:81229)

[AHS15] J. Aru, Y. Haung, and X. Sun. Two perspectives of the unit area quantum sphere and their equivalence. 2015. In preparation.

[AKSJ11] K. Astala, A. Kupiainen, E. Saksman, and P. Jones. Random conformal weldings. *Acta mathematica*, 207(2):203–254, 2011.

[Ald91a] D. Aldous. The continuum random tree. I. *Ann. Probab.*, 19(1):1–28, 1991. MR1085326 (91i:60024)

[Ald91b] D. Aldous. The continuum random tree. II. An overview. In *Stochastic analysis (Durham, 1990)*, volume 167 of *London Math. Soc. Lecture Note Ser.*, pages 23–70. Cambridge Univ. Press, Cambridge, 1991. MR1166406 (93f:60010)

[Ald93] D. Aldous. The continuum random tree. III. *Ann. Probab.*, 21(1):248–289, 1993. MR1207226 (94c:60015)

[Ang03] O. Angel. Growth and percolation on the uniform infinite planar triangulation. *Geom. Funct. Anal.*, 13(5):935–974, 2003. math/0208123. MR2024412 (2005b:60015)

[AR13] O. Angel and G. Ray. Classification of Half Planar Maps. *ArXiv e-prints*, March 2013, 1303.6582.

[AS03] O. Angel and O. Schramm. Uniform infinite planar triangulations. *Comm. Math. Phys.*, 241(2-3):191–213, 2003. math/0207153. MR2013797 (2005b:60021)

[AS08] T. Alberts and S. Sheffield. Hausdorff dimension of the SLE curve intersected with the real line. *Electron. J. Probab.*, 13:no. 40, 1166–1188, 2008. 0711.4070. MR2430703 (2009e:60025)

[AY09] M. Aspenberg and M. Yampolsky. Mating non-renormalizable quadratic polynomials. *Comm. Math. Phys.*, 287(1):1–40, 2009. math/0610343. MR2480740 (2009k:37098)

[BB88] M. T. Batchelor and H. W. J. Blöte. Conformal anomaly and scaling dimensions of the O(n) model from an exact solution on the honeycomb lattice. *Phys. Rev. Lett.*, 61(2):138–140, 1988. MR948142 (89g:82064a)

[Ber96] J. Bertoin. *Lévy processes*, volume 121 of *Cambridge Tracts in Mathematics*. Cambridge University Press, Cambridge, 1996. MR1406564 (98e:60117)

[BH12] S. H. Boyd and C. Henriksen. The Medusa algorithm for polynomial matings. *Conform. Geom. Dyn.*, 16:161–183, 2012. 1102.5047. MR2943594

[Bis07] C. J. Bishop. Conformal welding and Koebe's theorem. *Ann. of Math. (2)*, 166(3):613–656, 2007. MR2373370 (2009d:30010)

[BJRV13] J. Barral, X. Jin, R. Rhodes, and V. Vargas. Gaussian multiplicative chaos and KPZ duality. *Comm. Math. Phys.*, 323(2):451–485, 2013. 1202.5296. MR3096527

[BS93] M. T. Batchelor and J. Suzuki. Exact solution and surface critical behaviour of an O(n) model on the honeycomb lattice. *J. Phys. A*, 26(16):L729–L735, 1993. MR1236589 (94j:82024)

[Car84] J. L. Cardy. Conformal invariance and surface critical behavior. *Nuclear Phys. B*, 240:514–532, 1984.

[Car92] J. L. Cardy. Critical percolation in finite geometries. *J. Phys. A*, 25(4):L201–L206, 1992. hep-th/9111026. MR1151081 (92m:82048)

[Cha08] S. Chatterjee. Chaos, concentration, and multiple valleys. *ArXiv e-prints*, December 2008, 0810.4221.

[CK13] N. Curien and I. Kortchemski. Random stable looptrees. *ArXiv e-prints*, April 2013, 1304.1044.

[CL12] N. Curien and J.-F. Le Gall. The Brownian plane. *ArXiv e-prints*, April 2012, 1204.5921.

[CL14] N. Curien and J.-F. Le Gall. The hull process of the Brownian plane. *ArXiv e-prints*, September 2014, 1409.4026.

[Cur13] N. Curien. A glimpse of the conformal structure of random planar maps. *ArXiv e-prints*, August 2013, 1308.1807.

[Dav88] F. David. Conformal field theories coupled to 2-D gravity in the conformal gauge. *Modern Phys. Lett. A*, 3(17):1651–1656, 1988. MR981529 (89k:81138)

[DDSW90] S. R. Das, A. Dhar, A. M. Sengupta, and S. R. Wadia. New critical behavior in $d = 0$ large-N matrix models. *Modern Phys. Lett. A*, 5(13):1041–1056, 1990. MR1057913 (92a:81134)

[DFGZJ95] P. Di Francesco, P. Ginsparg, and J. Zinn-Justin. 2D gravity and random matrices. *Phys. Rep.*, 254:1–133, 1995, hep-th/9306153. MR1320471 (96c:81191)

[DK88a] B. Duplantier and I. Kostov. Conformal spectra of polymers on a random surface. *Phys. Rev. Lett.*, 61(13):1433–1437, 1988. MR960093 (89k:82067)

[DK88b] B. Duplantier and K.-H. Kwon. Conformal invariance and intersections of random walks. *Phys. Rev. Lett.*, 61:2514–2517, 1988.

[DK89] J. Distler and H. Kawai. Conformal field theory and 2D quantum gravity. *Nuclear Phys. B*, 321(2):509–527, 1989. MR1005268 (90g:81226)

[DK90] B. Duplantier and I. K. Kostov. Geometrical critical phenomena on a random surface of arbitrary genus. *Nuclear Phys. B*, 340(2-3):491–541, 1990. MR1068092 (91m:82056)

[DKRV14] F. David, A. Kupiainen, R. Rhodes, and V. Vargas. Liouville Quantum Gravity on the Riemann sphere. *ArXiv e-prints*, October 2014, 1410.7318.

[DLG02] T. Duquesne and J.-F. Le Gall. Random trees, Lévy processes and spatial branching processes. *Astérisque*, 281:vi+147, 2002. math/0509558. MR1954248 (2003m:60239)

[dN83] M. den Nijs. Extended scaling relations for the magnetic critical exponents of the Potts model. *Phys. Rev. B*, 27(3):1674–1679, 1983. MR690541 (85a:82028)

[DRSV14a] B. Duplantier, R. Rhodes, S. Sheffield, and V. Vargas. Critical gaussian multiplicative chaos: Convergence of the derivative martingale. *The Annals of Probability*, 42(5):1769–1808, 09 2014.

[DRSV14b] B. Duplantier, R. Rhodes, S. Sheffield, and V. Vargas. Renormalization of Critical Gaussian Multiplicative Chaos and KPZ Relation. *Comm. Math. Phys.*, 330(1):283–330, 2014. MR3215583

[DS86] B. Duplantier and H. Saleur. Exact surface and wedge exponents for polymers in two dimensions. *Phys. Rev. Lett.*, 57(25):3179–3182, 1986. MR869969 (88e:82022)

[DS87] B. Duplantier and H. Saleur. Exact critical properties of two-dimensional dense self-avoiding walks. *Nuclear Phys. B*, 290(3):291–326, 1987. MR919521 (89g:82049)

[DS88] B. Duplantier and H. Saleur. Winding-angle distributions of two-dimensional self-avoiding walks from conformal invariance. *Phys. Rev. Lett.*, 60(23):2343–2346, 1988. MR947310 (89e:82008)

[DS09] B. Duplantier and S. Sheffield. Duality and the Knizhnik-Polyakov-Zamolodchikov relation in Liouville quantum gravity. *Phys. Rev. Lett.*, 102(15):150603, 4, 2009. 0901.0277. MR2501276 (2010d:83106)

[DS11a] B. Duplantier and S. Sheffield. Liouville quantum gravity and KPZ. *Invent. Math.*, 185(2):333–393, 2011. 0808.1560. MR2819163 (2012f:81251)

[DS11b] B. Duplantier and S. Sheffield. Schramm-Loewner evolution and Liouville quantum gravity. *Phys. Rev. Lett.*, 107:131305, 2011. 1012.4800.

[Dub05] J. Dubédat. SLE(κ, ρ) martingales and duality. *Ann. Probab.*, 33(1):223–243, 2005. math/0303128. MR2118865 (2005j:60180)

[Dub09] J. Dubédat. Duality of Schramm-Loewner evolutions. *Ann. Sci. Éc. Norm. Supér. (4)*, 42(5):697–724, 2009. 0711.1884. MR2571956 (2011g:60151)

[Dup86] B. Duplantier. Exact critical exponents for two-dimensional dense polymers. *J. Phys. A*, 19(16):L1009–L1014, 1986. MR865722 (88a:82034)

[Dup87] B. Duplantier. Critical exponents of Manhattan Hamiltonian walks in two dimensions, from Potts and O(n) models. *J. Statist. Phys.*, 49(3-4):411–431, 1987. MR926190 (89b:82025)

[Dup89] B. Duplantier. Fractals in two dimensions and conformal invariance. *Physica D*, 38(1-3):71–87, 1989. Fractals in physics (Vence, 1989). MR1017710 (90i:82023)

[Dup98] B. Duplantier. Random walks and quantum gravity in two dimensions. *Phys. Rev. Lett.*, 81(25):5489–5492, 1998. MR1666816 (99j:83034)

[Dup99] B. Duplantier. Harmonic measure exponents for two-dimensional percolation. *Phys. Rev. Lett.*, 82(20):3940–3943, 1999, cond-mat/9901008. MR1688869 (99m:82029)

[Dup00] B. Duplantier. Conformally invariant fractals and potential theory. *Phys. Rev. Lett.*, 84(7):1363–1367, 2000, cond-mat/9908314. MR1740371 (2001c:82040)

[Dup03] B. Duplantier. Higher conformal multifractality. *J. Stat. Phys.*, 110:691–738, 2003, arXiv:cond-mat/0207743. Special issue in honor of Michael E. Fisher's 70th birthday (Piscataway, NJ, 2001). MR1964687 (2004b:82020)

[Dup04] B. Duplantier. Conformal fractal geometry & boundary quantum gravity. In M. L. Lapidus and M. van Frankenhuysen, editors, *Fractal geometry and applications: a jubilee of Benoît Mandelbrot, Part 2*, volume 72 of *Proc. Sympos. Pure Math.*, pages 365–482. Amer. Math. Soc., Providence, RI, 2004, math-ph/0608053. MR2112128 (2005m:82057)

[Dup06] B. Duplantier. Conformal random geometry. In A. Bovier, F. Dunlop, F. den Hollander, A. van Enter, and J. Dalibard, editors, *Mathematical statistical physics (Les Houches Summer School, Session LXXXIII, 2005)*, pages 101–217. Elsevier B. V., Amsterdam, 2006, arXiv:math-ph/0608053. MR2581884 (2012d:82017)

[Dup10] B. Duplantier. A rigorous perspective on Liouville quantum gravity and the KPZ relation. In S. Ouvry, J. Jacobsen, V. Pasquier, D. Serban, and

L. Cugliandolo, editors, *Exact methods in low-dimensional statistical physics and quantum theory (Les Houches Summer School LXXXIX, 2008)*, pages 529–561. Oxford Univ. Press, Oxford, 2010. MR2668656 (2011j:81292)

[Dur94] B. Durhuus. Multi-spin systems on a randomly triangulated surface. *Nuclear Phys. B*, 426(1):203–222, 1994. hep-th/9402052. MR1293688 (95g:82042)

[ES81] B. Efron and C. Stein. The jackknife estimate of variance. *Ann. Statist.*, 9(3):586–596, 1981. MR615434 (82k:62074)

[Eva85] S. N. Evans. On the Hausdorff dimension of Brownian cone points. *Math. Proc. Cambridge Philos. Soc.*, 98(2):343–353, 1985. MR795899 (86j:60185)

[Fat80] A. Fathi. Structure of the group of homeomorphisms preserving a good measure on a compact manifold. *Ann. Sci. École Norm. Sup. (4)*, 13(1):45–93, 1980. MR584082 (81k:58042)

[GHMS15] E. Gwynne, N. Holden, J. Miller, and X. Sun. Brownian motion correlation in the peanosphere for $\kappa \geq 8$. *ArXiv e-prints*, October 2015, 1510.04687.

[GKMW16] E. Gwynne, A. Kassel, J. Miller, and D. B. Wilson. Topologically-weighted spanning trees on planar maps and SLE-decorated Liouville quantum gravity for $\kappa \geq 8$. 2016. In preparation.

[GM93] P. Ginsparg and G. Moore. Lectures on 2D gravity and 2D string theory (TASI 1992). In J. Harvey and J. Polchinski, editors, *Recent direction in particle theory, Proceedings of the 1992 TASI*. World Scientific, Singapore, 1993, hep-th/9304011.

[GM16] E. Gwynne and J. Miller. Convergence of the topology of critical Fortuin-Kasteleyn planar maps to that of CLE_κ on a Liouville quantum surface. 2016. In preparation.

[GMS15] E. Gwynne, C. Mao, and X. Sun. Scaling limits for the critical Fortuin-Kasteleyn model on a random planar map I: cone times. 2015. arXiv:1502.00546.

[GS15a] E. Gwynne and X. Sun. Scaling limits for the critical Fortuin-Kastelyn model on a random planar map II: local estimates and empty reduced word exponent. 2015. arXiv:1505.03375.

[GS15b] E. Gwynne and X. Sun. Scaling limits for the critical Fortuin-Kastelyn model on a random planar map III: finite volume case. *ArXiv e-prints*, October 2015, 1510.06346.

[HMP10] X. Hu, J. Miller, and Y. Peres. Thick points of the Gaussian free field. *Ann. Probab.*, 38(2):896–926, 2010. 0902.3842. MR2642894 (2011c:60117)

[HR12] D. M. Halverson and D. Repovš. Survey on the Generalized RL Moore Problem. *arXiv e-prints*, January 2012, 1201.3897.

[IM74] K. Itô and H. P. McKean, Jr. *Diffusion processes and their sample paths*. Springer-Verlag, Berlin-New York, 1974. Second printing, corrected, Die Grundlehren der mathematischen Wissenschaften, Band 125. MR0345224 (49 #9963)

[JM92] S. Jain and S. D. Mathur. World-sheet geometry and baby universes in 2D quantum gravity. *Phys. Lett. B*, 286(3-4):239–246, 1992. hep-th/9204017. MR1175135 (93d:81160)

[JS00] P. W. Jones and S. K. Smirnov. Removability theorems for Sobolev functions and quasiconformal maps. *Ark. Mat.*, 38(2):263–279, 2000. MRMR1785402 (2001i:46049)

[Kah85] J.-P. Kahane. Sur le chaos multiplicatif. *Ann. Sci. Math. Québec*, 9(2):105–150, 1985. MR829798 (88h:60099a)

[Kah86] J.-P. Kahane. Une inégalité du type de Slepian et Gordon sur les processus gaussiens. *Israel J. Math.*, 55(1):109–110, 1986. MR858463 (88a:60075)

[Kal02] O. Kallenberg. *Foundations of modern probability*. Probability and its Applications (New York). Springer-Verlag, New York, second edition, 2002. MR1876169 (2002m:60002)

[KH95] I. R. Klebanov and A. Hashimoto. Non-perturbative solution of matrix models modified by trace-squared terms. *Nuclear Phys. B*, 434(1-2):264–282, 1995. hep-th/9409064. MR1312995 (95i:81180)

[KH96] I. R. Klebanov and A. Hashimoto. Wormholes, matrix models, and Liouville gravity. *Nuclear Phys. B Proc. Suppl.*, 45BC:135–148, 1996. String theory, gauge theory and quantum gravity (Trieste, 1995). MR1410550 (97h:81202)

[KK92] V. A. Kazakov and I. K. Kostov. Loop gas model for open strings. *Nuclear Phys. B*, 386(3):520–557, 1992. hep-th/9205059. MR1195992 (93m:81118)

[Kle95] I. R. Klebanov. Touching random surfaces and Liouville gravity. *Phys. Rev. D (3)*, 51(4):1836–1841, 1995. hep-th/9407167. MR1320922 (96h:81072)

[KMSW15] R. Kenyon, J. Miller, S. Sheffield, and D. B. Wilson. Bipolar orientations on planar maps and SLE_12. *ArXiv e-prints*, November 2015, 1511.04068.

[KN04] W. Kager and B. Nienhuis. A guide to stochastic Löwner evolution and its applications. *J. Statist. Phys.*, 115(5-6):1149–1229, 2004. math-ph/0312056. MR2065722 (2005f:82037)

[Kor92] G. P. Korchemsky. Matrix model perturbed by higher order curvature terms. *Modern Phys. Lett. A*, 7(33):3081–3100, 1992. hep-th/9205014. MR1186338 (93f:81135)

[Kos89] I. K. Kostov. O(n) vector model on a planar random lattice: spectrum of anomalous dimensions. *Modern Phys. Lett. A*, 4(3):217–226, 1989. MR1016518 (90h:81121)

[KPZ88] V. G. Knizhnik, A. M. Polyakov, and A. B. Zamolodchikov. Fractal structure of 2D-quantum gravity. *Modern Phys. Lett. A*, 3(8):819–826, 1988. MR947880 (89i:83039)

[Kri05] M. Krikun. Local structure of random quadrangulations. *ArXiv e-prints*, December 2005, math/0512304.

[KS91] I. Karatzas and S. E. Shreve. *Brownian motion and stochastic calculus*, volume 113 of *Graduate Texts in Mathematics*. Springer-Verlag, New York, second edition, 1991. MR1121940 (92h:60127)

[Lam67] J. Lamperti. Continuous state branching processes. *Bull. Amer. Math. Soc.*, 73:382–386, 1967. MR0208685 (34 #8494)

[Law13] G. F. Lawler. Continuity of radial and two-sided radial SLE at the terminal point. In *In the tradition of Ahlfors-Bers. VI*, volume 590 of *Contemp. Math.*, pages 101–124. Amer. Math. Soc., Providence, RI, 2013. 1104.1620. MR3087930

[Le 14] J.-F. Le Gall. Random geometry on the sphere. *ArXiv e-prints*, March 2014, 1403.7943.

[LG07] J.-F. Le Gall. The topological structure of scaling limits of large planar maps. *Invent. Math.*, 169(3):621–670, 2007, math/0607567. MR2336042 (2008i:60022)

[Lig05] T. M. Liggett. *Interacting particle systems*. Classics in Mathematics. Springer-Verlag, Berlin, 2005. Reprint of the 1985 original. MR2108619 (2006b:60003)

[LR12] G. F. Lawler and M. A. Rezaei. Minkowski content and natural parameterization for the Schramm-Loewner evolution. *ArXiv e-prints*, November 2012, 1211.4146.

[LS11] G. F. Lawler and S. Sheffield. A natural parametrization for the Schramm-Loewner evolution. *Ann. Probab.*, 39(5):1896–1937, 2011. 0906.3804. MR2884877

[LSW01a] G. F. Lawler, O. Schramm, and W. Werner. The dimension of the planar Brownian frontier is 4/3. *Math. Res. Lett.*, 8(4):401–411, 2001. math/0010165. MR1849257 (2003a:60127b)

[LSW01b] G. F. Lawler, O. Schramm, and W. Werner. Values of Brownian intersection exponents. I. Half-plane exponents. *Acta Math.*, 187(2):237–273, 2001. math/9911084. MR1879850 (2002m:60159a)

[LSW01c] G. F. Lawler, O. Schramm, and W. Werner. Values of Brownian intersection exponents. II. Plane exponents. *Acta Math.*, 187(2):275–308, 2001. math/0003156. MR1879851 (2002m:60159b)

[LSW02] G. F. Lawler, O. Schramm, and W. Werner. Values of Brownian intersection exponents. III. Two-sided exponents. *Ann. Inst. H. Poincaré Probab. Statist.*, 38(1):109–123, 2002. math/0005294. MR1899232 (2003d:60163)

[LSW04] G. F. Lawler, O. Schramm, and W. Werner. Conformal invariance of planar loop-erased random walks and uniform spanning trees. *Ann. Probab.*, 32(1B):939–995, 2004. math/0112234. MR2044671 (2005f:82043)

[LW99] G. F. Lawler and W. Werner. Intersection exponents for planar Brownian motion. *Ann. Probab.*, 27(4):1601–1642, 1999. MR1742883 (2000k:60165)

[LW00] G. F. Lawler and W. Werner. Universality for conformally invariant intersection exponents. *J. Eur. Math. Soc. (JEMS)*, 2(4):291–328, 2000. MR1796962 (2002g:60123)

[LZ13] G. F. Lawler and W. Zhou. *SLE* curves and natural parametrization. *Ann. Probab.*, 41(3A):1556–1584, 2013. 1006.4936. MR3098684

[Man72] B. B. Mandelbrot. Possible refinement of the lognormal hypothesis concerning the distribution of energy dissipation in intermittent turbulence. In *Statistical models and turbulence*, pages 333–351. Springer, 1972.

[Mil04] J. Milnor. Pasting together Julia sets: a worked out example of mating. *Experiment. Math.*, 13(1):55–92, 2004. MR2065568 (2005c:37087)

[Mil06] J. Milnor. *Dynamics in one complex variable*, volume 160 of *Annals of Mathematics Studies*. Princeton University Press, Princeton, NJ, third edition, 2006. MR2193309 (2006g:37070)

[Moo25] R. L. Moore. Concerning upper semi-continuous collections of continua. *Trans. Amer. Math. Soc.*, 27(4):416–428, 1925. MR1501320

[MP83] S. A. Morris and V. C. Peck. A note on homeomorphic measures on topological groups. *Proc. Edinburgh Math. Soc. (2)*, 26(2):169–171, 1983. MR705260 (85a:22006)

[MS12a] J. Miller and S. Sheffield. Imaginary Geometry I: Interacting SLEs. *ArXiv e-prints*, January 2012, 1201.1496. To appear in Probability Theory and Related Fields.

[MS12b] J. Miller and S. Sheffield. Imaginary geometry II: reversibility of $\mathrm{SLE}_\kappa(\rho_1;\rho_2)$ for $\kappa \in (0,4)$. *ArXiv e-prints*, January 2012, 1201.1497. To appear in Annals of Probability.

[MS12c] J. Miller and S. Sheffield. Imaginary geometry III: reversibility of SLE_κ for $\kappa \in (4,8)$. *ArXiv e-prints*, January 2012, 1201.1498. To appear in Annals of Math.

[MS13a] J. Miller and S. Sheffield. Imaginary geometry IV: interior rays, whole-plane reversibility, and space-filling trees. *ArXiv e-prints*, February 2013, 1302.4738.

[MS13b] J. Miller and S. Sheffield. Quantum Loewner Evolution. *ArXiv e-prints*, December 2013, 1312.5745. To appear in Duke Mathematical Journal.

[MS15a] J. Miller and S. Sheffield. An axiomatic characterization of the Brownian map. *ArXiv e-prints*, June 2015, 1506.03806.

[MS15b] J. Miller and S. Sheffield. Liouville quantum gravity and the Brownian map I: The QLE(8/3,0) metric. *ArXiv e-prints*, July 2015, 1507.00719.

[MS15c] J. Miller and S. Sheffield. Liouville quantum gravity spheres as matings of finite-diameter trees. *ArXiv e-prints*, June 2015, 1506.03804.

[MS16a] J. Miller and S. Sheffield. Liouville quantum gravity and the Brownian map II: geodesics and continuity of the embedding. 2016. In preparation.

[MS16b] J. Miller and S. Sheffield. Liouville quantum gravity and the Brownian map III: the conformal structure is determined. 2016. In preparation.

[MW13] J. Miller and H. Wu. Intersections of SLE Paths: the double and cut point dimension of SLE. *ArXiv e-prints*, March 2013, 1303.4725.

[Nak04] Y. Nakayama. Liouville field theory: a decade after the revolution. *Internat. J. Modern Phys. A*, 19(17-18):2771–2930, 2004. MR2073993 (2005j:81170)

[Nie82] B. Nienhuis. Exact critical point and critical exponents of O(n) models in two dimensions. *Phys. Rev. Lett.*, 49(15):1062–1065, 1982. MR675241 (84a:81035)

[Nie84] B. Nienhuis. Critical behavior of two-dimensional spin models and charge asymmetry in the Coulomb gas. *J. Statist. Phys.*, 34(5-6):731–761, 1984. MR751711 (85i:82074)

[Nie87] B. Nienhuis. Coulomb gas formulation of two-dimensional phase transitions. In C. Domb, M. Green, and J. Lebowitz, editors, *Phase transitions and critical phenomena, Vol. 11*, pages 1–53. Academic Press, London, 1987. MR942673 (90b:82023)

[Nol03] J. Nolan. *Stable distributions: models for heavy-tailed data*. Birkhäuser, 2003.

[OU41] J. C. Oxtoby and S. M. Ulam. Measure-preserving homeomorphisms and metrical transitivity. *Ann. of Math. (2)*, 42:874–920, 1941. MR0005803 (3,211b)

[Pol81] A. M. Polyakov. Quantum geometry of bosonic strings. *Phys. Lett. B*, 103(3):207–210, 1981. MR623209 (84h:81093a)

[PY82] J. Pitman and M. Yor. A decomposition of Bessel bridges. *Z. Wahrsch. Verw. Gebiete*, 59(4):425–457, 1982. MR656509 (84a:60091)

[PY96] J. Pitman and M. Yor. Decomposition at the maximum for excursions and bridges of one-dimensional diffusions. In *Itô's stochastic calculus and probability theory*, pages 293–310. Springer, Tokyo, 1996. MR1439532 (98f:60153)

[RS05] S. Rohde and O. Schramm. Basic properties of SLE. *Ann. of Math. (2)*, 161(2):883–924, 2005. math/0106036. MR2153402 (2006f:60093)

[Rud87] W. Rudin. *Real and complex analysis*. McGraw-Hill Book Co., New York, third edition, 1987. MR924157 (88k:00002)

[RV10] R. Robert and V. Vargas. Gaussian multiplicative chaos revisited. *Ann. Probab.*, 38(2):605–631, 2010. 0807.1030. MR2642887 (2011c:60160)

[RV11] R. Rhodes and V. Vargas. KPZ formula for log-infinitely divisible multifractal random measures. *ESAIM Probab. Stat.*, 15:358–371, 2011. 0807.1036. MR2870520

[RY99] D. Revuz and M. Yor. *Continuous martingales and Brownian motion*, volume 293 of *Grundlehren der Mathematischen Wissenschaften [Fundamental Principles of Mathematical Sciences]*. Springer-Verlag, Berlin, third edition, 1999. MR2000h:60050

[Sal86] H. Saleur. New exact exponents for two-dimensional self-avoiding walks. *J. Phys. A*, 19(13):L807–L810, 1986.

[Sch00] O. Schramm. Scaling limits of loop-erased random walks and uniform spanning trees. *Israel J. Math.*, 118:221–288, 2000. math/9904022. MR1776084 (2001m:60227)

[SD87] H. Saleur and B. Duplantier. Exact determination of the percolation hull exponent in two dimensions. *Phys. Rev. Lett.*, 58(22):2325–2328, 1987. MR889398 (88d:82073)

[Sei90] N. Seiberg. Notes on quantum Liouville theory and quantum gravity. *Progr. Theoret. Phys. Suppl.*, (102):319–349 (1991), 1990. Common trends in mathematics and quantum field theories (Kyoto, 1990). MR1182173 (93h:81136)

[She07] S. Sheffield. Gaussian free fields for mathematicians. *Probab. Theory Related Fields*, 139(3-4):521–541, 2007. math/0312099. MR2322706 (2008d:60120)

[She09] S. Sheffield. Exploration trees and conformal loop ensembles. *Duke Math. J.*, 147(1):79–129, 2009. math/0609167. MR2494457 (2010g:60184)

[She10] S. Sheffield. Conformal weldings of random surfaces: SLE and the quantum gravity zipper. *ArXiv e-prints*, December 2010, 1012.4797. To appear in Annals of Probability.

[She11] S. Sheffield. Quantum gravity and inventory accumulation. *ArXiv e-prints*, August 2011, 1108.2241. To appear in Annals of Probability.

[Spi58] F. Spitzer. Some theorems concerning 2-dimensional Brownian motion. *Trans. Amer. Math. Soc.*, 87:187–197, 1958. MR0104296 (21 #3051)

[Ste10] K. Stephenson. CirclePack. `http://www.math.utk.edu/~kens/CirclePack/`, 1992–2010.

[SW05] O. Schramm and D. B. Wilson. SLE coordinate changes. *New York J. Math.*, 11:659–669 (electronic), 2005. math/0505368. MR2188260 (2007e:82019)

[Tim10] V. Timorin. Topological regluing of rational functions. *Invent. Math.*, 179(3):461–506, 2010. 0810.5559. MR2587338 (2011c:37098)

[YZ01] M. Yampolsky and S. Zakeri. Mating Siegel quadratic polynomials. *J. Amer. Math. Soc.*, 14(1):25–78 (electronic), 2001. math/9808009. MR1800348 (2001k:37064)

[Zha08] D. Zhan. Reversibility of chordal SLE. *Ann. Probab.*, 36(4):1472–1494, 2008. 0808.3649. MR2435856 (2010a:60284)

Institute for Theoretical Physics
CEA/Saclay
91191 Gif-sur-Yvette, France

Department of Mathematics
Massachusetts Institute of Technology
Cambridge, MA, USA